Application to
U.S. Department of Energy
Office of Energy Efficiency and Renewable Energy
Golden Field Office

for
Enhanced (Engineered) Geothermal Systems (EGS)
Research and Development (R&D)
Solicitation DE-PS36-04GO94001

Project:
Evaluation of Oil-Industry Stimulation Practices for Engineered Geothermal Systems

submitted by
Pinnacle Technologies, Inc.
San Francisco, California
DUNS Number 82-492-6976

with the participation of
GeothermEx, Inc.
Richmond, California
DUNS Number 07-652-5757

October 2007

CONTENTS

1 PROJECT SUMMARY

Geothermal energy extraction is typically achieved by use of long open-hole intervals in an attempt to connect the well with the greatest possible rock mass. This presents a problem for the development of Enhanced (Engineered) Geothermal Systems (EGS), owing to the challenge of obtaining uniform stimulation throughout the open-hole interval. Fluids are often injected in only a fraction of that interval, reducing heat transfer efficiency and increasing energy cost.

Pinnacle Technologies, Inc. and GeothermEx, Inc. evaluated a variety of techniques and methods that are commonly used for hydraulic fracturing of oil and gas wells to increase and evaluate stimulation effectiveness in EGS wells. Headed by Leen Weijers, formerly Manager of Technical Development at Pinnacle Technologies, Inc., the project ran from August 1, 2004 to July 31, 2006 in two one-year periods to address the following tasks and milestones:

1) Analyze stimulation results from the closest oil-field equivalents for EGS applications in the United States (e.g., the Barnett Shale in North Texas) (section 3 on page 8). Pinnacle Technologies, Inc. has collected fracture growth data from thousands of stimulations (section 3.1 on page 12). This data was further evaluated in the context of:
   a) Identifying techniques best suited to developing a stimulated EGS fracture network (section 3.2 on page 29), and
   b) quantifying the growth of the network under various conditions to develop a calibrated model for fracture network growth (section 3.3 on page 30).

The developed model can be used to design optimized EGS fracture networks that maximize contact with the heat source and minimize short-circuiting (section 3.4 on page 38).

2) Evaluate methods used in oil field applications to improve fluid diversion and penetration and determine their applicability to EGS (section 4 on page 50). These methods include, but are not limited to:
   a) Stimulation strategies (propped fracturing versus water fracturing versus injecting fluid below fracturing gradients) (section 4.1 on page 50);
   b) zonal isolation methods (by use of perforated casing or packers) (section 4.2 on page 57);
   c) fracture re-orientation and fracture network growth techniques (e.g., by use of alternating high- and low-rate injections) (section 4.4 on page 74); and
   d) fluid diversion methods (by use of the SurgiFrac technique, the StimGun perforation technique, or stress shadowing).

This project task is to be completed in the first project year, enabling the most promising techniques to be field tested and evaluated in the second project year.

3) Study the applicability of the methods listed above by utilizing several techniques (section 5 on page 75) including, but not limited to:
   a) Hydraulic Impedance Testing (HIT) to determine the location of open hydraulic fractures along a open-hole interval;
   b) pressure transient testing to determine reservoir permeability, pore pressure, and closure stress; and
   c) treatment well tilt mapping or microseismic mapping to evaluate fracture coverage.

These techniques were reviewed for their potential application for EGS in the first project year (section 5.1 on page 75). This study also includes further analysis of any field testing that will be conducted in the Desert Peak area in Nevada for ORMAT Nevada, Inc. (section 5.2 on page 86), with the aim to close the loop to provide reliable calibrated fracture model results.

Developed through its hydraulic fracture consulting business, techniques of Pinnacle Technologies, Inc. for stimulating and analyzing fracture growth have helped the oil and gas industry to improve hydraulic fracturing from both a technical and economic perspective. In addition to more than 30 years of experience in the development of geothermal energy for commercial power generation throughout the world, GeothermEx, Inc. brings to the project:

1) Detailed information about specific developed and potential EGS reservoirs,
2) experience with geothermal well design, completion, and testing practices, and
3) a direct connection to the Desert Peak EGS project.

2 INTRODUCTION

This section describes the context (section 2.1), the problem statement (section 2.2), the proposed solution (section 2.3), the objectives (section 2.4), and the methodology (section 2.5) of this project.

2.1 Context

Geothermal systems are of interest primarily in terms of the production of power obtained with heat from the interior of the Earth. Below the surface of much of the Earth, the temperature increases with a gradient of ~ 26°F/1,000 ft in the first 33,000 ft. In certain places, the temperature gradient can be much greater. The Earth therefore contains an immense storage of energy in the part of its upper crust that is accessible by drilling. Most conventional hydrothermal resources are positioned in regions of active volcanism, or, more generally, along the active boundaries of tectonic plates. The greatest potential of geothermal systems lies in the generation of electricity. However, while geothermal energy is plentiful, geothermal power is not. This is because the required combination of heat and permeability does not exist everywhere. In fact, on a global scale, this combination is relatively rare: Most areas with elevated temperature gradients are hot but have a relatively low permeability. The concept of mining the crustal heat by circulating water between wells in a reservoir with artificially enhanced permeability would enable significantly more of the accessible crustal heat to be recovered as useful energy than can be derived from conventional hydrothermal resources alone. The extraction of geothermal energy from hot rock with a low permeability depends on the ability of a well or group of wells to mine heat from the largest possible mass of fractured rock. In geothermal wells, contact with the fractured rock mass is maximized with long, open-hole well intervals.

2.2 Problem Statement

The extraction of geothermal energy from hot rock with a low permeability depends on:
1) The ability to create a large, complex network of permeable fractures in which water can be circulated to mine its heat content; and
2) the ability to connect wells with the greatest possible mass of artificially fractured rock.

While long, open-hole intervals are common in geothermal developments, it is difficult to obtain a uniform stimulation throughout the open-hole interval. That is, fluids are often injected in only a fraction of the entire interval, resulting in a decrease of the direct area of contact between the well and the far-field system of fractures. This presents a problem for the development of Enhanced or Engineered Geothermal Systems (EGS) in that it reduces the efficiency of the transfer of heat, and increases the cost of the produced energy. To realize the potential of EGS power, the efficiency of creating and operating the artificially enhanced fracture network (i.e., the reservoir) needs to be improved.

2.3 Proposed Solution

The creation of complex networks of fractures is among the very few feasible methods to extract heat economically from hot rock with naturally low permeability. The hydraulic stimulation of rock to create fractures and networks of fractures is routinely conducted in the oil and gas industry. Typically, this procedure involves creating and extending one or more fractures within a formation that produces hydrocarbons. It greatly increases the direct contact area between the well and the reservoir. Hence, it accelerates the extraction of hydrocarbons from the reservoir. Other methods (e.g., chemical stimulation by injecting mineral dissolution agents or thermal stimulation by injecting colder fluids) may also be used, generally in conjunction with hydraulic stimulation.

In EGS, hydraulic stimulation could also be used to obtain contact with a significant volume of rock surrounding a geothermal well. Therefore, the ability to stimulate a network of fractures successfully is required to improve the economic viability of EGS. However, massive hydraulic stimulation adds significantly to the cost of the development of geothermal fields. In addition, controlling the development of the created fracture network and analyzing the results of stimulation are among the most difficult problems in EGS.

Consequently, it is logical for EGS efforts to build on what has already been learned and accomplished in tight hydrocarbon reservoirs (e.g., the Barnett Shale). A variety of techniques that is commonly used in the hydraulic fracturing of oil and gas wells is evaluated herein in the context of increasing and evaluating the effectiveness of EGS well stimulation. Two recent developments in the oil industry make this evaluation important for EGS:

1) The development of direct fracture diagnostic tools that can now be used on a commercial basis on many fracture stimulation treatments, and
2) the development of several of techniques to stimulate effectively and economically a variety of extreme hydrocarbon environments.

2.4 Objectives

As in the oil and gas development, the principal objectives of hydraulic stimulation treatments for EGS are to:

1) Maximize production of energy,
2) minimize costs, and
3) minimize risk.

To maximize the production of energy, the sub-goals are to:

1) Maximize the area of contact between the hot rock and the circulation fluid,
2) maximize the permeability of the network of fractures, and
3) eliminate or minimize short-circuiting of the circulation fluid in the network of fractures.

To minimize the costs, the sub-goals are to:

1) Minimize the amount (and therefore the costs) of the hydraulic fracturing fluids, proppants and additives, and
2) minimize the post-stimulation clean up efforts.

To minimize the risk, the sub-goal is to maximize the probability of creating a network of fractures in the pay-zone by use of proven technology and accurate predictive modeling.

2.5 Methodology

The knowledge obtained from and the techniques used for the stimulation of hydrocarbon reservoirs is transferred to the stimulation of EGS reservoirs.

3 OIL-FIELD EQUIVALENTS FOR EGS APPLICATIONS

Pinnacle Technologies, Inc. and GeothermEx, Inc. identified oil-field analogues for EGS applications in the United States. Pinnacle Technologies, Inc. has collected fracture growth data, together with treatment data, well and completion information and reservoir properties from thousands of hydraulic fracture treatments. We worked with our clients to evaluate further this data. From these findings, Pinnacle Technologies, Inc. developed a calibrated fracture growth model that approximates fracture growth in EGS applications.

To date, EGS experimentation has been largely undertaken in massive crystalline basement rock, e.g.:
1) The initial Hot Dry Rock project at Fenton Hill, New Mexico;
2) the Coso EGS project in south-eastern California;
3) the Hot Dry Rock project in the Cooper Basin in southern Australia (section 3.1.1 on page 14);
4) the European Hot Dry Rock project at Soultz-sous-Forêts in eastern France (section 3.1.2 on page 16); and
5) the Desert Peak EGS project in western Nevada.

However, there is significant near-term potential for EGS development in sedimentary and metamorphic rock types, most probably in the Salton Trough, and Basin and Range geologic provinces. Indeed, the Desert Peak project, positioned in the Basin and Range, has a metamorphic rock sequence overlying a massive granitic intrusion. As such, consideration has been given to stimulating some of these layered rocks. Another proposed EGS project at Lightning Dock, New Mexico, targeted limestone for hydraulic stimulation. In the Salton Sea, conventional hydrothermal production is derived from naturally fractured shales and sandstones. There is significant EGS potential in peripheral areas of the field where temperatures remain high. However, permeabilities in the sedimentary sequence are low. Therefore, although there has been an initial focus on crystalline rock for EGS development, sedimentary and layered metamorphic units are likely to be considered as potential EGS reservoir rocks in the not-so-distant future.

The EGS projects currently under development (e.g., Soultz, Cooper Basin, Coso, and Desert Peak) have all targeted massive intrusions for reservoir creation and enhancement. Unlike the other three, Coso stands out in that the intrusive rocks is either exposed at the surface or covered by a relatively thin veneer of recent volcanics and alluvium, greatly facilitating seismic data acquisition. At the other three, a thick layer of sedimentary and metamorphic rocks overlies the target intrusives. Primary heat sources include radioactive decay (in the case of the Cooper Basin), and regional high heat flow (for the other three), sometimes enhanced by nearby volcanism (Coso) and on-going high-temperature (resource grade) hydrothermal convection (certainly this is the case in Coso and Desert Peak). The intrusive target rocks are generally felsic. They have all experienced some degree of hydrothermal alteration. This indicates the presence of convecting fluids, in either the past or the present. Rock strengths are generally high, which is thought to be favorable for brittle failure during stimulation.

The oil-field analogues that we looked for exhibit complex fracture growth with growth of networks of fractures. One clear example of this fracture growth behavior is in the Barnett Shale in North Texas (section 3.1.3 on page 22), where an extensive fracture network [*Fisher et al.,* 2002] is created. This network has a length of several thousands of feet, and a width of several hundreds of feet.

For comparison, typical properties for existing EGS versus those for the Barnett Shale are listed in

Table 3.1.

Table 3.1: Typical properties for existing EGS versus Barnett Shale.

parameter	units	EGS (Coso)	EGS (Soultz)	EGS (Desert Peak)	Barnett Shale		
rock							
type		intrusive (granitic)	intrusive (granitic)	intrusive (granitic) or metamorphic	shale (non-siliciclastic rocks; quartz, clay)		
texture		massive, zoned	massive, altered	typically massive	organic-rich, fine grained		
natural fractures		yes, including some open ones	yes, including some open ones	yes; however few are open	yes		
Young's modulus	10^6 psi	7.7 to 11.6		6 to 10	3.7	3.7	2.5 to 7.9
Poisson's ratio		0.14 to 0.31		0.17 to 0.28	0.21	0.29	0.30 to 0.34
					Lower	**Upper**	**surrounding**
reservoir							
pore pressure	psi	hydrostatic	hydrostatic	hydrostatic			
Sw	%	100	100	100			
closure stress	psi/ft	0.69 to 0.75		likely ~ 0.50 to 0.63	0.50 to 0.61	0.70 to 0.74	0.69 to 0.80
permeability	10^{-3} mD			1.3 to 4.0	0.07 to 5.0; 1.0	7.0	
porosity	%	< 1		2 to 5	4 to 6		
depth	10^3 ft	5 to 10	11.5 and 16.5	7 to 10	6.8 to 9.0		
thickness	ft	1,000 to 4,000	typically 1,640 ft open-hole	1,000 to 3,000	200 to 800		
fracture toughness	10^3 psi $in^{½}$				0.5	0.5	1.0 to 1.5
completion							
type		open-hole	open-hole with floating string completion for production casing	open-hole	open-hole, perforated, slotted liner		
well orientation		deviated (not horizontal)	deviated	vertical	vertical	horizontal	
interval length	10^3 ft	entire open-hole	entire open-hole	entire open-hole		2 to > 3	
treatment							
injection rate	bbl/min	0.48 to 2.4 (planned)	7.5 to 34 (typically 15 to 19)		45 to 75	140 to 200	
fluid		plain water (perhaps brine slug	heavy brine first followed by plain water	plain water		slickwater	

		first)					
fluid volume	10^3 bbl	< 85.0	< 314	595 to 714	10 to 100		
proppants		none	none	none		sand	
proppant weight	10^6 lbm	n/a	n/a	n/a	0.075 to 0.25	0.50 to 1.0	
proppant concentration	lbm/gal	n/a	n/a	n/a	0.1 to 1.0		
parameter	**units**	**EGS (Coso)**	**EGS (Soultz)**	**EGS (Desert Peak)**	**Barnett Shale**		

The following sub-sections present the review of existing mapping datasets (section 3.1 on page 12), relevant fracture growth physics in EGS applications (section 3.2 on page 29), calibrated fracture models for EGS applications (section 3.3 on page 30), and a sensitivity study for stimulation treatment design tests (section 3.4 on page 38).

3.1 Review of Existing Mapping Datasets

Pinnacle Technologies, Inc. has collected fracture growth data, together with treatment data, well and completion information and reservoir properties from thousands of hydraulic fracture treatments. Many of these treatments have been conducted in low-permeability applications.

Pinnacle Technologies, Inc. has mapped more than 100 fracture treatments in the Barnett Shale. Some of this data has been published at oil-field conferences. The creation of complex networks such as these is among the only possibilities to contact a large body of heated rock and to extract heat from it economically.

We created an extensive database that contains fracture treatment data, well and completion information, reservoir properties and fracture mapping results. We developed empirical relationships between the size of the network of fractures (i.e., the length and width of the network system) versus given parameters (e.g., reservoir characteristics and rock-mechanical characteristics), and controllable parameters (e.g., fracture treatment design and well completion).

Hydraulic fracturing is routinely conducted in the oil and gas industry to accelerate the extraction of hydrocarbons from reservoirs, and some of this technology is directly applicable to the stimulation of geothermal reservoirs. Hydraulic fracturing for stimulation of oil or gas reservoirs generally aims to create a single, wide propped hydraulic fracture that penetrates hundreds to thousands of feet into the reservoir (Figure 3.1a). The width and length of the created fracture are generally engineered so that the conductivity of the fracture system is sufficiently high for the propped fracture not to act as the bottleneck for production response. In practice, however, creation of a single fracture is virtually impossible because of heterogeneous nature of rock, and the simultaneous propagation of parallel bands of multiple hydraulic fractures has been directly observed in many core-throughs and mine backs experiments (Figure 3.1b). In some oil and gas reservoirs (e.g., the Barnett Shale and the Cotton Valley Sandstone), an even more complex type of fracture growth is observed, as displayed in Figure 3.1c, with fracture growth along two orthogonal directions.

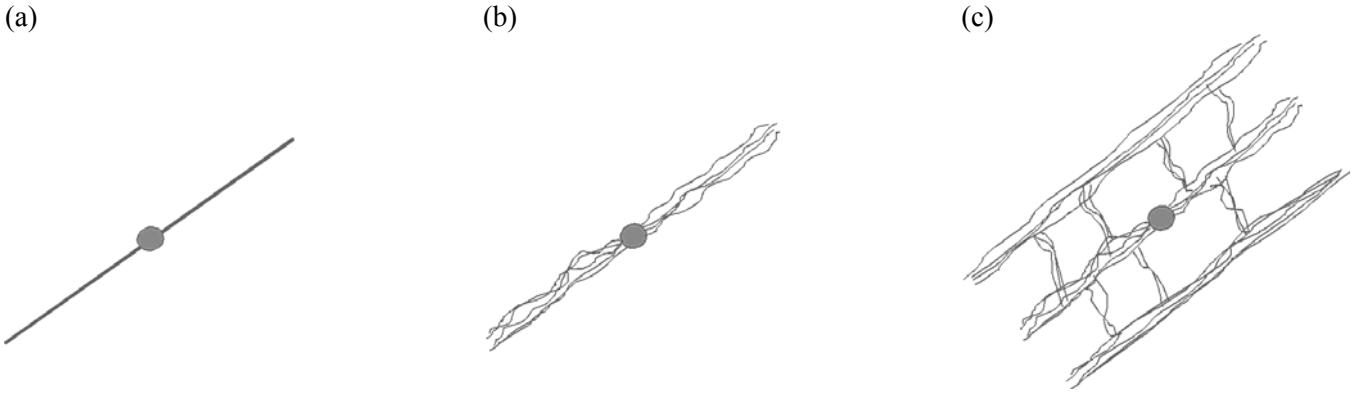

Figure 3.1: Examples of increasing fracture complexity: (a) Simple (most common), (b) complex, and (c) extremely complex (relatively rare) [*Fisher et al.,* 2002].

Although this extremely complex behavior is generally not desired in most hydraulic fracturing applications in the oil and gas industry, because both the fracture width and conductivity created are insufficient, it is actually desired for some specific applications where the reservoir permeability is extremely low. Similar to EGS for mining heat, successful stimulation of oil or gas production in ultra-low permeability reservoirs requires maximizing of the contact area between the created fracture system and the reservoir volume.

Hydraulic fracturing for oil or gas well stimulation has been conducted for more than five decades. However, until a few years ago the mechanisms of fracture growth were considered a black box, as it has been very difficult to determine what was actually achieved during typical propped fracture treatments. During the last decade, however, various technologies

have been developed and commercialized [*Warpinski et al.,* 2001; *Wright et al.,* 1999; *Wright et al.,* 1998a] that allow for real-time mapping of hydraulically created fractures. These direct diagnostics have literally opened engineers' eyes to the actual growth behavior of hydraulically created fractures under many conditions and circumstances. The oil and gas industry has now started to make changes to hydraulic fracture stimulation design and execution to account for this observed behavior. Out of the 35,000 fracture treatments that are performed in the oil and gas industry every year, ~ 1,500 are now mapped by use of either tiltmeter or microseismic fracture mapping. A total of ~ 10,000 hydraulic fracture treatments have been mapped for the oil and gas industry to date.

Published data from several EGS projects demonstrate the growth of the EGS reservoir resulting from hydraulic stimulation. Perhaps the most illustrative are:
1) the European Hot Dry Rock project at Soultz-sous-Fôrets in France (section 3.1.1 Cooper Basin on page 14), and
2) the project of Geodynamics, Ltd. in the Cooper Basin of South Australia (section 3.1.2 Soultz-sous-Fôrets on page 16).

The main technique that has been used to map the stimulations is microseismic monitoring, although other techniques have been used (particularly at Soultz).

Some major concerns about hydraulic fracturing that were noted [*Verity,* 1984] and addressed by the U.S. Department of Energy Geothermal Reservoir Well Stimulation Program (GRWSP) [*Entingh,* 2000]:
1) Hydraulic fractures in fractured formations may merely parallel the predominant natural fractures in the reservoir and fail to connect effectively with them. The results of the work by GRWSP remain consistent with this concept.
2) Rapid thermal degradation of polymer fracturing fluids could prevent the effective growth and propping of hydraulic fractures. Propping appeared to work in at least the experiments at East Mesa in California, and perhaps at Baca in New Mexico.
3) Conventional downhole mechanical equipment could be inadequate for fracturing in wells with elevated temperatures. This concern seems to have been allayed successfully by running pre-treatments (i.e., pre-pads) of cool water.
4) Available proppants may degrade in the saline environment with elevated temperatures. The fieldwork seemed not to have studied this issue (e.g., with long-term tests of productivity from stimulated wells).
5) The possibility of excessive fluid leakoff, especially in naturally fractured formations, could result in an early termination of hydraulic fracture growth. Some of the GRWSP results (e.g., at Raft River in Idaho) were interpreted to be consistent with this idea.

To identify reasonable analogues for EGS, data that describe the reservoirs, wells, treatments, hydraulic fractures, and completions from thousands of cases have been studied, in a variety of fields and formations (section 10.4 on page 191), e.g.:
1) The East Texas Cotton Valley sandstone,
2) the Elk Hills Gusher formation,
3) the North Texas Bossier Sandstone formation,
4) the San Juan Pictured Cliffs formation,
5) the Almond Coal in Wyoming,
6) the San Andres Dolomite,
7) the Clear Fork Carbonate in West Texas, and
8) the Lance formation in the Jonah field.

The clearest example of a gas field where a complex and extensive fracture network has been created that is also desirable for EGS applications, and where mapping data is extremely prolific (hundreds of hydraulic fracture stimulation treatments), is the Barnett Shale in North Texas (section 3.1.3 on page 22, and section 8 on page 102). Because the Barnett Shale has a very low permeability and it is naturally fractured, it could be a useful analogue for EGS. In addition, large fracture networks have been created by hydraulic stimulation, which is the intent in EGS development. Hence, valuable lessons can be learned from the Barnett Shale to improve stimulations of EGS.

3.1.1 Cooper Basin

The Cooper Basin is positioned within an area of known elevated heat flow in South Australia. It is well known from oil and gas exploration and production. Hydrocarbons are contained with late Carboniferous to Triassic (and sometimes older) sediments. They are locally underlain by intrusive mid-Carboniferous intrusive rocks, which are the host rocks for the evolving EGS development. Two geothermal wells (Habanero-1 and -2) have been drilled into the intrusive basement rocks. Both encountered significant overpressure (~ 5,000 psi). It is suggested [*Karner,* 2005a; *Karner,* 2005b] that the basement granite encountered in Habanero-1 and -2 is currently in communication with the overlying basin sediments. In addition, it is estimated that that the magnitudes of the in-situ fluid pressure and the overburden stress (i.e., the least compressive stress) are quite similar. Furthermore, it is speculated that the observed sub-horizontal fractures are representative of a previously created fracture network, yielding a relatively low tensile strength of the reservoir rock, and the ability to re-activate pre-existing weaknesses.

Habanero-1

Habanero-1 was completed at a depth of 14,500 ft in September 2003. Temperatures in excess of 480°F were observed. Granitic basement was encountered at 12,000 ft. Image logs suggest the presence of pre-existing sub-horizontal fractures within specific intervals. Because of the over-pressure, heavy muds were used during drilling to keep the well from flowing. In addition, lost circulation material was placed in several loss zones. Because the exploration company (Geodynamics, Ltd.) plans to use Habanero-1 as the injection well for the EGS development, the well was completed with an inner tubing string that would enable injection at high pressures. Although fractures and natural permeable zones were encountered, pre-stimulation testing of injection suggested sub-commercial hydraulic characteristics. To stimulate the reservoir and extend the fracture network, a total of ~ 1,300 bbl of fresh water was injected into this well in several phases during a periods of three weeks, with well-head pressures up to 9,400 psi. Adequate summaries of the stimulation and its results have been presented [*Asanuma et al.,* 2004; *Wyborn et al.,* 2004].

The microseismic network that was set up to monitor the stimulation consisted of the following [*Wyborn et al.,* 2005]:
1) Four wells with a depth of 330 ft at distances of ~ 16,500 ft from Habanero-1 (wells WA1 to WA4);
2) three wells with a depth of 2,800 ft positioned at a distance of ~ 6,600 ft from Habanero-1 (wells MW1 to MW3); the sensors were set at a depth of 1,500 ft in wells MW1 and MW3, and at a depth of 700 ft in well M2; this deployment is shallower than originally planned; and
3) the previously drilled well McLeod-1, which is at a distance of 1,500 ft from Habanero-1; the sensor was set at a depth of 5,900 ft where the rock temperature was 273°F.

A velocity model with six layers was developed to define the system, from previous seismic data collected in or around the McLeod well [*Wyborn et al.,* 2005]. The sediments are represented by five layers, and the intrusive rocks are represented by the sixth layer. The velocity in the granite was initially estimated at 990,000 ft/min from information from other locations. However, this velocity model yielded event locations near the bottom of well Habanero-1, which was deeper than expected from the locations of outflow zones identified from pressure-temperature-spinner (PTS) logging. The velocity of the granite was therefore increased to enable the gently dipping (i.e., ~ 25° to the south-west) seismically active zone to intersect well Habanero-1 at ~ 14,000 ft, where PTS logs demonstrated the outflow of injected water.

The stimulation created induced microseismicity in a large, NE-trending, sub-horizontal zone. From microseismic hypocenter locations, this zone has a maximum length of ~ 9.800 ft, and a maximum width of ~ 6,600 ft. Focal depths are mostly in the range of 13,000 to 15,500 ft.

Additional processing of the seismic data has resulted in a more compact zone of microseismicity [*Asanuma et al.,* 2005b; *Kumano et al.,* 2005]. The refinement of hypo central locations permits the evaluation of the geometry and growth patterns of the reservoir. It was concluded that a series (i.e., two or three) of long, parallel planes could be observed in the reservoir, dipping to the W at 25° or less. Each planar seismic cluster has an overall thickness of less than 170 ft. The total thickness of all clusters or zones appears to be less than 650 ft. Bounding structures were defined in the first few days by sharp edges to event location clusters, which are crossed after nine days of pumping, to develop a new plane of seismic

events ~ 320 ft above the first and implying a sub-vertical hydraulic connection between the two. The collapsing re-location method suggests further compaction of the overall thickness of the reservoir to ~ 320 to 500 ft. The presence of an a-seismic zone around the injection well is determined. This is attributed to previous relaxation of stresses from earlier testing of the main permeable zone in Habanero-1. Considering the over-pressure in the area, it is concluded that sub-horizontal fractures were at a critical or even over-critical state of stress for shear slip.

The significance of events of greater magnitude that occurred during the Habanerao-1 stimulation was analyzed [*Asanuma et al.,* 2005a]. The event of greatest magnitude had a moment magnitude of 3.0. This and other events with great magnitude were positioned throughout the seismic cloud, indicating no preference for a particular geologic structure. They occurred throughout the stimulation, apparently without correlation to pumping rate or pressure. Of 30 events with great magnitude, 11 occurred after shut-in. It was concluded that the physical processes creating the events with greater magnitude are the same as those for the more numerous small events. It was further postulated that the events with greater magnitude represent the breakdown of greater asperities along a fracturing plane. Increased extension of the reservoir after these events supports this conclusion.

Habanero-2

Well Habanero-2, drilled from a surface location at a distance of ~ 1,650 ft SW of Habanero-1, was completed in late 2004 and early 2005 as the production well of the EGS doublet. The results of drilling and preliminary flow testing indicated that the two Habanero wells are hydraulically connected via the stimulated zone created by injecting into Habanero-1 (referred to as the Bottom Zone reservoir). A series of diagnostic tests were undertaken earlier this year to evaluate this connection. This indicated a less-than-optimal connection of Habanero-2 to the Bottom Zone reservoir.

Habanero-2 was then stimulated, creating another sub-horizontal zone (referred to as the Top Zone reservoir) ~ 430 ft higher than the Bottom Zone, as displayed in Figure 3.2. Geodynamics, Ltd. believes that this Top Zone coincides with a fracture zone encountered near the casing shoe in Habanero-1 [*Geodynamics,* 2005]. To date, no seismic mapping data have been provided for this second phase of stimulation. Furthermore, it is stated that the connection between the two wells in the Bottom Zone reservoir is currently being improved by injecting into Habanero-1 and producing from Habanero-2 in a series of clean up flows. To improve the connection and to extend the reservoir, Geodynamics, Ltd. reports that it is injecting into Habanero-1 at the highest possible rates that can be achieved given the frictional resistance of the inner tubing string (maximum rates of ~ 15 bbl/min are reported) and allowing the water to flow out of Habanero-2.

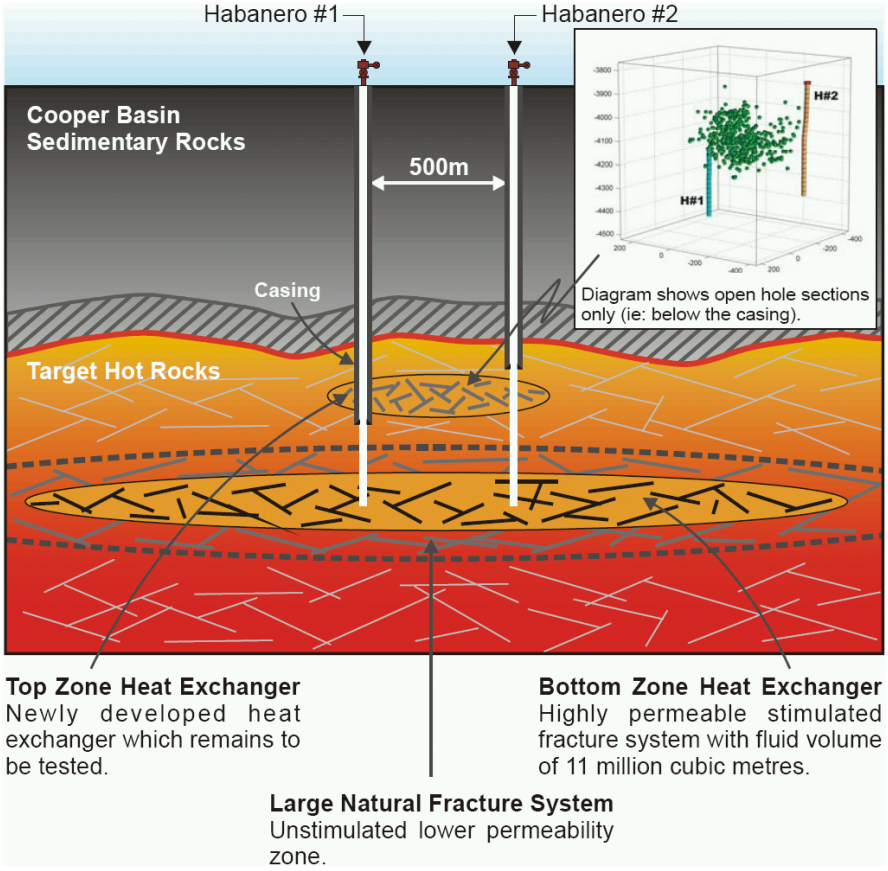

Figure 3.2: Stimulation of Habanero-2, creating another sub-horizontal top zone reservoir that is positioned ~ 430 ft above the bottom zone [*Geodynamics,* 2005].

3.1.2 Soultz-sous-Fôrets

Soultz-sous-Fôrets is positioned in northeastern France, near the western edge of the Rhine Graben rift system. Cenozoic sediments are underlain by a Triassic-Jurassic sedimentary sequence that is in turn underlain by early-Carboniferous granitic rocks [*Bächler,* 2003]. The Rhine Graben is characterized by relatively high thermal gradients and heat flow, as demonstrated by temperature data from the many oil and gas exploration wells in the region. The granitic basement at Soultz-sous-Fôrets lies beneath ~ 4,600 ft of sedimentary rock.

Nine boreholes currently exist at the site, including four full-diameter wells (GPK-1 to -4) and five seismic monitoring wells. Several of the monitoring wells were old oil exploration wells that were re-entered and deepened to reach the granitic basement. The first of the recently drilled full-diameter wells (GPK-1) has been converted to a deep seismic monitoring well, as displayed in Figure 3.3. At various times, the four full-diameter wells have been used for injection and production tests and have been subjected to hydraulic stimulation. Wells GPK-2, -3 and -4 now form the EGS triplet that is used to supply a pilot power plant, with injection into GPK-3 and production from GPK-2 and -4.

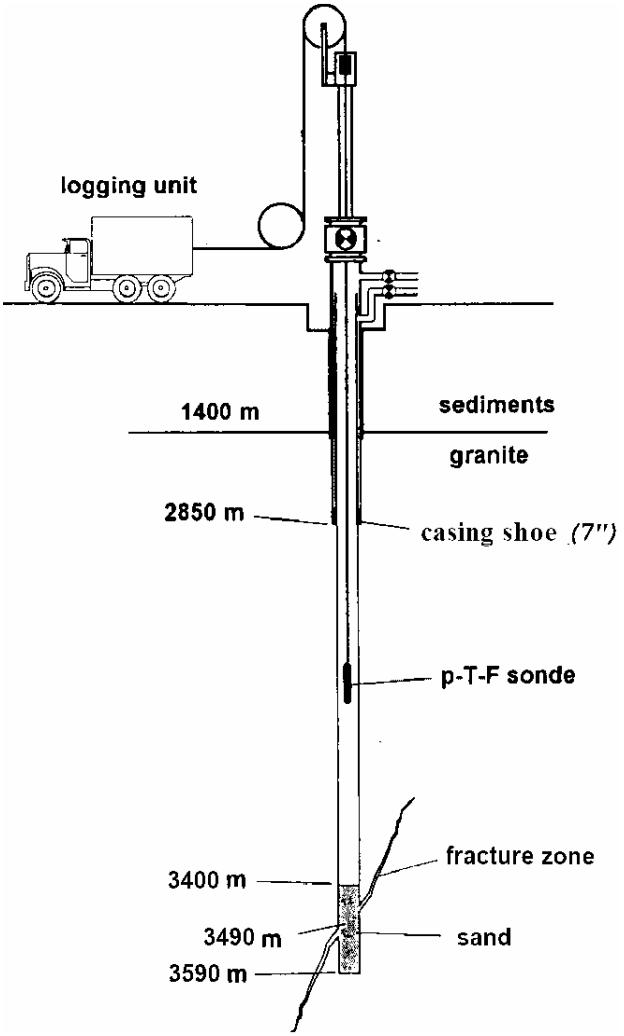

Figure 3.3: The first of the recently drilled full-diameter wells (GPK-1) that has been converted to a deep seismic monitoring well [*Jung et al.,* 1995].

During reservoir development at Soultz, numerous hydraulic injection tests were performed [*Karner,* 2005a; *Karner,* 2005b]. Based on data from these tests, the stress state for the depth range of 4,800 to 11,500 ft has been described empirically as follows [*Baria et al.,* 2005a; *Klee and Rummel,* 1993]:

1) Minimum horizontal stress: $\sigma_h = 2{,}290 + 0.659(z - 4{,}780)$,
2) maximum horizontal stress: $\sigma_H = 3{,}440 + 1.46(z - 4{,}780)$, and
3) vertical stress: $\sigma_V = 4{,}900 + 1.13(z - 4{,}520)$

where the stresses σ are measured in psi, and the depth z is in ft. These relations indicate a depth-dependent transition from normal faulting above ~ 9,900 ft to strike-slip faulting below that level. This is consistent with recent analyses of moment tensor solutions derived from stimulation-induced microseismicity [*Cuenot et al.,* 2005].

The following is a summary of the stimulations undertaken in the full-diameter wells:

1) In 1991, well GPK1 was stimulated at a depth of 4,700 to 6,600 ft.
2) In 1993, well GPK1 was stimulated at a depth of 9,400 and 11,200 ft at flow rates between 0.057 to 14 bbl/min with nearly constant well-head pressures of ~ 1,500 psi for the greater flow rates [*Jung et al.,* 1995];
3) In 1995, well GPK2 was first stimulated between 10,600 to 12,700 ft at a flow rate of ~ 5.7 bbl/min which generated downhole pressures of ~ 6,400 psi. Subsequently, flow rates were systematically varied from 2.3, 4.8, 7.1, and 9.8

bbl/min to generate pressures (measured at 10,500 ft) of ~ 4,800, 4,900, 5,100, and 5,400 psi, respectively [*Kohl et al.,* 1996].

4) In 2000, well GPK2 was stimulated at a deeper level of 14,500 to 14,600 ft with a downhole pressure of ~ 8,100 psi for flow rates of 11, 16, 19 bbl/min [*Weidler et al.,* 2002].
5) In May 2003, well GPK3 was stimulated at 13,900 ft with a downhole pressure (measured at 13,900 ft) of ~ 8,400 psi and flow rates of ~ 11 and 16 bbl/min [*Mégel et al.,* 2005].
6) In 2004, well GPK4 was stimulated at between the depths of ~ 15,400 ft and ~ 16,600 ft with a majority of the injected fluid entering the reservoir at ~ 16,500 ft and at a downhole pressure of ~ 8,800 psi for a predominant rate of ~ 11 bbl/min [*Baria et al.,* 2005b].

As in the Cooper Basin, the Soultz reservoir has a significant pre-existing fracture network. At Soultz, the dominant N-S orientation is consistent with the regional stress field [*André et al,* 2001]. This has been exploited during stimulation, and seismic monitoring has been used to map stimulation progress and results. Originally, well GPK-2 was completed at a depth of ~ 11,500 ft, where temperatures were ~ 300°F. It was deepened to 16,400 ft in 1999 to reach greater temperatures of ~ 390°F. As mentioned above, this deepened GPK-2 well was stimulated first in 2000. A total volume of 148×10^3 bbl was injected in three steps: 12, 16, and 19 bbl/min. Because of stimulation, the injectivity of GPK-2 was improved from between 0.0026 and 0.0052 bbl/min/psi to ~ 0.0079 bbl/min/psi [*Baria et al.,* 2004]. During the stimulation, 40,000 microseismic events were recorded, of which 14,000 could be positioned.

Seismic monitoring of the GPK-2 stimulation and other analyses allowed a drilling target to be chosen for well GPK-3. This second well of the triplet was completed at a depth of 16,400 ft in 2002, with the casing shoe set at 15,000 ft. The trajectory of GPK-3 lies within but near the edge of the stimulated area around GPK-2. The stimulation of GPK-3 was undertaken in four phases, as displayed in Figure 3.4 and Figure 3.5a-d [*Baria et al.,* 2005a]:

1) Fluid was injected into well GPK-3 only, at rates up to 23 bbl/min. The stimulation began by injecting heavy brine (density of 421 lbm/bbl) to initiate stimulation in the deeper, hotter section of the open-hole portion of the well. The brine flow rate was 11 bbl/min. This was followed by fresh water injection at the same rate, with the total period being approximately three days (for both brine and freshwater injection at this rate). The injection rate was then increased to 19 bbl/min (with a short peak at 33 bbl/min). Seismicity began to occur when an overpressure of 380 psi was reached. This suggests that the stimulated joints or fractures were near-critically stressed. Seismicity was initially positioned around the main flowing zone detected by TPS logging at 15,600 ft and then migrated toward GPK-2 in a downward direction, and to the N and S (Figure 3.5a).
2) Simultaneous injection in GPK-2 and -3. This idea, which is referred to as focused stimulation, was considered after a reduction in pore pressure and seismicity was observed while simultaneously stimulating GPK-2 and flowing GPK-1. The implication for the simultaneous injection in GPK-2 and GPK-3 was the opposite: That injection pressures could be superposed, elevating the pressure between the wells more than could be achieved with only a single stimulation. The choice of the term focused was made because it may enable selective stimulation of a region hydraulically connected to two wells. The injection rate in GPK-3 was continued at ~ 19 bbl/min when injection was started into GPK-2 at ~ 7.548 bbl/min. Seismic activity was concentrated in the upper part of the reservoir, and a deeper zone developed. Little seismicity was observed adjacent to GPK-2, where stressed had been relaxed by previous stimulation (Figure 3.5b).
3) GPK-2 is shut in but injection into GPK-3 continues at an increased rate of 34 bbl/min for a few hours. Thereafter, the rate was gradually decreased to avoid any large seismic events induced by a sudden rapid pressure drop. This phase of stimulation continued the development mostly in the upper part of the reservoir. However, this also initiated more activity in the deeper zone that had begun to develop during the second phase (Figure 3.5c).
4) Both wells are shut in and the pressure in GPK-2 is relieved by flowing the well back at ~ 229 bbl/min for five days (Figure 3.5d). During this phase, seismicity continued for as long as two months, in contrast to the rapid decay in event frequency associated with the shallower stimulation of this well at 11,800 ft. Most seismic activity was at the periphery of the area of seismicity that developed during earlier phases of the same stimulation. Many occurred near the top of the reservoir, perhaps owing to heating and buoyancy effects. The occurrence of two relatively large events (2.9 and 2.7 ML) necessitated the reduction of sub-surface pressures by venting of GPK-2 at ~ 3.8 bbl/min.

(a)

(b)

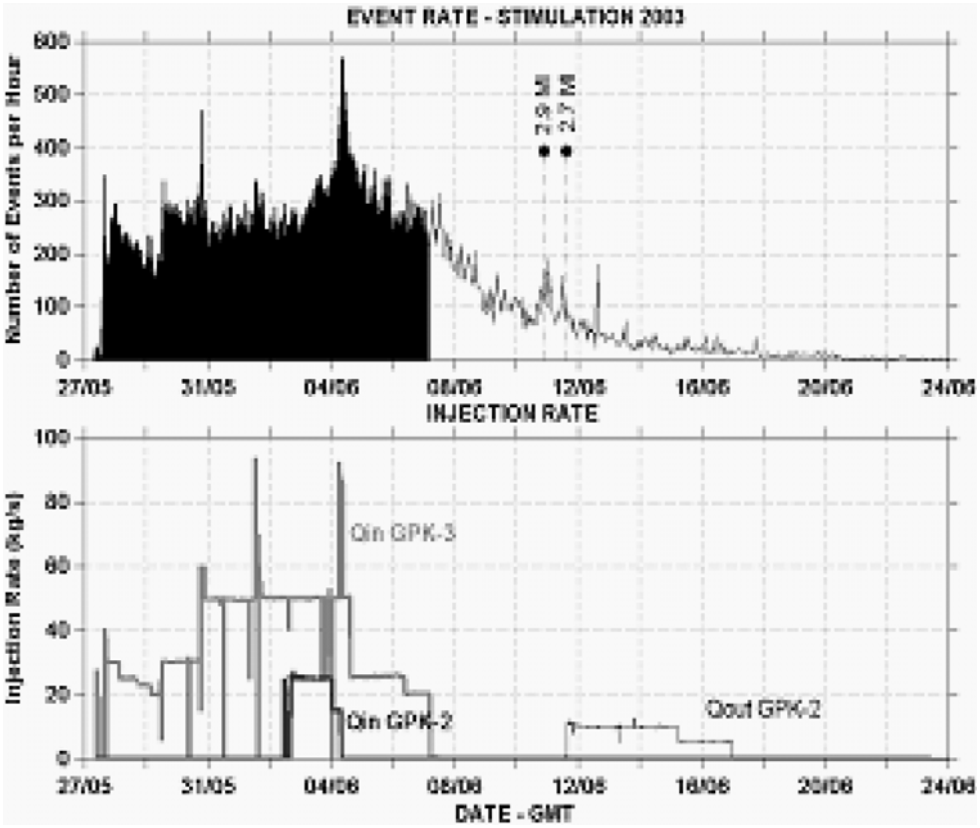

Figure 3.4: Stimulation of GPK-3 that was undertaken in four phases: (a) Avent rate, and (b) injection rate [*Baria et al.,* 2005a].

(a)

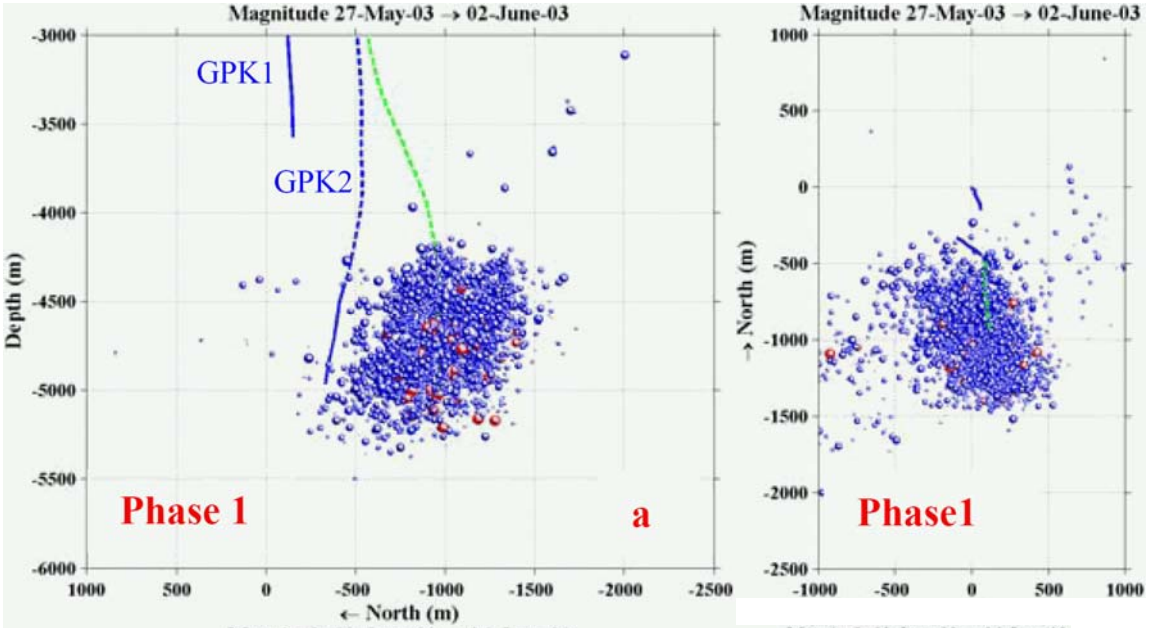
Magnitude 27-May-03 → 02-June-03
GPK1
GPK2
Depth (m)
-3000
-3500
-4000
-4500
-5000
-5500
-6000
Phase 1
a
1000
500
0
-500
-1000
-1500
-2000
-2500
← North (m)
Magnitude 27-May-03 → 02-June-03
→ North (m)
1000
500
0
-500
-1000
-1500
-2000
-2500
Phase1

(b)

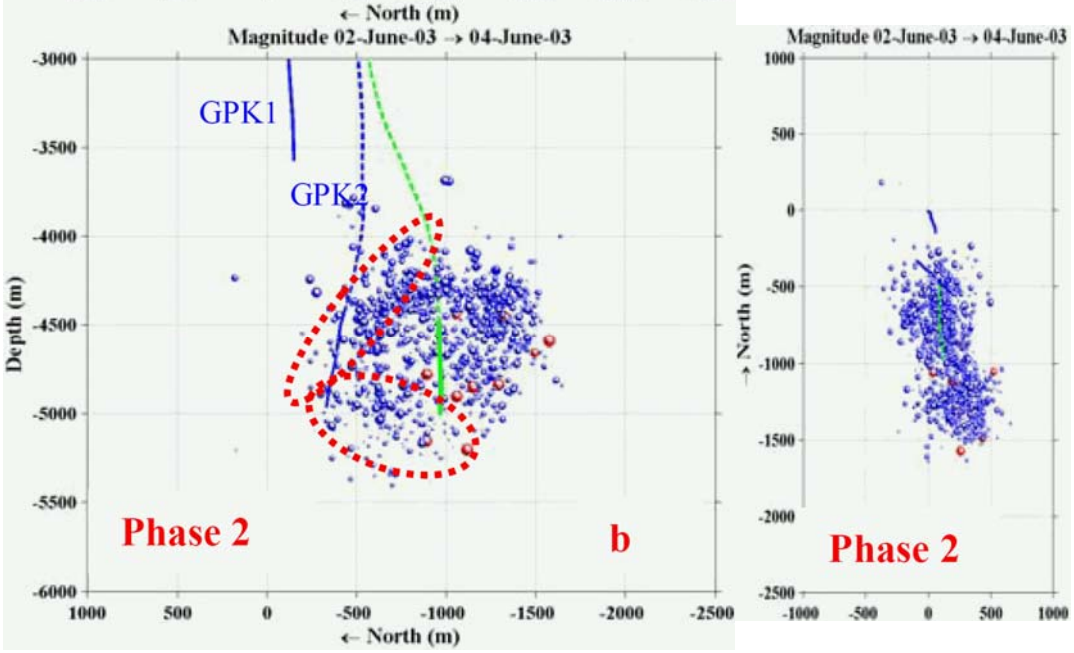
Magnitude 02-June-03 → 04-June-03
GPK1
GPK2
Depth (m)
-3000
-3500
-4000
-4500
-5000
-5500
-6000
Phase 2
b
1000
500
0
-500
-1000
-1500
-2000
-2500
← North (m)
Magnitude 02-June-03 → 04-June-03
→ North (m)
1000
500
0
-500
-1000
-1500
-2000
-2500
Phase 2

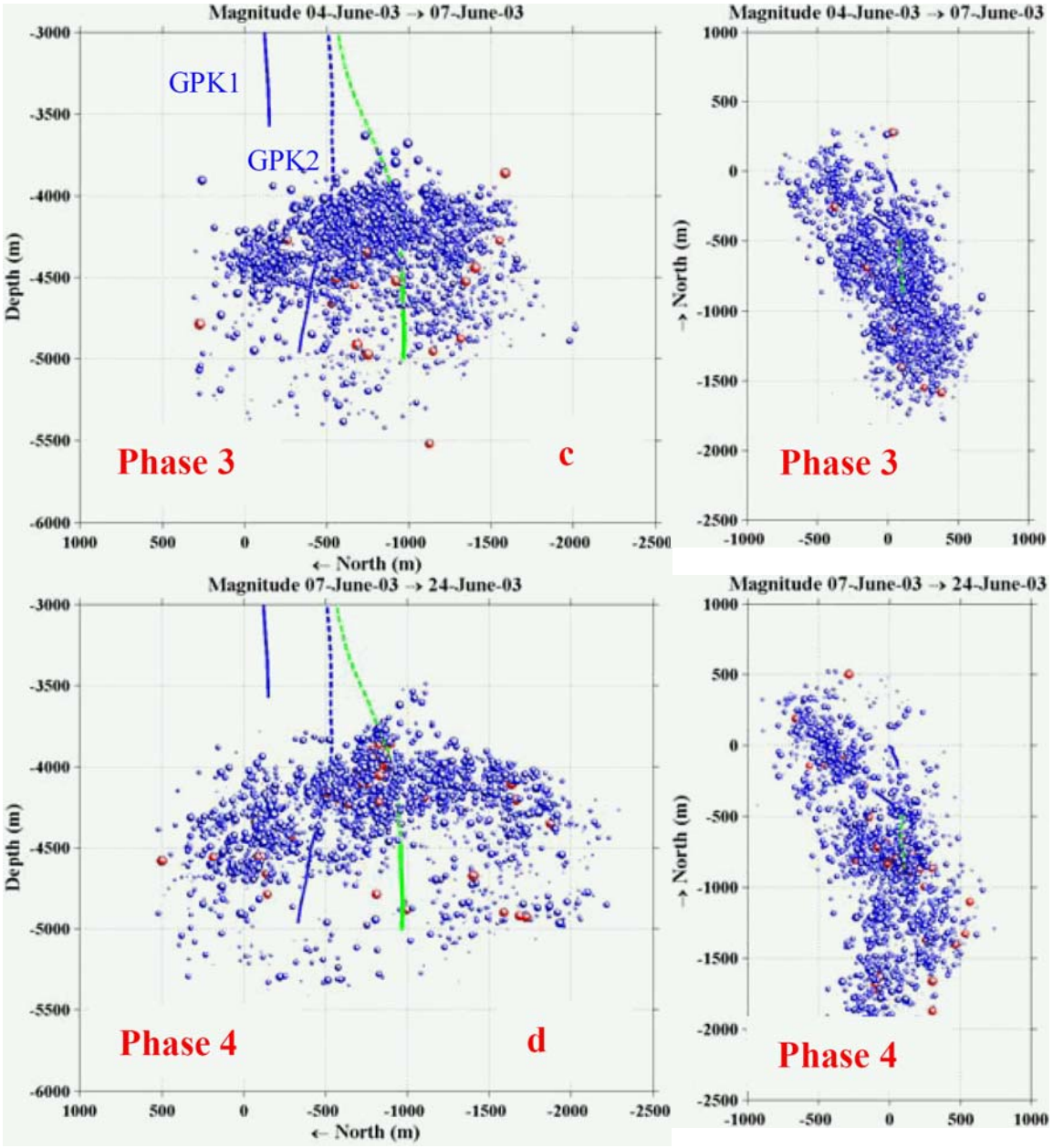

Figure 3.5: Vertical north to south sections through the seismic event distributions during the four stimulation phases of GPK-3: (a) Phase 1, (b) phase 2, (c) phase 3, and (d) phase 4 (event magnitudes: blue spheres M < 1.5, and red spheres: M ≥ 1.5) [*Baria et al.,* 2005a].

Post-stimulation circulation testing between wells GPK-2 and -3 indicated a productivity of 0.0260 bbl/min/psi for GPK-2 and an injectivity of 0.00781 bbl/min/psi for GPK-3. A total of ~ 314,500 bbl were injected into GPK-3 during the multi-phase stimulation [*Baria et al.,* 2005b].

Well GPK-4 was stimulated during a period of five days in September 2004. While this stimulation appears to have generated a significant seismically active volume, the overall injectivity is low. An acid stimulation in 2005 apparently did not appreciably improve this.

A consensus seems to be evolving that while GPK-2 has been stimulated sufficiently, this is not the case for either GPK-3 or GPK-4. The connection between GPK-3 (injector) and -2 (producer) is better than that between GPK-3 and -4. The

operational result would be an unbalanced system. Additional stimulation (perhaps another focused stimulation, or the use of viscous gels or higher flow rates than used previously at Soultz) appears likely [*Baria et al.,* 2005b].

In summarizing the results of EGS stimulations to date, the activities in the Cooper Basin and at Soultz have not resulted in fracturing intact rock [*Karner,* 2005a; *Karner,* 2005b]. However, are rather opening optimally oriented pre-existing fabric. While the creation of new fractures in intact rock could be possible in extensional or strike-slip systems, compressional settings probably require the presence of a pre-existing fabric with bulk strength lower than that of the intact reservoir rock.

It is clear that the stimulations at Soultz and Cooper Basin, and those likely to take place at Coso and Desert Peak, involve large volumes of mostly slickwater. Proppants have not been used but could be needed to increase near-well permeability, enabling a greater overall volume of rock to be stimulated. The only diversion techniques that have been used are high-density brines (at Soultz) and the emplacement of salt pills (at Cooper Basin). Experience from Fenton Hill and other early stimulation work [*Entingh,* 2000] demonstrates that typical oil field approaches (e.g., fracturing through perforated casing) does not yield commercial results. One of the main reasons for this is the difference in the energy content of the produced fluid. However, recent advances in diversion and fracturing techniques used in hydrocarbon reservoir offer some utility in EGS development.

3.1.3 Barnett Shale

The Barnett Shale is a marine shelf deposit of Mississippian age that lies unconformably on the Ordovician Viola Limestone and the laminated shales and sands of the Ellenburger Group. It is overlain conformably by the Pennsylvanian Marble Falls Limestone. The type log, displayed in Figure 8.2 on page 103, displays effective height growth barriers above the Barnett Shale (i.e., Barnett and Marble Falls Limestones) and below the Barnett Shale (i.e., Viola Limestone). This generally results in created hydraulic fractures that are effectively confined to the Barnett Shale. The depth to the top of the Barnett Shale in the core area varies from 6,800 to 9,000 ft. The thickness of the Barnett Shale ranges from 200 to 800 ft and from 300 to 500 ft in the core area. The productive formation is typically described as black, organic-rich shale composed of fine grained, non-siliciclastic rocks. Its very low permeability ranges from 7×10^{-5} to 5×10^{-4} mD. It is believed to be its own source rock, and it is over-pressured. The dominant hydraulic fracture orientation is NE-SW. The minimum horizontal stress is oriented NW-SE. An interesting phenomenon in the Barnett Shale is that natural fractures are prolific in a NW-SE orientation, roughly perpendicular to the preferred stress plane in which hydraulic fractures normally tend to grow. For detailed information, refer to section 8 on page 102.

Hydraulic Fracturing by use of Viscous Gels

Because of its very low permeability, the Barnett Shale needs to be effectively stimulated to obtain commercial production. Before 1998, most wells in the Barnett Shale were stimulated with hydraulic fracture treatments by use of one- to two-thousand barrels of crosslinked, gelled fluids (apparent viscosities of more than 1,000 cP) that carried significant amounts (often exceeding 100,000 lbm) of proppant (typically sand) up to relatively high proppant loadings of ~ 8,000 lbm/1,000 gal of gel. Most of these treatments did not yield sufficient productivity increases, because of the very low permeability of the shale and the inability to clean up efficiently the damage from gel residue with the proppant pack of the created hydraulic fractures. Conventional propped hydraulic fracturing may also not yield the desired results for EGS for the same reason, and for the additional reason that single, propped fractures does not provide sufficient heat transfer area to heat sufficiently the fluids that pass through them in the EGS circulation loop.

Hydraulic Fracturing by use of Water

In 1998, the application of water-based, low-viscosity (e.g., ≤ 10 cP), low-proppant-loading (up to 0.5 to 1.0 lbm/gal) hydraulic fracturing stimulation was gaining new acceptance and was successfully used to stimulate the Cotton Valley Sandstone [*Mayerhofer et al.,* 1997]. Since then, water fracturing has been widely used in various fields including the Barnett Shale. In addition to the changes from high- to low-viscosity fluids and overall reduction of proppant loading, typical treatment sizes increased from ~ 1,000 bbl to much greater treatment sizes of ~ 30,000 bbl to date. For detailed information, refer to section 8.3 on page 119.

These three fracture treatment changes are believed to cause the following changes relative to hydraulic fracture treatments by use of viscous gels:

1) Increase of the fracture-to-reservoir contact area. The thinner fluid can penetrate more easily from the initially created hydraulic fracture into the existing natural fractures, thus encouraging the creation of a complex fracture network. The greater treatment volume results in deeper penetration of the fracturing slurry into the reservoir.
2) Minimization of the damage to the proppant pack inside the hydraulic fractures associated with gel residue. High-viscosity gels may sometimes not effectively break into low viscosity fluids after the hydraulic fracture stimulation is completed, making it impossible to flow this residue back to the well during the initial oil or gas production following the fracture stimulation treatment. A primary cause is that water leakoff into the matrix concentrates the polymer level in the fracture, often increasing the concentration from 20 to 40 lbm/1,000 gal to more than 300 lbm/1,000 gal. This gel residue can permanently impair the permeability of the created proppant pack. Low-viscosity fluids (used in water fractures) do not contain these potentially damaging levels of polymers.
3) Creation of a fracture conductivity that is adequate for the ultra-low permeability of the Barnett Shale. In earlier fracture stimulation treatments where high proppant loadings were pumped as part of smaller slurry volumes, shorter but wider fracture were created, with actual fracture conductivity far exceeding the minimum required conductivity to prevent the created hydraulic fracture from being the bottleneck of production response. Approximately the same amount of proppant is used in the newer treatment. However, this proppant is distributed in a far greater slurry volume. This creates longer but narrower fractures, and the created hydraulic fracture width is still adequate to prevent the created hydraulic fracture from being the bottleneck of production response.

These three effects contribute to increased post-stimulation productivity.

Summarizing, the results of water fracturing in the Barnett Shale and other tight oil or gas reservoirs (e.g., the Cotton Valley Sandstone) indicate that, compared to conventional propped fracturing, this stimulation technique allows for the creation of longer and wider networks of fractures with less formation damage at lower cost. Materials costs are less but pumping costs are probably greater because of the longer period of the treatments. In contrast to oilfield stimulations, the application of sand as a proppant at the elevated temperatures in EGS reservoirs (especially when exceeding 300°F) is not feasible because of the significant and rapid reduction of the proppant permeability and conductivity due to stress corrosion cracking. Instead, ceramic proppants would be the only material that would withstand the conditions of EGS. Because experience in the Barnett Shale demonstrates that relatively small amounts of proppant can be sufficient for water fracturing in ultra-low permeability formations, the use of ceramic proppant could still be economically feasible in an EGS development. It is possible that the rock type (i.e., shale in the case of the Barnett Shale) dictates the need for proppant, or that shearing which might result in self-propped fractures is not the near well mechanism in the Barnett, such that proppant is needed.

Since:

1) an EGS development will either involve water circulation or cyclic water injection,
2) the viscosity of water is much (i.e., a factor of more than 10) greater than that of Barnett gas,
3) flow rates of a general geothermal well are very high (i.e., 1,000's of bbl/d) to get a reasonable amount of energy production, and
4) with wellbore drawdown, multiple-phase flow (i.e., steam and water) is likely.

Consequently, it seems likely that significantly higher fracture conductivity will be required in EGS compared to the Barnett Shale. This is discussed later in this chapter. To provide sufficient conductivity, perhaps simply changing the proppant to ceramic may suffice. However, perhaps the treatment design strategy may need to be dramatically changed (i.e., the use of conventional fracturing fluid and high proppant loadings).

Horizontal Wells

As for many other oil and gas reservoirs, in some areas of the Barnett Shale, horizontal wells have been drilled recently to optimize the production of gas. Horizontal wells can:

1) minimize the required surface development locations,
2) maximize the volume and surface area of a semi-horizontal network of fractures (e.g., those developing in the Barnett Shale), and
3) produce the field effectively with fewer (vertical) wells.

Although horizontal wells are not used in geothermal so far, the practice of drilling several deviated wells from a single pad is quite common in areas of rugged terrain (e.g., at The Geysers).

When multiple hydraulic fracture stimulation treatments are desired in a horizontal well, it used to be common in the oil and gas industry to case and cement the entire horizontal section of the well, so that there would be control of fluid diversions through perforated intervals that would be shot after setting and cementing the casing. Recently, however, the oil and gas industry has been experimenting with the use of uncemented slotted or perforated liner along the entire horizontal portion of the well [*Minner et al.,* 2003]. Although this can result in a loss of control over fluid diversion, the associated cost saving can be significant. Both the uncemented and the cemented horizontal well completions strategy have been tested in the Barnett Shale, and as the uncemented case is very similar to open-hole completions that are often used in EGS, it makes this case more suitable as an oilfield EGS equivalent. Liners are used in geothermal wells in locations where the formation could be unstable. Open-hole completions are probably more common. In a geothermal well, liners can potentiallyhave the problem of the frictional pressure drop through the slots. A geothermal well needs a far greater flow rate than an oil or gas well due to the far lower energy content of the produced fluid.

One consideration in the placement of the horizontal well trajectory is its orientation with respect to the least principal stress direction. A horizontal well that is drilled in the direction of the maximum stress is sometimes preferable in certain oil or gas reservoirs, because this enables the creation of wider, more conductive fractures parallel with the horizontal lateral and because it is generally easier to transport proppant through the favorable well-to-fracture connection area near the horizontal well. Most horizontal wells, however, are drilled in the direction of the least principal stress, as the resulting transverse hydraulic fractures cut across the well, and each separate stimulation stage simulates a single vertical well (with converging flow into a point source perforation interval). This would be more analogous to the EGS case and even the conventional geothermal case, where maximizing fracture intersections would be important. However, the overall system probably develops in the direction of the maximum horizontal stress. It is desirable to drain as much of the stimulated zone as possible. Then, the orientation or layout of the doublet or triplet (i.e., one injector and two producers) would probably be in the direction of $\sigma_{H,max}$, unless it is situation similar to Cooper Basin (i.e., $\sigma_{H,min}$ is vertical) which would impose far less constraints on system orientation and layout.

For effective stimulation of the production in oil or gas reservoirs, hydraulic fracturing from horizontal wells raises the following issues:
1) Cemented versus un-cemented horizontal section;
2) single stimulation stage versus multiple stimulation stages;
3) diversion and effective coverage of multiple stages along a un-cemented and a cemented lateral;
4) hydraulic fracturing of the adjacent target layers above or below the horizontal well when the well is placed in a particular layer;
5) orientation of the lateral relative to preferred hydraulic and natural fracture orientations; and
6) extent of the lateral.

Many of these issues can be evaluated through the combination of fracture mapping tools with fracture engineering and production correlations.

If vertical wells yield unsatisfactory productivity results, then the application of horizontal wells may be the solution. However, the benefits and disadvantages of horizontal wells associated with hydrocarbon production will also apply to EGS wells. To address the added complexities of horizontal well completions, a more thorough analysis of the stimulation results (e.g., via direct fracture diagnostics) is needed.

Diagnostics

Numerous diagnostic technologies that have been developed for various oil and gas reservoirs have been used for the Barnett Shale to evaluate the effectiveness of hydraulic fracture stimulation. These include real-data (net pressure) fracture modeling, production and well-test analysis, radioactive tracers, production logging, surface and downhole tilt mapping, and microseismic mapping [*Barree et al.,* 2002; *Cipolla and Wright,* 2002; *Warpinski et al.,* 2001; *Wright et al.,* 1999; *Wright et al.,* 1998a].

Most of the recent hydraulic fracturing treatments have been mapped with microseismic and tiltmeters in the core area of the Barnett Shale to understand the geometry of the created fractures. The obtained information is used to:
1) Determine the spacing and locations of the in-fill wells,
2) evaluate the impact of horizontal well lateral orientation
3) evaluate the designs of the stimulations,
4) determine the effectiveness of staging, and
5) test alternative techniques before their introduction in as-yet undeveloped parts of the reservoirs.

In addition, surface tilt mapping of hydraulic fractures is very valuable for horizontal completions, because they can measure the orientations of fractures, and determine the distribution of the volume of slurry along the lateral [*Minner et al.,* 2003].

The experience gained in the Barnett Shale and other stimulated hydrocarbon reservoir with fracture diagnostics, particularly (real-time) fracture mapping, can be directly applied to monitoring hydraulic stimulations in EGS development. Tiltmetering in EGS would provide the equivalent of the slurry volume distribution (i.e., an estimate of the hydraulically active reservoir). This needs to be combined with seismic mapping to determine shearing versus hydraulically relevant fracturing. There is not sufficient information on this yet in EGS. It is generally assumed that where shearing occurs the fractures are hydraulically connected. However, the degree of connection is not always adequate. In the last well at Soultz (GPK 4), the well was sited within the seismic cloud but was not as well connected to the injection well (GPK 3) as the other well of the triplet (GPK 2), which resulted in an unbalanced system. It is possible that tiltmetering would have told them to do the stimulation differently.

Results for Vertical Wells

In the Barnett Shale, the hydraulic fracture stimulation of a vertical well typically results in extremely complex networks of fractures [*Fisher et al.,* 2002]. These large networks of fractures typically have an extent of 1 mi and a width of 500 to 1,200 ft. These networks exist because the hydraulic fractures that grow in the NE-SW direction crosscut the natural fractures that are oriented in the NW-SE direction, and open them up. These natural fractures represent a significant part (i.e., 20 to 60%) of the total created volume of the network of fractures. Such complex fracturing and the creation of such large networks is relatively uncommon in most oil and gas reservoirs, and has only been observed to a lesser extent (i.e., with narrower networks) in a few locations other than the Barnett Shale (e.g., the Cotton Valley Sandstone).

The geometry of the induced hydraulic fractures is relatively predictable. However, the development of the network of fractures is quite variable as it forms from both induced hydraulic fractures and natural fractures that open during stimulation. The growth of the height of the hydraulically induced fractures is well contained within the target intervals. It is believed that adequate hydraulic fracture height containment is obtained through higher fracture closure stresses in the formations above and below the Barnett Shale, and because of the laminated nature of the shale, which causes a composite layering effect as the fracture grows vertically through the laminations. The recovery of gas and the drainage patterns are controlled by the total extent, width, and area of the networks of fractures, instead of the conventional half-length of the individual fractures.

These results indicate that it could be possible to create similar networks of fractures in naturally fractured EGS with a low permeability. If the target interval of the EGS is bounded by discontinuities of stress (e.g., different formations) and layer laminations, then it could be possible to create a network that is relatively well contained. Although EGS to date has focused on massive intrusive rocks, layered EGS target formations may exist in both the Salton Trough and the Basin and Range

geologic provinces, where temperature gradients are abnormally high and many conventional geothermal systems have been developed. EGS developments in these areas could be quite analogous to the experience in the Barnett Shale

Results for Horizontal Wells

In the Barnett Shale, the horizontal wells are often drilled in the NW-SE direction of the least principal stress. As a result, the networks of fractures are created transverse to the horizontal orientation of the wells. The initial sizes of the stimulations were designed to cover the same fracture pattern that would have been achieved with the drilling of multiple vertical wells over the same area. The horizontal lateral lengths are largely determined by the number of undrilled (vertical) locations that can be accessed. Because the density of vertical wells generally needs to be high (30 to 50 acre well spacing), the horizontal wells with their associated induced hydraulic fracture network may replace the induced hydraulic fracture network of two to three vertical wells. To achieve this reduction in drilling in the Barnett Shale, horizontal wells require a lateral length of 2,000 to 3,000 feet.

Several techniques for the diversion of fluid flow were used to divert effectively slurry flow over the entire lateral section:
1) Multiple fracture stimulation treatments (one per perforation cluster) in cemented horizontal wells;
2) single fracture stimulation treatments into multiple perforation clusters in uncemented horizontal wells;
3) multiple fracture stimulation treatments into multiple perforation clusters separated by setting sand plugs within the uncemented horizontal well.

Stress shadowing, the perturbation of the stress field by the presence of nearby fractures that develop during hydraulic fracture stimulation, can have an impact on the way the fracture network develops. In horizontal well treatment programs, stress shadows have two major impacts:
1) Increased compressive stress near a fracture tends to close-off or inhibit the initiation of nearby parallel fractures, providing a natural diversion mechanism along the well. If perforation clusters or fracture initiation points are too close together, then stress shadows tend to inhibit fracture growth along the mid-section of horizontal wells and encourage fracture growth at the heel and toe of wells.
2) An increase in the local minimum stress magnitude tends to encourage fracture growth in orthogonal directions. Even in fields where fracture orientation in vertical wells is relatively uniform, stress shadow effects often induce orthogonal fracture growth when stimulating long intervals in horizontal wells.

If managed properly, then stress shadowing can prove beneficial in creating the kinds of fractured networks that are required to drain effectively the Barnett Shale. Because of the phenomenon of stress shadowing, one or two clusters of perforation are preferred to three or more.

Greater volumes of injected fracturing fluid do not necessarily increase the extent of the network of fractures and the productivity of the wells. The growth of orthogonal vertical fractures (i.e., fracture networks) occurs even in vertical wells in the Barnett Shale because of a low in-situ horizontal deviatoric stress and the presence of natural fractures orthogonal to the current maximum stress direction (NE-SW).

For a typical single-stage stimulation from an uncemented horizontal in the Barnett Shale, the four networks of fractures have a length of 2,000 ft and a width of 500 ft at each location, which is shorter and narrower, respectively, than an average network resulting from the stimulation of a typical vertical well. However, their cumulative width is 2,000 ft, which is nearly the same as the length of the lateral of 2,400 ft. If the entire lateral were completely stimulated, then this would be expected. The location of the fractures is not strongly correlated to the location of the clusters of perforations. That is, the fracture network grows where in-situ conditions along the horizontal lateral dictate, and not exactly where the perforations are shot along the uncemented liner.

The second stage of a two-stage stimulation from an uncemented horizontal well in the Lower Barnett Shale is diverted sufficiently up-hole (toward the kick-off point or heel of the well) and away from the first stage to effectively cover the entire length of the lateral. The height of the fracture network was effectively confined to the Barnett Shale interval only.

From the cumulative frequency for all 23 horizontal wells plus seven vertical wells in the Barnett Shale, it is evident that the horizontal wells outperform their vertical neighbors by a factor of 2 to 3 during the first 180 days of production. It is also evident from the distribution that a significant group of the uncemented horizontal wells outperformed the cemented wells in this same area.

From the correlation between post-stimulation production rates and the gross contact volume in the reservoir, it is evident that the gross volume of the fractured reservoir is defined as the product of the average fracture length, the cumulative network width, and the fracture height. Evidently, the total volume of reservoir in contact with the fracture network is immense, and the increase by a factor of 2 to 3 in production in horizontal wells in comparison to vertical wells is most likely because of the increase in gross reservoir contact volume. A typical reservoir volume of 2.2×10^9 ft^3 equates to more than 50,500 acre-ft of reservoir potentially in contact with a fracture system on a single horizontal well.

Consequently, to stimulate EGS, drilling horizontal wells in the direction of the least principal stress with transverse hydraulic fractures could be beneficial and cost-effective, compared to vertical wells. However, while this is effective at draining a large volume of the hydrocarbon reservoir, this is complicated by the temperature effect in EGS. In addition to the requirement of draining the area, this needs to be accomplished sufficiently slow or through a sufficiently large volume to transfer adequately the heat to the fluid. Similar to oil and gas field applications, uncemented (in contrast to cemented) wells with single or double clusters of perforations are believed to be preferable for EGS.

Notably, the extent of the network of fractures and the productivity of the wells may not necessarily increase with greater volumes of injected fracturing fluid. At Soultz, a point of diminishing returns with volume was reached, and the pumping costs become significant (e.g., the simulation of the dual or focused stimulation [*Baria et al.,* 2005b]). It appears that most of the volume is stimulated after approximately one day, and then the increase in stimulated volume becomes progressively smaller with each additional day. It is indeed possible that the cumulative width of the networks can approach the length of the lateral. However, as the uncemented liner really acts as an open-hole well with regard to fluid diversion, it is possible to initiate a hydraulic fracture system anywhere, not just at the location of the perforated intervals. As there is no reliable control of fluid diversion, some areas along the horizontal lateral may remain unstimulated. To eliminate these unstimulated areas, conducting multiple stimulation treatment stages could be required. As an EGS analogy, perhaps it would be possible to set casing and stimulate the well, then drill ahead and stimulate the well again, perhaps starting with heavy brine the second time to divert the focus to the deeper zone. Local multiple-stage stimulations of uncemented laterals have involved perforating and fracturing the deepest portion, then set the bridge plug in the lateral and perforate and fracture the upper interval. This strategy relies on the distance between stages to inhibit growth of the fracture of the second stage in the interval of the first stage.

Conclusions

In the Barnett Shale, extensive mapping of hydraulic stimulations demonstrates that hydraulic fractures grow in a complex network because of their interaction with pre-existing, natural fractures. The creation of such networks is expected to be highly beneficial for EGS reservoirs, because of their extensive volume and surface areas. For EGS reservoirs that are well bounded by neighboring layers with a higher fracture closure stress or by significant composite layering effects, it is expected that the fractures will be well contained within the target interval. The total length and surface area of the network of fractures, instead of the length of the individual fractures, is expected to control the overall fluid flow patterns in EGS.

From many hydraulic fracture stimulations of oilfield reservoirs, in particular the Barnett Shale, it is likely that fracture mapping can provide valuable insight into the geometry of the network of fractures. This is accepted practice in EGS, although the number of projects is still small. This technique can also be used for real-time modification of the design of hydraulic stimulations.

Similar to the Barnett Shale, water fracturing in EGS is expected to result in lower fracture conductivity than from conventional propped fracturing. However, the treatment cost will be significantly lower, and such treatments likely result in a greater extension of the fractures and an easier clean up of the viscous fracturing fluids (i.e., gels). Although the

application of gels in EGS is generally not considered due to the elevated temperatures, perhaps the use of viscous fracturing fluids should still be considered.

While vertical wells may yield satisfactory results, the application of uncemented horizontal wells may have benefits for EGS: As in oil or gas reservoirs, horizontal EGS wells would alleviate the problem of inadequate locations at the surface, and maximize the lateral extent of the network of fractures. An interesting (albeit costly) concept is to combine the two technologies by stimulating horizontal injection and production wells to obtain a sufficiently large network.

Summarizing, the lessons learned from the vast amount of information that has been collected from the Barnett Shale can contribute to the development of hydraulic stimulations in EGS. In addition to determining the state of stress and the mechanical properties of the potential reservoir rock, it important to determine the density, geometry and connectivity of pre-existing networks of natural fractures, and the existence of bounding layers. This information can then contribute to the design and locations of the wells, and the design of the stimulation itself.

3.2 Relevant Fracture Growth Physics in EGS Applications

FracproPT (FPPT) by Pinnacle Technologies, Inc. is the world's leading fracture analysis system. It is used by more than 1,000 engineers in the oil and gas industry (including corporate licenses for companies such as Anadarko, BJ Services, ChevronTexaco, and Halliburton) for fracture treatment design, analysis, and post-fracture evaluation. Oilfield fracture models, e.g., FPPT, have the capability to approximate fracture growth in a complex network. They have been used to develop calibrated fracture growth models for environments that are similar to the Barnett Shale. A methodology must be developed to account for some of the fracture growth physics in EGS applications and the longer time scale associated with EGS applications in comparison to the fracture treatments (i.e., modeling longer-term impact on fracture growth). As part of this project, we developed:

1) A two-dimensional (2D) fracture-reservoir heat transfer algorithm, by extending the existing one-dimensional (1D) heat transfer algorithms for heat transfer between the fracture and the reservoir near the fracture face (section 9.12.1 on page 173); this addition is necessary to account for the longer time scale associated with EGS applications, thus requiring the modeling of heat transfer in both horizontal directions, not just in a direction perpendicular to the fracture plane;
2) a 2D leakoff algorithm, by extending the existing 1D leakoff algorithms for leakoff from the hydraulic fracture system into the reservoir (section 9.12.2 on page 176);
3) an empirical model for fracture growth orientation and fracture complexity from three-dimensional (3D) state-of-stress, rock mechanical characteristics, natural fracture orientation, and fracture treatment characteristics (section 9.12.3 on page 179);
4) an improved model of fracture closure stress changes (i.e., back stress) because of increases in reservoir pore pressure and reduction in reservoir temperature throughout fracture treatments (section 9.12.4 on page 181);
5) an improved pressure dependent-leakoff functionality, because in naturally fractured reservoirs, fluid leakoff from a main fracture can accelerate dramatically once the fracture pressure in the main fracture approaches the maximum horizontal stress because of the opening of fissures (section 9.12.5 on page 181); and
6) an approximate visualization of the fracture network in the reservoir in addition to the overall fracture geometry (section 9.12.5 on page 181).

3.3 Calibrated Fracture Models for EGS Applications

Pinnacle Technologies, Inc. has developed calibrated fracture growth models for many reservoirs, including the complex fracture growth processes that occur (e.g., in the Barnett Shale). These calibrated models have been developed by matching results from predictive fracture growth models (i.e., the FracproPT system by Pinnacle Technologies, Inc.) to both fracture treatment (i.e., pressure and injection rate) data records and direct far-field measurements of fracture dimensions (e.g., microseismic and tiltmeter fracture mapping). From the improved capabilities explained in project subtask 1b (section 3.2 on page 29), we derived a calibration that represents EGS applications as closely as possible utilizing oil-field analogies.

This section describes predictive hydraulic fracturing modeling (section 3.3.1 below), calibrated hydraulic fracturing modeling (section 3.3.2 on page 31), net pressure history matching (section 3.3.3 on page 31), fracture model calibration (section 3.3.4 on page 33), benefits and limitations of calibrated models (section 3.3.5 on page 36), and application of modeling to the Barnett Shale (section 3.3.6 on page 36).

3.3.1 Predictive Hydraulic Fracturing Modeling

Predictive modeling of fracture dimensions and the associated production stimulation has often been more an art than a science [*Weijers et al.,* 2005]. The first problem of fracture models is that the inputs for the model are typically not very well defined. The three most critical input parameters for fracture models, which are to be determined along the depth interval of interest, are generally:

1) The Young's modulus of the rock,
2) the permeability, and
3) the fracture closure stress.

These parameters greatly affect fracture height growth. However, these critical parameters are typically not measured. The problem of non-existent or poor input measurements can be addressed by conducting better measurement of these critical input parameters. However, this is neither easy nor affordable:

1) Young's modulus can be measured from core. However, the industry is now routinely measuring dynamic modulus by use of sonic logging tools, providing a reasonable input for this parameter.
2) The industry has also made advances in permeability measurements [*Mayerhofer and Economides,* 1997], obtaining better estimates of the permeability-height product by use of before- and after-closure fracture analysis.
3) The profile of closure stress across the fracture height remains a critical model input parameter that is generally not known very well. Attempts to measure the closure stress through dipole sonic interpretation are notoriously flawed [*Wright et al.,* 1998b], and the best method to determine fracture closure is to do a pump-in / shut-in. The fracture closure stress is now routinely measured in the pay interval by use of a breakdown injection / pressure decline before the main fracture treatment. However, this only provides a single average measurement in the breakdown interval. Our plan for Desert Peak is to use rock strength data and a sonic log to determine $\sigma_{H,min}$ all along the interval of interest for stimulation. It is only in joint industry-science projects that it is sometimes possible to measure the closure stress directly in layers outside the pay-zone. For fracture modeling on typical fracture treatments, it is hoped that educated estimates can be made about the closure stress in zones outside the pay through:
   a) dipole sonic measurements,
   b) the interpretation of reservoir pore pressure and depletion, and
   c) fracture model calibration to observed geometry results.

   However, significant uncertainties remain, and can significantly alter fracture growth in the model.

It is in these well-defined cases of these joint industry projects where the second problem associated with the use of fracture models becomes apparent. Even in cases where all the critical model input parameters have been measured directly, the physics of the model is often not consistent with what really happens. This is because all the mechanisms that are important in hydraulic fracture growth are still not known and understood, and what input parameters should be provided for these unknown mechanisms are certainly not understood. This shortcoming of models can be addressed by calibrating fracture models with direct fracture diagnostics. Although not all physical mechanisms that play a role in hydraulic fracture growth

could be completely understood, the data from tilt mapping and microseismic mapping can be used to empirically train the model. Even in the absence of a full understanding of the physics, a fracture design provided with a calibrated model can approximate what actually happens during a fracture treatment much more accurately than an empirical design could ever estimate.

3.3.2 Calibrated Hydraulic Fracturing Modeling

With the development of pseudo 3D fracture growth models in the early 1980s, the industry was very excited that there were finally models available that could reliably predict fracture growth [*Weijers et al.,* 2005. However, direct measurements [*Shlyapobersky et al.,* 1988] of levels of fracture pressure soon demonstrated that actual net pressures were much greater than predicted by any of these pseudo 3D models. In addition, these models predicted a significant sensitivity to fluid viscosity, which was not observed to that degree in these field measurements. Fracture growth predictions for these models generally demonstrated fractures contained to the pay-zone, as low net pressure did not permit fracture growth through barriers below and above the pay-zone.

As a direct result of this discrepancy between model and measurement of net pressure, new lumped parameter and full 3D models were developed with a more flexible approach to honor the message contained in these fracture pressure measurements. Assumptions about the physics of fracture growth were changed so the user could match the observed net pressure response with a model net pressure response. To account for higher net pressure and observed sensitivity to fluid viscosity, the following changes were made:

1) The incorporation of complex fracture growth (i.e., multiple hydraulic fractures), which results in competition between opening fractures; and
2) increased fracture growth resistance at the fracture tip caused by plastic deformation and creation of micro-fractures in the process zone.

Fracture growth predictions by use of these new models generally demonstrated significantly less confinement than previous models, and thus much shorter fracture half-length.

3.3.3 Net Pressure History Matching

About a handful of commercial fracture growth simulators are currently available, and most allow a stimulation engineer to history-match bottom-hole treatment data or observed net fracturing pressure with output from the model to match or just determine what occurred during a treatment [*Weijers et al.,* 2005]. This step can be performed after the treatment by use of various simulators, and a few allow matching to be performed while the treatment is being executed in real time.

Minimum Model Input Requirements

For many engineers it has become standard practice to use the same fracture model from treatment design to treatment execution onsite and post-fracture treatment analysis. As a first step, the modeler has to provide several minimum model inputs, including [*Weijers et al.,* 2005]:

1) mechanical rock properties
   a) Young's modulus profile (from core test or sonic log)
   b) closure stress profile (injection / decline data or sonic log)
   c) permeability, i.e., from pressure transient analysis (PTA) or injection / falloff analysis
2) well completion and perforations
3) treatment schedule, proppant and fluid characteristics
4) fracture treatment data
   a) anchor points from diagnostic injections for closure stress analysis (breakdown injection), leakoff calibration (fluid efficiency test or mini-fracture) and friction analysis (step down test)
   b) recorded pressure, slurry rate and proppant concentration
      i) surface (i.e., well head) pressure is sufficient for decline match
      ii) dead string (i.e., tubing or annulus with a packerless completion that is used to monitor bottom hole data) or bottom hole pressure gauge required for matching while pumping

The anchor points 4)a) (i.e., the now no longer uncertain parameters) obtained from these diagnostic injections are used to calibrate the fracture model in a simple sense. Closure stress 1)b) and leakoff behavior 1)c) for the pay-zone are thus determined and re-entered into the model.

Determining Observed Net Pressure

The first activity in net pressure analysis is to obtain the correct observed net pressure from measured data. Obtaining the correct observed net pressure from measured surface pressure revolves around [*Weijers et al.,* 2005]:

1) The service company measures the surface pressure throughout the treatment;
2) Hydrostatic head is calculated by knowing what is pumped into the well and what the individual densities of these components are;
3) Frictional components, comprising well friction (determined by service companies in flow loop tests), perforation friction and near-well friction (estimated by use of rate step down tests); and,
4) Fracture closure stress in the pay-zone is obtained from pressure decline analysis following a water or slickwater breakdown injection, which is essentially a mini-fracture.

When dealing with the uncertainty of high frictional components, the focus of net pressure history matching is generally on the shut-in decline periods where frictional components are zero.

The collection of anchor points is critical for fracture pressure analysis, and focus of this analysis is on the determination of fracture closure stress. Fracture closure is found by use of various methods that attempt to linearize leakoff behavior from a fracture (e.g., plotting pressure versus square-root time, G-function time [*Nolte,* 1979], and log-log diagnostic plots of pressure change).

Net Pressure Matching

Net pressure history matching is the activity of changing model inputs and assumptions to calculate a model net pressure that matches the observed net pressure response. Net pressure-history matching is still perceived as a very complex activity. However, when by use of a simple, systematic approach, the number of parameters that a user has to adjust to obtain a net pressure history match is limited to a handful. These matching parameters are general and do not pertain to any specific model. The reason that these parameters can be used as matching parameters is that their exact value is typically not known. However, the observed net pressure response can give us clues for their approximate value. A net pressure match can generally be obtained by matching both level (i.e., constant in time) and decline of net pressure by use of the following eight level and slope parameters. Level net pressure parameters include the following [*Weijers et al.,* 2005]:

1) Fracture complexity (or simultaneous propagation of multiple fractures): Numerous core-throughs and mine backs have demonstrated that multiple fracture growth is the rule rather than the exception [*Weijers et al.,* 2000]. Competition between multiple fractures increases net pressures, and needs to be accounted for in any fracture growth simulator.
2) Fracture tip effects, which reflect the resistance for fracture growth at the tip: Apart from matching higher net pressures, this parameter can also be used to change the sensitivity of net pressure to the apparent viscosity of the fluid that is being pumped. Increased fracture growth resistance at the fracture tip can be caused by plastic deformation and creation of micro-fractures in the process zone.
3) Closure stress contrast between pay and neighboring layers: Closure stress contrast is considered one of the classical fracture confinement mechanisms that is included in all industry models. The closure stress in layers outside the pay can be estimated by interpreting dipole sonic data and by evaluating parameters (e.g., Poisson's ratio and pore pressure depletion). If there is a significant contrast between closure stress in the pay-zone and the surrounding layers, then this increases the net fracturing pressures, because the fracture grows in a more confined manner.
4) Proppant drag: Fluid friction along the fracture (between well and fracture tip) increases as proppant is pumped, just as well friction increases when proppant-laden slurry is pumped following clean fluid. The exact increase in friction along the fracture face, however, is dependent on a multitude of parameters (including, e.g., fracture wall roughness). As these parameters are not known, a multiplier of the theoretical effect is used in net pressure matching.

5) Fracture compliance change during tip screen-out (TSO): This refers to treatments where proppant bridges at the fracture tip during the treatment, and the dehydrated proppant bank works its way back to the wellbore. The resulting change in fracture compliance needs to be accounted for as the fracture is packed with proppant back to the well. By changing this parameter in net pressure matching, how fracture length and height affect the width calculation can be controlled.

Slope or decline net pressure matching parameters include the following [*Weijers et al.,* 2005]:
1) Formation permeability: Leakoff from a slickwater injection can be matched by changing formation permeability. The estimated permeability is under elevated fracturing pressures, which could be higher than the one observed when producing the well.
2) Wallbuilding coefficient: This is a measure of the additional resistance to fluid leakoff from gel filter-cake. This filter cake builds up on the fracture walls during fluid leakoff. Once permeability is determined from a breakdown injection, leakoff from a crosslinked gel mini-fracture can be used to determine the wall-building coefficient.
3) Pressure-dependent leakoff: Once the permeability and leakoff coefficient are established, actual leakoff during a propped-fracture treatment can be higher than for a mini-fracture because of fissure opening at elevated fracturing pressures.

These eight general parameters are usually sufficient to create a net pressure history match for any fracture treatment. Once the model net pressure matches the observed net pressure, and the right assumptions are made in the model, it is hoped that the model reflects the nature of the fracture growth and that the fracture half-length and height have been estimated. Unfortunately, that hope is not often justified, as there are various shortcomings in the net pressure matching process:
1) Net pressure matching is an indirect diagnostic technique (i.e., the fracture geometry is inferred from net pressure and leakoff behavior); and
2) solutions are non-unique, such that careful and consistent application is required to obtain useful results.

The net pressure matching technique is therefore most useful when results are integrated or calibrated with results from other diagnostics (e.g., production and well test analysis data), and with direct fracture diagnostics (e.g., tilt and microseismic mapping data).

3.3.4 Fracture Model Calibration

To match both fracture geometry and net pressure response, it is determined first whether changes are necessary to the previously mentioned matching parameters *Weijers et al.,* 2005. The sensitivity to these parameters is explored by bringing them to their physical bound. For example, closure stress is brought to a bounding zone up to 1.0 to 1.1 psi/ft or a modulus is brought to the highest realistic value for the type of rock in an attempt to match the level of the observed net pressures.

In practice, this works as follows: Let us first consider the un-calibrated net pressure match in Figure 3.6 and its associated fracture geometry prediction in Figure 3.7a [*Weijers et al.,* 2005]. This geometry demonstrates significant out-of-zone growth. This match was conducted by use of the classical confinement mechanism of the contrast of the closure stress of the fractures. To match the high initial net pressures during the breakdown injection, significant tip effects were used. To match the increasing net pressure throughout most of the propped fracture treatment, it was assumed that increasing fracture growth complexity. Even though the barrier, pay-zone closure stress contrast is significant, it is lower than the 2,000 psi of net pressure observed during the propped fracture treatment. Therefore, this net pressure match results in significant out-of-zone growth with fracture half-length and total fracture height of ~ 250 ft.

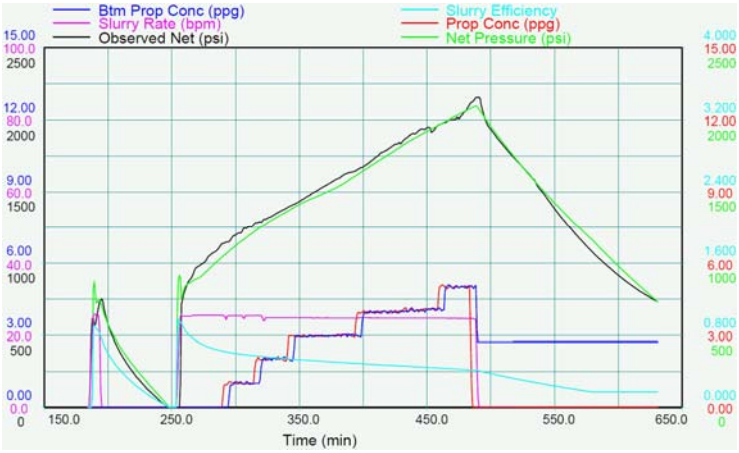

Figure 3.6: Observed net pressure (black) and match with model net pressure (green). The model net pressure response from the un-calibrated model and the calibrated model are almost identical [*Weijers et al.,* 2005].

(a)

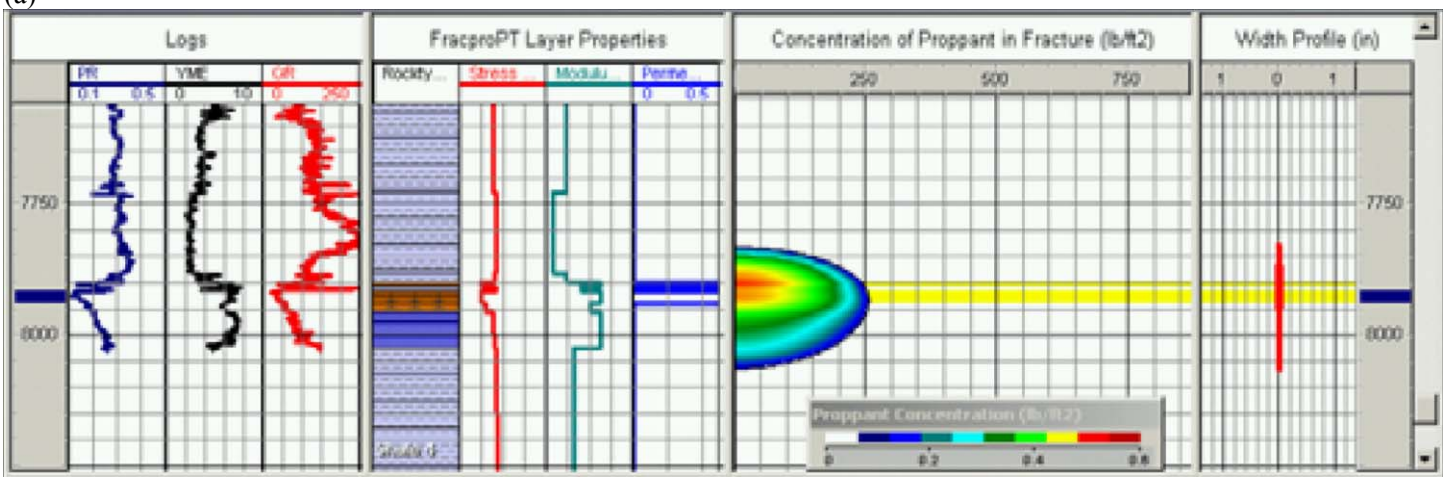

(b)

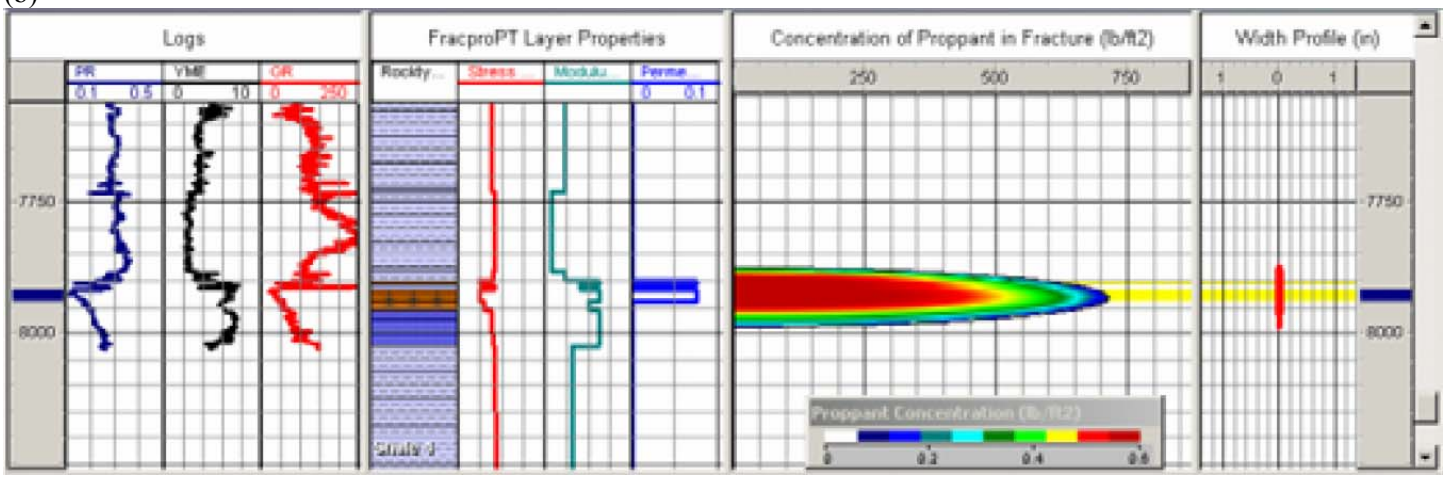

Figure 3.7: Estimated fracture geometry for net pressure history match: (a): classical model assumptions, and (b) matching of both net pressure history and directly observed fracture geometry by use of additional containment effects (e.g., composite layering) [*Weijers et al.,* 2005].

However, microseismic mapping demonstrated an actual fracture height of only 130 ft and a fracture half-length of 700 ft, which is very different from the un-calibrated pressure matching result. Net pressure history matching was repeated to match the directly observed geometry. First, it was determined that a closure stress gradient in excess of 1 psi/ft was required in the shales around the pay-zone to obtain the observed confinement, and this was considered unrealistic. Therefore, a composite layering effect was introduced to match the level of confinement observed. Additional confinement increases net pressures, and both tip effects and fracture complexity had to be reduced to maintain a net pressure match. As the fracture surface area in the pay-zone increased significantly, the reservoir permeability and wallbuilding coefficient had to be reduced to maintain a match of leakoff behavior. The final fracture geometry from the calibrated model is displayed in Figure 3.7b.

Once a calibrated model has been obtained by matching net pressure response and directly measured fracture dimensions, the fracture model can be executed in predictive mode to evaluate alternative designs. In this particular example, production data demonstrated that effective propped half-length was far shorter than the hydraulic fracture half-length of 700 ft, most likely because of insufficient cleanup farther away in the fracture. Significant cost savings have been achieved by pumping smaller treatments on subsequent jobs, reducing hydraulic fracture half-length while maintaining effective propped fracture half-length and production response.

3.3.5 Calibrated Model Benefits and Limitations

It was demonstrated that there are cases where current fracture growth modeling can provide accurate estimates of fracture geometry [*Weijers et al.,* 2005]. Classical mechanisms to confine fracture height growth (e.g., closure stress or permeability barriers), are incorporated in most models of fracture growth, and are sometimes sufficient to describe fracture growth behavior. However, there is not yet a lot of confidence in the ability to predict in which environments fracture growth is dictated by these classical mechanisms. Models today are more sophisticated than twenty years ago. However, often still do not accurately predict fracture growth. This is because of poor characterization of rock, reservoir, and geology, and an incomplete understanding of relevant physics.

Calibrated models have allowed us to narrow down the possible solutions for a fracture model and decrease the degrees of freedom to obtain a match. However, even the solution of a calibrated model is not necessarily unique, as values for other input parameters could be assumed that are not correct (in the absence of their measurement), and other model parameters may have to be over-corrected to obtain a calibrated match. This problem of not truly calibrating a model within reasonable bounds can be minimized by evaluating several basic measurements for fracture model input parameters and by conducting mapping on a series of treatments (as opposed to a single treatment). These basic measurements should include:

1) Fracture closure stress in pay-zone (from pressure decline analysis following a breakdown injection);
2) End-of-job slurry efficiency to determine fracture volume (from pressure decline behavior following the fracture treatment); and
3) Conduct a limited series of tests to determine bounding layers stresses. The industry needs to explore more methods to determine fracture closure in layers other than the pay-zone.

The model calibration that was described in this paper is empirical, by matching both observed net pressures and observed fracture geometries. Perhaps this empirical approach leads to improved physics in models. With time, it may then become possible to achieve the ultimate goal for a fracture modeler: A combined fracture, reservoir, and production model integrated with direct real-time fracture diagnostics.

Summarizing, it can be concluded that:

1) Direct diagnostic observations on more than 1,000 hydraulic fracture treatments have revealed the surprising complexity and variability of hydraulic fracturing;
2) fracture model calibration has proved both heartening and humbling. However, it clearly demonstrates how a fracture model can be adjusted to match most diagnostic results and the observed net pressure behavior;
3) fracture height confinement is in many cases more significant than earlier expected, and is most likely caused by layer interface effects; and
4) the physics of fracture growth along and through layer interfaces is not well understood and is not captured well in most current models.

These problems are also relevant when modeling EGS stimulations, since they are not only relevant for tensile fractures. However, they are also relevant for networks of smaller shear fractures. Consequently, the complexities of model matching would likely be comparable for EGS stimulations, except for a lack of data and experience.

3.3.6 Barnett Shale

A combination of mini-hydraulic fracturing analysis with step-down tests, fracture modeling, and post-hydraulic fracturing analysis of treatment and production data was applied for fracture engineering [*Fisher et al.,* 2002]. An investigation of the mapping results indicates that the initial well productivity was independent of the half-length of the fracture. However, there appears to be a correlation to the size and complexity of the created fracture network, as would be expected in EGS situations. Other production correlations that support this finding (i.e., that the complexity of the fracture was the primary driver for productivity) included:

1) The volume of the fracture for the NW component from surface tiltmeters (i.e., cross-cutting natural fractures),
2) the width of the fracture network (i.e., the width of the microseismic event cloud), and
3) the degree of the increase of the net pressure during the treatment.

One of the benefits of direct measurements of the fracture geometry is the ability to calibrate a fracture model. This results in an effective modeling tool for optimizing future designs of hydraulic fracturing treatments. While fracture diagnostics are critical for understanding how fractures grow, modeling is required to predict the performance of future designs and to evaluate design changes. The previously discussed measured fracture geometries were used to develop a calibrated model for the Barnett Shale in two different areas. A 3D fracture simulator was used to model the measured geometry of the fracture while incorporating the pressure, volume, and rates of the treatment. To achieve a match, several of the input calibration parameters or settings were adjusted from the default values. The final calibrated model settings can now be used for predicting growth in single zone treatments, and is reasonable for application in the combination treatments.

The net pressure was history matched for each fracturing treatment. An example of the net pressure match for a single zone (i.e., Lower Barnett Shale fracturing treatment) is displayed in Figure 3.8. The model matches the magnitude and character of the net pressure throughout the treatment. The modeled geometry of the fracture is displayed in Figure 3.9. As is evident from the tiltmeter and microseismic mapping measurements, the fracture is fairly well contained to the Lower Barnett Shale. It does not grow up into the Upper Barnett Shale.

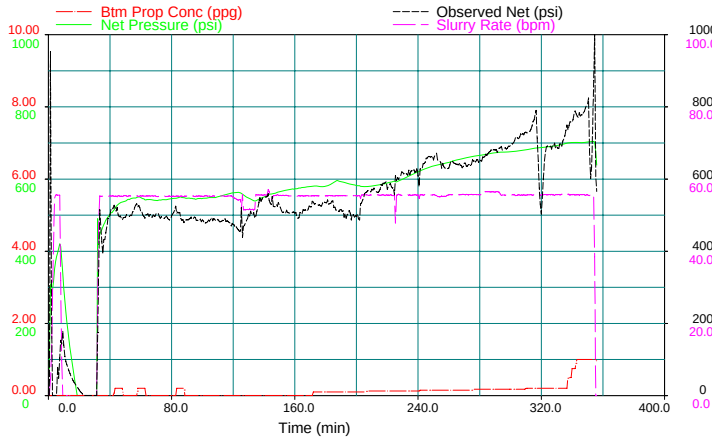

Figure 3.8: Net pressure match from Lower Barnett Shale treatment [*Fisher et al.,* 2002].

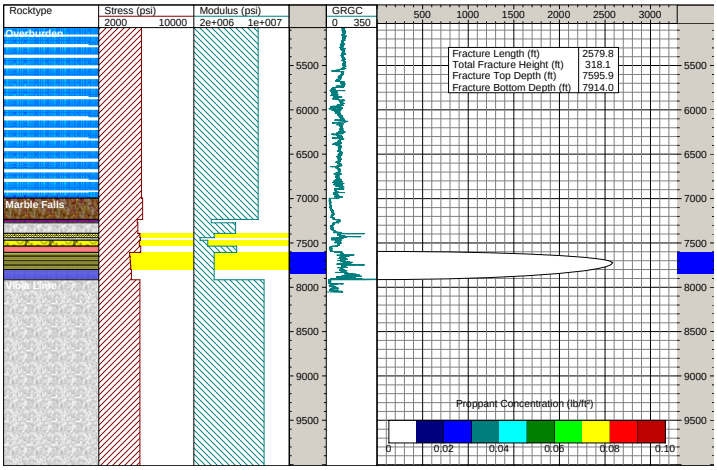

Figure 3.9: 3D fracture model output by use of measured fracture dimensions, treatment parameters, and net pressure matching [*Fisher et al.,* 2002].

The settings developed for the calibrated model match the single-zone Upper Barnett Shale and Lower Barnett Shale treatments very well, especially for the half-lengths of the fracture. It is more difficult to model the combination of hydraulic fracturing treatments in both the upper and lower zones, because of the differences in closure pressure and changing fluid split rates. However, the model still works reasonably well for the combination hydraulic fracturing treatments.

3.4 Sensitivity Study for Stimulation Treatment Design Test

Once the EGS calibration has been developed, it will be possible to design a fracture treatment that is optimized for its ability to maximize contact to a large reservoir volume. By use of the calibrated fracture growth model, the means by which controllable fracture treatment parameters change the fracture length and network width can be evaluated. The impact of completion parameters discussed in project task 2 (section 4 on page 50) can also be determined. However, because project subtasks 3b and 3c (section 5.2 on page 86) were cancelled, this sensitivity study was not performed. Instead, an analysis of production modeling versus microseismic mapping results was performed.

3.4.1 Integration of Microseismic Mapping and Production Modeling

For a vertical well in the Barnett Shale, a history match of production is performed [*Mayerhofer et al.,* 2006]. Results from microseismic mapping were used directly to approximate a fracture network in a reservoir simulator. This resulted in an estimate of the effective length of the fracture network. This real field case is followed by a parametric study for a horizontal well that investigates the impact on production of various parameters of the fracture network.

Vertical Well

A numerical reservoir simulator for black oil was used to approximate the effective geometry of a fracture network of a single vertical well. The well was hydraulically fractured with a large treatment using light sand. The created fractures are modeled as a discrete network of linear segments in both principal fracture directions (NE-SW and NW-SE). The conductivity of the fractures was given by the product of width and permeability of the fracture blocks. The simulations did not include:

1) Clean up of the fracturing fluid,
2) water production, and
3) gas desorption.

The well used in this example is a vertical well located in the core area of the Barnett Shale. This well was fracture treated and mapped in 2001. Microseismic mapping clearly illustrates that very large fracture networks are generated. The pre-dominate azimuth of the hydraulic fractures is in the NE direction. A secondary component is oriented orthogonal to that direction. It is unknown how much of the generated network is actually effective during production. The results from microseismic mapping are displayed in Figure 3.10. The fracture network has a total extent of more than 2,700 ft, with apparent asymmetric growth to the SW. The NE wing of the network structure did not develop as effectively, based on the observed microseismic events. The observation well was in a position that should have detected growth on the NE side. The width of the network of ~ 350 ft is small in this case, and the height of the network demonstrates adequate coverage of the Lower Barnett interval. The Upper Barnett was also stimulated in this well. This stimulation displayed a smaller network structure. The network structure (shown as red lines in Figure 3.10) represents the effective network modeled in the reservoir simulator as an approximation of the microseismic results. This is the final structure of the network, which was used to match the history of the production of the well. This final structure is a result of several iterations that explored alternate answers. Once the permeability of the matrix is fixed, the resulting total effective length (i.e., the sum of all open segments) and conductivity of the network are unique.

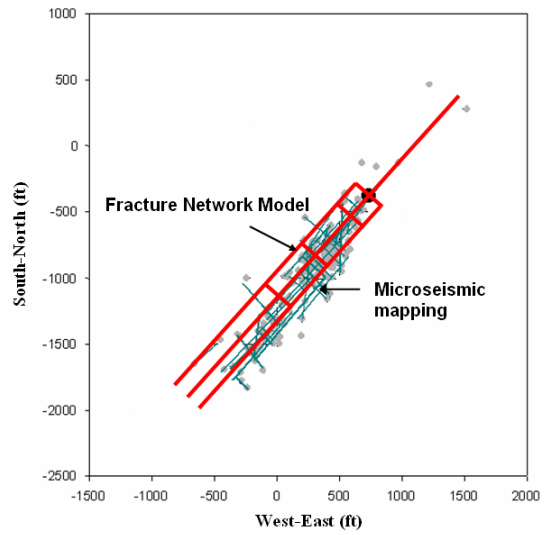

Figure 3.10: Fracture network as determined from microseismic mapping which is approximated with a numerical network model (overlayed as red lines) [*Mayerhofer et al.,* 2006].

The reservoir input parameters used in the simulation are displayed in Table 3.2. Three parameters were varied to obtain the history match for the:

1) Fracture length,
2) fracture density, and
3) fracture conductivity.

Table 3.2: Reservoir parameters for the vertical well.

parameter	units	value
depth	ft	7,000
net thickness	ft	415
porosity	%	6
water saturation	%	30
initial pressure	psi	3,800
temperature	°F	180
gas gravity	-	0.6

The actual gas rate was used as a constraint, as displayed in Figure 3.11. The total well history includes four years of production.

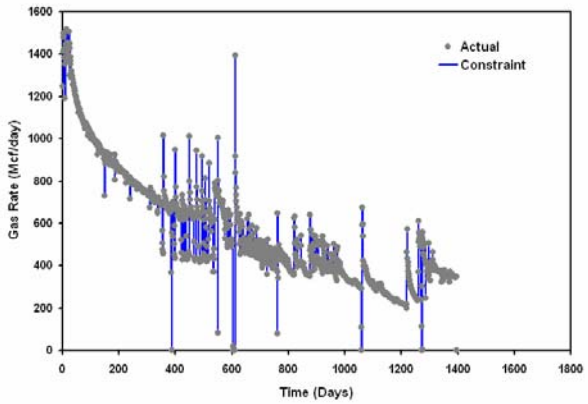

Figure 3.11: Gas flow rate versus time, which was used as a constraint for production modeling [*Mayerhofer et al.,* 2006].

The history match of flowing tubing and casing pressures versus time is displayed in Figure 3.12. The model predicts higher wellhead flowing pressures in late time, which track the surface annulus pressure (i.e., open-ended tubing), and represents liquid loading. The loading condition was confirmed by higher flow rates after foam clean out. Although this match is not entirely unique, the effective total fracture network length (i.e., the sum of all fracture segments open to flow in the two principal fracturing directions) is ~ 6,000 to 7,800 ft with an average conductivity of 4 mD-ft. The permeability of the matrix was fixed at 0.0001 mD or 100 nD, which was estimated from core tests. The effective network width was modeled to be 180 ft (90 ft fracture spacing in the NE direction and four orthogonal stringers) with a network extent of ~ 2,000 ft in the SW direction. While the total effective network length (i.e., the sum of all open segments) must fall within the range of 6,000 to 7,800 ft, the aspect ratio of effective network extent to width could vary to some degree. An alternate match, which would also be within the microseismically mapped network area, was achieved with a network with a width of 360 ft (i.e., 180 ft fracture spacing) and shorter extent of 1,300 ft in the SW direction. Decreasing the permeability of the matrix by an order of magnitude (i.e., 10 nD) would result in a similar pressure history match. However, the effective total length of the fracture network would have to be increased to ~ 16,500 ft. This would result in a closer fracture spacing of 60 ft with a network width of 360 ft and a total extent of 2,700 ft. The exact position, aspect ratio of effective network width to length, and fracture spacing within can only be uniquely determined with the help of production data for multiple wells.

The pressure distribution after one year of production is displayed in Figure 3.13. Sub-μD permeabilities of the matrix do not drain very far beyond the created network. Additionally, low conductivities of the fractures play an important role as they create greater gradients of pressure in the network. This results in less efficient drainage farther from the well.

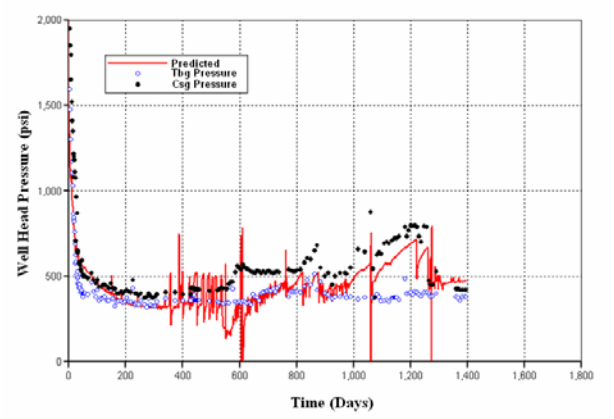

Figure 3.12: History match of flowing tubing and casing pressures for open-ended tubing [*Mayerhofer et al.,* 2006].

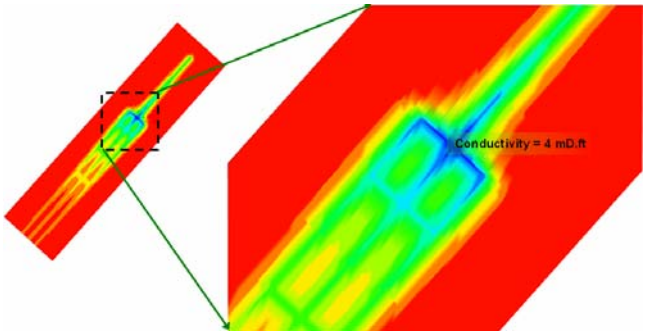

Figure 3.13: Pressure distribution after one year of production [*Mayerhofer et al.,* 2006].

Impact of Non-Darcy Flow on Pressure History Match

The modeling of non-Darcy flow effects required a reduction of the size of the fracture grid block (i.e., the fracture width) to 0.001 ft (i.e., 0.012 in) to describe more accurately the actual width of the fractures and the flow velocities that are important for non-Darcy flow effects. A comparison of different widths of the blocks demonstrated that the simulator was still stable at these small widths, and that numerical results were not impacted.

Incorporating non-Darcy flow affects the pressure match. A reduction of predicted flowing pressure of 200 psi in early time (i.e., ~ 12% of the drawdown) due to including non-Darcy flow effects is displayed in Figure 3.14. Re-achieving a pressure history match would require an increase of total network length or fracture conductivity.

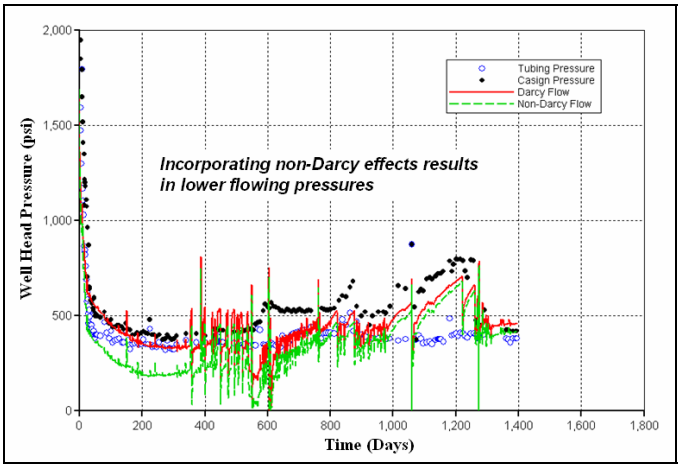

Figure 3.14: Effect of non-Darcy flow on pressure match for a simulated width of the fractures of 0.001 ft [*Mayerhofer et al.,* 2006].

3.4.2 Horizontal Well Parametric Study

The following parametric study for horizontal wells demonstrates how the productivity of horizontal well is affected by:
1) The size of the fracture network,
2) the density of the fracture network,
3) the conductivity of the fractures,

4) the permeability of the matrix, and
5) gaps in the network.

Simulations on the effect of skin damage of the fracture face along the network, and tapered conductivity of the fracture network that decreases away from the well are also discussed.

Impact of Network Size

Correlations demonstrate that larger fracture networks result in better well performance. For the core area of the Barnett Shale, the cumulative production of gas versus the stimulated reservoir volume (SRV) during 6 months is displayed in Figure 3.15. The SRV is defined as the product of gross stimulated area as measured by microseismic mapping and the thickness of the Barnett Shale (if microseismic mapping indicated that the entire Barnett Shale pay zone was stimulated). While there is some variability in the correlation, the trend clearly shows that higher SRV results in a better performance of the wells. This can also be demonstrated with generic reservoir simulations. The simulation for a network generated from a horizontal well with a length of 2,000 ft with a spacing of the fractures of 400 ft and a total extent of the fracture network normal to the lateral of 2,000 ft is displayed in Figure 3.16. The simulation was performed with half-symmetry. This equates to a total SRV of $1{,}200\times10^6$ ft^3. A constant conductivity of the fractures of 4 mD-ft was used in all simulations. The distribution of the pressure in the network after 15 years of production illustrates that the drainage area does not reach far beyond the area that has been stimulated, due to the sub-μD permeability of the shale.

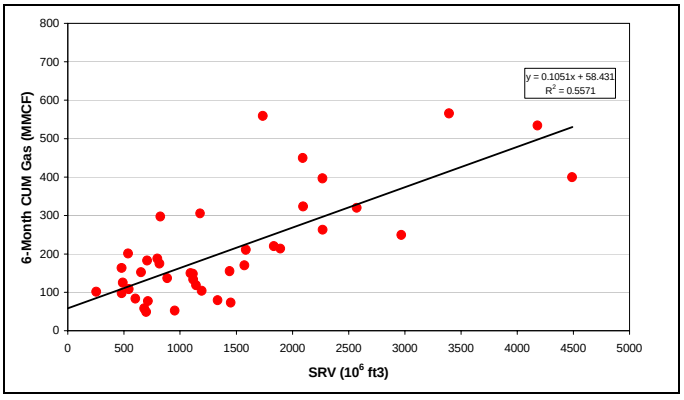

Figure 3.15: Stimulated Reservoir Volume (SRV) versus well performance [*Mayerhofer et al.,* 2006].

The impact of the size of the network (i.e., the stimulated reservoir volume, SRV) on the cumulative production of gas is displayed in Figure 3.17. Doubling the SRV from 600×10^6 to $1{,}200\times10^6$ ft^3 almost doubles the production. However, as the network becomes even larger, the relative benefit of size diminishes. The result of an increase of the SRV from $1{,}200\times10^6$ to $1{,}800\times10^6$ ft^3 is a less than proportional increase of production of 25%. This can be attributed to the low conductivity of the fractures that create large gradients of pressure within the network. These pressure gradients make it more difficult to drain distant portions of the network. Thus, larger networks provide better production with some diminished returns as a function of the conductivity of the fractures when the network becomes very large. Practical limitations to the size of the network of course include:

1) Existing spacing of the wells,
2) faults,
3) potential vertical growth into water-bearing layers,
4) operational limits,
5) operational cost, and
6) operational risk.

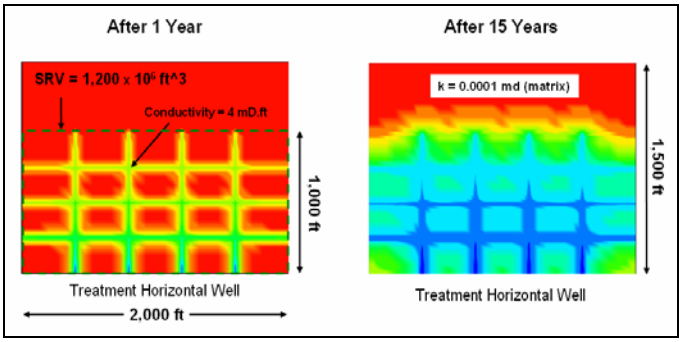

Figure 3.16: Impact of network size (SRV=1,200×10^6 ft^3). Half square drainage area versus pressure distribution [*Mayerhofer et al.,* 2006].

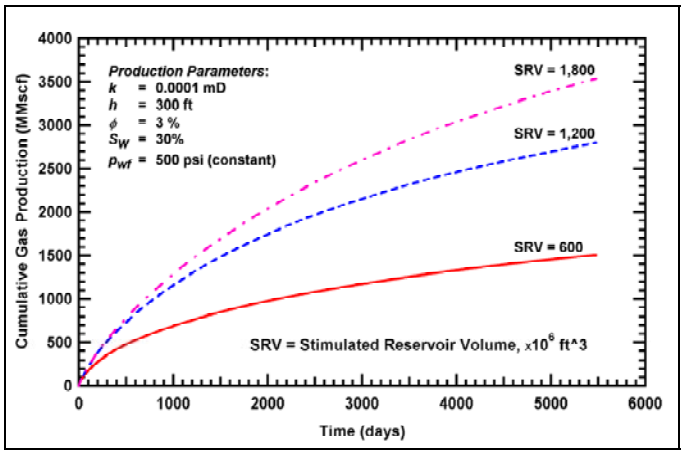

Figure 3.17: Impact of network size on cumulative gas production [*Mayerhofer et al.,* 2006].

Impact of Sub-Optimal Horizontal Well Fracture Staging Resulting in a Network Gap

The means by which sub-optimal fracture staging results in a network gap along the lateral can diminish well performance is displayed in Figure 3.18 and Figure 3.19. In this example, 20% of the lateral (i.e., equal to 400 ft) was not stimulated. This results in a roughly proportional loss of production of 20%, which demonstrates the importance of proper staging along the lateral.

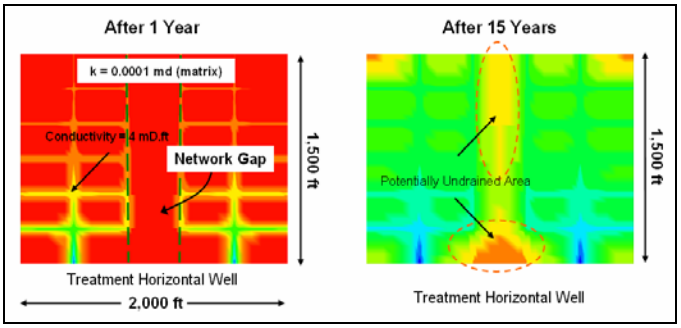

Figure 3.18: Impact of sub-optimal fracture staging with network gap equal to 20% of lateral [*Mayerhofer et al.,* 2006].

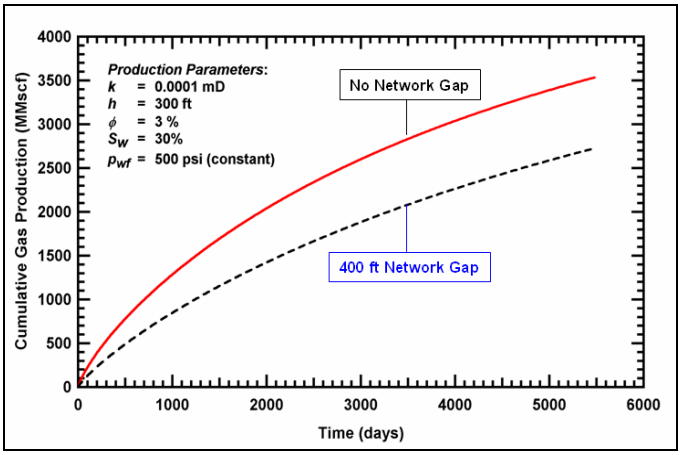

Figure 3.19: Impact of sub-optimal fracture staging with network gap on production [*Mayerhofer et al.,* 2006].

Impact of Network Density (Fracture Spacing)

The calculations of the SRV do not capture the density of the fracture network (i.e., the spacing of the fractures within the overall structure of the network). The density also has an important impact on the sub-μD permeabilities of the shale. The impact of the spacing of the fractures on the recovery factors of gas for a permeability of 100 nD are displayed in Figure 3.20 and Figure 3.21. The acceleration of production is significant even for a small spacing of the fractures of 25 ft. However, the maximum ultimate recovery of gas of 80% is already reached at a spacing of the fractures of 50 ft, and it is very close to maximum at a spacing of 100 ft.

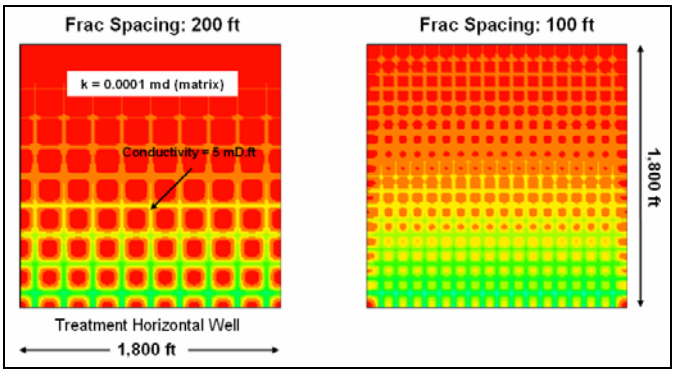

Figure 3.20: Impact of the density of the network (i.e., fracture spacing) [*Mayerhofer et al.,* 2006].

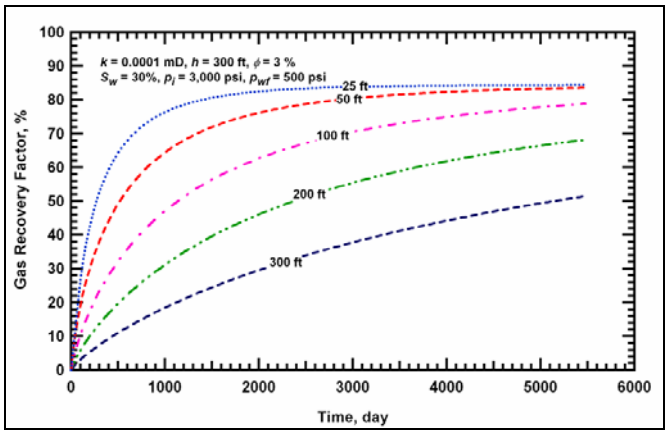

Figure 3.21: Impact of the spacing of the fractures on the recovery factor of gas for a permeability of the shale of 100 nD [*Mayerhofer et al.,* 2006].

Based on intuition and supported by production data, the best completion strategy should be to generate the largest possible fracture network with the highest possible density of fractures to achieve the maximum surface area of fractures and recovery. This could include, e.g., drilling longer laterals, larger treatments, more fracture stages, diversion, simultaneous multi-well fracturing repeated fracturing of the same interval. The two questions are:

1) How to achieve this economically, when the point of diminishing returns is reached; and
2) how to balance creating a dense network while also maximizing overall network size (i.e. creating a dense network through diversion may hinder generating more aerial extent).

Impact of Network Conductivity

At first glance, based on the definition of the dimensionless conductivity of fractures, it is expected that the conductivity of the fractures would be of secondary importance in rock with sub-μD permeability. Water fracture treatments and lack of proppant transport beyond a few hundred feet from the well bore likely results in very low average conductivities of the fractures of less than 10 mD-ft. This may be sufficient for a single hydraulic fracture with a length of 500 to 1,000 ft. However, network structures in the Barnett Shale are so large that the conductivity of the fractures starts to become important again. Consequently, very low conductivities result in a loss of production. For the same created volume of the fracture network, a very low conductivity of 0.5 mD-ft generates very large pressure drops in the network. This results in substantially less effective fracture network (less than 20%) after a well life of one year as compared to a conductivity of 5 or 20 mD-ft. This comparison is displayed in Figure 3.22. The effect on production is displayed in Figure 3.23, which illustrates that higher conductivities result in higher production. Realistically, it is difficult to generate average conductivities of fractures more than 5 mD-ft. However, the significant incremental improvement from 0.5 to 5 mD-ft may warrant a closer examination of proppants with small mesh size and higher quality, ultra light weight proppants, and how they could be transported farther into the network.

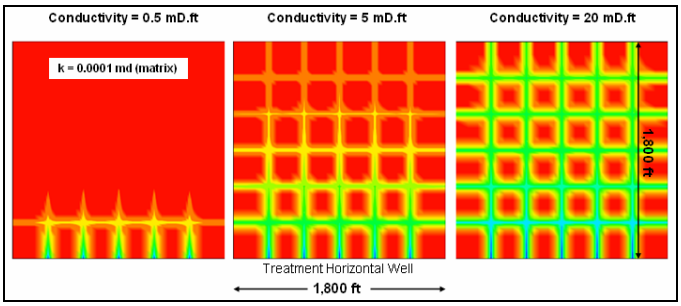

Figure 3.22: Impact of overall conductivity of the fracture network: Pressure distribution after one year of well life [*Mayerhofer et al.,* 2006].

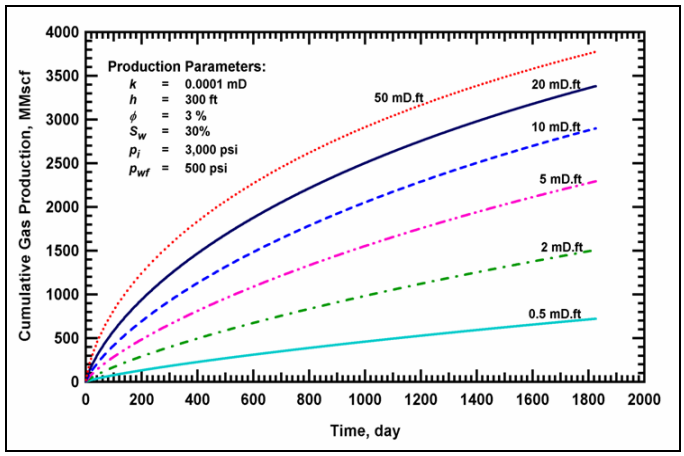

Figure 3.23: Cumulative gas production as affected by the overall conductivity of the network [*Mayerhofer et al.,* 2006].

Effect of High Near-Well Fracture Conductivity

In contrast to the effect of overall conductivity on production, the enhancement of near-well fracture conductivity (a few hundred feet from the well bore) is easier to control and achieve by pumping at the end of the treatments:

1) Larger proppant sizes,
2) higher concentrations of proppant, and
3) proppant of higher quality.

The comparison of the effect of the conductivity of the fractures near the well (i.e., extending 300 ft from the well) on production is displayed in Figure 3.24 and Figure 3.25. Increasing the conductivity from 5 to 50 mD-ft results in an increase of production of 15%. However, the relative benefit is very small beyond 20 mD-ft. While these numbers indicate that enhancement of production is not as significant as for other parameters (e.g., network size and overall conductivity), it can still be important especially if the conductivity near the well is less than expected (e.g., due to poor communication between the fracture near the well fracture and the well bore). Achieving higher conductivities of the network with more aggressive proppant pump schedules should only be considered if this action does not result in a simultaneous decrease of the overall size of the network (i.e., partial screen-outs within the network that make it harder to increase the size of the network). A conceivable approach could be to pump a fracture treatment with standard size and low concentrations of proppant to ensure a maximum extent of the network. This could then be followed by a more aggressive tail-in of proppant with a higher quality.

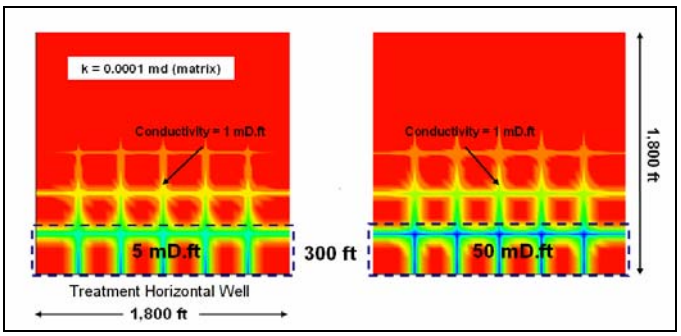

Figure 3.24: Effect of tapered conductivity of fractures for greater near-well conductivity with 300 ft of 5 mD-ft versus 50 mD-ft [*Mayerhofer et al.,* 2006].

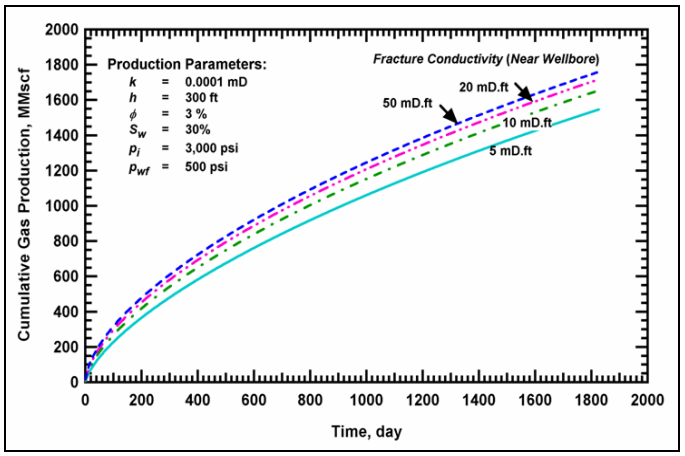

Figure 3.25: Effect of high near-well fracture conductivity [*Mayerhofer et al.,* 2006].

Convergence of flow into fewer, smaller perforated intervals from a large network may result in some inefficiencies, especially if the flow rate were high and near-well conductivity were low. Consequently, it is important to have more access points into the well bore. This could be an advantage for uncemented laterals, since these would allow more near-well reservoir contact. However, other issues (e.g., controlled placement of fracture stages, growth into the water-bearing Ellenberger formation through fault interaction) preclude the wide scale applicability of uncemented horizontals. The corrosion of external casing may also be a potential problem with uncemented laterals.

Impact of Fracture Face Skin Damage

The impact of skin damage of the face of the fracture along the fracture network that extends 1 ft into the reservoir is displayed in Figure 3.26. The effect of skin damage is not significant until it exceeds about 95% near the fracture. This is to be expected, and this is consistent with original findings, which demonstrated the impact of fracture face skin on production [*Cinco and Samaniego,* 1981].

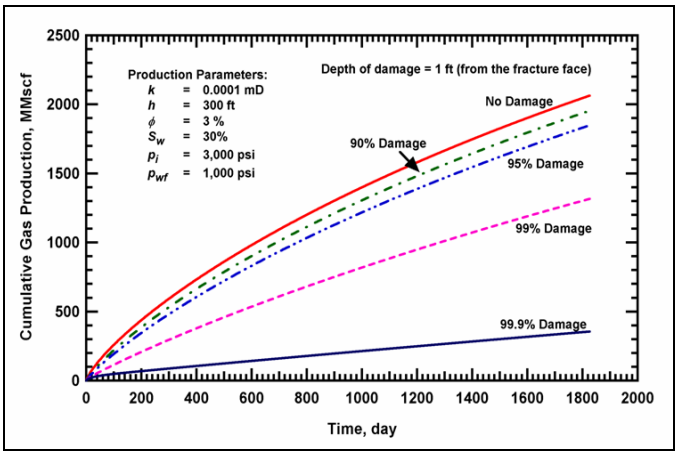

Figure 3.26: Impact of skin damage of the face of the fracture [*Mayerhofer et al.,* 2006].

Pressure Transient Testing (Buildup) to Evaluate Fracture Network Effectiveness and Conductivity

The numerical reservoir simulator was used to generate different pressure buildup responses during a period of 14 days as a function of fracture network characteristics (e.g., conductivity and effective network length). The purpose of the evaluation was to determine if a pressure buildup test could provide both qualitative and quantitative answers about network characteristics.

A comparison of the response of the pressure build-up of network with a low and high conductivity in a vertical well is displayed in Figure 3.27. The total length is 18,000 ft, the permeability is 10 nD, and the spacing of the fractures is 300 ft. The comparison shows that a network with a low conductivity yields more bi-linear flow. In contrast, the high conductivity case yields a linear flow regime. The spacing of the fractures is too large to yield dual-porosity behavior.

A comparison of the response of pressure build-up of a short, single fracture with a length of 300 ft and a large fracture network with a total segment length of 18,000 ft is displayed in Figure 3.28. As expected, the short, single fracture transitions into linear flow very quickly. In contrast, the fracture network has a longer transition preceded by bi-linear flow. If the same reservoir permeability is used in the interpretation, then an analysis of the output of the numerical simulation with a program for conventional analysis of pressure transients provided answers similar to the input of the simulation in both cases. This implies that if the permeability of the matrix were given within a certain range, then it would be possible to estimate a range of effective total lengths of the fracture network from the data of the pressure build-up.

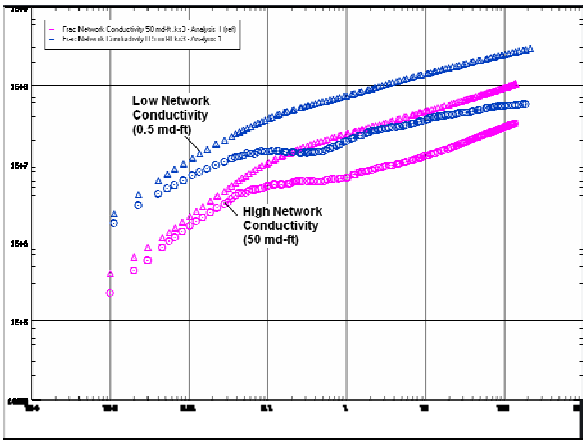

Figure 3.27: Simulated test of pressure build-up: Log-log diagnostic plot comparing a conductivity of the fractures of 0.5 and 50 mD-ft [*Mayerhofer et al.,* 2006].

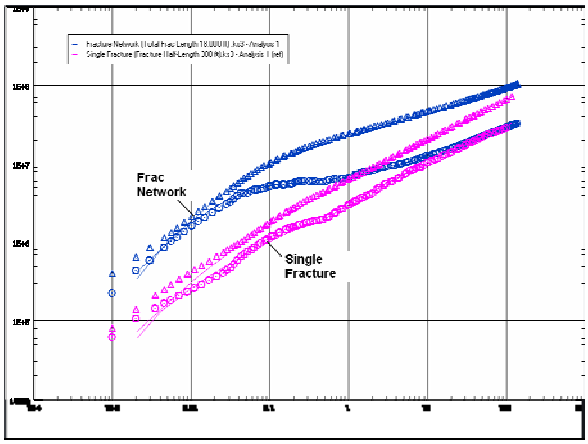

Figure 3.28: Simulated test of pressure build-up: Log-Log diagnostic plot comparing a single 300 ft fracture with a large fracture network for a total segment length of 18,000 ft [*Mayerhofer et al.,* 2006].

A comparison of different spacings of the fractures and their impact on the response of the pressure build-up did not yield any clear distinguishing features within the time frame of the build-up, except that dual-porosity behavior may become visible at very small spacings of the fractures.

3.4.3 Conclusions

1) Barnett Shale production can be modeled numerically using a discrete number of fracture segments that resemble the aerial extent of the microseismic fracture image. Once the permeability of the shale matrix is fixed, the resulting total effective length (i.e., the sum of all open segments) and conductivity of the fracture network are unique.
2) Estimating the position, the aspect ratio of the effective width to length of the network, and the spacing of the fractures would require the use of additional data (e.g., of simulations of the production from multiple wells).
3) Larger fracture networks with higher stimulated reservoir volume (SRV) result in better well performance. However, as the network becomes very large, the relative benefit of the size diminishes due to the low conductivity of the fractures. The drainage area is largely confined to the stimulated network area due to the sub-µD permeability of the shale. This concept is indeed the basis of the goal of obtaining a large SRV for EGS. Moreover, in contrast to producing gas in the Barnett Shale, the pumping of water in EGS may further confine the drainage area.
4) The spacing of the fractures within the overall network structure also has an important impact on the production in the sub-µD permeabilities of the shale. For a permeability of the matrix of 100 nD, the acceleration of the production is significant, even for a small spacing of the fractures of 25 ft. However, the maximum ultimate recovery of gas of 80% is already achieved with a spacing of the fractures of 50 ft for a permeability of the shale of 100 nD. Similar to conclusion 3), this notion is indeed the basis of the goal of obtaining relatively dense fracture spacing for EGS. Interestingly, this conclusion demonstrates that the economically optimum fracture spacing (e.g., 50 ft) may not necessarily be the smallest feasible spacing (e.g., 25 ft).
5) Sub-optimal fracture staging results in network gaps along the horizontal well. This results in a loss of production that is approximately proportional to the percentage of unstimulated lateral. This highlights the fact that investments made in fluid diversion and penetration are critical to succesful creation of EGS.
6) Fracture network structures in the Barnett Shale are so large that fracture conductivity starts to become important again despite the ultra low permeability of the shale. Very low conductivities of the fractures result in a loss of production due to the inability to move gas from the far reaches of the network. Again, pumping of water instead of gas likely amplifies this problem further. Consequently, simply creating a large fracture network with a proper spacing may still not be optimal for succesful EGS, if the conductivity of the fractures is not sufficient. Proper selection of proppants (e.g., ceramics) may be beneficial to mitigate this problem.

7) If more aggressive proppant pump schedules do not result in a decrease of overall network size at the same time, then increasing the near-well conductivity could also provide improved production. A conceivable approach could be to pump a full size fracture treatment with low proppant concentrations first, followed by a more aggressive tail-in of higher quality proppant. This may be a feasible technique for EGS where proppants (e.g., ceramics) are pumped.
8) If the permeability of the shale is fixed within a certain range, it may be possible to estimate a range for the effective total lengths of the fracture network using test data for pressure buildup. Consequently, pressure diagnostics, in addition to fracturing diagnostics, appear to be critical to estimating and predicting the success of EGS stimulations.
9) The goal of any completion strategy in the Barnett Shale should be to generate the largest possible fracture network with the highest possible density of fractures, but limited by the issue mentioned in conclusion 4). This maximizes the total surface area of the fracture, and allows obtaining a recovery that is within economic limits. This strategy could include, e.g., drilling longer laterals, larger treatments, more fracture stages, diversion, simultaneous fracturing of multiple wells, and repeated fracturing of the same interval. All of these techniques are likely also applicable to EGS.
10) Caution is needed when trying to balance the creation of a dense fracture network while also maximizing the overall size of the network. The reason is that creating a dense network through aggressive diversion may be detrimental to generating a larger network. This balance is likely equally important for EGS.

4 METHODS TO IMPROVE FLUID DIVERSION AND PENETRATION

Pinnacle Technologies, Inc. and GeothermEx, Inc. conducted a study to evaluate methods in oil field applications that could have a positive impact on fluid flow diversion and fluid penetration from a long open-hole completion typical of geothermal wells. The result of more uniform fluid diversion and penetration along a well is an increased direct contact area between the well and the far-field fracture system. A combination of available literature, publications from oil-field related societies, and the vast database of fracture treatment data from Pinnacle Technologies, Inc. were used to complete this project task.

The methods that we evaluated include (but are not limited to):
1) Propped fracturing versus water fracturing versus injecting fluid below fracture gradients (section 4.1 below);
2) zonal isolation by use of perforated casing or packers and fluid diversion by use of the SurgiFrac or StimGun perforation technique or by use of stress shadowing (section 4.2 on page 57); and
3) fracture re-orientation and fracture network growth techniques by use of alternating high- and low-rate injections or alternating high- and low-viscosity fluids (section 4.4 on page 74).

This project task was conducted in the first project year. The most promising techniques are recommended for further evaluation in future EGS field tests conducted in the Desert Peak area in Nevada for ORMAT Nevada, Inc. (section 5 on page 75).

4.1 Propped Fracturing versus Water Fractures

Classical hydraulic fracture treatments conducted in the oil and gas industry typically called for a gelled water-based fluid and a proppant (i.e., either sand or ceramic) that would be used to keep the fracture open after the pumping pressure is released (section 4.1.1 on page 51). In hydraulic fracturing, the ideal conductivity of the (propped) fracture system predominantly depends on the permeability of the reservoir that requires stimulation.

During the last few years, the oil and gas industry has made significant progress to design fracture treatments utilizing a dimensionless conductivity. In ultra-low (i.e., micro-Darcies) matrix permeability reservoirs, this has led to the implementation of low proppant concentration fracture treatments, where in addition to minor propping, the roughness of the fracture walls that are created and inability of the fracture to perfectly close on itself result in an intrinsic fracture conductivity (section 4.1.2 on page 52). In EGS, this is referred to as self-propping. Dr. Michael Mayerhofer at Pinnacle Technologies, Inc. has been a pioneer in development of this technology [*Mayerhofer et al.,* 1997], which is directly applicable to EGS development.

Alternative techniques (i.e., light weight proppants, explosive slurry, and nitrogen gas injection) are presented in section 4.1.3 on page 55.

In reservoirs with a greater permeability, models have been developed to take into account more accurately turbulent non-Darcy and multiphase flow effects on proppant pack damage. Turbulent non-Darcy flow occurs because of the relatively high flow rates of the focused flow inside the narrow fracture. It is important to account for these effects when high flow rates through fractures are expected, as it can dramatically change the ideal conductivity needed to prevent the fracture from being the bottleneck to the production response of a well. The fracture analysis system FracproPT of Pinnacle Technology, Inc. can model the effects from turbulent non-Darcy and multiphase flow. However, the capability of FracproPT to model heat transfer as well as fluid transfer is very limited (section 9.10 on page 171). That is, FracproPT does not account for thermal contraction and its effect on permeability and porosity, and thus injectivity and productivity. Consequently, FracproPT is generally not used for steam floods or other multiple phase enhanced oil recovery (EOR). FracproPT is currently not very well suited for hydrothermal and geothermal situations.

Propped and non-propped fracture treatments were also compared to injections where bottom-hole pressures remain below the minimum principal stress (i.e., fracture closure stress). The oil industry utilizes matrix acidizing techniques, where various acids (i.e., mixtures) are pumped into the pore space of the reservoir rock to clean out damage caused by completion and drilling activities. Although this technique may not truly stimulate the reservoir, it can sometimes be the best economic

alternative, as it is relatively cheap to implement. Acidizing is also used in conventional hydrothermal and EGS wells, generally to increase near-well permeability. Sometimes this is because of mud damage and sometimes because the fractures are filled with calcite (hydrochloric acid is used in this case) or silica (hydrofluoric acid appears to be the acid of choice for this problem). The hope in either case (near well mud damage or mineral-filled fractures) is that the problem is only near the well and that acidizing links into a permeable fracture system. At Soultz, well GPK-4 or GPK-3 was recently acidized to improve the connection between them. However, this did not have any effect. Perhaps an insufficient amount of acid was pumped into the well, and it all reacted with the near-well fractures and very little acid was able to penetrate any further. Consequently, it seems that in EGS, acidizing is likely only useful as a supplement to hydraulic fracturing.

We evaluated the appropriateness of all these different stimulation techniques and concepts for EGS applications, both from a technical and from an economic perspective. We also provided an application range (if relevant) for these techniques for the specific reservoir properties that need to be met for these techniques to be successful.

Historically, the emphasis in fracturing low-permeability reservoirs was on the productive fracture half-length x_f. For greater permeability reservoirs, the fracture conductivity $k_f w$ (i.e., the product of fracture permeability and fracture width) is equally or more important, and the two are balanced by the formation permeability k [*Economides and Nolte,* 2004]. This critical balance was first discussed more than 10 years after the introduction of fracturing, with the important concept of dimensionless fracture conductivity. Mathematical analysis was used to conduct a comprehensive consideration of finite-conductivity fractures with the assumption of steady-state flow (i.e., constant-pressure boundaries). The dimensionless conductivity is equal to

$$C_{fD} = \frac{k_f w}{k x_f} \tag{4.1}$$

This dimensionless conductivity is the ratio of the ability of the fracture to carry flow divided by the ability of the formation to feed the fracture. In general, these two production characteristics should be in balance. In fact, for a fixed volume of proppant, maximum production is achieved for a value of C_{fD} between 1 and 2 in high permeability reservoirs, and above 10 in low permeability reservoirs. Similar principles are perhaps also valid for fracture networks in EGS.

4.1.1 Propped Hydraulic Fracturing

The research and development of hydraulic fracturing has highly emphasized the effective placement of propping agents to provide and maintain the conductivity after releasing the fracturing pressure [*Mayerhofer et al.,* 1997]. For this purpose, the service industry has developed sophisticated fluid systems and an extensive recipe of chemical additives for hydraulic fracturing. The fluid systems are engineered to change the viscosity during its journey from the surface to the fracture, and afterwards during the clean up of the fractures. The sole reason for the design of these fluid systems is to:
1) Place the proppant,
2) minimize the damage to the formations, and
3) ensure proper clean up of the fractures.
In turn, the proppant has no other function than to maintain a conductive fracture during the production from the well.

The first decade of stimulation treatments in the Barnett Shale was dominated by massive hydraulic fracturing treatments withmore than 1×10^6 lbm of 20 to 40 mesh sand [*Lancaster et al.,* 1992] carried in highly viscous crosslinked gelled fluids [*Coulter et al.,* 2004; *Fisher et al.,* 2004; *Fisher et al.,* 2002]. The production was variable with vertical wells producing up to 1×10^9 ft^3 estimated ultimate recovery (EUR).

Because of the extremely low permeability of the Barnett Shale, its inability to efficiently clean up the damage to the fractures from gels, and the high cost of massive hydraulic stimulations, most treatments did not provide an adequate return of investment (ROI) *Fisher et al.,* 2004.

4.1.2 Light Sand and Water Fracturing

In 1997, Devon Energy Corp., formerly Mitchell Energy and Development Corp., began experimenting with water fracturing (WF) or light sand fracturing (LSF) treatments.

Principle

Water fracturing is defined as the application of a water-based hydraulic fracturing fluid with a low-viscosity (e.g., ≤ 10 cP) [*Grieser et al.,* 2003]. Average concentrations of proppant are less than 0.5 lbm/gal, which is very low compared to conventional hydraulic fractures. Concentrations of guar gel vary from 0.5 to 20 lbm/1,000 gal. The gel is primarily used as a friction reducer, not as transport medium for proppant. Other additives include long-chained polymer friction reducers at concentrations of 0.5 to 2.0 lbm/1,000 gal, surfactants, biocides, and clay-stabilizers.

In many reservoirs with low- or ultra-low-permeability, light sand fracturing is successfully applied to reduce the cost of stimulations without decreasing the production [*Fisher et al.,* 2004; *Walker et al.,* 1998]. An example of such a reservoir is the Cotton Valley Sand in East Texas. This is a gas reservoir with a low permeability. It is located at a distance of approximately 100 miles to the east of the Fort Worth Basin. Water fracturing was successfully re-introduced (i.e., from other reservoirs such as the Austin Chalk) to the Cotton Valley Sand partly to reduce costs, which were very high due to large, expensive crosslinked fracturing treatments, but mainly based on surprisingly improved well performance after water fracturing [*Mayerhofer et al.,* 1997]. Another example is the naturally fractured Austin Chalk, where water-fracturing treatments are pumped without any propping agents and are very succesful. Even a few oil-producing reservoirs have responded favorably to such treatments [*East et al.,* 2004]. It was believed that similar success would be achieved in the Barnett Shale with treatments consisting of large volumes of slickwater. Subsequently, several versions of these treatments were tested, before evolving to the current design.

Application to Barnett Shale

In the Barnett Shale, water or light sand fracturing has been successful. It is now widely used for a different reason: it provides a much greater surface area of contact with the reservoir, and minimizes fracture damage. This results in an improved productivity [*Fisher et al.,* 2004]. Currently, nearly every treatment is performed by use of light sand fracturing with high injection rates of water, plus a friction reducer to enable reasonable rates of injection given the completion, scale inhibitor and biocide, or some permutation of this technique [*Grieser et al.,* 2003]. This has proven to be the most important advancement in the resurgence of development programs in this basin [*East et al.,* 2004]. The use of water or light sand fracturing treatments has considerably improved both the production and the economics in this reservoir [*Fisher et al.,* 2002].

The parameters for hydraulic fracturing depend on the location within the Barnett Shale, the viability of barriers of limestone surrounding the Barnett Shale intervals, and the net thickness of the pay-zone. A typical treatment may generally consist of vertical cased wells, light sand water fracturing with large volumes of slickwater, and 20/40 and 40/70 mesh sand. The parameters of such fracturing treatments are listed in
. In many cases, the sand stages are pumped intermittently with sweep stages without proppant. More recently, proppant concentrations as high as 3 lbm/gal have been used in later stages of these water fracturing treatments.

Table 4.1: Parameters of hydraulic fracturing for stimulation treatment in Barnett Shale.

well orientation	slickwater volume (10^3 bbl)	sand mass (10^3 lbm)	sand concentration (lbm/gal)	injection rate (bbl/min)
vertical	12 to 36	75 to 250	0.1 to 2	45 to 75
horizontal	24	100 to 300	0.1	65 to > 200
horizontal, un-cemented	20 to 100	500 to > 1,000	0.1	< 140 or 200
horizontal, cemented (per stage)	24 to 60	150 to 400	0.1	< 140 or 200

In contrast to the vertical completions, most horizontal completions use more water with more sand at greater pumped rates. In a few wells, fluid volumes exceeded 143,000 bbl. Some horizontal completions in the Barnett Shale are re-completions of vertical wells. However, most have been newly drilled wells.

Mechanisms

There are several possible reasons for the success of water fracturing treatments with high injection rates, large volumes, and low concentrations of sand [*East et al.,* 2004; *Mayerhofer et al.,* 1998; *Mayerhofer et al.,* 1997]:

1) A fracture can be described at different scales. At a large scale, the faces of the fracture may appear to close smoothly. However, at the small scale, the faces of the fracture do not match. This certainly occurs for the scale of the grain size. For example, Cotton Valley Sand has grain sizes of ~ $^1/_{16}$ to 1 mm. However, this may also occur on the large scale of layering, natural fractures, and fracture branching. The faces of the fracture deform permanently. The resulting rough asperities are in contact. This results in a highly conductive, residual opening of the fractures because of misalignment that remains after mechanical closure, even at high closure stresses [*Zimmerman et al.,* 1990; *Hopkins et al.,* 1990; *Barton et al.,* 1985; *Bandis et al.,* 1983]. This conductivity can be adequate in rock with low permeability. Residual conductivity has been observed in various laboratory environments and in field scale experiments [*Branagan et al.,* 1996]. That is, a fracture can actually retain a sufficient conductivity with very little or no proppant. For example, at the multiple well experiment (MWX) site, downhole tiltmeters were used to observe substantial residual hydraulic fracturing width (several months after shut-in) after pumping a mini-hydraulic fracturing without proppant. This is also observed in EGS projects, notably at Soultz.
2) Shear slip can cause an offset and possibly branching of the hydraulic fracture. It may also change the natural permeability near the fracture. The points of offset can produce shear forces within the hydraulic fracture that additionally help create mismatch and asperities once the fracture closes. These also cause obstructions where the proppant can accumulate, which can is considered problematic for EGS.
3) The effect of normal and shear stresses, either natural or artificial, on a fracture dictate its conductivity. When loading a fracture under high stresses (i.e., 5,000 to 11,800 psi), the contact area between the adjacent two fracture walls is only between 40 to 70% [*Bandis et al.,* 1983]. This depends on the roughness and the strength of the walls. Such natural mismatches and the resulting creation of asperities could occur when shear forces displace the fracture walls out of their original position. Experiments performed on an Austin Chalk core demonstrated that a shear displacement of the walls of the fracture by merely 2 to 3 mm resulted in an increase of the conductivity of an order of magnitude of 2 to 3 [*Olsson and Brown,* 1993]. The effects of these forces on the propagation of fractures are just now beginning to be investigated. This is critically important in EGS. The hydro-mechanical response of natural fractures has been addressed in the rock mechanics literature [*Zimmerman et al.,* 1990; *Brown,* 1989]. It is an extremely important issue in the field of the underground disposal of nuclear waste.
4) Conventional propped fracturing treatments do not clean up efficiently [*Stim-Lab,* 1996]. An inferior effective conductivity of fractures can be caused by gel damage, two-phase flow and other mechanisms [*Willberg et al.,* 1997]. That is, proppant along with gel residue and filter cake [*Fisher et al.,* 2004; *Fisher et al.,* 2002] could actually impair fracture permeability and its ability to clean up. The forces of inertia (i.e., because of high viscosity, surface

tension, and relative permeability) fail to clean out the gel residue in the proppant pack and the two-phase flow in the proppant pack may create effective lengths of hydraulic fracturing that are only a small percentage of the actual created length. This becomes especially severe in reservoirs with a pressure depletion. Water fractures create a propped fracture with a length that is comparable to the portion that cleans up during conventional jobs (i.e., the effective fracture lengths can be the same in water versus conventional fractures. Both water fractures and conventional treatments are sub-optimal, because the effective fracture length is generally much less than the obtained total fracture length. However, water fracturing costs less. In addition, hydraulic fracturing fluids with low viscosity appear to achieve longer fractures [*Warpinski et al.,* 1998], and hydraulic fracturing fluid cleanup is made easier. The extension of fractures with adequate conductivity is the key design parameter in reservoirs with low permeability, for both conventional and water fractures.

5) The use of low proppant loads and thin fluids may promote the settling of proppant near obstructions or into small vertical offsets inside the fractures that serve as a ledge for proppant to accumulate. This in turn could act as a wedge, or extended asperity, keeping the other parts of the fracture open (while such proppant settling could also reduce the fracture permeability). The conductivity is then given by channels in between the asperities and the proppant, rather than by a proppant pack, similar to partial mono-layers.
6) Rock debris created during the hydraulic fracturing (especially in shales) may act as a self-propping agent, which is well known for EGS.
7) More recently, and especially in completions in the Barnett Shale, a network or network of multiple inter-communicating fractures is formed [*Fisher et al.,* 2004]. This is in contrast to the traditional concept of only a single highly dominant fracture plane, or at least a very small number of dominant fracture planes [*Soliman et al.,* 2004]. That is, when a hydraulic fracture propagates, it can open pre-existing natural fractures, faults, and plains of weaknesses by inducing shear slip. This can occur both ahead of the fracture tip but also near the fracture because of leakoff. This causes an offset and possibly branching of the hydraulic fracture.

Currently, it is not known which mechanism, or combination of mechanisms, depending on the specific formation properties, is dominant [*Mayerhofer et al.,* 1998]. It is important to determine the overall conductivity of these flow channels during the history of production [*Mayerhofer et al.,* 1997]. In rock with low permeability, it does not require much open aperture to provide fractures with relatively great conductivity. For example, in the case of a rock with a permeability of 0.01 mD and a fracture with a length of 500 ft, an aperture of only 9×10^{-4} in is needed. These points may have a tremendous impact on the costs of a hydraulic fracturing operation. Gelling agents, proppant, and associated chemical additives comprise a significant part of the cost of hydraulic fracturing. In the early literature, self-propping and partial mono-layers of fractures haze been discussed. In general, however, the idea has been discarded by the oil and gas industry. This is a significant point of difference between conventional hydraulic fracturing in the oilfield as compared to EGS, which has been broached by the recent experience in the Barnett Shale.

Design

Even with the success enjoyed with light sand fracturing treatments, not every area of the Barnett Shale has proven as successful to date as the core area in the counties of Wise and Denton [*Fisher et al.,* 2004]. The quality and quantity of pay-zone varies substantially from the traditional core area to the newer plays on the fringes. Successful development in the newer fringe areas likely requires additional changes in techniques for completion (i.e., a different approach in the construction, completion, and stimulation of wells). Several new strategies are being tested in both core and fringe areas.

The basic methodology for the design of fractures has not been aggressively applied to water fracturing [*Grieser et al.,* 2003]. This could be because:

1) The suspected complex geometry indicated by microseismic imaging, and the uncertainty of the deposition of proppant in fluids with low viscosity; and
2) water fracturing may have been considered a low technology practice of completion, used mainly in reservoirs with marginal capability of production.

Instead, rules of thumb are offered for the design of water fractures. When they are used, little consideration is given in the design of water fractures to the permeability of the reservoir, and its relationship to the conductivity of fractures. This necessitates the search for a different design approach.

Hence, existing methods for the coupling of the design of water fractures and the quality of the reservoir were used to highlight the specific characteristics that are unique to water fracturing. These characteristics include:
1) Low permeability of the formation,
2) long treatment intervals,
3) large treatment volumes,
4) low fluid viscosity,
5) poor proppant transport,
6) narrow width and complex geometry of the fractures, and
7) high injection rates.

The basis for the design of hydraulic fractures is not new. Based on successful water fracturing treatments in the Barnett, it could be possible to design a similar water fracturing treatment at Desert Peak.

4.1.3 Alternatives

In addition to conventional propped and water hydraulic fracturing, stimulation of low permeability formations can be achieved with light weight proppants, explosive liquid or slurry (e.g., in the Tipton Shale in Wyoming, and the Devonian Shale in West Virginia), and gas injection with or without proppant (e.g., in the Devonian Shale in West Virginia).

Light Weight Proppants

A major concern in utilizing large volumes of slickwater with low concentrations of proppant, and high flow rates as the only means to transport proppant into the reservoir, is the inefficiency of obtaining the most effective propped fracture [*Schein et al.,* 2004]. To improve the transport of proppant and increase the effective length of the fractures, lightweight proppants could be used. Their lower density allows the proppant to occupy the same volume, while utilizing approximately half of the weight of sand, while being able to withstand elevated temperatures. This allows the proppant to be transported farther from the well than sand in complex, naturally fractured shale with low permeability where proppant with greater mesh sizes has a tendency to bridge. The lightweight proppants experience much lower settling velocities during hydraulic fracturing with slickwater. Additional work needs to be performed to better optimize applications for this novel approach to maximize productivity.

Explosive Slurry

An explosive liquid or slurry that is displaced from a well into natural fractures or pre-generated horizontal hydraulic fractures can be detonated to produce a distributed fracture network with sufficient void and permeability.

In the Tipton Shale, numerous diagnostic and evaluation measurements were performed during the course of the experiment for initial site characterization, hydraulic fracture assessment, explosive displacement and detonation performance, and post detonation fracture and permeability assessment *Parrish et al.,* 1981. Results demonstrate that fractures were induced. The fractures were randomly distributed with no regions of extensive fracturing or shale dislocation. Enhancement of permeability was limited essentially to enlargement of the pre-generated hydraulic fracture horizons into which the explosive slurry was detonated.

In the Devonian Shale, early cumulative production from gas wells stimulated with a high-energy water gel explosive averaged a factor of 2 compared to nearby wells stimulated with dynamite [*Coursen,* 1983]. From an estimate of production loss because of well damage done by post-shot drilling in the shot zone, it is concluded that production from the wells stimulated with water gel would have averaged a factor of 5 compared to dynamite stimulations if no such drilling had been done. Consequently, this is probably not a useful technique, and there could perhaps be problems with charges going off prematurely due to the elevated temperatures in the geothermal environment.

Nitrogen Gas Injection

In the Devonian Shale, nitrogen gas without proppant was injected into a vertical well undergoing hydraulic fracturing [*Evans et al.,* 1982]. From downhole tiltmeter mapping, the surface deformations occurring near the well were analyzed to obtain a description of the geometry and the development of the resulting fracture. Significant upward and lateral growth of a near-vertical fracture aligned with the proposed direction of maximum tectonic compression is inferred to take place initially. However, after some time after the injection of the nitrogen gas, fracture growth in a horizontal plane began abruptly, and vertical growth ceased. No indication of this breakout is evident in the wellhead pressure or flow rate records. The state of stress near the well was estimated, and implications of the inferred fracture development behavior were analyzed.

The addition of sand as proppant to a nitrogen gas stimulation performed on a vertical well was operationally successful, except for minor problems with five out of nine treatments [*Gottschling et al.,* 1985]. This process has been developed and demonstrated in 17 field tests. A wide variety of stimulation conditions involving flow rates, total nitrogen, number of perforations, and well depths have been studied. The early production results from two offset wells demonstrate a significant improvement of the decline curve. Theories from observed data from well treatments have been developed. The displacement of proppant without the use of water or other liquids is a significant benefit both environmentally and economically. Additionally, the process causes no formation damage, and the well cleanup is rapid. The current major disadvantage is the small amounts of dplaced proppant, although improved process designs have already demonstrated an increase in sand quantities.

Nitrogen and carbon dioxide gas without sand, and foam with sand were injected from a horizontal well [*Layne and Siriwardane,* 1988]. The borehole intersects multiple natural fractures in the reservoir. Inflatable packers and casing port collars were used so that individual zones could be tested or stimulated along the well [*Layne and Siriwardane,* 1988]. In situ fracture diagnostics were used [*Layne and Siriwardane,* 1988]. Radioactive-tracer with spectral gamma-ray logging confirmed that both fluid pressure and stress perpendicular to the fracture affect the injection rate distribution along the well.

4.2 Zonal Isolation and Diversion Techniques

Zonal isolation is defined as separating a zone from other intervals through perforating and mechanical devices (e.g., plugs, packers) [*Economides and Nolte,* 2004]. Usually there are several potential producing zones penetrated by a well that must be hydraulically fractured. To ensure that each zone is stimulated effectively, these intervals must be isolated from one another. Several isolation methods have proved to be effective. These methods can be used only when the various formations and intervals are isolated from each other behind the casing with cement. While this is currently not deemed feasible for EGS, this should perhaps be considered in the long term.

Hydraulic fracturing is routinely conducted in oil and gas fields to accelerate the extraction of hydrocarbons. Over the last decade, the development and commercialization of direct hydraulic fracture diagnostics [*Cipolla and Wright,* 2000; *Wright et al.,* 1999] has helped to improve our understanding about the physics of fracture growth. Fracture diagnostics are now routinely used to determine fracture length, height, orientation, and proppant placement. These measurements help to improve stimulation design and execution in oil and gas applications. We can also utilize these lessons learned from the oilfield to evaluate the challenge to obtain an effective stimulation and fluid diversion in EGS wells.

In many oilfield applications, multiple target zones are penetrated by a single well. In some fields, the pay interval that contains hydrocarbons can have a thickness of several thousand feet. With the absence of an effective wellbore distribution strategy, hydraulic fractures typically grow in the layers that provide the least resistance (i.e., the zones in which the fracture closure stress is lowest). Consequently, a stimulation treatment that would target all pay zones at once could end up covering only a very small portion of the interval, as displayed in Figure 4.1. Many techniques have been developed in the oilfield to improve fluid diversion and fracture penetration over the entire thickness of the target zone.

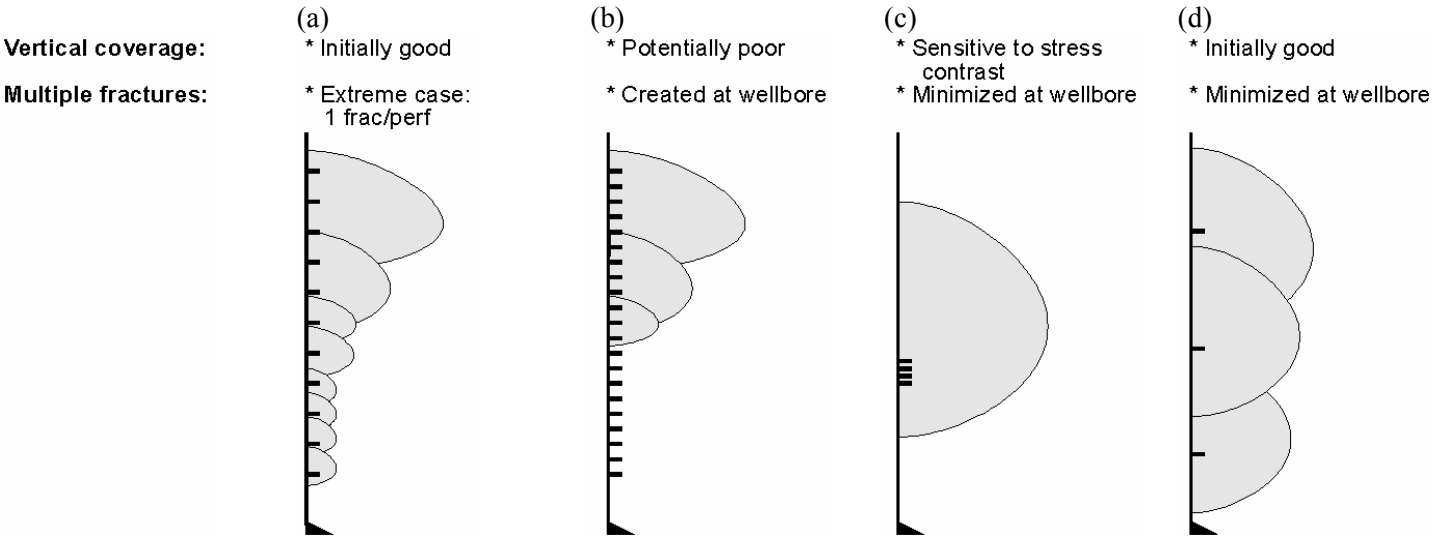

Figure 4.1: Conceptual illustration of the fracture interval coverage that may result from different perforation strategies [*Minner et al.,* 1996]: (a) Limited entry, (b) unrestricted entry, (c) point source, and (d) multiple point source / limited entry. The thickness of the target stage interval ranges from 150 to 300 ft. The multiple point source / limited entry strategy (d) has the advantages of good initial interval coverage and minimizes the well bore initiation of multiple fractures.

Until recently, the desire in oilfield stimulation has been to create and extend a simple fracture system within a reservoir. However, in several newly developed reservoirs (e.g., the Barnett Shale), the emphasis has been on creating a complex fracture network, since this is the only viable way to create an economic production response from ultra-low permeability rock. Similarly, for successful and cost-effective EGS development, it is also necessary to create an extensive and complex fracture network to achieve the maximum contact with the heat source while minimizing the potential for short-circuiting.

Various techniques have been developed by the oil and gas industry to encourage fluid diversion over the thickness of the target interval and lateral diversion throughout the reservoir. In EGS, the use of some of these diversion techniques is challenging, as most wells that have been used for EGS have long open-hole completions. This includes wells drilled specifically for EGS development (e.g., at the European HDR project in Soultz-sous-Fôrets) and wells of opportunity, which are typically non-productive or marginally productive geothermal wells (e.g., those investigated at the Coso and Desert Peak EGS projects in the United States).

This section is aimed directly at the practical goal of improving the effectiveness of EGS stimulations, to enable the delivery of more geothermal power at less cost. For this purpose, the report provides an overview of techniques that are commonly used for hydraulic fracturing in the oilfield, and evaluates their effectiveness in improving stimulation and diversion for EGS wells.

4.2.1 Zonal Isolation and Height Diversion Made Easy - Cased Wells

Cased and lined wells have a large diameter pipe placed and cemented along the entire well or along subsections, respectively. The casing and liner provide significant advantages over open hole completions:
1) Protect the up-hole layers from fluids, pressures, and well stability problems;
2) protect fresh-water formations; and,
3) isolate zones of lost returns or formations with significantly different pressure gradients.

In particular, the casing allows mechanical isolation, and the perforations in cased wells are beneficial for mechanical and chemical diversion. This makes cased wells very attractive for most stimulation and diversion techniques. While geothermal wells are cased above the reservoir for these same reasons, perforated casings through the production intervals of geothermal wells are not used because of the requirement for much greater per-well flow rates in geothermal compared to oil and gas wells. It has been found that perforating through cemented casings does not permit sufficient flow from the formation to the well bore for traditional geothermal (non-EGS) wells. However, since EGS development is experimental at this stage, EGS wells are not expected to yield the same production rates as traditional geothermal wells. That is, an EGS well with a perforated, cemented casing could be able to achieve the injection rates needed for stimulation and the flow rates or injection rates needed during routine operation. If so, then the cased and perforated completion and all the diversion techniques that are facilitated by this completion could be applicable to EGS.

Various isolation techniques can be used to temporarily isolate target zones from each other and from the rest of the well [*Economides and Nolte,* 2000]. These isolated zones can be stimulated separately or simultaneously. A first requirement for proper isolation is achieving a good cement bond between perforated intervals. Various types of casing plugs for zonal isolation are available for conventional bottom-to-top treatment stage stimulation. Typically, perforations are shot in the casing, a fracture stimulation treatment is conducted, and the stimulated zone is isolated from new perforations that are treated up-hole. Mechanical bridge plugs can be run on tubulars or wire line [*Brown et al.,* 2000]. Sand plugs can also be pumped (sometimes as part of the propped fracture treatment) to cover a previously stimulated perforated interval. Bridge plugs are the most reliable and commonly used method to provide adequate isolation between perforated zones. Fracture baffles are concentric baffle rings that are run as part of the casing string and are placed between individual target zones [*Brown et al.,* 2000; *Robert and Rossen,* 2000]. Isolation is achieved by dropping balls or running wire line plugs that seat in the baffle rings. Some of these techniques are limited to vertical or near-vertical wells.

There is always an economic trade-off between the number of fracture treatments and the ability to achieve effective fluid diversion. In cased wells, there are several perforation schemes that can help to create good vertical coverage (refer to Figure 4.1) [*Minner et al.,* 1996]:
1) Limited entry perforation distributions are used to obtain simultaneous fluid flow through certain perforations by creating a large frictional pressure drop across these perforations [*Elbel and Britt,* 2000]. The high frictional pressure drop is designed to offset the stress differences between target zones to enhance injection into all the perforated target zones [*Lagrone and Rasmussen,* 1963]. However, a sufficient injection rate must be available to maintain this high differential pressure across the perforations, both initially and as the perforations are eroded by proppant.

2) Unrestricted entry perforating using a long interval, somewhat similar to the use of an open hole interval. There is considerably less initial control over fracture treatment distribution, as differences in closure stresses along the depth of the well dictate where fracture growth occurs. Ball sealers are sometimes used in conjunction with unrestricted entry treatments. Ball sealers are small spheres that are added to the fracturing fluid to seal the perforations on the inside of the casing that accept the largest quantities of fluid [*Robert and Rossen,* 2000]. However, their sealing efficiency is very unpredictable.
3) Point source perforation distribution is used to obtain fluid flow through only very few perforations in a single, very limited part of the well [*Underwood and Kerley,* 2000]. This tends to produce very few fractures or only a single fracture. While it does not suffer from adverse fluid flow distributions and difficult proppant placement, it could stimulate only a very small target zone due to limited height growth because of fracture containment.
4) Multiple point source / limited entry perforating is a hybrid strategy that consists of limited entry (≥ 500 psi perforation pressure drop) implemented in the form of, e.g., three point source perforation intervals. This strategy would have the advantage of point source perforations of initiating fewer fracture multiples at the well bore, resulting in larger fracture dimensions and greater proppant concentration per fracture, and covering a larger interval using a single treatment.

In some cases where it is impossible to achieve the required high injection rates during a fracture treatment, high pressure or rates can be utilized during the perforation process. Extreme overbalance perforating is the application of a very high overbalance pressure during the perforating process, or the very high pressure surging of existing perforations [*Brown et al.,* 2000]. Pressurized liquid and / or gas (usually nitrogen, N_2) is utilized to inject various fluid systems into the formation. The primary objective is to create hydraulic fractures either as a pre-hydraulic fracture treatment or as a dynamic fluid diversion [*Handren et al.,* 1993; *Dees and Handren,* 1993]. Propellant-assisted perforating combines perforation breakdown with propellant in a single tool and operation [*Loman et al.,* 1996]. The perforating assembly has a propellant sleeve over a conventional perforating gun assembly. When the guns are detonated, the propellant sleeve is ignited, instantly producing a burst of high-pressure gas. The gas enters the perforations, breaks through any damage around the perforation tunnel, and creates short fractures near the well.

Although the multiple point source strategy can cover as much as ~ 300 ft of reservoir thickness per treatment, this is still not enough to effectively treat the long open hole intervals in EGS with a thickness of more than 1,000 ft in a single treatment. Therefore, this strategy requires multiple treatments separated by bridge plugs or sand plugs, making it a somewhat time-consuming process. In areas where this process is often used, as many as six fracture treatments can be performed during a single day. In some areas, up to 15 separate fracture stages are pumped in a single vertical well.

Several fracturing technologies with coiled tubing exist in the oil industry. One technique involves pumping the fracture treatments through a coiled tubing string. For this procedure, perforations are shot along the entire well first. Then, a bridge plug-packer assembly run on coiled tubing is used to place proppant into a selective set of perforations [*Zemlak et al.,* 1999]. The assembly is quickly pulled up after a fracture treatment, to conduct the fracture treatment in the next shallower set of perforations. This technique has the advantages that it isolates the wellhead and tubulars from treating pressures, and reduces execution time compared to stimulations in stages. However, because of the relatively small diameter of the coil, there are significant limitations to the slurry injection rates and pressures. In areas where this process is often used, as many as 20 fracture treatments can be completed during a single day. A second coiled tubing fracture technique involves running a jetting tool on coiled tubing into an unperforated well [*Hejl et al.,* 2006]. Perforations are cut into the casing by first pumping a low concentration of proppant slurry through the jetting tool. The propped fracture treatment is then pumped down the casing or coiled tubing annulus. After the fracture treatment is completed, the fractured perforation interval is covered with a sand plug to isolate it from the next fracture stage performed up the hole. After the fracture treatments are completed, the coiled tubing string is used to clean out the well. As many as eight fracture stages have been performed per day.

4.2.2 A Hybrid Alternative - Uncemented Slotted Liners in Horizontal Wells

Reducing cost in the oil industry has shown a tendency in some areas to omit cementing of a horizontal section, because this was often prone to technical difficulties, e.g., due to the presence of channels at the top of the annulus [*Minner et al.,* 2003; *Wright et al.,* 1996], and stage isolation often failed.

To enable at least some degree of selective fracture treatments or remedial work within the (e.g., horizontal) target zone, the liner has multiple point-source limited entry perforations in the open hole (uncemented) section. Liner perforations are either mechanically installed on the liner before running in the hole, or conventionally shot once the liner is in place downhole. An unrestricted slotted liner does not provide good diversion behind the pipe into the open hole annulus. With the point source perforation strategy, the hope is that the higher local pressure at each perforation cluster initiates a fracture system nearby.

A lateral of significant length can be effectively stimulated using this method in the Barnett Shale [*Fisher et al.,* 2005; *Fisher et al.,* 2004]. However, the location of the created fractures is not strongly correlated to the location of the clusters of perforations. That is, the fracture network grows where in-situ conditions along the horizontal lateral dictate, and not exactly where the perforations are shot along the uncemented liner.

In the Rose Field, a pioneering area for using the uncemented slotted liner concept, surface tilt mapping showed transverse fracture growth at the toe and heel of the well, with a large longitudinal component in the central portion of the lateral [*Minner et al.,* 2003]. Injection rates of 60 to 75 bbl/min were required to distribute fluids across the entire lateral.

Uncemented slotted liners are common in geothermal wells that are open to unstable formations. Selective slotting opposite lost-circulation zones has been used. However, in-flow or out-flow points are not only those zones that make themselves known during the drilling process. As in oil and gas wells, annular flow behind the liner is common, and it is unlikely that a particular zone in an EGS well could be successfully stimulated through an uncemented slotted liner.

4.2.3 Zonal Isolation and Height Diversion Challenges - Open Hole Wells

Wells used in EGS applications most often are completed as an open hole well through the section of interest. The open hole may have a length of ≥ 1,000 ft. The main limitations of open hole wells are:
1) The well is unsupported and may collapse; and
2) selective fracture treatments or remedial efforts within the target zone are more difficult.

Effective zonal isolation in open hole wells is virtually impossible. However, packers for open hole wells are available [*Freyer and Huse,* 2002]. The packers are configured with one large element that can be deformed easily to contact the uneven surface of the drilled hole, yet retain strength and sufficient integrity to withstand the anticipated differential pressures and temperatures. In applications where treatment pressures stay below fracturing pressures open hole packers could be successful, because the pressure differential across the packer would be more moderate. However, the use of these packers is generally not recommended for fracture treatments, as the fracture system typically initiates along the open hole section, and has a tendency to follow this open hole section along and past the packer. In addition, it is common that the fracture could initiate at the packer due to the compressive force exerted by the packer on the borehole wall.

To obtain height coverage during a stimulation treatment, diversion is therefore more difficult in the open hole. In the following section, we discuss a variety of techniques that are sometimes used to improved fracture height coverage over a thick target zone.

Chemical diversion can be conducted by adding chemicals to fracturing fluids that temporarily seal the perforations or fractures in an open hole well that accept most fluid flow. Chemical diversion includes:
1) Bridging materials (e.g., rock salt and benzoic acid flakes),
2) wax beads, and
3) foams.

Bridging materials (e.g., rock salt, benzoic acid flakes) are used to bridge in perforations and / or pre-existing fractures [*Brown et al.,* 2000]. They share many of the limitations of ball sealers and sand packs in that they are difficult to accurately place and keep in place.

Wax beads can be reliably placed in the cooled-down, near- well area during stimulations [*Johnson and Brown,* 1993]. After completion of the treatment, they melt as the bottom-hole temperature builds up [*Johnson and Brown,* 1993]. The wax beads need to have a melting point that is less than the bottom hole static temperature, and greater than the surface fluid temperature [*Johnson and Brown,* 1993]. The benefits of wax beads are [*Bell et al.,* 1993]:

1) They adhere to other wax particles;
2) they deform under pressure;
3) they are soluble in produced hydrocarbons fluids;
4) they are non-hazardous;
5) they are readily available at low cost; and
6) wax beads with differing melting points are available for treatments in various thermal environments [*Johnson and Brown,* 1993].

However, wax beads within blocked-off intervals can loosen or melt during the course of a treatment, and thus act as a source of pressure relief [*Johnson and Brown,* 1993]. Wax beads have been used for water fracturing open hole wells in naturally fractured chalk formations [*Bell et al.,* 1993].

Foams (e.g., with nitrogen gas) [*Logan et al.,* 1997; *Zerhboub et al.,* 1994] have been used particularly in cases where other diversion techniques are impractical or less efficient. Foams have the additional advantage of good cleanup with little or no potential for damage to the formation. The ratio of gas to fluid depends on the bottom-hole conditions during the treatment.

Water fracturing with alternating gel slugs [*Aud et al.,* 1994; *Hainey et al.,* 1995] utilizes lower pumping rates combined with higher viscosity fracturing fluids to minimize the creation of a complex near well bore geometry [*Elbel and Britt,* 2000; *Robert and Rossen,* 2000]. At the same time, the use of alternating gel slugs can ensure fracture growth in other zones. Very high injection rates are also used (> 100 bbl/min is common in horizontal well stimulations) in uncemented slotted liners to maximize zonal coverage of a fracture treatment.

The hydra-jet technique is the creation of closely spaced, undamaged jetted tunnels in open hole wells using a jetting tool at the end of a coiled tubing. Creation of the jetting tunnels is immediately followed by a fracture treatment by switching over from injection though the jet tool alone to slurry injection though the annulus [*Gilbert and Greenstreet,* 2005; *East et al.,* 2004; *Hoch et al.,* 2003]. The benefits of this technique are:

1) Reduction of the cost and time of completion;
2) the creation of fewer fractures, or even only a single dominant fracture plane; and
3) few near-well connectivity problems between the well and the hydraulic fractures.

4.2.4 Alternative Techniques for Lateral Diversion

Even if it is possible to stimulate effectively a target zone along the entire height of the well, then the created surface area could be insufficient for economic heat transfer. A solution to this shortcoming is to create more surface area in a lateral direction away from the main or initially created fracture system, and thus, as shown in Figure 4.2, to create an extremely complex fracture system as opposed to a simple fracture system.

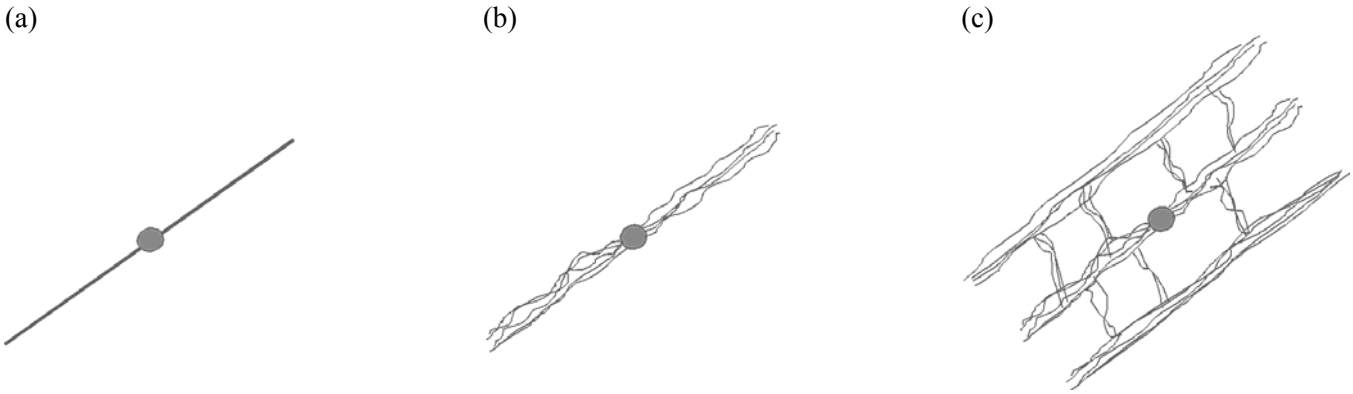

Figure 4.2: Examples of increasing fracture complexity: (a) Simple (most common), (b) complex, and (c) extremely complex (relatively rare) [*Fisher et al.,* 2002].

A more extensive lateral fracture system can be obtained manually through staged fracture treatments in deviated or horizontal wells [*Goktas and Ertekin,* 2000]. Horizontal wells are generally aligned either along the preferred fracture plane for longitudinal fractures, or perpendicular to the preferred fracture plane for transverse fractures [*Elbel and Britt,* 2000; *Lietard et al.,* 1996; *Pope and Handren,* 1992].

Many alternative techniques to enhance lateral diversion utilize some type of alternating of a specific parameter that controls fracture growth:
1) Alternating slurry injection rate;
2) alternating gel viscosity;
3) alternating proppant stages; and
4) alternating pump-ins / shut-ins.

Alternating slurry injection rate and fluid viscosity can potentially result in switching between mode I (opening mode) and mode II (shearing mode) fracture growth. In particular, fractures may grow along the plane of maximum shear stress at low rates or when injecting fluids (or gases) with very low viscosity. However, fractures may grow perpendicular to the least principal stress at greater rate [*Weijers et al.,* 1999].

Propellant stimulation may also create a more complex fracture network as initiation pressures typically temporarily exceed all principle stress components. Propellant, which has been used in geothermal wells, is conveyed on wire line and results in improved penetration (versus regular perforating) into the formation and greater connectivity of the reservoir fluids to the well, and minimizes formation damage during perforating and fracturing. However, the extent of the stimulation is very limited to only tens of feet away from the well bore, and must therefore be followed with a large size fracture treatment.

Proppant slugs are small volumes of low concentration proppant slurries that are pumped ahead of or during a fracturing treatment [*McDaniel et al.,* 2001a; *McDaniel et al.,* 2001b; *Stadulis,* 1995; *Cleary et al.,* 1993]. Their purpose is to screen out multiple-fractures such that they cease accepting fluid and propagating. In areas where there is complex fracture growth and natural fractures (e.g., the Barnett Shale), proppant slugs are believed to enhance fracture complexity. The proppant slugs can be pumped in various sizes, ranging from the actual proppant used in the treatment to 100 mesh sand.

Alternating proppant stages and the implementation of pump-ins / shut-ins relies on stress shadowing for lateral diversion. Stress shadowing [*Warpsinki and Branagan,* 1989] is the perturbation of the stress in the reservoir due to open hydraulic fractures. The rate at which this stress perturbation declines for an increasing distance away from the face of the fracture is controlled by the smallest aerial fracture dimension (i.e., the height or length) [*Fisher et al.,* 2004]. The presence of proppant during injection can create a permanent fracture opening on proppant, and shut-in periods between fracture treatments can ensure that this proppant is locked in place to create a stress shadow. Multiple fracture treatment stages in

a drill cuttings disposal project [*Griffin et al.,* 2000] showed that a fan-like fracture system with various fracture orientations can be achieved when fractures are given the time to close on solids between treatments.

These stress shadows have two major impacts [*East et al.,* 2004; *Fisher et al.,* 2004]:
1) The increased compressive stress near a fracture tends to close-off or inhibit the initiation of nearby parallel fractures which provides a diversion mechanism along the well; and
2) the increase in the magnitude of the local minimum stress tends to encourage fracture growth in orthogonal directions.

These two effects are beneficial for creating extensive and complex fracture networks for EGS. If multiple fractures are created from a single well (e.g., transverse fractures from a horizontal well, or fractures intersecting a vertical well at different depths [*East et al.,* 2004]), then these effects could be more significant. Stress shadowing has been observed with direct fracture diagnostics in naturally fractured, low permeability reservoirs [*East et al.,* 2004; *Fisher et al.,* 2004]. Stress shadowing can also be used to create height growth barriers by fracturing upper and lower bounding zones before the main hydraulic stimulation or by proppant banking, in particular in water fracturing.

Re-fracture treatments also rely on stress shadowing, as observed by direct fracture diagnostics [*Wright and Weijers,* 2001; *Siebrits et al.,* 2000; *Wright and Conant,* 1995]. Re-orientation in re-fracture treatments [*Wright et al.,* 1994a; *Wright et al.,* 1994b] can be caused by changes in the state of stress due to the presence of open hydraulic fractures or changes in pore pressure distribution in the reservoir. The benefits of re-fracturing treatments can be significant, as a new fracture treatment in a previously stimulated well accesses new reservoir if the fracture re-orients perpendicular to the initial fracture direction. In many instances in low permeability reservoirs, this has led to re-fractured wells that produce at almost the initial rate after the first completion, which was performed many years before the re-fracture treatment.

4.3 Commonly Used Zonal Isolation and Diversion Techniques

This section describes cement sheaths (section 4.3.1 below), fracture placement control (section 4.3.2 on page 64), mechanical bridge plugs (section 4.3.3 on page 64), sand plugs (section 4.3.4 on page 64), fracture baffles (section 4.3.5 on page 64), bridge plugs and packers (section 4.3.6 on page 65), diversion (section 4.3.7 on page 65), limited entry (section 4.3.8 on page 66), application to EGS (section 4.3.9 on page 67), horizontal drilling (section 4.3.10 on page 67), hydra-jet fracturing from horizontal wells (section 4.3.11 on page 69), stress shadows (section 4.3.12 on page 71), and alternatives to conventional fluid diversion (section 4.3.13 on page 73).

4.3.1 Cement Sheath

The cement sheath must provide zonal isolation during both production and stimulation operations [*Economides and Nolte,* 2004]. For a producing well, the cement seal between the pipe and formation must be tight to prevent fluids from flowing through the annular area. The permeability of a set Portland cement of normal density is in the low micro Darcy range. If the cement does not bond perfectly to either the pipe or the formation and a small channel remains, then the effective cement permeability can be significantly increased. Large permeabilities may result from channel widths that are quite small [*Nelson,* 1990]. For example, a channel width of only 1.4×10^{-4} in is sufficient to create an effective cement permeability of 1,000 mD. Channel permeabilities of this order may allow significant cross flow between zones.

During hydraulic fracturing these small channels, or micro annuli, are relatively insignificant. The effective cement permeability does not create a high leakoff risk for the fracturing fluid within the annulus. A leakoff rate for a micro-annulus is less than 0.024 bbl/min. If major channels within the cement can be avoided, then containment of the fracturing treatment should be possible.

The effects of fracturing pressures on the adhesion tension between the cement and casing or the cement and formation are not clearly understood. Consequently, the resulting condition of the cement sheath following hydraulic fracturing is difficult to predict. Sonic logs run after fracturing treatments typically indicate that the cement bond (i.e., hydraulic seal) across the fractured interval is destroyed. However, the bond farther up-hole remains intact. The loss of the cement bond across the fractured interval probably does not affect the placement or containment of the fracturing treatment. Cement of

relatively low compressive strength should prevent the fracture from migrating between the casing and the formation. However, alteration of the cement bond may occur during the treatment. Any failure of the hydraulic seal may result in a micro annulus that leads to the cross flow of reservoir fluids. This is somewhat applicable to open-hole EGS wells where it is desirable to avoid breaking down the cement at the casing shoe leading to the development of a micro annulus for water migration, potentially stimulating a shallower interval (possibly in cooler rock). At Soultz and in the Cooper Basin heavy brine slugs were used at the start of the stimulation to avoid this problem and to generate more permeability deeper in the well.

4.3.2 Fracture Placement Control

The most reliable method of controlling the placement of fracturing fluids is to limit perforations to a single zone [*Economides and Nolte,* 2004]. When several zones of a well are to be stimulated, the individual zones can be isolated from one another and stimulated individually. This can be accomplished through progressive perforation and stimulation. After a fracturing treatment has been placed in the first zone, it is isolated, and another zone of interest is perforated and treated in another single stage. Of course, this methodology works best when the deepest zone is completed first and subsequent zones are individually stimulated by working up-hole. Another effective multiple zone stimulation technique is coiled tubing-conveyed treatment.

4.3.3 Mechanical Bridge Plugs

Several mechanical methods are available to provide adequate isolation between perforated zones [*Economides and Nolte,* 2004]. The most reliable method is the use of mechanical bridge plugs, which can be run on tubulars or wire-line. Bridge plugs that are run on tubulars are retrievable and can be moved and reset several times. Wire-line bridge plugs cannot be moved once set, and their removal typically requires milling after the treatment. These bridge plugs are used when several treatments are attempted in one day or rig-less completions. They can be run in the hole quickly, and cleanout trips are not required between stages. The retrievable bridge plugs are used when zones are individually tested before another zone is opened. Any excess proppant must be circulated out of the hole before the tool is moved to prevent the proppant from sticking the tool. A typical treatment involves perforating the bottom zone, performing the hydraulic fracture treatment, and providing zonal isolation by setting a bridge plug just above the stimulated interval. The next zone is then perforated and fractured.

4.3.4 Sand Plugs

A similar method of isolation can be achieved with sand plugs after the fracturing treatment [*Economides and Nolte,* 2004]. The volume of sand necessary to cover the perforated interval is added to the casing. The sand plug is tested by applying pressure to the casing, and then the next zone is perforated and stimulated. Once all zones have been fracture stimulated, the sand can be circulated out of the well with either conventional or coiled tubing. The amount of sand required above the top perforations is generally small and can be calculated by applying Darcy's law to linear flow. For example, 20/40 mesh sand with a thickness of 10 ft in casing with a diameter of 5½ in creates a pressure drop of more than 6,000 psi for a 40 cp linear gel leaking through the sand pack at 0.5 bbl/min. If the permeability of the sand pack must be reduced to prevent flow through the pack, then a mixture of sand meshes can be used.

4.3.5 Fracture Baffles

Mechanical diversion can also be accomplished with fracture baffles [*Economides and Nolte,* 2004]. Fracture baffles are run as part of the casing string and are placed between individual producing zones. After the lowest interval is perforated and fractured, a ball is dropped down the casing. The ball seats on the baffle and prevents fluid flow below this point. The next zone can then be perforated and fracture stimulated. When multiple zones are isolated with baffles, care must be taken to place the baffles so that the baffle openings progressively decrease in size from top to bottom (i.e., the bottom fracture baffle has the smallest diameter opening). The first ball must be able to pass through the upper baffles and still seat in the bottom baffle. Similarly, the second ball must pass through the upper baffles and seat in the second baffle from the bottom, and so on. All baffles have an inherent weakness owing to the limited area available in the casing coupling. The pressure differential across the baffle should be limited to the specifications of the manufacturer.

4.3.6 Bridge Plugs and Packers

When completion practices do not allow the progressive order of fracturing to proceed from the lowest zone of interest up to higher intervals, bridge plugs must be used in conjunction with packers [*Economides and Nolte,* 2004]. The combination of a bridge plug and packer to straddle an interval provides an extremely reliable method of isolation, and with coiled tubing enables rapid one-day multiple-stage completions. These retrievable tools can easily be moved to cover any interval, provided the unperforated casing is sufficiently long to provide a packer seat. However, caution should be taken when open perforations are present above a packer because of the possibility of proppant entering into the annular area if the fracture reaches the open perforations. Small quantities of proppant on top of a retrievable packer can stick the tool-string.

4.3.7 Diversion

Diverting techniques are used in some cases to control the placement of fluid and slurry into the zones of interest [*Economides and Nolte,* 2004]. A diversion treatment may be advantageous compared to separately isolating individual zones because all the treatments can be pumped continually, and they are therefore more economical and time efficient. Although initially attractive, controlling placement through diversion carries many inherent risks. At a minimum, drilling damage can be bypassed. However, optimum stimulation of the formation cannot be achieved by use of diverting materials.

The use of bridging materials (e.g., rock salt and benzoic acid flakes), as the diverting medium usually results in an over-flushed fracture. Some of the bridging material enters the fracture and displaces the near-well proppant before diversion is achieved at the perforations. Conductivity near the well could be minimized, resulting in a choked fracture with limited production capabilities.

This problem is pronounced when high-viscosity crosslinked fluids are used for fracturing. These fluids are highly efficient at proppant transport and carry the proppant away from the perforations as they are displaced by the diverter slurry. If the fluids used in the treatment are of low viscosity and create an equilibrium proppant bank, then the diverter over-flush may not be a significant problem. With this type of proppant transport, the proppant bank is not destroyed during the over-flush of the diverter.

The application of conventional ball sealers to divert fracturing stages has many of the same inadequacies as bridging materials. It is extremely difficult to predict the seating efficiency of ball sealers. This problem is even more pronounced after proppant has eroded the perforations. In addition, the ball sealers must be introduced to the fluid while proppant is being added. The presence of proppant reduces the seating efficiencies. However, it is impossible to predict by how much. If the ball sealers are introduced to a clean fluid stage immediately following the proppant stages, then the clean fluid over-flushes proppant away from the perforations until the balls finally seat.

Designing a schedule that ensures precise proppant placement into multiple zones with diverter stages is almost impossible. When several zones are open to the well, it is extremely difficult to calculate which zone fractures first. The zones are almost surely different in size and have slightly different rock properties. Because it is not practically possible to know which zone fractures at a given time, most hydraulic fracturing schedules by use of diverters are simply divided into even stages. The uneven in-situ parameters cause slurry placement in the separate zones to create fractures of uneven geometries and conductivities.

It is also difficult to design and size the diverter stage so that all perforations in the zone being fractured become plugged and the other zones remain unaffected by the diverter. If a diverter stage is too large, then it may plug the unfractured intervals before the fracturing slurry designed for that stage has been pumped. If the diverter stage is too small, the first zone may not be adequately plugged and the original fracture may continue to accept fluid. Portions of the pad fluid intended for the second interval over-flush the proppant pack away from the immediate well. At the same time, the second zone is losing critical volumes of pad fluid, which may result in an early screen-out.

4.3.8 Limited Entry

Limited-entry treatments are designed to place fracturing fluids into multiple zones simultaneously [*Economides and Nolte,* 2004]. The limited-entry technique uses the pressure drop created across the perforations during pumping to divert the fracturing fluid into several different perforated intervals. Generally, a pressure differential of 500 to 1,000 psi is considered necessary to provide adequate control over fluid placement.

The total flow of fluid entering a given zone is restricted by controlling the size and number of perforations in that interval. The elevated pressure drop at the perforations forces fluid to go to another zone. This diversion technique has proved popular because of its simplicity and economics. The diversion does not require expensive tools, and it does not require running and retrieving tools or making cleanout trips. The only cost for applying this type of diversion is the excess hydraulic horsepower required to pump the treatment at higher pressure.

If a limited-entry treatment is not applied correctly, then each producing zone may not receive adequate treatment. Several factors must be considered when designing a limited-entry treatment. The number and size of perforations are calculated to divert the pad fluid. Smaller zones do not require as much fluid or proppant and therefore require fewer perforations. Some zones may require fewer than five perforations to control flow into that section. With a limited number of perforations available, the importance of the breakdown procedure becomes obvious. The loss of one or two perforations can significantly alter the flow distribution into all the zones.

Introducing sand into the fracturing fluid quickly erodes the perforations and changes the corresponding flow coefficient for each perforation. For example, after only 10,000 lbm of proppant, the pressure drop across the perforations reduces greatly. Therefore, diversion of the pad fluids could be successful. However, diversion of the proppant-laden stages cannot be presumed to be successful. After the perforations have been eroded, one zone is most likely to accept most of the fluid.

An accurate stress profile of the well is necessary to design a successful limited-entry treatment. Each zone has a different fracture gradient and therefore they break down and fracture at different pressures. If great contrast exists among the fracture gradients of individual zones, then the perforation scheme must be designed to reflect this difference.

Limited-entry designs usually do not consider the net pressure effects of the fracture. It is common for a fracturing treatment to create a net pressure of more than 500 psi. An imbalance in net pressures between zones can effectively negate the perforation pressure drop. Fracture height and Young's modulus are two parameters with a major effect on net pressure [*Economides and Nolte,* 2004]. Both parameters should be closely evaluated before the design of a limited-entry treatment.

The net pressure in the fracture is inversely proportional to the gross fracture height. Large zones have smaller net pressures and therefore tend to accept a disproportionate amount of fracturing fluid. Very small zones most likely remain unstimulated because they rapidly build high net pressures and do not accept significant volumes of fracturing fluids. The global Young's modulus of the zone has a similar effect: the greater the Young's modulus, the narrower the fracture and the higher the net pressure.

The final parameter with significant impact on the successful placement of fractures by use of the limited-entry technique is fluid leakoff. The size of the zone and the rate the fluid is pumped into the zone directly influence the fluid efficiency and hence the fracture penetration. With several zones accepting fluid at one time, the total pump rate into any one interval could be quite low. Zones with the lowest pump rates generally have poor fluid efficiency, which may result in an early screen-out.

Accurately placing proppant into multiple zones with limited entry is extremely difficult. Fracture penetration and width are most likely highly irregular among zones. Smaller zones may not accept any significant amount of fluid. The increased producing capabilities of several stimulated zones resulting from isolation and separate treatments should be carefully examined and weighed against the economic benefits of a limited-entry treatment before the fracturing strategy is selected. This could be analogous to a long open-hole EGS completion with several conductive zones intersecting the

well. In this case, if the characteristics of each zone were known to some extent, then the limited entry procedure could be used to force fluid into one set of zones or another.

4.3.9 Application to EGS

In most geothermal wells, long open-hole intervals are used to extract heat from the Earth. In such wells, however, it can be very difficult to distribute fluids uniformly along the well during stimulation. This is also a major challenge in the oil and gas industry, where impressive production gains can be made if a thick reservoir is effectively covered with hydraulic fractures over the entire height of the target interval. Direct fracture diagnostics have demonstrated that in many cases, coverage of the target reservoir is less than ideal.

Many techniques have been developed in the oil and gas industry to improve fluid diversion over a target interval, and to create some degree of fracture penetration at all depths along the reservoir. We provide an overview of these techniques. We also evaluated whether these can be used in EGS applications. Some of these techniques include (but are not limited to):

1) Setting casing and shooting perforation clusters or distributed limited entry perforations: This requires stimulating through casing perforations, which has not been demonstrated to be effective so far in either conventional hydrothermal or EGS.
2) Use of ball-out treatments to divert fluid flow into zones previously not stimulated by blocking perforations that have taken fluid: This is similar to the baffle balls. Consequently, they are only applicable to cased holes, and therefore of limited usefulness for EGS.
3) Methods such as SurgiFrac by Halliburton, open hole packers (e.g., PackersPlus by Packers Plus Energy Services) or StimGun by CoreLab: These techniques aim to achieve flow diversion while fluid contact with the reservoir is not physically restricted. They also aim for local pressurization to stimulate only a small target zone.
   a) For SurgiFrac, sand-laden fluid that is pumped through a hydra-jet tool impinges on the formation and creates a cavity. As the cavity is formed, pressure on the bottom of the cavity increases, which eventually initiates a fracture? Annular fluid is pulled into the fracture, helping to extend it.
   b) For StimGun, a cylindrical sleeve of gas is used that generates propellant that is simply slid in place over the outside of conventional hollow steel carrier perforating guns. The propellant is ignited by the pressure and shock wave of the shaped charges as they penetrate the gun, casing, and formation. This approach has the disadvantage of creating only limited extent of the stimulation (10 ft to 30 ft).
   c) Open-hole Packers (e.g. PackersPlus) have proven to be a feasible completion technique in recent horizontal well completions in shale and tight sandstone reservoirs. A pre-configured string of packers and ports is set in the open hole section. The packers provide zonal isolation, while balls or darts are dropped to open and close fracture stages. Balls are dropped at the end of each fracture treatment stage, thereby opening the port for the next stage. Consequently, this type of treatment is continuous and multiple fracture stages can be performed in one day. If components of the system and packers can withstand the high temperatures, then this may be a viable technique for EGS. Limitations and risks for this method are the same as for any other open hole packer configuration, where zonal isolation may not be guaranteed if fracturing takes place around the packers.

4.3.10 Horizontal Drilling

The success in outlying areas of the Barnett Shale has been greatly enhanced by the increased use of horizontal completions [*East et al.,* 2004].

Motivation

It is recognized that horizontal wells provide greater well contact with a greater volume of reservoir rock than vertical wells. Hence, they provide the ability to improve the economics of development [*Fisher et al.,* 2004]. Horizontal wells have also been used in an attempt to spread the energy of hydraulic fracturing over a greater area. This theoretically decreases the likelihood of excessive growth of the height of the fracture into unfavorable intervals. Additionally, some areas in the Fort Worth Basin present special challenges regarding surface locations from optimum well density to drain adequately areas with low permeability. With the very active drilling activity, in many cases horizontal completions are

necessitated by urban considerations (e.g., by the use of additions, surface access, and landowner restrictions, in almost every county) [*East et al.,* 2004]. Consequently, pad drilling of horizontal wells from a minimum number of surface locations is a viable option to reduce the footprint caused by multiple vertical wells, and to retain the ability to contact large areas of this productive resource.

Configuration

Most horizontal wells in the Barnett Shale have been drilled in the direction of the least principal horizontal stress, toward the NW-SE direction. In contrast, the maximum horizontal stress direction is NE-SW. Consequently, fracture networks develop transverse to the wells of the horizontal lateral. This allows a single horizontal well to replace multiple vertical wells, depending upon the length of the lateral. The initial sizes of the stimulation treatment were designed to cover the same fracture pattern that would have been achieved with the drilling of multiple vertical wells over the same area. Lateral lengths are largely determined by how many undrilled locations can be accessed with the horizontal well. Horizontal well lengths are typically 2,000 to 3,000 ft. They may replace two to more than three vertical wells.

A comparison of ideal fractures resulting from different orientations of vertical and horizontal wells with respect to the horizontal stress directions is displayed in Figure 4.3.

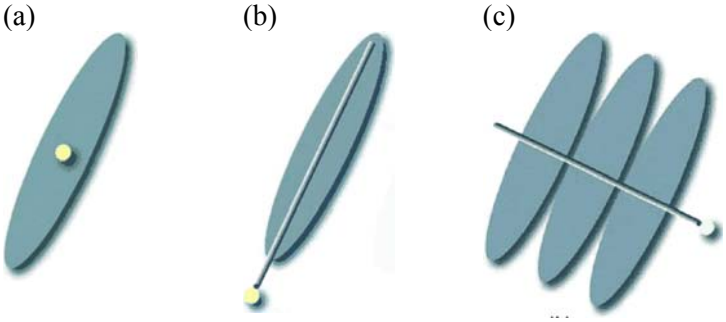

Figure 4.3: Expected fracture orientations for: (a) vertical, (b) horizontal longitudinal, and (c) horizontal transverse wells [*East et al.,* 2004; *Fisher et al.,* 2004].

Most formations that consist of hard rock with horizontal wells are drilled similar to the horizontal transverse geometry as displayed in Figure 4.3c. This generates fractures that cut across the well. Each transverse fracture simulates a single vertical well. In environments with greater permeability, the horizontal longitudinal geometry as displayed in Figure 4.3b might be preferable.

Even with hydraulic fracturing from vertical wells, the degrees of simplicity or complexity of the nature of hydraulic fracturing varies. This can range from a simple single fracture to extremely complex (Figure 8.3 on page 105). Additionally, a fracturing treatment from a horizontal well often behaves differently than it would from a vertical well in the same reservoir. Generally, the fracture growth in a horizontal well is more complex than in a vertical well, with more fracture planes and more development of multiple fractures. This is the case even in environments where vertical wells exhibit only simple fractures.

Hydraulic fracturing from horizontal wells raises the following issues:
1) cemented versus un-cemented liners;
2) single stage versus multiple stages;
3) diversion and effective coverage of multiple stages along an un-cemented and a cemented latera;
4) hydraulic fracturing of the Upper and Lower Barnett Shale when the well is placed only in the Lower Barnett Shale;
5) containment of fractures within the Barnett Shale interval;
6) direction of orientation of the lateral from previous experience with preferred hydraulic and natural fracture orientations; and

7) the extent of the lateral.

Application to Barnett Shale

Because fractures from vertical wells in the Barnett Shale tend to be very complex [*Fisher et al.,* 2002], the treatments from horizontal wells could be expected to exhibit extreme variances, depending on local geology, natural fracture characteristics, and stress shadowing.

4.3.11 Hydra-jet Fracturing from Horizontal Wells

From the early inception of hydra-jet hydraulic fracturing, one of its primary features is the undamaged nature of the jetted tunnels, and the closely clustered placement of these perforations [*East et al.,* 2004]. This helps to create fewer, or just a single, dominant fracture plane. In addition, near-well connectivity problems between the well and the hydraulic fracture seldom exist. The jetting tool assembly is then moved to the next desired location and another single-fracture system is created, with a result similar to that illustrated in Figure 4.4. The technique has demonstrated the ability to improve the placement of fractures by the stimulation treatment fluid in horizontal well completions. It is suggested that it can reduce the time and cost of completion, or enhance the economic recovery (ER) by improving the coverage over the reservoir. Obviously, to accomplish both is the ultimate goal. However, in naturally fractured reservoirs, water fracturing treatments open, or dilate, a great number of these natural fractures. Then, a single dominant fracture plane may have less value for the effective stimulation of the production of these reservoirs. The Barnett Shale reservoir could be the consummate example of such a reservoir.

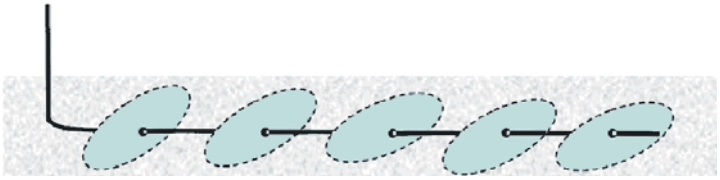

Figure 4.4: Typical multi-stage hydraulic fracturing result of hydra-jet stimulation treatment from single, horizontal well. No mechanical isolation is needed [*East et al.,* 2004].

Injection via Tubing Annulus

For hydra-jet fracturing, a water fracturing treatment with a high rate of injection is placed where the desired rates of injection are usually a factor of 2 to 5 greater than what would be used for a treatment with gelled fluid in the same reservoir [*East et al.,* 2004]. To increase meaningfully the quantity of sand that can be placed in a large-volume hydra-jet fracturing treatment, without concerns for tool or jet failures, the job design would be need to be modified. Under current consideration is a job design where sand is pumped down the annulus, at least during portions of each hydraulic fracturing stage (i.e., Halliburton's CobraMax). Typically, only 20% to 30% of the total injection rate, and all the proppant, is pumped through the annulus and out of the jet nozzles. However, when total job volumes may exceed 24,000 bbl, the accompanying sand volumes of 250,000 to 350,000 lbm can present a challenge to the life of the jet nozzles in the bottom-hole assembly (BHA). Hence, this procedure normally has not been a viable consideration for horizontal applications of hydra-jet hydraulic fracturing. However, for completions in the Barnett Shale with no open perforations above the BHA, and with very high rates of injection through the annulus, it is considered a very realistic design change. This alteration of the job design could greatly increase the quantity of sand placed with essentially no increase in time or cost of the job other than for the added sand used.

The net result of changing the technique to pumping most of the rate through the annulus is lower overall horsepower requirements than when most of the rate is through the tubing string. With most of the rate of injection through the annulus, conventional tubulars can be used, while total hydraulic fracturing rates as high as 65 to 70 bbl/min are achieved. If the annulus above the BHA is open to the reservoir, then a potentially negative side effect is that greater pressures may occur in the annulus between the heel and the BHA where generally fractures should not form. This effect is not present in a well

with only blank pipe, where the only perforations are those created by hydra-jet hydraulic fracturing before each fracturing stage. To date, non-perforated casing, cemented or un-cemented, is the only way hydra-jet fracturing has been used successfully in a Barnett Shale well. The hydra-jet fracturing technique has been used successfully in an open-hole completion without liner in another reservoir [*Sneddon and Elliott,* 1946].

Application to Barnett Shale

In the Barnett Shale, hydra-jet fracturing has been applied only for a few wells. In this reservoir, the accurate determination of the values of economic recovery (ER) with data for production during short times is difficult [*East et al.,* 2004]. However, it seems that with the early attempts of hydra-jet fracturing in these wells, the response of the production was not increased to the degree that was expected (i.e., from the apparent improvement in the coverage for the reservoir that was observed in the results of fracture mapping). Evidence of the improved efficiency of the placement of the treatment fluid is offered by two case history wells, where the analysis of microseismic fracture-monitoring data was collected from an offset well. The data offers comparisons between conventional water fracturing stimulations with hydra-jet fracturing treatments with twenty and twelve stages, both in completions with both cemented and un-cemented liner.

Hydra-jet fracturing appears to be very successful in generating significant activity of hydraulic fracturing, and giving equal or superior coverage along the entire lateral. This could be useful for initiating fracture network stimulations along a long open-hole interval in EGS. However, these early wells may or may not give the lower rates of the decline of production that were expected from these treatments following the observed high degree of response and effective coverage along the lateral. One shortcoming of the very early applications of hydra-jet fracturing could be the smaller relative volumes of sand placed. Early jobs also used great numbers of stages and relatively lower volumes of fluid than most horizontal completions to which they are now being compared. Some of the later treatments, for which data of fracture mapping is not yet available, have used fewer, greater stages. It is still undetermined whether this is an improvement to the process.

Improved Production

In general, the recorded relative recovery of fluid from the two case histories for hydra-jet fracturing treatments was only ~ 50% of that for typical horizontal Barnett Shale wells with conventional water fracturing stimulation [*East et al.,* 2004]. This lower percentage of the recovery of the load has led to the speculation that, with less sand placed, the system of joints could be closing back either more completely, or simply faster, than after typical conventional water fracturing treatments.

A review of more than 80 completions in the Barnett Shale indicated a distinct correlation between greater quantities of sand yields and an improved production in this reservoir [*Coulter et al.,* 2004]. If this is an accurate assumption that would extrapolate to general horizontal completions in the Barnett Shale, then the development of designs for hydra-jet fracturing treatments that can place much greater concentrations of sand could be necessary to make this design more of an economic success in the Barnett Shale and other reservoirs.

Containment

From horizontal wells in the core area, approximately 50% of the fractures grew into the Upper Barnett Shale. In contrast, the remainder was confined within the Lower Barnett Shale [*Fisher et al.,* 2004]. While it is too early to draw a conclusion from the limited data, hydra-jet fracturing is expected to help minimize the growth of the height of the fractures. This is very desirable in areas where the bounding limestones are not present. In addition, nearby aquifers pose a risk to the production should they become connected to the Barnett Shale during a fracturing treatment [*East et al.,* 2004].

Benefits Compared to Conventional Horizontal Well Fracturing

At least in the Barnett Shale, it is believed that eliminating the simultaneous generation of multiple fractures is not desirable through the use of hydra-jet fracturing [*East et al.,* 2004]. However, the capability of hydra-jet hydraulic fracturing to concentrate the initial creation of these multiple fractures within a few feet along the well, at multiple specific locations along a horizontal lateral, could be a significant change in the application of water fracturing for horizontal completions. By

varying from basic hydra-jet-hydraulic fracturing and by use of very high rates of injection through the annulus (i.e., Halliburton's CobraMax), the requirements for high rates of injection for water fracturing stimulations can be achieved. Each hydraulic fracturing stage can then be more similar to what would be used on a single-stage completion from a vertical well. In addition, ideally, each stage can achieve that degree of stimulation at multiple points along a horizontal well without packers, bridges, or chemical plugs, and with a single well intervention. This can be beneficial for EGS.

Thus, hydra-jet fracturing offers significant improvements over some conventional processes, particularly for open-hole horizontal completions without a liner. To-date, hydra-jet-hydraulic fracturing has only been used in Barnett Shale wells for cemented, and un-cemented cased, horizontal wells because of concerns about possible formation caving or sloughing up-hole of the BHA that could stick the treating string. In reality, the attempt to use hydra-jet fracturing in the Barnett Shale reservoir is in its infancy, and new ways to improve the response of the production, as well as control the overall cost of the completion of the wells may still be found.

4.3.12 Stress Shadowing

Stress shadowing has been a factor in the success of horizontal treatments in the Barnett Shale [*Fisher et al.,* 2004; *Fisher et al.,* 2002]. On many of the fracturing treatments on horizontal wells, a stress shadow effect is clearly observed in the mapping results [*East et al.,* 2004]. When a hydraulic fracture is opened, the compressive stress normal to the fracture faces is increased above the initial in-situ stress by a quantity equal to the net hydraulic fracturing pressure. This elevation in stress is greatest right at the face of the fracture. However, the perturbation of the stress radiates out into the reservoir for hundreds of feet. The stress shadow that is cast by an open hydraulic fracture is displayed in Figure 4.5 and Figure 4.6. The rate at which this stress perturbation declines with distance from the face of the fracture is controlled by the smallest aerial fracture dimension (i.e., height or length). In the Barnett Shale, the heights of fractures are generally much less than the lengths of the fractures. Hence, the distance impacted by the stress shadow is controlled by the height of the fracture. The stress shadow becomes quite small when the offset distance is a factor of ~ 1.5 greater than the fracture height. In the core area of the Barnett Shale, the heights of fractures are typically ~ 300 to 400 ft. Hence, it is expected that the stress shadow to dissipate at a distance of ~ 500 ft away from the opening of a fracture. Experience supports this estimated shadow distance, as evidenced by the regularly spaced crosscutting fractures that tend to appear at intervals of ~ 500 ft regardless of the location of the perforation cluster.

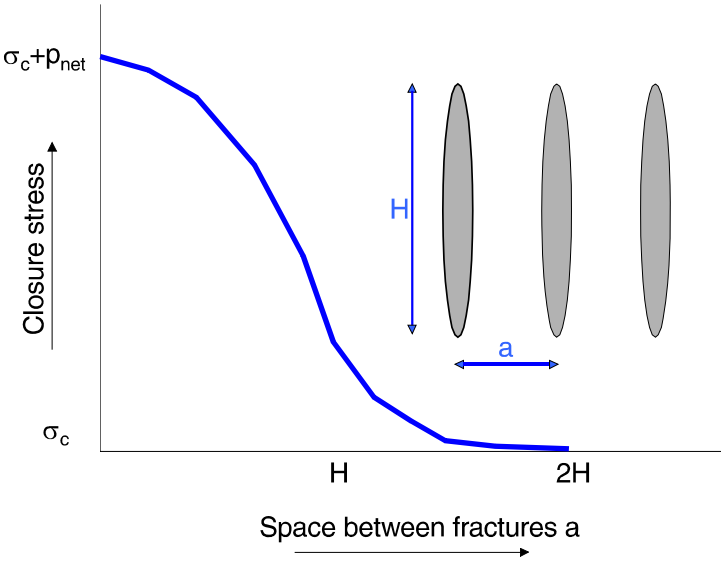

Figure 4.5: Relationship between closure stress increase as a function of distance away from fracture (stress shadow) expressed in terms of fracture height [*Warpsinki and Branagan,* 1989].

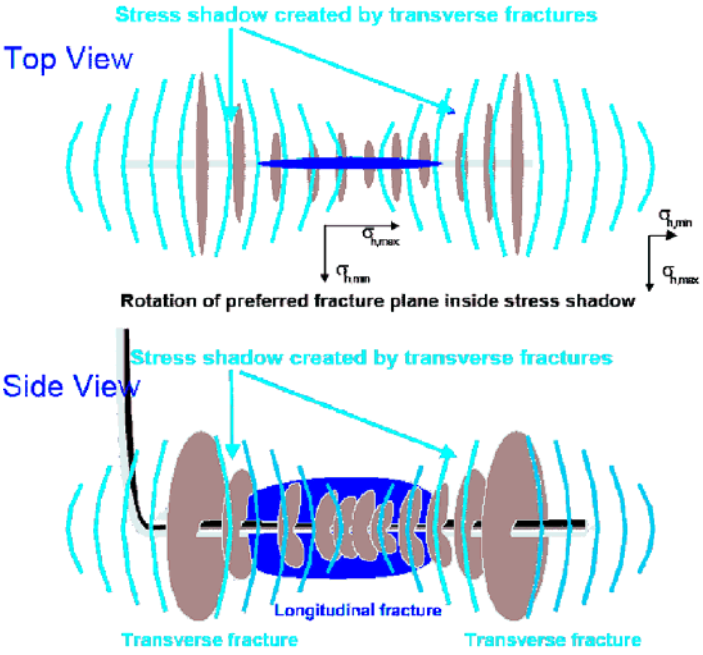

Figure 4.6: Stress shadow effects on transverse fracture growth [*Fisher et al.,* 2004].

Stress shadow effects have been discussed for more than 15 years and documented with fracture mapping data for 10 years [*Minner et al.,* 2003; *Minner et al.,* 2002; *Wright et al.,* 1997; *Wright et al.,* 1995; *Warpsinki and Branagan,* 1989]. However, they were confined to special cases of tightly-spaced wells, and were mostly because of long-term production and injection operations [*Fisher et al.,* 2004]. However, these stress-shadow effects are critical to the design of completions and fracturing treatment strategies for horizontal wells [*East et al.,* 2004]. Yet, the importance of stress shadows remains underappreciated.

Stress shadows in horizontal well hydraulic fracturing have two major impacts: First, the increased compressive stress near a fracture tends to close-off or inhibit the initiation of near by parallel fractures. This provides a natural diversion mechanism along the well. If perforation clusters or fracture initiation points are too close together, then stress shadows tend to inhibit fracture growth along the mid-section of horizontal wells. Instead, fracture growth at the heel and toe of wells is encouraged. Second, the increase in the magnitude of the local minimum stress tends to encourage fracture growth in orthogonal directions. Even when the orientation of fractures from vertical wells is relatively uniform, stress shadow effects often induce orthogonal fracture growth when stimulating long intervals in horizontal wells. These impacts are illustrated in Figure 8.13 on page 117.

Both effects are important for completions from horizontal wells. The growth of orthogonal vertical fractures, or fracture networks, occurs even in vertical wells in the Barnett Shale because of a low in-situ horizontal deviatoric stress and the presence of natural fractures orthogonal to the current maximum stress direction, which is NE-SW. Stress shadows from simultaneously growing and competing fractures that have initiated along a horizontal well tend to enhance further the fracture growth in the orthogonal direction, which is NW-SE. This enhancement is positive because the contact area with the reservoir is enlarged (i.e., the size of the network, and density of the network are both believed to contribute to the productivity of the well).

Recently, the mechanisms of the alteration of a stress field in the surroundings of a created hydraulic fracture that could potentially affect other hydraulic fractures created from near by wells was discussed [*East et al.,* 2004; *Soliman et al.,* 2004]. If multiple fractures are created from a single well, then this effect could be more significant. Examples are creating multiple transverse fractures from a horizontal well, or multiple fractures intersecting a vertical well at different depths. The

presence of casing versus open-hole completion could also make a difference. From earlier solutions [*Sneddon,* 1946; *Sneddon and Elliott,* 1946], the effect of the presence of multiple fractures on the pressure of hydraulic fracturing, the magnitude of the stress field, and even the potential change of the orientation of the stress were presented. Depending on the dimensions of the fracture, the distances between the various already created fractures exhibit a higher treating pressure, and may even cause changes in the orientation of the stress-field. The is sufficiently significant to warrant consideration in the design and optimization of the number of fractures.

4.3.13 Alternatives to Conventional Fluid Diversion

Wax Beads

Wax beads can be reliably placed in the cooled-down, near- well area during stimulations [*Johnson and Brown,* 1993]. After completion of the treatment, they melt as the bottom-hole temperature builds up. The wax beads need to have a melting point that is less than the bottom hole static temperature, and greater than the surface fluid temperature. The benefits of wax beads are [*Bell et al.,* 1993]:

1) They adhere to other wax particles;
2) they deform under pressure;
3) they are soluble in produced hydrocarbons fluids;
4) they are non-hazardous;
5) they are readily available at low cost; and
6) wax beads with differing melting points are available for treatments in various thermal environments.

However, wax beads within blocked-off intervals can loosen or melt during the course of a treatment, and thus act as a source of pressure relief. Wax beads have been used for water fracturing open-hole wells in naturally fractured chalk formations.

Wax beads were used for fluid diversion in horizontal wells in the Austin Chalk in Texas and the Niobrara in Wyoming. The selection of an effective diverting agent to optimize the slickwater fracture stimulation of horizontal wells has evolved from treatments utilizing graded salt, benzoic acid, paraformaldehyde, and naphthalene to the current use of wax beads. Its product availability, high solubility in hydrocarbons and low melting point (for ease of cleanup), variable shape, low cost, and the lower concentrations required to achieve diversion make the non-hazardous wax the diverter of choice for horizontal well slickwater treatments. Consequently, wax beads have been successfully applied to divert these treatments in open-hole laterals.

In the Austin Chalk, micro resistivity logs for well analysis and radioactive tracer logs of pre- and post-production levels demonstrate that wax diverters contribute significantly to the stimulation of horizontal wells.

In the Niobrara, early bottom-hole treating pressure responses and post-treatment production are related to the extent of natural fracturing exposed within the horizontal sections. The lack of sustained productivity after the treatments indicates that horizontal wells in the Niobrara respond differently than those in the Austin Chalk after stimulations with large volumes and high rates. The most likely explanation for this difference is that fractures opened during large-volume, high-rate treatments in the Niobrara either close during production or do not provide sustainable connectivity to fractures with high conductivity.

4.4 Methods for Alternating Fracture Growth Mode or Fracture Re-orientation

By use of the diagnostic tools of Pinnacle Technologies, Inc., we have observed three mechanisms [*Wright and Weijers,* 2001; *Siebrits et al.,* 2000; *Weijers et al.,* 1999; *Wright and Conant,* 1995] in fracture growth that can be very promising for the geothermal industry to access the largest amount of heated rock possible from a single well:

1) Fracture re-orientation caused by a change in the 3D state of stress due to the presence of previously created hydraulic fractures;
2) fracture re-orientation induced by changes in pore pressure and reservoir temperature; and
3) changes in fracture azimuth and dip resulting from changes in the injection rate or viscosity of the injected fluid.

The oil and gas industry has performed hundreds of re-fracturing treatments in recent years that aim to exploit the re-fracture re-orientation mechanism. If the fracture re-orients itself ~ 90° with respect to the initial fracture orientation, then a new fracture treatment in a previously stimulated well accesses new reservoir. The benefits of such a re-fracturing treatment can be significant. In many instances in low-permeability reservoirs, this has led to re-fractured wells that produce oil or gas at almost the original rate when the well was first completed (i.e., many years before the re-fracture treatment). Pinnacle Technologies, Inc. has been a pioneer in the industry for directly measuring the re-fracture re-orientation in many wells, and for developing the technology from theoretical design to practical implementation.

The improved modeling capabilities that we developed in project subtask 1b (section 3.2 on page 29) make it possible to determine the change in fracture closure stress and fracture azimuth due to temporal changes in temperature and pore pressure. This could also be applied to EGS to fan out subsequent fractures to obtain a much greater stimulated reservoir volume.

The mechanism of fracture orientation changes due to modifications in injection rates or fluid viscosity has been observed in secondary recovery projects in the oil industry. Utilizing the surface tilt mapping technology of Pinnacle Technologies, Inc., it was observed that fractures may grow along the plane of maximum shear stress at low rates, whereas the fracture system grows perpendicular to the least principal stress at greater rate. This mechanism is caused by increases in pore pressure along the direction in which shear fractures enhance permeability. This re-orientation process has been observed [*Weijers et al.,* 1999] in low-rate water-injection water, and in greater rate steam-injection treatments and CO_2-injection treatments.

The effect of altering the injection rate and the treatment viscosity is similar to the effect of changing the injection pressure. Adjusting the injection rate and viscosity could be beneficial for EGS, because it is desirable to keep the injection pressure below $\sigma_{H,min}$ while creating a large volume of stimulated pre-existing fractures.

5 FIELD TESTING

Pinnacle Technologies, Inc. and GeothermEx, Inc. studied the applicability of methods listed in project task 2 (section 4 on page 50) by use of several hydraulic fracture diagnostic techniques, including, but not limited to:
1) Hydraulic Impedance Testing (HIT) to determine the location of open hydraulic fractures along a open-hole interval;
2) pressure transient testing to determine reservoir permeability, pore pressure and closure stress; and
3) tilt mapping in treatment wells or microseismic mapping to evaluate hydraulic fracture coverage.

We intended to use the results from project task 1 (section 3 on page 8) and task 2 (section 4 on page 50) and the recommendations for direct hydraulic fracture diagnostics from project subtask 3a (section 5.1 below) to design the best possible diagnostic injections for application in the Desert Peak EGS area. We planned to provide these designs to ORMAT Nevada, Inc. for their consideration.

We have started task 3a (section 5.1 below). However, continuation of this task was not possible, as fieldwork in the Desert Peak area for ORMAT Nevada, Inc. has been delayed owing to problems with re-completing the well of interest (DP 23-1). The stimulation work did not commence before the current project was finalized. Consequently, subtasks 3b and 3c (section 5.2 on page 86) were removed from the project.

This section discusses the applicability of various hydraulic fracture diagnostic techniques for EGS (section 5.1 below), EGS field test data, and post treatment evaluation and reconciliation with calibrated model of this data (section 5.2 on page 86).

5.1 Applicability of Various Hydraulic Fracture Diagnostic Techniques for EGS

Pinnacle Technologies, Inc. and GeothermEx, Inc. evaluated a multitude of diagnostic tools that are currently used for hydraulic fracture diagnostics for their applicability in EGS applications. This study provides benefits and disadvantages of all these technologies and list their major capabilities and limitations for application in EGS.

The indirect (section 5.1.1 on page 77), direct near well (section 5.1.2 on page 79), and far field (section 5.1.3 on page 80) hydraulic fracture diagnostic tools that were evaluated include (but are not limited to):
1) Surface, offset well and treatment well tilt mapping,
2) microseismic mapping,
3) hydraulic impedance testing (HIT),
4) tracer logging,
5) temperature logging,
6) diagnostic fracture injection test (DFIT) / Mayerhofer pressure decline analysis techniques,
7) pressure transient testing,
8) interference testing,
9) an-elastic strain recovery stress measurements, and
10) formation micro imaging (FMI) log interpretation.

The principal abilities and limitations of the available diagnostic tools are displayed in Figure 5.1.

From this evaluation, we provide a list of recommended diagnostic techniques that can be used in the Desert Peak area for ORMAT Nevada, Inc.

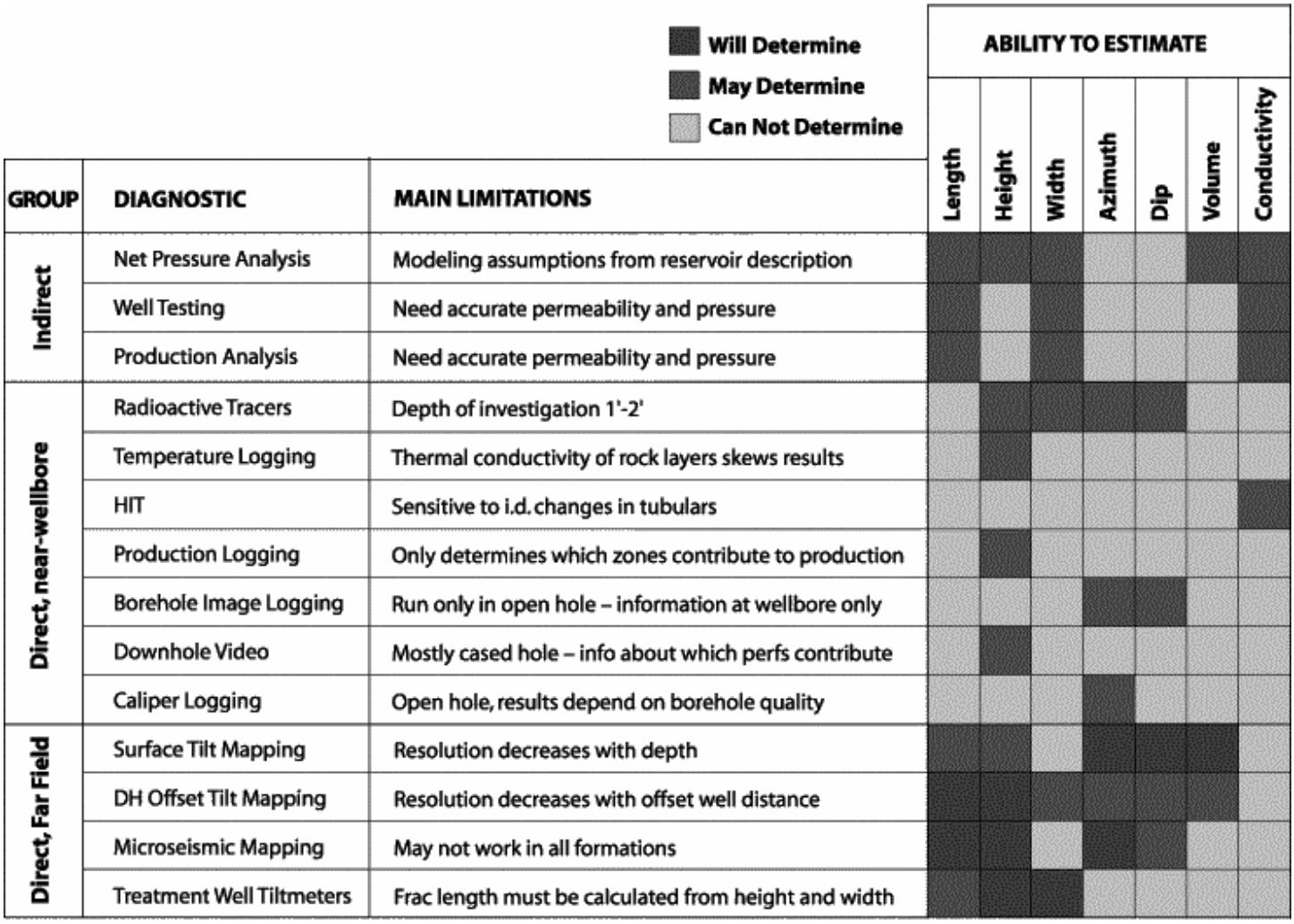

Figure 5.1: Available diagnostic tools and their principal abilities and limitations [*Barree et al.,* 2002].

Hydraulic fracture diagnostics is critical in understanding the details of actual subsurface growth of hydraulic fractures, especially in cases of complex geometries of hydraulic fractures [*Maxwell et al.,* 2002]. Numerous diagnostic tools for hydraulic fracturing have been successfully applied in the Barnett Shale [*East et al.,* 2004]. Hydraulic fracture diagnostics can be broken into two principal groups, as displayed in Figure 5.1 [*Barree et al.,* 2002]:

1) Indirect techniques that include hydraulic fracture modeling, well testing, and production analysis (section 5.1.1 on page 77), and
2) Direct diagnostic measurements that are further subdivided into:
   a) Near -well (e.g., radioactive tracers, temperature, and production logs) (section 5.1.2 on page 79), and
   b) far-field (e.g., tiltmeter and microseismic mapping) (section 5.1.3 on page 80).

The near- and far-field diagnostics provide distinctly different viewpoints of a hydraulic fracture. Near-well diagnostics is an intricate, well-log scale view of a hydraulic fracture with depths of investigation with a range of the order of a few feet. It provides a relatively detailed look at the area of contact of the hydraulic fracture within the perforated interval, concentrations and height of the proppant at the well, or a profile of the entry of the production into the well [*Warpinski,* 1996].

Far-field diagnostics have a depth of investigation of many tens to hundreds of feet. They provide large-scale macroscopic views of the gross dimensions of the hydraulic fractures. However, they do not have the well-log scale detail of the near-field tools.

In many cases both near- and far-field technologies are combined to obtain the best possible picture of hydraulic fracture growth. These data are then used to calibrate a simulator for hydraulic fracturing. This provides an accurate model of how the growth of hydraulic fractures occurs under actual reservoir conditions. This calibrated model is then used for the prediction of how (e.g., different systems of hydraulic fracturing fluids), changes of the rate of injection, and varying concentrations and volumes of proppant would change the created geometry of the hydraulic fracture and net present value (NPV) for this and future treatments.

Modeling versus diagnostics is discussed in section 5.1.4 on page 84.

5.1.1 Indirect Diagnostics

Indirect diagnostics of hydraulic fracturing include net pressure analysis, or modeling, well testing, and production analysis.

Net Pressure Analysis (Modeling)

Net pressure analysis by the numerical modeling of the propagation of hydraulic fractures is more of a hopeful prediction than an actual treatment diagnostic [*Weijers et al.,* 2005]. Models of the flow of fluids, the transport of solids, and the evolution of the geometry of the hydraulic fractures are from simplifying assumptions. This makes the numerical solution of the complex problem tractable and practical for routine use of the models. The input to the models consists of stress, pore pressure, and distributions of the elastic properties of the rock. These data are constrained by measurements of the pressure in the well and various open-hole and cased-hole logs. Even with accurate input data, the models are further limited by their assumptions of linear-elastic fracture mechanics and homogeneous, coupled deformation of the rock. Simulators that allow for a deviation from these homogenizing assumptions can model more discontinuous hydraulic fracture geometries. However, they require data to describe the in-situ discontinuities of the rock. Such data is normally not available.

When used as diagnostic tool, the models are calibrated by changing their input data to match some observed job parameter. This usually occurs after the treatment. However, this sometimes happens in real-time. Unfortunately, the parameter that is commonly used as a match is the observed treating pressure. The observed pressure is often a treating pressure at the surface that is removed from the actual fluid pressure inside the hydraulic fracture by the hydrostatic head, and the friction because of the flow in the hydraulic fracture, near the well, in the perforation and in the pipe. All these dynamic inputs to the pressure change continuously during the job, and may not be accurately predictable.

Even if an accurate treating pressure at bottom-hole is available, then sensitivity analysis demonstrates that the treating pressure is very weakly coupled to the hydraulic fracture geometry, which is the ultimate predictive goal of the models. For example, in an assumed Perkins-Kern geometry of the hydraulic fracture (i.e., a well-contained vertical hydraulic fracture, the observed net pressure is a function of the created length of the hydraulic fracture raised to the power of ¼). When this insensitivity is combined with the unknowns of changing frictional dynamics, it is difficult to determine the actual created length of the hydraulic fracture from matching the pressures. In general, the use of models for hydraulic fracturing as a diagnostic tool leads to non-unique solutions and inadequate results. In fact, the treating pressure is more often affected by the transport of proppant and the rheology of the fluid near the well, than by the far-field geometry of the hydraulic fracture. However, models of the geometry of the hydraulic fracture, in conjunction with other direct diagnostic tools, can be effectively calibrated using direct measurements in an operating area. Then, they can be used to predict accurately the created geometry of the hydraulic fracture, and to design effective hydraulic fracturing treatments.

Well Testing

Well testing can assist in defining the geometry of hydraulic fractures only in the same way that production analysis is able to [*Barree et al.,* 2002]. In fact, there could be other limitations to the conventional analysis of pressure build-up that yield

different results (i.e., as compared to those obtained from the dynamic analysis of production). Well transient testing involves the interpretation of the transmission of a pressure transient through the reservoir and near-well environment of the hydraulic fracture. If the well test is an analysis of the build-up of the pressure, then the transient is caused by the shut-in at the well. Some evidence from the field suggests that this shut-in transient behaves differently than the pressure transient established by drawdown at high pumping rates [*Barree et al.,* 2002]. An example, demonstrating post-fracture production and a subsequent buildup analysis on the same well, is displayed in Figure 5.2 and Figure 5.3. The rate of production demonstrates a detailed match of the post-fracture production by use of a three-dimensional (3D) simulator of the reservoir. The far-field effective permeability of the reservoir is 0.27 mD. The apparent effective half-length of the created hydraulic fracture is 28 ft. The dashed line is the predicted rate of production for an effective length of the hydraulic fracture of 300 ft. All lengths of the hydraulic fractures are from an assumed infinite conductivity.

The log-log type curve in Figure 5.3 displays the results of a build-up test conducted at the end of the flow period of the reservoir. The build-up confirmed the same permeability, thickness, and initial pressure of the reservoir as the match of the production analysis. However, the effective half-length of the hydraulic fracture calculated from the build-up test was 350 ft, with an infinite conductivity. This discrepancy could be caused by high-rate, non-Darcy flow effects that exist during production but dissipate during the shut-in. Theoretical estimates of the effect of non-Darcy flow indicate that changes in the apparent length of the hydraulic fracture of this magnitude are possible if non-Darcy pressure losses are ignored.

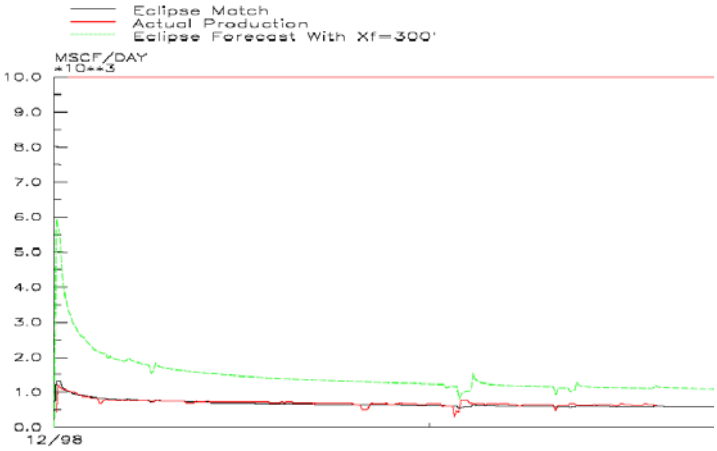

Figure 5.2: Production history match of post-hydraulic fracturing well performance indicates effective hydraulic fracture length of 28 ft. Red line represents actual production, and green line represents expected production fracture length of 300 ft [*Barree et al.,* 2002].

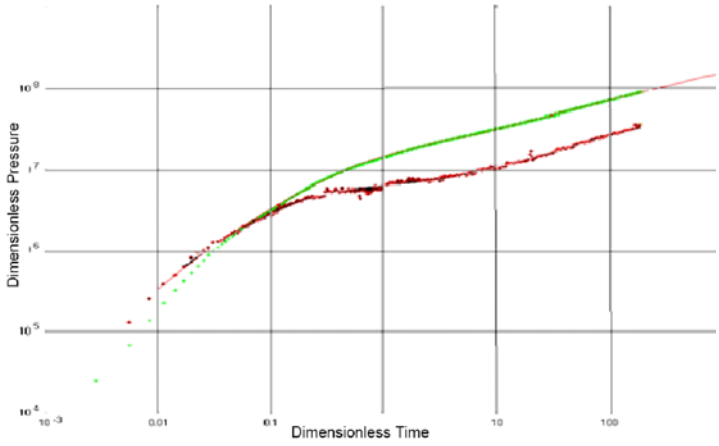

Figure 5.3: Pressure buildup analysis of the fractured well (from Figure 5.2) with hydraulic fracture length of 355 ft. Far-field reservoir properties are the same for both build-up and production history match analyses [*Barree et al.,* 2002].

This example further points out the difficulty in by use of indirect hydraulic fracturing diagnostics to evaluate the effectiveness of the hydraulic fracturing treatment. All the indirect measurements respond to primary system variables that actually control the response of the measured parameter to the dynamics of the system. If these variables are not considered in the overall analysis, then the interpretation of the measurements can be incorrect, even if the measurements themselves are correct.

Production Analysis

The post-fracturing analysis of well production, either with a numerical simulator for the reservoir or with type-curve models, is an indirect diagnostic tool to determine the geometry of hydraulic fractures. The difficulty with this technique, when applied separately, is that the apparent length of the hydraulic fracture responds only to the ultimately cleaned-up, or effective, length of the hydraulic fracture, not the actually created or even propped length. In addition, production analysis does not provide detailed information about the growth of the height of the hydraulic fracture or its containment. In almost

all cases, the effective producing length of the hydraulic fracture is less (often much less) than the created or propped length. This discrepancy has been at the root of many mistaken assumptions of the geometry of the hydraulic fractures that have been used to incorrectly constrain or calibrate models in the past.

For example, it is common that a design of a hydraulic fracture treatment was expected to create a half-length of 500 ft with adequate proppant concentration. However, the post-hydraulic fracturing production or build-up analysis indicated an effective length of 100 ft. The explanation has previously focused on the created length of the hydraulic fracture, the overall geometry, and the containment of the height. In some cases, this led to models that predict a massive growth of height, great widths of hydraulic fractures, and short created lengths in an effort to force-fit the geometry of the model to the apparent effective length. This result has adversely affected the modeling of the geometry of hydraulic fractures and their interpretation for years. This is a very adequate example of the misinterpretation of data resulting from the application of two indirect measurements with direct diagnostic measurement as a constraint.

With a more direct measurement of the length and the containment of hydraulic fractures, a different picture emerges. It now appears that many hydraulic fractures are much better contained in height. In addition, they can be extensive in their created length. This indicates that the difference between the effective producing length and the created length is not primarily an issue of geometry. It is an issue of the effective conductivity of the proppant pack, and clean-up of hydraulic fracturing fluids. The new interpretation suggests that some of the hydraulic fracturing fluids and breaker systems commonly being used do not clean up as effectively as previously believed. This observation has already led to the development of a new generation of cleaner systems for hydraulic fracturing fluids. Of course, the extreme complexity of hydraulic fractures (e.g., the true dendritic fracture patterns in some reservoirs) also contributes to short effective lengths of hydraulic fractures in some cases. These instances can easily be detected with direct diagnostics. However, they could be completely misinterpreted by the analysis of production.

5.1.2 Direct, Near-Well Diagnostics

The direct, near-well diagnostics of hydraulic fracturing include radioactive tracers, temperature logging, hydraulic impedance testing (HIT), production logging, borehole image logging, downhole video, and caliper logging. The direct near -well tools suffer from a shallow depth of investigation of ~ 1 to 2 ft. Thus, they do not always provide a complete picture of the growth of the height or length of hydraulic fractures away from the well [*East et al.,* 2004].

Radioactive Tracers

Historically, radioactive tracing and spectral gamma ray logging have been used to determine the vertical height of hydraulic fractures that is associated with a propped or an acid hydraulic fracturing treatment, and the location where proppant is placed adjacent to the well. Consequently, it is easily determined from the tracers which perforations are open during a treatment, and which are not accepting hydraulic fracturing slurry [*East et al.,* 2004]. Early radioactive tracers suffered from plating-out of the liquids and poor integrity of the radioactive-coated sand grains. Early spectral gamma ray tools were limited by the number of spectral channels available for distinguishing between multiple radioactive isotopes. In the last two decades, the introduction of non-wash-off radioactive ceramic bead tracers and spectral gamma ray logging tools with more than 500 spectral channels for isotope resolution has extended the precision and reliability of this diagnostic technology. These quantum improvements in the technology have been supplemented by mathematical algorithms that enable the spatial identification of the placement of the tracer within the area of investigation of the spectral gamma ray (GR) tool of 24 to 30 in. Additional algorithms enable the computation of traced concentrations of the proppant near the well and associated widths of the propped hydraulic fracture. Radioactive tracers have been frequently used in the Barnett Shale.

Temperature and Production Logging

Temperature and production logging, in one form or another, has been applied for decades. The sensors used for temperature logging have also advanced, from the infancy of a temperature survey to what is now considered a full production logging string of temperature, pressure, fluid density, dielectric and spinner. With the increase in the resolution of the tools, production logging expanded from a problem-solving log to a tool used in hydraulic fracture diagnostics. The principal uses of the individual sensors are:

1) temperature to identify the entry points of the production and to verify channeling behind the pipe;
2) pressure to determine the density within the well and to convert the production of the reservoir to production at the surface;
3) fluid density to determine the density within the well and the ratio of the amount of gas versus that of the fluid;
4) dielectric to determine the ratio between the amount of water and that of the hydrocarbons which is critical in three-phase determinations; and
5) spinner to profile the production to determine the effectiveness of the treatment.

Hydraulic Impedance Testing (HIT)

Hydraulic impedance testing (HIT) can determine whether a hydraulic fracture is present in a well. It can also determine the location of the hydraulic fracture. It is a completely non-invasive method, by use of only equipment at the surface to perform downhole measurements of the hydraulic fracture. The technique is used predominantly to detect the presence and location of hydraulic fractures in injection wells. It can also provide an accurate measurement of the closure stress of the formation (i.e., the minimum in-situ stress). This is used to assist with the engineering of hydraulic fractures, and to monitor water injection wells. Compared to other downhole measurement technologies, it does not require the placement of any tools into the well, and is more cost efficient.

Borehole Image Logging

Borehole image logging is a valuable tool in both structural and sedimentological interpretations of data from wells. It can be used to match core to log depth, assist with the characterization of facies, and provide accurate information on the dip for paleo-current analysis. It is also very useful for the interpretation of hydraulic fractures in reservoirs, especially in determining whether hydraulic fractures are induced naturally or by drilling. Borehole breakout analysis is another use of this type of data. Because of the high resolution of borehole image logging, it can often provide insight into the thickness and distribution of thin beds in a sequence.

Downhole Video

Downhole video yields high-resolution, real-time images of the direct environment (i.e., surface) of the well. It can visualize well fluids and their entry points, downhole mechanical equipment, leaks of the casing or tubing, deposits of minerals, scale corrosion, and microbial build-up. Rock formations are easily viewed in open-hole wells. However, when drilling mud is used, it is opaque and usually prohibits the use of downhole video. Therefore, the tools must be in clean fluid.

Caliper Logging

Caliper logging uses a device with at least three arms to measures the internal diameter of completions with casings or open-holes. This information is crucial to all types of production logging, to calculate an accurate rate of fluid flow.

5.1.3 Direct, Far Field Diagnostics (Hydraulic Fracture Mapping)

Direct, far-field diagnostics of hydraulic fracturing include surface, downhole offset and treatment well tilt mapping, and microseismic imaging. Numerous technical publications are available that present more detailed information on the commonly used hydraulic fracture mapping technologies, tiltmeter and microseismic mapping [*Barree et al.,* 2002; *Cipolla and Wright,* 2002; *Warpinski et al.,* 2001 *Wright et al.,* 1999; *Wright et al.,* 1998a]. These diagnostic tools are now quite commonly applied in the Barnett Shale and other gas reservoirs with a low permeability [*East et al.,* 2004].

Principles

These tools do not have the fine resolution of 1 to 2 ft provided by the near-well tools. However, they do provide a complete picture of the azimuth, the gross height, and the length of hydraulic fractures [*East et al.,* 2004]. These mapping technologies for hydraulic fractures are complementary. Because they directly measure the actual geometry of hydraulic fractures, they can be used to develop an accurate image of the growth of hydraulic fractures, even during the treatment

[*Fisher et al.,* 2002]. Consequently, they allow for a better understanding of the different aspects of the mechanisms of the propagation of these hydraulic fractures. They also provide insight into the dynamics of the depletion of the reservoir, and significantly help optimize the management of the reservoir. The real-time results can be used to diagnose the effectiveness of both ongoing and planned operations [*Maxwell et al.,* 2002]. For example, the hydraulic fracture can be imaged, and the injection parameters can be changed to gain the desired characteristics of the hydraulic fracture, and to assess the effectiveness of controlling the complex growth of the hydraulic fracture. In addition, a post-mortem analysis of the hydraulic fracture enables the calibration of numerical simulations, the prediction of drainage patterns, and the assessment of changes to and optimization of the design of hydraulic fracturing.

Application to Barnett Shale

The primary application of hydraulic fracture mapping is the characterization of hydraulic fracture networks. Hydraulic fracture mapping has been used extensively in the core area to determine the spacing and locations of infill wells, to evaluate various designs and techniques of stimulation treatments, to identify candidates for re-fracturing, to determine the effectiveness of staging, and to test alternative techniques before their introduction in the fringe areas of exploitation [*Fisher et al.,* 2004].

The production results are strongly correlated to the orthogonal growth of the hydraulic fractures [*Fisher et al.,* 2002]. This is visualized in the results of the surface tiltmeters as the NW component, and in the microseismic data as a wide band of seismic activity. Clearly, utilizing two independent mapping technologies allowed for a more complete image of the hydraulic fracture network.

Tiltmeter and microseismic mapping provides key information, including the orientation and dimensions of hydraulic fractures. The combination of direct hydraulic fracture diagnostics and soundly engineered modeling of hydraulic fracturing determines:

1) Whether the hydraulic fracture covers the entire pay-zone as designed,
2) whether it is confined to that zone,
3) whether the staging of the treatments (e.g., proper number of stages, optimal-sized stages, proper volume and concentration of proppant) are efficient,
4) the dimensions (e.g., top, bottom and length) of the hydraulic fracture,
5) the comparison of the dimensions of the hydraulic fracture with the modeled dimensions and resultant estimates of production, and
6) how the hydraulic fracture orientation and length affect the choice of spacing of wells well and the locations of infill drilling to drain effectively this reservoir.

Tilt Mapping

The tiltmeter can sense very small changes in the gradient of displacement, or tilt [*Fisher et al.,* 2002]. The tiltmeter cube illustrated in Figure 5.4 displays the expected deformation pattern resulting from a simple hydraulic fracture as observed at the surface and from an offset well. Tilt mapping has been commercially available for more than ten years. Thus far, more than 6,000 hydraulic fractures have been mapped.

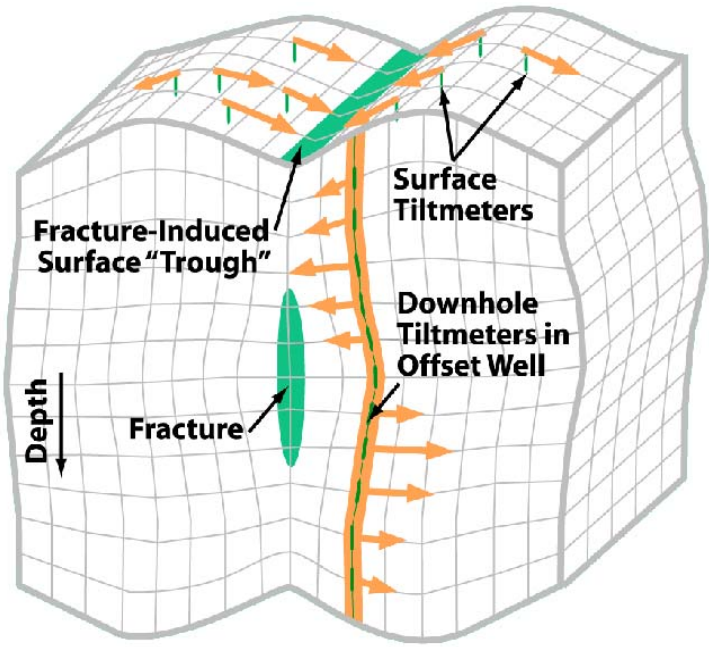

Figure 5.4: Pattern of deformation resulting from a hydraulic fracture, detected by surface and downhole tiltmeters [*Fisher et al.,* 2002].

Principles

A tiltmeter is a very sensitive device, similar to an electronic carpenter's level. It can measure changes in the tilt of the Earth from deformation caused by a displacement of a hydraulic fracture down to 1 ppb (part per billion) or 1 nano radian [*Barree et al.,* 2002; *Fisher et al.,* 2002]. Depending upon the location of the instruments, tiltmeters can measure the azimuth, dip, height, length, and width of hydraulic fractures. As a hydraulic fracture displaces the Earth as it grows, tiltmeters are able to measure the pattern of deformation caused by these displacements. Inversion of the pattern of deformation allows for the calculation of the size and orientation of the hydraulic fracture or fractures that created the deformation.

Limitations

Limitations are typically a result of the proper observation vantage point: being sufficiently near to the hydraulic fracture to be able to measure the resulting deformation. Consequently, for surface tilt mapping in wells deeper than 10,000 ft, hydraulic fractures must be relatively large. Downhole tilt mapping is most successful when performed in near by observation wells that are located within 500 to 1,000 ft away from the treatment well. Tilt mapping works in any type of lithology from very soft, unconsolidated rock to very stiff carbonates.

Surface Tilt Mapping

Surface tilt mapping is utilized on more than 1,000 treatments per year to map the deformation caused at the surface of the Earth by hydraulic fractures or dislocations in the sub-surface [*Fisher et al.,* 2002]. The deformation of the surface, measured by tiltmeter arrays, is used to determine directly the azimuth and dip of a hydraulic fracture, and the fraction of the treatment volume placed in each plane or orientation when hydraulic fracture growth occurs in multiple planes [*Wright et al.,* 1998a]. Surface tiltmeters are very valuable for horizontal completions because they can measure the orientation of hydraulic fractures and the distribution of the volume of the slurry along the lateral [*Fisher et al.,* 2004]. This determines whether the majority of the slurry goes only in the heel, the middle or the toe of the lateral, or whether it is evenly distributed along the length of its lateral.

Downhole Offset and Treatment Well Tilt Mapping

Downhole offset and treatment well tilt mapping is a separate application of the surface tilt mapping [*Cipolla and Wright,* 2000; *Wright et al.,* 1998a]. By ruggedizing the surface tiltmeter instruments and placing them in offsetting wells to the treatment wells, the dimensions (i.e., height and length) of hydraulic fractures can be determined [*Barree et al.,* 2002; *Fisher et al.,* 2002]. A new generation of downhole tiltmeters can be placed in the treatment well itself. This eliminates the need for an offset observation well. This also provides direct measurements of the height of a hydraulic fracture during a mini-fracture, water or acid fracturing [*Wright et al.,* 2001].

In some field experiments for downhole tilt mapping, the treatments are monitored with two arrays of downhole tiltmeters. One is placed near the end of each wing of the hydraulic fracture network to determine the location of top and bottom of the hydraulic fracture, and the total length of each wing [*Fisher et al.,* 2002]. To measure the length of the hydraulic fractures, the downhole tiltmeter arrays are placed in the general direction that the hydraulic fractures are expected to propagate.

Microseismic Mapping

For more than twenty years, microseismic mapping has been used to measure how hydraulic fractures grow with time [*East et al.,* 2004]. It also allows on-the-fly changes to optimize the treatment parameters.

Principles

Microseismic mapping originates in Earthquake seismology [*East et al.,* 2004]. When the pore pressure is increased during a hydraulic fracture treatment because of leakoff and hydraulic fracture opening, the formation is stressed [*Barree et al.,* 2002]. This affects the stability of existing planes of weakness in the formation near the hydraulic fracture (e.g., natural fractures, flaws, bedding planes), many of which are likely to fail. The increasing pore pressure reduces the net effective stress that holds these planes of weaknesses together. This in effect lubricates them, so that they can slip and fail, similar to Earthquakes along faults. These shear slippages (i.e., micro-Earthquakes, or microseisms), emit acoustic energy, or elastic waves or sound. This can be detected by sensitive listening instrumentation [*Albright and Pearson,* 1982].

These seismic receivers consist of arrays of tri-axial geophones and accelerometers. They are placed in an offset well [*Fisher et al.,* 2002]. The receivers can detect the emitted sound at distances of up to 1 mi.

The general concept of microseismic hydraulic fracture mapping is illustrated in Figure 5.5. The tools have three component sensors to obtain the two-dimensional (2D) orientation of each detected event. The height of the vertical array of 5 to 12 devices, typically more than 400 ft, allows for the triangulation in the vertical plane and thus the measurement of the height of each event and the distance from the monitor well. After orienting each tool in the array, usually during the perforating procedure in the treatment well, the microseisms created by the hydraulic fracturing treatment are detected, oriented, and positioned within the reservoir.

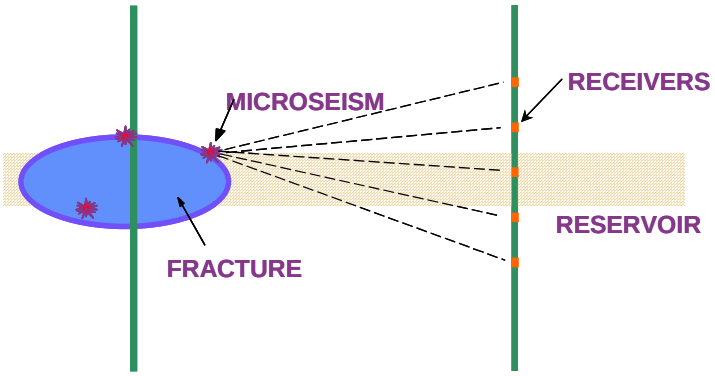

Figure 5.5: Location of microseismic events [*Fisher et al.,* 2002].

By use of the difference in velocity between the arrivals of compressional and shear waves, the distance to and depth of each microseism emission can be measured. From this information and the application of hodogram analyses, the direction to each microseism is found. This allows a map to be built in real-time as a hydraulic fracture is growing, pinpointing the 3D location of each of these microseismic events. In plan view, this map provides the orientation of the hydraulic fracture as well as indicating other hydraulic fractures (which may splinter off in additional planes), and the overall complexity of hydraulic fracture growth. From the side view, the height (top and bottom) and length of the hydraulic fractures can be observed.

Limitations

The limitations of microseismic mapping include its application to certain lithologies, and the availability, location and distance of observation wells. The formations that are most conducive to generating and transmitting microseisms are typically sands with low permeability, limestones, and hard and naturally fractured shales. Soft formations with high porosity and interestingly, dolomites, typically require a smaller distance between the observation and the treatment well than a typical formation. The preferred location is near the center of the hydraulic fracture, and normal to the treatment well. Observation distances are dictated by the ability of the formation to transmit acoustic energy. Typically, the ideal distance is 1,000 to 2,000 ft from the hydraulic fracturing well. The observation well must be extremely quiet with perforations isolated temporarily during the monitoring operation. Typically, existing production wells are temporarily used as an observation well, after pulling the production tubing and setting a temporary bridge plug above the reservoir [*Maxwell et al.,* 2002]. Once deployed, the wire-line array is mechanically clamped in place to ensure the mechanical coupling with the rock.

5.1.4 Modeling versus Diagnostics

Currently, several different diagnostic technologies for hydraulic fracturing are available that estimate or measure key hydraulic fracture parameters [*Weijers et al.,* 2005]. Each diagnostic technique has inherent strengths and weaknesses. In some cases, more than one method needs to be applied to describe adequately the parameters of hydraulic fractures that are most important to the individual treatment. Even with the availability of these diagnostic technologies, it is important to understand that simply measuring the dimensions of a hydraulic fracture is still a post-process picture. It does not predict how a different design of hydraulic fracturing in the same well would have grown. It does also not predict how the same design would behave in a different well. Hydraulic fracture design models are the most widely applied (and misapplied) diagnostic tool. They are useful as a predictive tool for the optimization of hydraulic fracturing. However, they all suffer from an incomplete understanding of the mechanics of the propagation of a hydraulic fracture in a formation. Therefore, the two technologies must be combined such that direct physical measurements of the growth of a hydraulic fracture can be coupled to a 3D simulator of hydraulic fracturing. This results in a calibrated hydraulic fracture model. This model can capture the essential physics of the growth of hydraulic fractures in a given reservoir, while honoring the direct diagnostic measurements of hydraulic fracture geometry and the signature of the net pressure from the treatment.

A complete picture of the growth and geometry of hydraulic fractures can only be realized when hydraulic fracture diagnostics and physically consistent models are combined at multiple scales. For example, tracer, temperature, or other near-well diagnostics are required to pinpoint the entry of the hydraulic fracturing fluid and proppant into the hydraulic fracture, and to determine which perforations are open during each phase of the treatment. This knowledge is necessary as a first constraint to the modeling. However, by itself this is not adequate to constrain the model. The far-field geometry of the hydraulic fracture must also be defined by tiltmeter or microseismic mapping to determine the general size and shape of the hydraulic fracture, and to identify potential confining layers and mechanisms. These direct measurements must be integrated into a numerical model of hydraulic fracturing that recognizes and accounts for the identified physical processes of the flow of fluids, the transport of solids, the deformation of the rock, and the containment of the hydraulic fractures. The input parameters to the model, while from the best available well log and reservoir information, must be calibrated from the direct diagnostic measurements to assign the correct level of importance to various mechanisms of the containment of the hydraulic fractures. Only with this degree of diagnostic characterization of the hydraulic fracture and coupled modeling is it possible to understand truly the controls on the evolution of the geometry of hydraulic fractures. With this integrated approach, a predictive model for the design of hydraulic fracturing can be developed for a reservoir. By use of the predictive, calibrated model, the stimulation can be optimized to provide the required conductivity and maximum effective length of the hydraulic fracture to maximize the production economics.

5.2 EGS Field Test Data, Post Treatment Evaluation, and Reconciliation with Calibrated Model

ORMAT Nevada, Inc. has been very eager to work with GeothermEx, Inc. and to implement new technologies to evaluate created hydraulic fracture networks and to test out new methodologies that can maximize contact between the hydraulic fracture system and the reservoir. The eagerness of this operator to try things out was a main benefit of this project.

Recommended Treatment Methodologies

Water fracturing in EGS is expected to result in an effective fracture conductivity that is equal or better than that from conventional propped fracturing, at significantly lower cost. In addition, such treatments will likely result in a greater extension of the fractures and an easier clean up. Refer to section 4.1 on page 50.

In addition to determining the state of stress and the mechanical properties of the potential reservoir rock, it important to determine the density, geometry and connectivity of pre-existing networks of natural fractures, and the existence of any bounding layers. This information can then contribute to the design and locations of the wells, and the design of the stimulation itself. Refer to section 3.1 on page 12.

The recommended treatment methodologies that have been theoretically tested one versus the other to determine which should work best at Desert Peak and other places are (in order of best expected performance):

1) Deviated and horizontal cased well bore for excellent control of height and lateral diversion; coiled tubing fracture treatments for quick execution (but with severe rate limitations), combined with implementation of alternating rates, gel viscosities, proppant slugs and pump ins and shut ins to create stress shadowing for lateral and vertical diversion. A series of directional wells could be used, with the well azimuth in the direction of the least principle stress to maximize the number of active fracture intersections. While transverse fracture systems are effective in draining a large volume of the hydrocarbon reservoir, the rate of heat transfer needs to be balanced with respect to the capacity of the reservoir to prevent the reduction of the heat and flow gradients. As in the oilfield, horizontal EGS wells would alleviate the problem of inadequate locations at the surface, and maximize the lateral extent of the network of fractures. It could be possible to stimulate through horizontal wells to obtain the largest network but then produce from and inject into vertical wells to maximize heat transfer or inject into vertical wells and produce from horizontal wells.
2) Deviated and horizontal uncemented slotted liner with various perforation intervals for limited entry fracturing with single treatment at very high slurry rate, combined with implementation of alternating rates, gel viscosities, proppant slugs and pump-ins - shut-ins to create stress shadowing for lateral diversion. As there is no reliable control of fluid diversion, some areas along the well may remain unstimulated. To eliminate these unstimulated areas, conducting multiple stimulation treatment stages with fluid diversion could be required. While vertical wells probably yield satisfactory results, the application of uncemented horizontal wells may have advantages for EGS.
3) Horizontal open hole with hydra-jet or propellant initiation strategy, combined with implementation of alternating rates, gel viscosities, proppant slugs, and pump-ins and shut-ins to create stress shadowing for lateral diversion. Hydra-jet and propellant assisted initiation aim to achieve flow diversion while fluid contact with the reservoir is not physically restricted by locally pressurizing and thus stimulating only a small target zone. As such, these two techniques could be useful for initiating fracture network stimulations along a long open hole interval in EGS.
4) Regularly scheduling re-fracture treatments in EGS projects may also be an effective way to stimulate continuously other parts of the reservoir, as the state of stress in the reservoir is changes by placement of proppant, pore pressure and heat transfer changes.
5) Fluid diversion and penetration are critical to succesful creation of EGS to prevent sub-optimal fracture staging that results in network gaps along the horizontal well and thus a loss of production that is approximately proportional to the percentage of unstimulated lateral.
6) Proper selection of proppants (e.g., ceramics) is important to mitigate the fact that the required fracture network structures are so large that fracture conductivity starts to become important again despite the ultra low permeability of the reservoir. Very low conductivities of the fractures result in a loss of production due to the inability to move fluids from the far reaches of the network. That is, simply creating a large fracture network with a proper spacing may still not be optimal for succesful EGS, if the conductivity of the fractures is not sufficient.

7) Pumping a full size fracture treatment with low proppant concentrations first, followed by a more aggressive tail-in of higher quality proppant to increase the near-well conductivity to improve production. This may be a feasible technique for EGS where proppants (e.g., ceramics) are pumped if more aggressive proppant pump schedules do not result in a decrease of overall network size at the same time.
8) Pressure diagnostics, in addition to fracturing diagnostics, are critical to estimating and predicting the success of EGS stimulations. Using test data for pressure buildup, if the permeability of the reservoir is known to be within a certain range, it may be possible to estimate a range for the effective total lengths of the fracture network.
9) It is important to balance the creation of a dense fracture network while also maximizing the overall size of the network. The reason is that creating a dense network through aggressive diversion may be detrimental to generating a larger network.

For items 1) to 4), refer to section 4.2 on page 57, and for items 5) to 9), refer to section 3.4 on page 38.

Analysis of Diagnostic Results

It is likely that fracture mapping can provide valuable insight into the geometry of the network of fractures. This technique can also be used for real-time modification of the design of hydraulic stimulations. Refer to section 3.1 on page 12.

Although this project did not include any co-founding for the implementation of direct hydraulic fracture diagnostic techniques, we believe that there would have been several opportunities in the Desert Peak areas to collect this data independently from this project during the second project year of the project. We were supposed to dedicate time in our project to analyze the collected data from these hydraulic fracture diagnostics, but most of this work was cancelled.

Data collected by use of microseismic mapping and other technologies during the field test was supposed be analyzed to determine the dimensions and orientation of the hydraulic fracture system that is created while by use of the design injection sequences recommended in project task 2 (section 4 on page 50).

The primary application of hydraulic fracture mapping is the characterization of hydraulic fracture networks. Hydraulic fracture mapping can be used to determine the spacing and locations of infill wells, to evaluate various designs and techniques of stimulation treatments, to identify candidates for re-fracturing, to determine the effectiveness of staging, and to test alternative techniques before their introduction in new areas of exploitation.

The growth of a hydraulic fracture network can be visualized by surface tiltmeters, and microseismic mapping as a wide band of seismic activity. Clearly, utilizing two independent mapping technologies allows for a more complete image of the hydraulic fracture network.

Tiltmeter and microseismic mapping provides key information, including the orientation and dimensions of hydraulic fractures. The combination of direct hydraulic fracture diagnostics and soundly engineered modeling of hydraulic fracturing determines:

1) Whether the hydraulic fracture covers the entire pay-zone as designed,
2) whether it is confined to that zone,
3) whether the staging of the treatments (e.g., proper number of stages, optimal-sized stages, proper volume and concentration of proppant) are efficient,
4) the dimensions (e.g., top, bottom and length) of the hydraulic fracture,
5) the comparison of the dimensions of the hydraulic fracture with the modeled dimensions and resultant estimates of production, and
6) how the hydraulic fracture orientation and length affect the choice of spacing of wells well and the locations of infill drilling to effectively drain the reservoir.

Refer to section 5.1 on page 75.

While most of task 3 has been cancelled, we still expect that the methodologies that we developed will be applied at Desert Peak, albeit not necessarily as part of this project. This cancellation also resulted in the cancellation of project subtask 1d (section 3.4 on page 38).

Calibrated Model

The results of the analysis of the diagnostic results were supposed to be compared with the calibrated model that was developed in project subtask 1c (section 3.3 on page 30).

Current models often still do not accurately predict fracture growth. This is due to poor characterization of rock, reservoir, and geology, and an incomplete understanding of relevant physics. However, calibrated models allow narrowing down the possible solutions for a fracture model and decreasing the degrees of freedom to obtain a match. Yet, even the solution of a calibrated model is not necessarily unique, as it is possible to assume values for other input parameters that are incorrect (in the absence of their measurement). Consequently, it could be necessary to over-correct other model parameters to obtain a calibrated match. This problem of not truly calibrating a model within reasonable bounds can be minimized by evaluating several basic measurements for fracture model input parameters and by conducting mapping on a series of treatments (as opposed to a single treatment). These basic measurements should include:

1) Fracture closure stress in pay zone (from pressure decline analysis following a breakdown injection);
2) end-of-job slurry efficiency to determine fracture volume (from pressure decline behavior following the fracture treatment), and
3) a limited series of tests to determine bounding layers stresses.

Model calibration is empirical, by matching both observed net pressures and observed fracture geometries. This empirical approach perhaps leads to improved physics in models. With time, it may then become possible to achieve the ultimate goal for a fracture modeler: a combined fracture, reservoir, and production model integrated with direct real-time fracture diagnostics. Refer to section 3.3 on page 30.

This project task was therefore supposed to close the loop on the development of a calibrated model for EGS applications. Starting with a calibrated hydraulic fracture model for oil-field analogues, we were supposed to test this calibrated model with directly measured hydraulic fracture dimensions. The calibrated model was supposed to be adjusted if necessary.

Once a calibrated model has been developed and verified, it can be used to predict what happens in other EGS applications more accurately. The calibrated hydraulic fracture growth model for EGS applications was supposed to be the vehicle to disperse knowledge about hydraulic fracture growth in EGS applications beyond the Desert Peak EGS area.

6 DISCUSSION AND CONCLUSIONS

In the Barnett Shale, extensive mapping of hydraulic stimulations shows that hydraulic fractures grow in a complex network because of their interaction with pre-existing natural fractures. The creation of such networks is expected to be highly beneficial for EGS reservoirs, due to their extensive volume and surface areas. For EGS reservoirs that are well bounded by neighboring layers with a higher fracture closure stress or by significant composite layering due to fracture growth through laminations, it is expected that the fractures will be well contained within the target interval. The total length and surface area of the network of fractures, instead of the length of the individual fractures, is expected to control the overall fluid flow patterns in EGS.

Based on many hydraulic fracture stimulations of oilfield reservoirs, in particular the Barnett Shale, it is likely that fracture mapping can provide valuable insight into the geometry of the network of fractures. This technique can also be used for real-time modification of the design of hydraulic stimulations. Like in the Barnett Shale, water fracturing in EGS is expected to result in an effective fracture conductivity that is equal or better than that from conventional propped fracturing, at significantly lower cost. In addition, such treatments will likely result in a greater extension of the fractures and an easier clean up. While vertical wells probably yield satisfactory results, the application of uncemented horizontal wells may have advantages for EGS: As in oil or gas reservoirs, horizontal EGS wells would alleviate the problem of inadequate locations at the surface, and maximize the lateral extent of the network of fractures.

For oilfield and EGS reservoirs, stimulation and diversion presents a challenging problem. In terms of stimulation and diversion, the main differences between oilfield and EGS are:

1) The volumes injected are significantly greater in EGS, because of the limited nature of the hydrocarbon-bearing strata relative to the presumably much larger target volume for EGS;
2) EGS rock is stronger than oildfield rock (however, while at first glance it may seem that stronger EGS rock is more difficult to fracture, it is actually more likely to benefit from natural fractures or other pre-existing weaknesses, as compared to weaker oilfield rock, due to fracture shearing combined with propping of asperities); and
3) most of the EGS developments have a more or less hydrostatic pressure gradient, in contrast to oilfield reservoirs (of which some can be over- or under-pressurized, although many are at or near hydrostatic pressure).

Based on the lessons learned from diversion of fluid flow in oil field environments, the following recommendations apply to development of EGS (in order of best expected performance through effective vertical and lateral diversion):

1) Deviated and horizontal cased well bore for excellent control of height and lateral diversion; coiled tubing fracture treatments for quick execution (but with severe rate limitations), combined with implementation of alternating rates, gel viscosities, proppant slugs and pump ins and shut ins to create stress shadowing for lateral and vertical diversion. A series of directional wells could be used, with the well azimuth in the direction of the least principle stress to maximize the number of active fracture intersections. While transverse fracture systems are effective in draining a large volume of the hydrocarbon reservoir, the rate of heat transfer needs to be balanced with respect to the capacity of the reservoir to prevent the reduction of the heat and flow gradients. As in the oilfield, horizontal EGS wells would alleviate the problem of inadequate locations at the surface, and maximize the lateral extent of the network of fractures. It could be possible to stimulate through horizontal wells to obtain the largest network but then produce from and inject into vertical wells to maximize heat transfer or inject into vertical wells and produce from horizontal wells. This would be an interesting, but probably costly, method to combine these two technologies.
2) Deviated and horizontal uncemented slotted liner with various perforation intervals for limited entry fracturing with single treatment at very high slurry rate, combined with implementation of alternating rates, gel viscosities, proppant slugs and pump-ins - shut-ins to create stress shadowing for lateral diversion. As there is no reliable control of fluid diversion, some areas along the well may remain unstimulated. To eliminate these unstimulated areas, conducting multiple stimulation treatment stages with fluid diversion could be required. While vertical wells probably yield satisfactory results, the application of uncemented horizontal wells may have advantages for EGS, similar to the advantages observed in oilfield applications.
3) Horizontal open hole with hydra-jet or propellant initiation strategy, combined with implementation of alternating rates, gel viscosities, proppant slugs, and pump-ins and shut-ins to create stress shadowing for lateral diversion. Hydra-jet and

propellant assisted initiation aim to achieve flow diversion while fluid contact with the reservoir is not physically restricted by locally pressurizing and thus stimulating only a small target zone. As such, these two techniques could be useful for initiating fracture network stimulations along a long open hole interval in EGS.

Regularly scheduling re-fracture treatments in EGS projects may also be an effective way to stimulate continuously other parts of the reservoir, as the state of stress in the reservoir is changes by placement of proppant, pore pressure and heat transfer changes.

There are cases where current fracture growth modeling can provide accurate estimates of fracture geometry. Classical mechanisms to confine fracture height growth (e.g., closure stress or permeability barriers), are incorporated in most models of fracture growth, and are sometimes sufficient to describe fracture growth behavior. However, the ability to predict in which environments these classical mechanisms dictate fracture growth is still limited. It appears that composite layering is the dominant mechanism to control fracture confinement. It is still not fully understood when this mechanism is more prevalent and when it is not. For example, we have observed composite layering is more important in laminated formations. In addition, layers with a mechanical contrast compared to neighboring layers (e.g., coal, which has a much lower modulus than most other rock types) often provide significant confinement.

Models today are more sophisticated than twenty years ago. However, they often still do not accurately predict fracture growth. This is due to poor characterization of rock, reservoir, and geology, and an incomplete understanding of relevant physics. However, calibrated models allow narrowing down the possible solutions for a fracture model and decreasing the degrees of freedom to obtain a match. However, even the solution of a calibrated model is not necessarily unique, as it is possible to assume values for other input parameters that are not correct (in the absence of their measurement). Consequently, it could be necessary to over-correct other model parameters to obtain a calibrated match. This problem of not truly calibrating a model within reasonable bounds can be minimized by evaluating several basic measurements for fracture model input parameters and by conducting mapping on a series of treatments (as opposed to a single treatment). These basic measurements should include:

1) Fracture closure stress in pay zone (from pressure decline analysis following a breakdown injection);
2) end-of-job slurry efficiency to determine fracture volume (from pressure decline behavior following the fracture treatment),
3) a limited series of tests to determine bounding layers stresses.

Model calibration is empirical, by matching both observed net pressures and observed fracture geometries. This empirical approach perhaps leads to improved physics in models. With time, it may then become possible to achieve the ultimate goal for a fracture modeler: a combined fracture, reservoir, and production model integrated with direct real-time fracture diagnostics.

Summarizing, these lessons learned from the vast amount of information that has been collected for the Barnett Shale could contribute to the development of hydraulic stimulations in EGS. In addition to determining the state of stress and the mechanical properties of the potential reservoir rock, it important to determine the density, geometry and connectivity of pre-existing networks of natural fractures, and the existence of bounding layers. This information can then contribute to the design and locations of the wells, and the design of the stimulation itself.

While a number of stimulation and diversion techniques from the oilfield can be applied to EGS, the differences between oilfield and EGS applications necessitate further study. The overview and discussion presented in this report is intended as inspiration to discover novel and improved techniques to improve the effectiveness of the development of EGS.

Direct diagnostic observations on more than 1,000 hydraulic fracture treatments have revealed the surprising complexity and variability of hydraulic fracturing. Fracture model calibration has proved both heartening and humbling. However, we have learned how a fracture model can be adjusted to match most diagnostic results and the observed net pressure behavior. Fracture height confinement is in many cases is more significant than earlier expected, and is most likely caused by layer interface effects. The physics of fracture growth along and through layer interfaces is not well understood and is not captured well in most current models.

7 REFERENCES

ABAQUS: "ABAQUS / Standard Version 6.5 Data Sheet," 2005a.

ABAQUS: "ABAQUS / Standard Version 6.5 Product Profile," 2005b.

Advani, S.H., Lee, T.S., and Lee, J.K.: "Three-dimensional Modeling of Hydraulic Fractures in Layered Media - Part I - Finite Element Formulations," Journal of Energy Resources Technology, Vol. 112, pp. 1-9, 1990.

Albright, J.N., and Pearson, C.F.: "Acoustic Emissions as a Tool for Hydraulic Fracture Location: Experience at the Fenton Hill Hot Dry Rock Site," Society of Petroleum Engineers Journal, Vol. 22 (1982), pp. 523-530, Society of Petroleum Engineers paper 09509.

André, A.-S., Saussee, J., and Lespinasse, M.: "New Approach for the Quantification of Paleostress Magnitudes: Application to the Soultz Vein System (Rhine Graben, France)," Tectonophysics, Vol. 336 (2001), pp. 215-231.

Asanuma, H., Kumano, Y., Izumi, T., Soma, N., Kaeida, H., Aoyagi, Y., Tezuka, K., Wyborn, D., and Niitsuma, H.: "Microseismic Monitoring of a Stimulation of HDR Reservoir at Cooper Basin, Australia by the Japanese Team," Geothermal Resources Council Transactions, Vol. 28 (2004), pp. 191-195.

Asanuma, H., Nozaki, H., Niitsuma, H., Wyborn, D.: "Interpretation of Microseismic Events with Larger Magnitude Collected at Cooper Basin, Australia," Geothermal Resources Council Transactions, Vol. 29 (2005), pp. 87-91.

Asanuma, H., Soma, N., Kaieda, H., Kumano, Y., Izumi, T., Tezuka, K., Niitsuma, H., and Wyborn, D.: "Microseismic Monitoring of Hydraulic Stimulation at the Australian HDR Project in Cooper Basin," Proceedings of the International Geothermal Association 2005 World Geothermal Congress, Antalya, Turkey, 24-29 April.

Aud, W.W., Wright, T.B., Cipolla, C.L., Harkrider, J.D., and Hansen, J.T.: "The Effect of Viscosity on Near- well Tortuosity and Premature Screenouts," Society of Petroleum Engineers paper 28492, 1994.

Bächler, D.: "Coupled Thermal-hydraulic-chemical Modeling at the Soultz-sous-Forêts HDR Reservoir (France)," Ph.D. thesis (2003), ETH Zürich, Switzerland, 151 pp.

Bagheri, M., and Settari, A.: "Modeling of Geomechanics in Naturally Fractured Reservoirs," Society of Petroleum Engineers paper 93083, 2005.

Bandis, S.C., Lumsden, A.C., and Barton, N.R.: "Fundamentals of Rock Joint Deformation," International Journal of Rock Mechanics and Mining Sciences and Geomechanics Abstracts, Vol. 20 (1983), No. 6, pp. 249-268.

Baria, R., Michelet, S., Baumgärtner J., Dyer, B., Gerard, A., Nicholls, J., Hettkamp, T., Teza, D., Soma, N., Asanuma, H., Garnish, J., and Mégel, T..: "Microseismic Monitoring of the World's Largest Potential HDR Reservoir," 29th Workshop on Geothermal Reservoir Engineering, Stanford, California, January 26-28, 2004.

Baria, R., Michelet, S., Baumgärtner, J., Dyer, B., Gerard, A., Hettkamp, T., Teza, D., Soma, N., Asanuma, H., and Garnish, J.: "Creation and Mapping of 5000 m Deep HDR / HFR Reservoir to Produce Electricity," Proceedings of the International Geothermal Association 2005 World Geothermal Congress, Antalya, Turkey, 24-29 April.

Baria, R., Michelet, S., Baumgärtner, J., Dyer, B., Nicholls, J., Hettkamp, T., Teza, D., Soma, N., Asanuma, H., Garnish, J., Megel, T., Kohl, T., and Kueperkoch, L.: "A 5000m Deep Reservoir Development at the European HDR Site at Soultz," Proceedings of the 30th Workshop on Geothermal Reservoir Engineering, Stanford, California, January 31-February 2, 2005, pp. 291-298.

Barree, R.D., Fisher, M.K., and Woodroof, R.A.: "A Practical Guide to Hydraulic Fracture Diagnostic Technologies", Society of Petroleum Engineers paper 77442, 2002.

Barree, R.D.: "A New Look at Fracture-tip Screenout Behavior," Journal of Petroleum Technology, Vol. 138 (1991), Society of Petroleum Engineers paper 18955, Transactions of the American Institute of Mining, Metallurgical, and Petroleum Engineers, Vol. 291, pp. 138-147.

Barree, R.D.: "A Practical Numerical Simulator for Three-dimensional Fracture Propagation in Heterogeneous Media," Society of Petroleum Engineers paper 12273, 1983.

Barton, N.R., Bandis, S.C., Bakhtar, K.: "Strength, Deformation and Conductivity Coupling of Rock Joints," International Journal of Rock Mechanics and Mining Sciences and Geomechanics Abstracts, Vol. 22 (1985), No. 3, pp. 121-140.

Batycky, R.P., Blunt, M.J, and Thiele, M.R.: "A 3D Filed Scale Streamline-Based Reservoir Simulator," Society of Petroleum Engineers Reservoir Engineering, (November 1997), pp. 246-254.

Bell, C.E., Holmes, B.W., and Rickards, A.R.: "Effective Diverting on Horizontal Wells in the Austin Chalk," Society of Petroleum Engineers paper 26582, 1993.

Bellinger, C.E.: "Horizontal Well in the Devonian Shale, Martin County, Kentucky," Society of Petroleum Engineers paper 23447, 1991.

Berchenko, I., and Detournay, E.: "Deviation of Hydraulic Fractures through Poroelastic Stress Changes Induced by Fluid Injection and Pumping", International Journal of Rock Mechanics and Mining Sciences and Geomechanics Abstracts, Vol. 34 (1997), No. 6, pp. 1,009-1,019.

Biglarbigi, K., Mohan, H., Ray, R.M., and Meehan, D.N.: "Potential for Horizontal Well Technology in the U.S.," Journal of Petroleum Technology, Vol. 52 (2000), No. 6, pp. 68-75, Society of Petroleum Engineers paper 62619 and 59360.

Branagan, P.T., Warpinski, N.R., Engler, B., and Wilmer, R.: "Measuring the Hydraulic Fracture-induced Deformation of Reservoirs and Adjacent Rocks Employing a Deeply Buried Inclinometer Array: GRUDOE Multi-site Project," Society of Petroleum Engineers paper 36451, 1996 Annual Technical Conference held in Denver, 6-9 October.

Brown, J.E., Thrasher, R.W., and Behrmann, L.A.: "Fracturing Operations," Chapter 11 in Economides, M.J. and Nolte, K.G. (editors): "Reservoir Stimulation," third edition, John Wiley and Sons, New York, New York, 2000, 856 pp.

Brown, S.R.: "Transport of Fluid and Electric Current through a Single Fracture," Journal of Geophysical Research, Vol. 94 (1989), pp. 9,429-9,438.

Bruno, M.S., and Nakagawa, F.M.: "Pore Pressure Influence on Tensile Fracture Propagation in Sedimentary Rock," International Journal of Rock Mechanics and Mining Sciences and Geomechanics Abstracts, Vol. 28 (1991), No. 4, pp. 261-273.

Buchsteiner, H., Warpkinski, N.R., and Economides, M.J.: "Stress Induced Permeability Reduction in Fissured Reservoirs," Society of Petroleum Engineers paper 26513, 1993.

Carter, B.J, Desroches, J., Ingraffea, A.R. and Wawrzynek, P.A.: "Simulating Fully 3D Hydraulic Fracturing," in Zaman, M., Gioda, G., and Booker, J.: "Modeling in Geomechanics" (2000), Wiley Publishers, 730 pp.

Carter, R.D.: "Derivation of the General Equation for Estimating the Extent of the Fractured Area," Appendix I of "Optimum Fluid Characteristics for Fracture Extension," Drilling and Production Practice, Howard, G.C., and Fast, C.R., New York, New York, American Petroleum Institute (1957), pp. 261-269.

Cinco L.H., and Samaniego V.F.: "Transient Pressure Analysis: Finite Conductivity Fracture Case Versus Damaged Fracture Case," Society of Petroleum Engineers paper 10179, 1981.

Cipolla, C.I., and Wright, C.A., "Diagnostic Techniques to Understand Hydraulic fracturing: What? Why? And How?" Society of Petroleum Engineers - Production and Facilities, Vol. 17 (2002), No. 1, pp. 23-35, Society of Petroleum Engineers paper 75359.

Cipolla, C.L., and Wright, C.A., "State-of-the-art in Hydraulic Fracture Diagnostics," Society of Petroleum Engineers paper 64434, 2000.

Cleary, M.P., and Fonseca, A. Jr.: "Proppant Convection and Encapsulation in Hydraulic Fracturing: Practical Implications of Computer and Laboratory Simulations," Society of Petroleum Engineers paper 24825, 1992r.

Cleary, M.P., Johnson, D.E., Kogsbøll, H-H., Owens, K.A., Perry, K.F., de Pater, C.J., Stachel, A., Schmidt, H., and Tambini, M.: "Field Implementation of Proppant Slugs To Avoid Premature Screen-Out of Hydraulic Fractures With Adequate Proppant Concentration," Society of Petroleum Engineers paper 25892, 1993.

Cleary, M.P., Keck, R.G., and Mear, M.E.: "Microcomputer Models for the Design of Hydraulic Fractures," Society of Petroleum Engineers / Department of Energy paper 11628, 1983.

Cleary, M.P., Wright, C.A., and Wright, T.B.: "Experimental and Modeling Evidence for Major Changes in Hydraulic Fracturing Design and Field Procedures," Society of Petroleum Engineers paper 21494, 1991.

Cleary, M.P.: "Analysis of Mechanisms and Procedures for Producing Favorable Shapes of Hydraulic Fractures," Society of Petroleum Engineers paper 09260, 1980a.

Cleary, M.P.: "Comprehensive Design Formulae for Hydraulic Fracturing," Society of Petroleum Engineers paper 09259, 1980b.

Clifton, R.J., and Abou-Sayed, A.S.: "A Variational Approach to the Prediction of the Three-dimensional Geometry of Hydraulic Fractures," Society of Petroleum Engineers paper 9879, 1981. .

Clifton, R.J., and Abou-Sayed, A.S.: "On the Computation of the Three-dimensional Geometry of Hydraulic Fractures," Society of Petroleum Engineers paper 7943, 1979. .

Clifton, R.J., and Wang, J.J.: "Adaptive Optimal Mesh Generator for Hydraulic Fracturing Modeling," Proceedings of the 32nd U.S. Rock Mechanics Symposium, 1991.

Clifton, R.J., and Wang, J.J.: "Modeling of Poroelastic Effects in Hydraulic Fracturing," Society of Petroleum Engineers paper 21871, 1991.

Clifton, R.J., and Wang, J.J.: "Multiple Fluids, Proppant Transport, and Thermal Effects in Three-dimensional Simulation of Hydraulic Fracturing," Society of Petroleum Engineers paper 18198, 1988. .

Clifton, R.J.: "Three-dimensional Fracture-propagation Models," chapter 5 in Gidley, J.L.: "Recent Advances in Hydraulic Fracturing," Society of Petroleum Engineers - Monograph Series, Vol. 12 (1989), Richardson, Texas.

Computer Modeling Group: "STARS Version 2003," User's Guide, Calgary, Alberta, Canada.

Computer Modelling Group Ltd.: "STARS - User's Guide," 2005, 881 pp.

Cooke, C.E., Jr., "Conductivity of Fracture Proppants in Multiple Layers," Journal of Petroleum Technology (September 1973), pp. 1,101-1,107, Society of Petroleum Engineers paper 4117.

Core Lab: "GOHFER School," 2003.

Coulter, G.R., and Wells, R.D.: "The Advantages of High Proppant Concentration in Fracture Stimulation," Journal of Petroleum Technology (June 1972), pp. 643-650, Society of Petroleum Engineers paper 3298.

Coulter, G.R., Benton, E.G., and Thomson, C.L.: "Water Fractures and Sand Quantity: A Barnett Shale Example," Society of Petroleum Engineers paper 90891, 2004.

Coursen, D.L.: "Early Production from Some Devonian Shale Gas Wells Stimulated with Several Kinds of Explosive Charge," Society of Petroleum Engineers paper 12322, 1983.

Cramer, D.D.: "The Application of Limited-entry Techniques in Massive Hydraulic Fracturing Treatments," Society of Petroleum Engineers paper 16189, 1987.

Crockett, A.R., and Okusu, N.M., and Cleary, M.P.: "A Complete Integrated Model for Design and Real-time Analysis of Hydraulic Fracturing Operations," Society of Petroleum Engineers paper 15069, 1986.

Crockett, A.R., Willis, R.M. and Cleary, M.P.: "Improvement of Hydraulic Fracture Predictions by Real-time History Matching on Observed Pressures," Society of Petroleum Engineers - Production Engineering Vol. 4 (1989), No. 4, pp. 408-416, Society of Petroleum Engineers paper 15264.

Cuenot, N., Charléty, J., Dorbath, L., and Haessler, H.: "Faulting Mechanisms and Stress Tensor at the European HDR Site of Soultz-sous-Forêts," Proceedings of the 30th Workshop on Geothermal Reservoir Engineering (2005), Stanford, California, 31 January-2 February.

Dees, J.M. and Handren, P.J.: "A New Method of Overbalance Perforating and Surging of Resin for Sand Control," Society of Petroleum Engineers paper 26545, 1993.

Dershowitz, W., Hurley, N., and Been, K.: "Stochastic Discrete Fracture Modeling of Heterogeneous and Fractured Reservoirs," Proceedings of the 1992 3rd European Conference on the Mathematics of Oil Recovery, Delft, The Netherlands.

East, L.E. Jr., Grieser, W., McDaniel, B.W., Johnson, B., Jackson, R., and Fisher, K.: "Successful Application of Hydra-jet Hydraulic Fracturing on Horizontal Wells Completed in a Thick Shale Reservoir," Society of Petroleum Engineers paper 91435, 2004.

Eberhard, M.J., Schlosser, D.E.: "Current Use of Limited-entry Hydraulic Fracturing in the Codell / Niobrara Formations - DJ Basin," Society of Petroleum Engineers paper 29553, 1995.

Economides, M.J. and Nolte, K.G. (editors): "Reservoir Stimulation," third edition, John Wiley and Sons, New York, New York, 2000, 856 pp.

Economides, M.J., and Nolte, K.G. (editors): "Reservoir Stimulation," third edition, 2000, pp. 9.21-9.24, John Wiley and Sons, Ltd, New York.

Economides, M.J., and Nolte, K.G.: "Reservoir Stimulation," Schlumberger, 2004.

Elbel, J. and Britt, L.: "Fracture Treatment Design," chapter 10 in M.J. Economides and K.G. Nolte (editors): "Reservoir Stimulation," third edition, John Wiley and Sons, New York, New York, 2000, 856 pp.

Elbel, J.L., and Mack M.G.: "Refracturing: Observations and Theories," Society of Petroleum Engineers paper 25464, 1993 Production Operations Symposium, Oklahoma City, 21-23 March.

Entingh, D.J.: "Geothermal Well Stimulation Experiments in the United States," Proceedings of the International Geothermal Association 2000 World Geothermal Congress held in Kyushu - Tohoku, Japan, 28 May-10 June.

Evans, K., Holzhausen, G., and Wood, D.M.: "The Geometry of a Large-scale Nitrogen Gas Hydraulic Fracture Formed in Devonian Shale: An Example of Fracture Mapping with Tiltmeters," Society of Petroleum Engineers Journal, Vol. 22 (1982), No. 5, pp. 755-763, Society of Petroleum Engineers paper 08933.

Fan, Y. and Economides, M.J.: "Fracturing Fluid Leakoff and Net Pressure Behavior in Frac and Pack Stimulation," Society of Petroleum Engineers paper 29988, 1995

Fan, Y.: "A New Interpretation Model for Fracture Calibration Treatments," Society of Petroleum Engineers paper 37401, 1997.

Fisher, M.K., Heinze, J.R., Harris, C.D., Davidson, B.M., Wright, C.A., and Dunn, K.P.: "Optimizing Horizontal Completion Techniques in the Barnett Shale Using Microseismic Fracture Mapping," Society of Petroleum Engineers paper 90051, 2004 Annual Technical Conference and Exhibition held in Houston, Texas, 26-29 September.

Fisher, M.K., Wright, C.A., Davidson, B.M., Goodwin, A.K., Fielder, E.O., Buckler, W.S., and Steinsberger,N.P.: "Integrating Fracture-Mapping Technologies To Improve Stimulations in the Barnett Shale," Society of Petroleum Engineers paper 77441, 2005.

Fisher, M.K., Wright, C.A., Davidson, B.M., Satisfactorywin, A.K., Fielder, E.O., Buckler, W.S., and Steinsberger, N.P.: "Integrating Fracture Mapping Technologies to Optimize Stimulations in the Barnett Shale," Society of Petroleum Engineers paper 77441, 2002.

Fix, J.E., Frantz Jr., J.H., and Lancaster, D.E.: "Application of Microseismic Technology in a Devonian Shale Well in the Appalachian Basin," Society of Petroleum Engineers paper 23425, 1991.

Freyer, R. and Huse, A.: "Swelling Packer for Zonal Isolation in Open Hole Screen Completions," Society of Petroleum Engineers paper 78312, 2002.

Ganong, B.L., Hansen, C., Connolly, P., and Barree, B.: "Rose Field: A McLure Shale, Monterey Formation Development Story," Society of Petroleum Engineers paper 83501, 2003.

Gentier, S., Rachez, X., Dezayes, C., Blaisonneau, A., and Genter A.: "How to Understand the Effect of the Hydraulic Stimulation in Terms of Hydro-Mechanical Behavior at Soultz-sous-Forêts (France)," Geothermal Resources Council Transactions, Vol. 29 (2005), pp. 159-166.

Geodynamics, Ltd.: "Cooper Basin HFR Geothermal Project - Major Upgrade of Underground Heat Exchanger and Development of Second Reservoir," Australian Stock Exchange (ASX) Announcement, 7 September 2005, 3 pp.

Gheissary, G., Fokker, P.A., Eggbertts, P.J.P., Floris, F.J.T., Sommerauer, G., and Kenter, C.J.: "Simulation of Fractures Induced by Produced Water Reinjection in a Multilayer Reservoir," Society of Petroleum Engineers paper 54735, 1998.

Gilbert, J. and Greenstreet, C.: "Application of Pinpoint Fracturing in the Cooper Basin, Australia," Society of Petroleum Engineers paper 97004, 2005.

Goktas, B. and Ertekin T.: "Performances of Openhole Completed and Cased Horizontal/Undulating Wells in Thin–Bedded, Tight Sand Gas Reservoirs," Society of Petroleum Engineers paper 65619, 2000.

Gottschling, J.C., Royce, T.N., and Shuck, L.Z.: "Nitrogen Gas and Sand: A New Technique for Stimulation of Devonian Shale," Journal of Petroleum Technology (May 1985), pp. 901-907, Society of Petroleum Engineers paper 12313.

Green, A.E., and Sneddon, I.N.: "The Stress Distribution in the Neighborhood of a Fat Elliptical Crack in an Elastic Solid," Proceedings of the Cambridge Philosophical Society, Vol. 46 (1950), pp. 159-164.

Grieser, B., Hobbs, J., Hunter, J., and Ables, J.: "The Rocket Science behind Water Fracturing Design," Society of Petroleum Engineers paper 80933, 2003.

Griffin, L.G., Sullivan, R.B., Wolhart, S.L., Waltman, C.K., Wright, C.A., Weijers, L., and Warpinski, N.R.: "Hydraulic Fracture Mapping of the High-temperature, High-pressure Bossier Sands in East Texas," Society of Petroleum Engineers paper 84489, 2003.

Griffin, L.G., Wright, C.A., Davis, E.J., Wolhart, S.L., and Moschovidis, Z.A.: "Surface and Downhole Tiltmeter Mapping: An Effective Tool for Monitoring Downhole Drill Cuttings Disposal," Society of Petroleum Engineers paper 63032, 2000.

Gringarten, A.C., Ramey Jr., H., and Raghavan, R.: "Unsteady-State Pressure Distributions Created by a Well with a Single Infinite-Conductivity Vertical Fracture," Society of Petroleum Engineers Journal, (August 1974), p. 347.

Gulrajani, S.N., and Nolte, K.G.: "Fracture Evaluation Using Pressure Diagnostics," chapter 9 in Economides, M.J., and Nolte, K.G. (editors): "Reservoir Stimulation," third edition, 2000, pp. 9.21-9.24, John Wiley and Sons, New York, New York.

Hagel, M., and Meyer, B.: "Utilizing Mini-fracture Data to Improve Design and Production," Journal of Canadian Petroleum Technology, Vol. 33 (1994), No. 3, Canadian Institute of Mining, Metallurgy and Petroleum paper 92-40, 1992.

Hainey, B.W., Weng, X., and Stoisits, R.F.: "Mitigation of Multiple Fractures from Deviated wells," Society of Petroleum Engineers paper 30482, 1995.

Handren, P.J., Jupp, T.B., and Dees, J.M.: "Overbalance Perforating and Stimulation Method for Wells," Society of Petroleum Engineers paper 26515, 1993.

Hannah, R.R., Park, E.I., Porter, D.A., Black, J.W.: "Combination Fracturing/Gravel-Packing Completion Technique on the Amberjack, Mississippi Canyon 109 Field," Society of Petroleum Engineers - Production and Facilities (November 1994), p. 262, Society of Petroleum Engineers paper 26562.

Hejl, K.A., Madding, A.M., Morea, M.F., Glatz, C.W., Luna, J., Minner, W.A., Singh, T., and Stanley, R.R.: "Extreme Multistage Fracturing Improves Vertical Coverage and Well Performance in the Lost Hills Field," Society of Petroleum Engineers paper 101840, 2006.

Hoch, O., Stromquist, M., Love, G., and Argan, J.:. "Multiple Precision Hydraulic Fractures of Low-Permeability Horizontal Openhole Sandstone Wells," Society of Petroleum Engineers paper 84163, 2003.

Hole, J.A., and Zelt, B.C.: "3-D Finite Difference Reflection Traveltimes," Geophysics Journal International, Vol. 121 (1995), pp. 427-434.

Hopkins, C.W., Rosen, R.L., and Hill, D.G.: "Characterization of an Induced Hydraulic Fracture Completion in a Naturally Fractured Antrim Shale Reservoir," Society of Petroleum Engineers paper 51068, 1998.

Hopkins, D.L., Cook, N.G.W., and Myer, L.R.: "Normal Joint Stiffness as a Function of Spatial Geometry and Surface Roughness," Rock Joints (1990), Barton and Stephansson (editors), Balkema, Rotterdam, pp. 203-210.

House, L.: "Locating Microearthquakes Induced by Hydraulic Fracturing in Crystalline Rock," Geophysical Research Letters, Vol. 14 (1987), pp. 919-921.

Huang, W., Di Donato, G., and Blunt, M.J.: "Comparison of streamline-based and grid-based dual porosity simulation," Journal of Petroleum Science and Engineering, Vol. 43 (2004), pp. 129-137.

Itasca Consulting Group: "3DEC - 3 Dimensional Distinct Element Code - User's Guide," 2005.

Jaeger, J.C., and Cook, N.G.W.: "Fundamentals of Rock Mechanics," Chapman and Hall, London, United Kingdom, 515 pp., 1976.

Ji, L., Settari, A., Sullivan, R.B., and Orr, D.: "Methods For Modeling Dynamic Fractures in Coupled Reservoir and Geomechanics Simulation," Society of Petroleum Engineers paper 90874, 2004.

Johnson, R.L. Jr., and Brown, T.D.: "Large-volume, High-rate Stimulation Treatments in Horizontal Wells in the Niobrara Formation, Silo Field, Laramie County, Wyoming," Society of Petroleum Engineers paper 25926, 1993.

Johnson, R.L., Dunn, K.P., Bastian, P.A., Hopkins, C.W., and Conway, M.W.: "Qualifying Hydraulic fracturing Effectiveness in Tight, Naturally Fractured Reservoirs by Combining Three-dimensional Hydraulic fracturing and Reservoir Simulators," Society of Petroleum Engineers paper 49048, 1998.

Jung, R., Richard, J. W., Nicholls, J., Bertozzi, A., and Heinemann, B.: "Evaluation of Hydraulic Tests at Soultz-sous-Forêts, European HDR-site,", International Geothermal Association 1995 World Geothermal Congress held in Florence, Italy, 18-31 May 1995, pp. 2,611-2,616.

Karner, S.L.: "Creating Permeable Fracture Networks for EGS: Engineered Systems versus Nature," Geothermal Resources Council Transactions, Vol. 29 (2005), pp. 167-172, 2005a.

Karner, S.L.: "Stimulation Techniques Used in Enhanced Geothermal Systems: Perspectives from Geomechanics and Rock Physics," Proceedings of the 30th Stanford Geothermal Workshop (2005), 2005b.

Keck, R.G., Cleary, M.P., and Crockett, A.: "A Lumped Numerical Model for the Design of Hydraulic Fractures," Society of Petroleum Engineers paper 12884, 1984.

Klee, G., and Rummel, F.: "Hydrofrac Stress Data for the European HDR Research Test Site Soultz-sous-Forêts," International Journal of Rock Mechanics Sciences and Geomechanics Abstracts, Vol. 30 (1993), No. 7, pp. 973-976.

Kohl T., Jung, R., Hopkirk, R.J., and Rybach, L.: "Non-linear Flow Transients in Fractured Rock Masses - The 1995 Injection Experiment in Soultz," Proceedings of the 21st Workshop for Geothermal Reservoir Engineering (1996), Stanford, California, 22-24 January, pp.157-164.

Kohl, T., and Mégel, T.: "Predictive Modeling of Reservoir Response to Hydraulic Stimulations at the European EGS Site Soultz-sous-Forêts," International Journal of Rock Mechanics, submitted (2005), 20 pp, 2005b.

Kohl, T., and Mégel, T.: "Coupled Hydro-mechanical Modeling of the GPK3 Reservoir Stimulation at the European EGS Site Soultz-Sous-Forêts," paper SGP-TR-176 in Proceedings of the 2005 13th Workshop on Geothermal Reservoir Engineering held in Stanford, California, 31 January-2 February, 2005a.

Koning, E.J.L.: "Waterflooding under Fracturing Conditions," Ph.D. dissertation, Technical University of Delft, The Netherlands, 1988.

Kucuk, F. and Brigham, E.W.: "Transient Flow in Elliptical Systems," Society of Petroleum Engineers Journal (June 1981), p. 309.

Kumano, Y., Moriya, H., Wyborn, D., and Niitsuma, H.: "Estimation of Detailed Reservoir Structure at Cooper Basin HDR Field, Australia by Using Microseismic Multiplet," Geothermal Resources Council Transactions, Vol. 29 (2005), pp. 93-97.

Kuuskraa, V.A., Koperna, G., Schmoker, J.W., and Quinn, J.C.: "Barnett Shale-rising Star in Fort Worth Basin," Oil and Gas Journal (May 1998), pp. 67-76.

Lagrone, K.W., and Rasmussen, J.W.: "A New Development in Completion Methods- The Limited Entry Technique," Journal of Petroleum Technology (July 1963), pp. 695-702, Society of Petroleum Engineers paper 00530.

Lamb, H.: "Hydrodynamics," 6th edition (1932), Dover Publications, New York, New York, pp. 581-587.

Lancaster, D.E., McKetta, S.F., Hill, R.E., Guidry, F.K., and Jochen, J.E.: "Reservoir Evaluation, Completion Techniques, and Recent Results from Barnett Shale Development in the Fort Worth Basin," Society of Petroleum Engineers paper 24884, 1992.

Layne, A.W., and Siriwardane, H.J.: "Insights into Hydraulic Fracturing of a Horizontal Well in a Naturally Fractured Formation," Society of Petroleum Engineers paper 18255, 1988.

Lietard, O., Ayoub, J., and Pearson, A.: "Hydraulic Fracturing of Horizontal Wells: An Update of Design and Execution Guidelines," Society of Petroleum Engineers paper 37122, 1996.

Logan, E.D., Bjornen, K.H., and Sarver, D.R.: "Foamed Diversion in the Chase Series of Hugoton Field in the Mid-Continent," Society of Petroleum Engineers paper 37432, 1997.

Loman, G., Phillips, D.T., and Cicon, H.N.: "Stimulation of Horizontal Wells Using the Dynamic Gas Pulse Loading Technique," Society of Petroleum Engineers paper 37097, 1996.

Ma, M.J. and Yew, C.H. "A 3D Fracture Simulator for Soft Formation," in Amadei, B., Kranz, R.L., Scott, G.A., and Smeallie, P.H. (editors): "Rock Mechanics for Industry," Balkema, Rotterdam, The Netherlands, pp. 1079–1084, 1999.

Mack, M.G., and Warpinkski, N.R.: "Mechanics of Hydraulic Fracturing," chapter 6 in Economides, M.J., and Nolte, K.G.: "Reservoir Stimulation," (2000), third edition, Wiley Publishers, 750 pp.

Makurat, A., Gutierreq, M.: "Fracture Flow and Fracture Cross Flow Experiments," Society of Petroleum Engineers paper 36732, 1996.

Maxwell, S.C, Urbancic, T.I, Falls, S.D., and Zinno, R.: "Real-time Microseismic Mapping of Hydraulic Fractures in Carthage, Texas,", Society of Exploration Geophysicists 2000t.

Maxwell, S.C, Urbancic, T.I., Steinsberger, N., and Zinno, R.: "Microseismic Imaging of Hydraulic Fracture Complexity in the Barnett Shale," Society of Petroleum Engineers paper 77440, 2002r.

Mayerhofer, M.J., and Economides, M.J.: "Fracture Injection Test Interpretation: Leakoff Coefficient vs. Permeability Estimation," Society of Petroleum Engineers - Production and Facilities, Vol. 12 (1997), No. 4, pp. 231-236, Society of Petroleum Engineers paper 28562.

Mayerhofer, M.J., and Meehan, D.: "Water fractures - Results from 50 Cotton Valley Wells," Society of Petroleum Engineers paper 49104, 1998.

Mayerhofer, M.J., Ehlig-Economides, C.A., and Economides, M.J.: "Pressure Transient Analysis of Fracture Calibration Tests," Society of Petroleum Engineers paper 26527, 1993.

Mayerhofer, M.J., Lolon, E.P., Youngblood, J.E., and Heinze, J.R.: "Integration of Microseismic Fracture Mapping Results with Numerical Fracture Network Production Modeling in the Barnett Shale," Society of Petroleum Engineers paper 102103, 2006.

Mayerhofer, M.J., Richardson, M.F., Walker, R.N. Jr., Meehan, D.N., Ohler, M.W., and Browning, R.R. Jr.: "Proppants? We Don't Need No Proppants," Society of Petroleum Engineers paper 38611, 1997.

Mayerhofer, M.J., Walker, R.N. Jr., Urbancic, T., and Rutledge, J.T.: "East Texas Hydraulic Fracture Imaging Project: Measuring Hydraulic Fracture Growth of Conventional Sandfracs and Water fractures," Society of Petroleum Engineers paper 63034, 2000.

McDaniel, B.W., McMechan, D.E., and Stegent, N.A.: "Proper Use of Proppant Slugs and Viscous Gel Slugs Can Improve Proppant Placement During Hydraulic Fracturing Applications," Society of Petroleum Engineers paper 71661, 2001a.

McDaniel, B.W., Stegent, N.A., and Ellis, R.: "How Proppant Slugs and Viscous Gel Slugs Have Influenced the Success of Hydraulic Fracturing Applications," Society of Petroleum Engineers paper 71073, 2001b.

McDaniel, B.W., Willett, R.M., and Underwood, P.J.: "Limited-entry Fracture Applications on Long Intervals of Highly Deviated or Horizontal Wells," Society of Petroleum Engineers paper 56780, 1999.

McEvilly, T.V. and Majer, E.L.: "ASP: An Automated Seismic Processor for Microearthquake Networks," Bulletin of the Seismological Society of America, Vol. 72 (1982), No. 1, pp. 303-325.

Meehan, D.N., and Pennington B.F.: "Numerical Simulation Results in the Carthage Cotton Valley Field," Journal of Petroleum Technology, Vol. 34 (1982), No. 9,838, pp. 189-198, Society of Petroleum Engineers paper 9838.

Meehan, D.N.: "Stimulation Results in the Giddings (Austin Chalk) Field," Society of Petroleum Engineers - Production and Facilities, Vol. 10 (1995), No. 2, pp. 96-102, Society of Petroleum Engineers paper 24783.

Mégel, T., Kohl, T., Gérard, A., Rybach, L., and Hopkirk, R.: "Downhole Pressures Derived from Wellhead Measurements during Hydraulic Experiments," Proceedings of the International Geothermal Association 2005 World Geothermal Congress, Antalya, Turkey, 24-29 April.

Meyer, B.R., Cooper, G.D., and Nelson, S.G.: "Real-time 3D Hydraulic Fracturing Simulation: Theory and Field Case Studies," Society of Petroleum Engineers paper 20658, 1990.

Meyer, B.R.: "Design Formulae for Two- and Three-dimensional Vertical Hydraulic Fractures: Model Comparison and Parametric Studies," Society of Petroleum Engineers paper 15240, 1986.

Meyer, B.R.: "Three-Dimensional Hydraulic Fracturing Simulation on Personal Computers: Theory and Comparison Studies," Society of Petroleum Engineers paper 19329, 1989.

Minner, W.A., Du, J., Ganong, B.L., Lackey, C.B., Demetrius, S.L., Wright, C.A.: "Rose Field: Surface Tilt Mapping Shows Complex Fracture Growth in 2500' Laterals Completed with Un-cemented Liners," Society of Petroleum Engineers paper 83503, 2003.

Minner, W.A., Wright, C.A., Stanley, G.R., de Pater, C.J., Gorham, T.L., Eckerfield, L.D., and Hejl, K.A.: "Waterflood and Production-induced Stress Changes Dramatically Affect Hydraulic Fracture Behavior in Lost Hills Infill Wells," Society of Petroleum Engineers paper 77536, 2002.

Minner, W.A., Wright, C.A., and Dobie, C.A.: "Treatment Diagnostics and Net Pressure Analysis Assist with Fracture Strategy Evaluation in the Belridge Diatomite," Society of Petroleum Engineers paper 35696, 1996.

Mroz, T.H., and Schuller, W.A.: "Geotechnical Evaluations for Siting Horizontal Wells in Devonian Shale Reservoirs," Society of Petroleum Engineers paper 21295, 1990.

Nelson, E.B.: "Introduction," in Nelson, E.B. (editor) "Well Cementing," Schlumberger (1990), Houston, Texas, pp. I-1 - I-3.

Nelson, G.D., and Vidale, J.E.: "Earthquake Locations by 3D Finite Difference Travel Times," Bulletin of the Seismological Society of America, Vol. 80 (1990), pp. 395.

Nolte, K.G., Mack, M.G., and Lie, W.L.: "A Systematic Method for Applying Fracturing Pressure Decline: Part 1," Society of Petroleum Engineers paper 25845, 1993.

Nolte, K.G.: "Determination of Fracture Parameters from Fracturing Pressure Decline," Society of Petroleum Engineers paper 08341, 1979.

Olsson, W.A., Brown, S.R.: "Hydromechanical Response of a Fracture Undergoing Compression and Shear," International Journal of Rock Mechanics and Mining Sciences and Geomechanics Abstract, Vol. 30 (1993), No. 7, pp. 845-851.

Overbey, W.K. Jr., Yost, A.B. II, and Wilkins, D.A.: "Inducing Multiple Hydraulic Fractures from a Horizontal Well," Society of Petroleum Engineers paper 18249, 1988.

Palmer, I.D.: "Induced Stresses Due to Propped Hydraulic Fracture Coalbed Methane Wells," Society of Petroleum Engineers paper 25861, 1993.

Parrish, R.L., Stevens A.L., and Turner T.F. Jr.: "A True In-situ Fracturing Experiment - Final Results," Journal of Petroleum Technology, Vol. 33 (1981), No. 7, pp. 1,297-1,304, Society of Petroleum Engineers paper 07513.

Pasarai, U., and Arihara, N.: "A Simulator for Predicting Thermal Recovery Behavior Based on Streamline Method," Society of Petroleum Engineers paper 97411, 2005.

Pasarai, U., and Arihara, N.: "Application of Streamline Method to Hot Water-Flooding Simulation for Heavy Oil Recovery," Society of Petroleum paper 93149, 2005.

Perkins, T.K., and Kern, L.R.: "Widths of Hydraulic Fractures," Journal of Petroleum Technology, Vol. 13 (1961), No. 9, pp. 937-949, Society of Petroleum Engineers paper 00089.

Phillips, W.S., Rutledge, J.T., Fairbanks, T.D., Gardner, T.L., Miller, M.E., and Schuessler, B.K.: "Reservoir Fracture Mapping using Microseisms: Austin Chalk, Giddings Field, TX and 76 Field, Clinton Co., KY," Society of Petroleum

Engineers - Reservoir Evaluation and Engineering, Vol. 1 (1998), No. 2, pp. 114-121, Society of Petroleum Engineers paper 36651.

Pope, C.D. and Handren, P.J.: "Completion Techniques for Horizontal Wells in the Pearsall Austin Chalk," Society of Petroleum Engineers - Production Engineering, May, p. 144–148, 1992, Society of Petroleum Engineers paper 20682.

Prats, M.: "Effect of Vertical Fractures on Reservoir Behavior - Incompressible Fluid Case," Society of Petroleum Engineers Journal, Vol. 1 (1961), No. 1, pp. 105-118, Society of Petroleum Engineers paper 1575-G.

Reeves, S.R., Cox, D.O., Smith, M.B., and Schatz, J.F.: "Stimulation Technology in the Antrim Shale," Society of Petroleum Engineers paper 26203, 1993a.

Reeves, S.R., Hill, D.G., and Cox, D.O.: "Production Optimization in the Antrim Shale," Society of Petroleum Engineers paper 25461, 1993b.

Robert, J.A. and Rossen, W.R.: "Fluid Placement and Pumping Strategy," chapter 19 in Economides, M.J. and Nolte, K.G. (editors): "Reservoir Stimulation," third edition, John Wiley and Sons, New York, New York, 2000, 856 pp.

Rutledge, J.T., and Phillips, W.S.: "A Comparison of Microseismicity Induced by Gel-proppant- and Water-injected Hydraulic Fractures, Carthage Cotton Valley Gas Field, East Texas,", 2002 Society of Exploration Geophysicists 72nd Annual International Meeting, Expanded Abstracts, pp. 2,393-2,396.

Rutledge, J.T., and Phillips, W.S.: "Hydraulic Stimulation of Natural Fractures as Revealed by Induced Microseisms, Carthage Cotton Valley Gas Field, East Texas," Geophysics, Vol. 68 (2003), pp. 441-452.

Rutledge, J.T., Phillips, W.S., and Mayerhofer, M.J., "Faulting Induced by Forced Fluid Injection and Fluid Flow Forced by Faulting: An Interpretation of Hydraulic-fracture Microseismicity, Carthage Cotton Valley Gas Field, Texas," Bulletin of the Seismology Society of America, Vol. 94 (2004), No. 5, pp. 1,817-1,830.

Rutledge, J.T., Phillips, W.S., House, L.S., and Zinno, R.J.: "Microseismic Mapping of a Cotton Valley Hydraulic Fracture using Decimated Downhole Arrays,", 1998 Society of Exploration Geophysicists 68th Annual International Meeting, Expanded Abstracts, pp. 338-341.

Sanyal, S.K., Butler, S.J., Swenson, D., and Hardeman, B.: "Review of the State-of-the-art of Numerical Simulation of Enhanced Geothermal Systems," Proceedings of the 2000 World Geothermal Congress held in Kyushu - Tohuku, Japan, 28 May- 10 June, pp. 3,853-3,858.

Sanyal, S.K., Lovekin, J.W., Henneberger, R.C., Robertson-Tait, A., and Brown, P.J.: "Injection Testing for an Enhanced Geothermal System Project at Desert Peak, Nevada," Geothermal Resources Council Transactions, Vol. 27 (2003), pp. 885-891.

Schein, G.W., Carr, P.D., Canan, P.A., and Richey, R.: "Ultra Lightweight Proppants: Their Use and Application in the Barnett Shale," Society of Petroleum Engineers paper 90838, 2004.

Schlumberger: "FracCADE, model formulation document," not dated.

Schlumberger: "FracCADE, User Guide 5.1," (2002).

Settari, A.: "Simulation of Hydraulic Fracturing Processes," Society of Petroleum Engineers Journal, Vol. 487 (December 1980).

Sharma, M.M., Gadde, P.B., Sullivan, R., Sigal, R., Fielder,R., Copeland, D., Griffin, L., and Weijers, L.: "Slickwater and Hybrid Fracs in the Bossier: Some Lessons Learnt," Society of Petroleum Engineers paper 89876, 2004.

Shelkholeslami, B.A., Schlottman, B.W., Seidel, F.A., and Button, D.M.: "Drilling and Production Aspects of Horizontal Wells in the Austin Chalk," Journal of Petroleum Technology, Vol. 43 (1991), No. 7, pp. 773-779, Society of Petroleum Engineers paper 19825.

Shlyapobersky, J., Wong, G.K., and Walhaug, W.W.: "Overpressure Calibrated Design of Hydraulic Fracture Stimulations," Society of Petroleum Engineers paper 18194, 1988.

Siebrits, E., Elbel, J.L., Detournay, E., Detournay-Piette, C., Christianson, M., Robinson, B.M., and Diyashev, I.R.: "Parameters Affecting Azimuth and Length of a Secondary Fracture during a Refracturing Treatment," Society of Petroleum Engineers paper 48928, 1998.

Siebrits, E., Elbel, J.L., Hoover, R.S., Diyashev, I.R., Griffin, L.G., Demetrius, S.L., Wright, C.A., Davidson, B.M., Steinsberger, N.P., and HiII, D.G.: "Refracture Re-orientation Enhances Gas Production in Barnett Shale Tight Gas Wells," Society of Petroleum Engineers paper 63030, 2000.

Smith, M. B., Klein, H. H., "Practical Applications of Coupling Fully Numerical 2-D transport Calculation With a PC-Based Fracture Geometry Simulator," Society of Petroleum Engineers paper 30505, 1995.

Smith, M.B., Bale, A.B., Britt, L.K., Klein, H.H., Siebrits, E., and Dang, X.: "Layered Modulus Effects on Fracture Propagation, Proppant Placement, and Fracture Modeling," Society of Petroleum Engineers paper 71654, 2001.

Smith, M.B., Bose, M., Klein, H.H., Ozenne, B.R., Vandersypen, R.S.: "High-Permeability Fracturing: "Carter" Fluid Loss or Not," Society of Petroleum Engineers paper 86550, 2004.

Sneddon, I.N., and Elliott, H.A.: "The Opening of a Griffith Crack under Internal Pressure," Quarterly of Applied Mathematics, Vol. IV (1946), No. 3, pp. 262-267.

Sneddon, I.N.: "The Distribution of Stress in the Neighborhood of a Crack in an Elastic Solid," Proceedings, Royal Society of London, Series A, Vol. 187 (1946), pp. 229-260.

Soliman, M.Y., East, L., and Adams, D.: "Geo-mechanics Aspects of Multiple Hydraulic Fracturing of Horizontal and Vertical Wells," Society of Petroleum Engineers paper 86992, 2004.

Stadulis, J.M.: "Development of a Completion Design to Control Screenouts Caused by Multiple Near- well Fractures," Society of Petroleum Engineers paper 29549, 1995.

Stimlab - Proppant Consortium, 1996, pp. 209-220.

Stright, D.H. Jr, and Robertson, R.D.: "An Integrated Approach to Evaluation of Horizontal Well Prospects in the Niobrara Shale," Society of Petroleum Engineers - Reservoir Engineering, Vol. 10 (1995), No. 4, pp. 247-252, Society of Petroleum Engineers paper 25923.

Taurus Reservoir Solutions: "Geosim - Software Description," 2003.

Tester, J.W., Murphy, H.D., Grigsby, C.O., Potter, R.M., and Robinson, B.A.: "Fractured Geothermal Reservoir Growth Induced by Heat Extraction," Society of Petroleum Engineers - Reservoir Engineering, Vol. 4 (1989), No. 1, pp. 97-104, Society of Petroleum Engineers paper 15124.

Thiele, M.R., Batycky, R.P., and Blunt, M.J.: "A Streamline-Based 3D Field-Scale Compositional Reservoir Simulator," Society of Petroleum Engineers paper 38889, 1997.

Underwood, P.J. and Kerley, L.A.: "Evaluation of Selective vs. Point-source Perforating for Hydraulic Fracturing," Society of Petroleum Engineers - Drilling and Completion, Vol. 15, p. 177-184, 2000, Society of Petroleum Engineers paper 65404 and 36480.

Urbancic, T.I., and Rutledge, J.: "Using Microseismicity to Map Cotton Valley Hydraulic Fractures,", 2000 Society of Exploration Geophysicists 70th Annual Meeting, Expanded Abstracts, pp. 1,444-1,448.

Valko, P., and Economides, M.J.: "Fluid Leakoff Delineation in High-Permeability Fracturing," Society of Petroleum Engineers paper 37403, 1997.

van Batenburg, D.W., and Hellman, T.J.: "Guidelines for the Design of Fracturing Treatments for Naturally Fractured Formations," Society of Petroleum Engineers paper 78230, 2002.

van den Hoek, P.J., Matsuura, T., de Krron, M., and Gheissary. G.: "Simulation of Produced Water Reinjection under Fracturing Conditions," Society of Petroleum Engineers - Production and Facilities, Vol. 166 (August 1999), Society of Petroleum Engineers paper 36846.

van den Hoek, P.J.: "A Simple and Accurate Description of Nonlinear Fluid Leakoff in High-Permeability Fracturing," Society of Petroleum Engineers paper 77183, 2002.

Verity, R.V.: "The Geothermal Well Stimulation Program and Experiments in the Imperial Valley," Proceedings of the Geothermal Program Review III (1984), U.S. Department of Energy, Washington, D.C., pp. 171-180.

Vidale, J.E.: "Finite-Difference Calculation of Traveltimes in Three Dimensions," Geophysics, Vol. 55 (1990), No. 5, pp. 521-526.

Walker, R.N. Jr., Hunter, J.L., Brake, A.C., Fagin, P.A., and Steinsberger, N.P.: "Proppants, We Still Don't Need No Proppants - A Perspective of Several Operators," Society of Petroleum Engineers paper 49106, 1998.

Walsh, J.B.: "Effect of Pore Pressure and Confining Pressure on Fracture Permeability," International Journal of Rock Mechanics and Mining Sciences and Geomechanics Abstracts, Vol. 18 (1981), pp. 429-435.

Warpinski, N.R., and Branagan, P.T.: "Altered-stress Hydraulic Fracturing," Journal of Petroleum Technology, Vol. 41 (1989), No. 9, pp. 990-997, Society of Petroleum Engineers paper 17533.

Warpinski, N.R., Branagan, P.T., Engler, B.P., Wilmer, R., and Wolhart, S.L.: "Evaluation of a Downhole Tiltmeter Array for Monitoring Hydraulic Fractures," International Journal of Rock Mechanics and Mining Sciences, Vol. 34 (1997), No. 3-4, pp. 438.

Warpinski, N.R., Branagan, P.T., Peterson, R.E., Wolhart, S.L., and Uhl, J.E.: "Mapping Hydraulic Fracture Growth Using Microseismic Events Detected by a Wireline Retrievable Accelerometer Array," Society of Petroleum Engineers paper 40014, 1998.

Warpinski, N.R., Kramm, R.C., Heinze, J.R., and Waltman, C.K.: "Comparison of Single- and Dual-Array Microseismic Mapping Techniques in the Barnett Shale," Society of Petroleum Engineers paper 95568, , 2005a.

Warpinski, N.R., Moschovidis, Z.A., Parker, C.D., and Abou-Sayed, I.S.: "Comparison Study of Hydraulic Fracturing Models - Test Case: GRI Staged Field Experiment No 3," Society of Petroleum Engineers - Production and Facilities, Vol. 9, (1994), No. 1, pp. 7-16, Society of Petroleum Engineers paper 25890.

Warpinski, N.R., Sullivan, R.B., Uhl, J.E., Waltman, C.K., and Machovoe, S.R.: "Improved Microseismic Fracture Mapping Using Perforation Timing Measurements for Velocity Calibration," Society of Petroleum Engineers Journal, Vol. 10 (2005), No. 1, pp. 14-23, Society of Petroleum Engineers paper 84488, 2005b.

Warpinski, N.R., Wolhart, S.L., and Wright, C.A.: "Analysis and Prediction of Microseismicity Induced by Hydraulic Fracturing," Society of Petroleum Engineers Journal, Vol. 9 (2004), No. 1, pp. 24-33.

Warpinski, N.R., Wolhart, S.L., and Wright, C.A.: "Analysis and Prediction of Microseismicity Induced by Hydraulic Fracturing," Society of Petroleum Engineers paper 71649, 2001.

Warpinski, N.R.: "Hydraulic Fracture Diagnostics," Journal of Petroleum Technology (October 1996), Society of Petroleum Engineers paper 36361.

Warpinski, N.R.: "Hydraulic Fracturing in Tight, Fissured Media," Journal of Petroleum Technology, Vol. 43 (1991), No. 2, pp. 146-152 and 208-209, Society of Petroleum Engineers paper 21054.

Weidler, R., Gerard, A., Baria, R., Daumgärtner, J., and Jung, R.: "Hydraulic and Microseismic Results of a Massive Stimulation Test at 5 km Depth at the European Hot-dry Rock Test Site Soultz, France," Proceedings of the 2002 27th Workshop on Geothermal Reservoir Engineering, Stanford, California, pp. 95-100.

Weijers, L., Wright, C., Mayerhofer, M., and Cipolla, C.: "Developing Calibrated Fracture Growth Models for Various Formations and Regions Across the United States," Society of Petroleum Engineers paper 96080, 2005.

Weijers, L., Wright, C.A., Demetrius, S.L., Wang, G., Davis, E.J., Emanuele, M.A., Broussard, J.B., Golich, G.M.: "Fracture Growth and Re-orientation in Steam Injection Wells," Society of Petroleum Engineers paper 54079, 1999.

Weijers, L., Wright, C.A., Sugiyama, H, Sato, K., and Zhigang, L.: "Simultaneous Propagation of Multiple Hydraulic Fractures: Evidence, Impact and Modeling Implications," Society of Petroleum Engineers paper 64772, 2000.

Wiley, C., Barree, B., Eberhard, M., and Lantz, T.: "Improved Horizontal Well Stimulations in the Bakken Formation, Williston Basin, Montana," Society of Petroleum Engineers paper 90697, 2004.

Willberg, D.M., Card, R.J., Britt, L.K., Samuel, M., England, K.W., Cawiezel, K.E., and Krus, H.: "Determination of the Effect of Formation Water on Fracture Fluid Cleanup Through Field Testing in the East Texas Cotton Valley," Society of Petroleum Engineers paper 38620, 1997.

Williams, B.B.: "Fluid Loss from Hydraulically Induced Fractures," Journal of Petroleum Technology, Vol. 22 (1970), No. 6, pp. 882- 888, Society of Petroleum Engineers paper 2769.

Wong, G.K., Fors, R.R., Casassa, J.S., and Hite, R.H.: "Design, Execution and Evaluation of Frac and Pack (F&P) Treatments in Unconsolidated Sand Formations in the Gulf of Mexico," Society of Petroleum Engineers paper 26563, 1993.

Wright, C.A., and Conant, R.A.: "Hydraulic Fracture Re-orientation in Primary and Secondary Recovery from Low-permeability Reservoirs," Society of Petroleum Engineers paper 30484, 1995.

Wright, C.A., and Weijers, L.: "Hydraulic Fracture Re-orientation: Does It Occur? Does It Matter?" The Leading Edge, Vol. 20 (2001), No. 10, pp. 1,185-1,189.

Wright, C.A., Conant, R.A., Golich, G.M., Bondor, P.L., Murer, A.S., and Dobie, C.A.: "Hydraulic Fracture Orientation and Production / Injection Induced Reservoir Stress Changes in Diatomite Waterfloods," Society of Petroleum Engineers paper 29625, 1995.

Wright, C.A., Conant, R.A., Stewart, D.W., and Byerly, P.M.: "Re-orientation of Propped Refracture Treatments," Society of Petroleum Engineers paper 28078, 1994b.

Wright, C.A., Conant, R.A., Stewart, D.W., and Byerly, P.M.: "Re-orientation of Propped Refracturing Treatments," Society of Petroleum Engineers paper 28078, 1994a.

Wright, C.A., Davis, E.J., Minner, W.A., Ward, J.F., Weijers, L., Schell, E.J., and Hunter, S.P.: "Surface Tiltmeter Fracture Mapping Reaches New Depths—10,000 Feet, and Beyond?" Society of Petroleum Engineers paper 39919, 1998.

Wright, C.A., Davis, E.J., Ward, J.F., Griffin, L.G., Fisher, M.K., Lehman, L.V., Fulton, D.D., Podowski, J., and Grieser, W.V.: "Real-time Fracture Mapping from the "Live" Treatment Well," Society of Petroleum Engineers paper 71648, 2001.

Wright, C.A., Davis, E.J., Weijers, L., Golich, G.M., Ward, J.F., Demetrius, S.L., and Minner, W.A.: "Downhole Tiltmeter Fracture Mapping: A New Tool for Directly Measuring Hydraulic Fracture Growth," Society of Petroleum Engineers paper 49193, 1999.

Wright, C.A., Davis, E.J., Weijers, L., Minner, W.A., Henigan, C.M., and Golich, G.M.: "Horizontal Hydraulic Fractures: Oddball Occurrences or Practical Engineering Concern?" Society of Petroleum Engineers paper 38324, 1997.

Wright, C.A., Stewart, D.W., Emanuel, M.A., and Wright, W.W.: "Re-orientation of Propped Refracturing Treatments in the Lost Hills Field," Society of Petroleum Engineers paper 27896, 1994, 1994a.

Wright, C.A., Stewart, D.W., Emanuele, M.A., and Wright, W.W.: "Re-orientation of Propped Refracture Treatments in the Lost Hills Field," Society of Petroleum Engineers paper 27896, 1994b.

Wright, C.A., Weijers, L., Germani, G.A., MacIvor, K.H., Wilson, M.K., and Whitman, B.A.: "Fracture Treatment Design and Evaluation in the Pakenham Field: A Real-Data Approach," Society of Petroleum Engineers paper 36471, 1996.

Wright, C.A., Weijers, L., Germani, G.A., MacIvor, K.H., Wilson, M.K., and Wohitman, B.A.: "Fracture Treatment Design and Evaluation in the Pakenham Field: A Real-Data Approach," Society of Petroleum Engineers paper 36471, 1998.

Wyborn, D., De Graaf, L., and Hann, S.: "Enhanced Geothermal Development in the Cooper Basin Area, South Australia," Geothermal Resources Council Transactions, Vol. 29 (2005), pp. 151-155.

Wyborn, D., De Graaf, L., Davidson, S., and Hann, S.: "Development of Australia's First Hot Fractured Rock (HFR) Underground Heat Exchanger, Cooper Basin, South Australia," 2004.

Yost, A.B. II, and Overbey, W.K. Jr.: "Production and Stimulation Analysis of Multiple Hydraulic Fracturing of a 2,000-ft Horizontal Well," Society of Petroleum Engineers paper 19090, 1989.

Yost, A.B. II, Overbey, W.K., and Carden, R.S.: "Drilling a 2,000-ft Horizontal Well in the Devonian Shale," Society of Petroleum Engineers paper 16681, 1987a.

Yost, A.B. II, Overbey, W.K., Salamy, S.P., and Saradji, B.S.: "Devonian Shale Horizontal Well: Rationale for Wellsite Selection and Well Design," Society of Petroleum Engineers paper 16410, 1987b.

Zammerilli, A.M.: "A Simulation Study of Horizontal, High-angle, and Vertical Wells in Eastern Devonian Shale," Society of Petroleum Engineers paper 18998, 1989.

Zemlak, W., Lemp, S., and McCollum, R.: "Selective Hydraulic Fracturing of Multiple Perforated Intervals with a Coiled Tubing Conduit: A Case History of the Unique Process, Economic Impact and Related Production Improvements," Society of Petroleum Engineers paper 54474, 1999.

Zerhboub, M., Touboul, E., Ben-Naceur, K., and Thomas, R.L.: "Matrix Acidizing: A Novel Approach to Foam Diversion," Society of Petroleum Engineers - Production and Facilities (May 1994), pp. 121-126.

Zimmermann, R.W., Chen, D.W., Long, J.C.S., and Cook, N.G.W.: "Hydromechanical Coupling between Stress, Stiffness, and Hydraulic Conductivity of Rock Joints and Fractures," Rock Joints (1990), Barton and Stephansson (editors), Balkema, Rotterdam ISBN 906191-109-5, pp. 571-577.

Zuber, M.D., Lee, W.J., and Gatens, J.M. III: "Effect of Stimulation on the Performance of Devonian Shale Gas Wells," Society of Petroleum Engineers - Production Engineering, (November 1987), pp. 250-256, Society of Petroleum Engineers paper 14508.

Zuber, M.D., Lee, W.J., and Gatens, J.M. III: "Effect of Stimulation on the Performance of Devonian Shale Gas Wells," Society of Petroleum Engineers - Production Engineering, (November 1987), pp. 250-256, Society of Petroleum Engineers paper 14508.

8 APPENDIX A: FRACTURE GROWTH IN THE BARNETT SHALE

This section discusses general information (section 8.1 below), fracture mapping results (section 8.2 on page 106), water fracturing in the Barnett Shale (section 8.3 on page 119), the correlation of fracture parameters to production (section 8.4 on page 125), and the two-well mapping approach (section 8.5 on page 137).

8.1 General Information

The oil field analogues that were evaluated exhibit a complex growth of fractures, because of the development of networks of fractures. One clear example of this behavior is found in the Barnett Shale in North Texas. Here, a fracture network is created with a length of more than 1,000 ft and a width of several 100 ft. Pinnacle Technologies, Inc. has mapped more than 800 fracturing treatments in the Barnett Shale. A selection of this data has been published at oil field conferences. In an EGS development, the creation of a complex network of fractures is desired to contact a large body of hot rock, and to extract heat from it economically.

This section describes the geography (section 8.1.1 below), the geology (section 8.1.2 below), the thickness (section 8.1.3 on page 103), the porosity and permeability (section 8.1.4 on page 104), the production (section 8.1.5 on page 104), the production stimulation (section 8.1.6 on page 104), and hydraulic fracture geometry (section 8.1.7 on page 104) of the Barnett Shale.

8.1.1 Geography

The Barnett Shale covers a large area, from the Fort Worth Basin, out past the Permian Basin of West Texas and New Mexico [*Fisher et al.,* 2004]. The extent of the Barnett Shale with the core area is displayed in Figure 8.1.

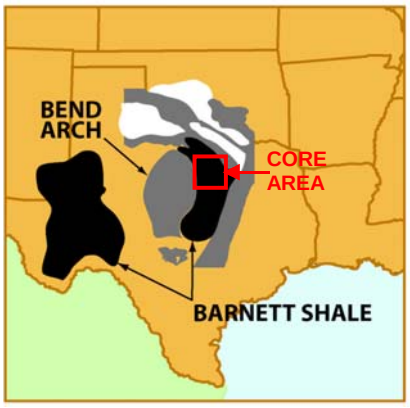

Figure 8.1: Extent of Barnett Shale (marked by two black shaded areas), with core area in Wise and Denton counties (outlined by a red square) [*Fisher et al.,* 2004].

8.1.2 Geology

The Geology of the Barnett Shale has been discussed in numerous technical papers [*Coulter et al.,* 2004], including an overview [*Kuuskra et al.,* 1998]. The Barnett Shale is of Mississippian age *Fisher et al.,* 2004; *Fisher et al.,* 2002]. It is a marine shelf deposit. It lies unconformably on the Viola/Simpson Limestone and Ellenburger Group of early to middle Ordovician age. It is conformably overlain by the Marble Falls Limestone of Pennsylvanian age. The Viola Limestone and Ellenburger Group formations below the Lower Barnett Shale are porous and often completely water-saturated. In some

areas, the Barnett Shale is divided into an upper and lower layer, and is separated by the Forestburg Limestone. A type log from the core area is displayed in Figure 8.2. Several of the areas currently under development outside of the core area contain a Barnett Shale interval that is not as well-bounded above. More importantly, it lacks a significant barrier below, except when the Viola Limestone is present. When the Viola Limestone is absent (e.g., in the W and SW), the Ellenburger is not a barrier and it is also wet.

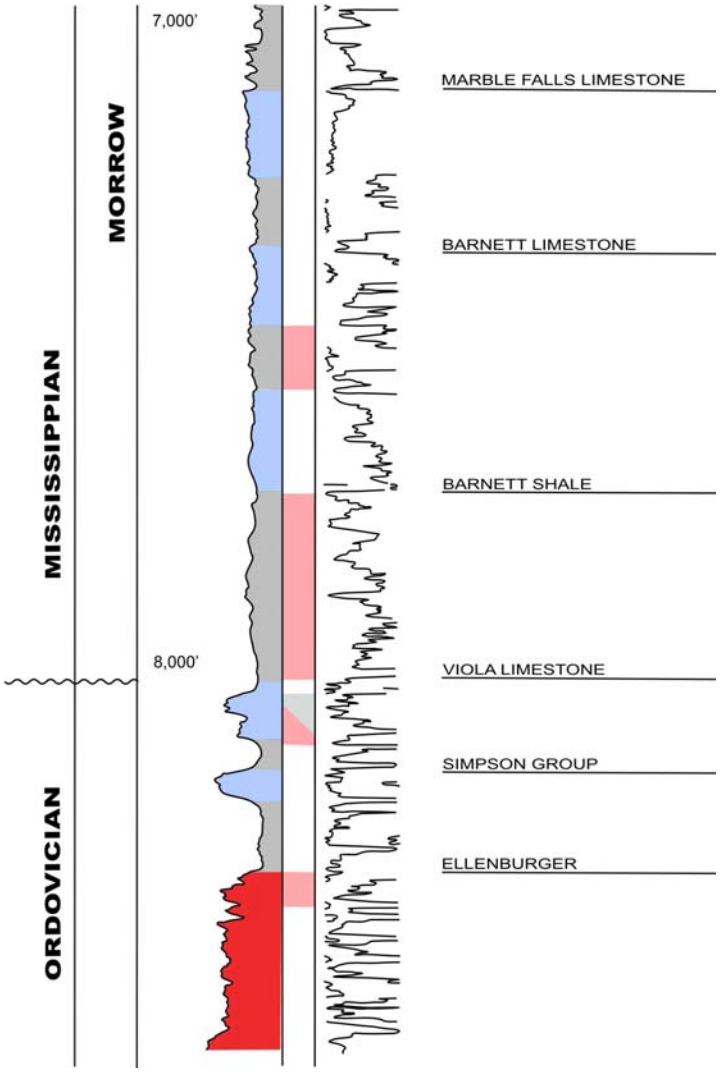

Figure 8.2: Type log of Barnett Shale in core area displaying under- and overlying limestones [*Fisher et al.,* 2004].

The productive Barnett Shale is typically a black, organic-rich shale composed of fine grained, non-siliciclastic rocks (i.e., primarily quartz and clay). It is classified as shale [*East et al.,* 2004]. However, it is more complex and inhomogeneous. Where the shale is more dolomitic, there is less organic matter. The traditional log analysis is further complicated by the presence of minerals (e.g., calcite, dolomite, and pyrite). Natural fractures are sometimes sealed with calcium carbonate.

8.1.3 Thickness

The depth of the Barnett Shale in the core area varies from ~ 6,800 to 9,000 ft [*Coulter et al.,* 2004]. Within the Fort Worth Basin, it has a thickness of 200 to 800 ft [*Fisher et al.,* 2004; *Fisher et al.,* 2002]. In the core area, it has a thickness of ~ 500 ft.

8.1.4 Porosity and Permeability

The Barnett Shale has a low primary porosity of 4 to 6% [*Coulter et al.,* 2004]. With the secondary porosity, the total porosity can be considerably greater. It has an extremely low permeability of 7×10^{-5} to 5×10^{-3} mD *Fisher et al.,* 2004; *Fisher et al.,* 2002]. Most of its porosity and permeability developed from the thermal transformation, or cracking, of its organic matter from liquid to gas [*East et al.,* 2004]. Because of this reaction, the volume increased by up to a factor of 10. This resulted in micro-fractures induced by maturation. The pores of the matrix have a radius of ~ 0.005 µm. Much of the gas is stored in the micro-fractures. In addition, 40 to 60% of the gas is absorbed in the solid organic matter, or kerogen. The total organic content (TOC) averages 2.5%. The quantity of gas in place is estimated at 120×10^{9} ft^3/mi^2. The current recovery is estimated at less than 12%. It is the only known productive rock on the east shelf of the Fort Worth Basin that is believed to its own source, reservoir, trap, and seal.

8.1.5 Production

The Barnett Shale is abnormally pressured in the core area [*Fisher et al.,* 2004; *Fisher et al.,* 2002]. Gas shows on a mud log are sometimes an adequate indicator of the permeability and gas storage [*East et al.,* 2004]. Additionally, it is believed that the reflectance of vitrinite could be correlated to the potential for production. Wells that display natural fractures in electrical micro imaging (EMI) logs tend to produce better.

8.1.6 Production Stimulation

Because of the very low permeability of the Barnett Shale, it is imperative that extremely great surface areas of fractures are created by hydraulic fracturing treatments for commercial production [*Coulter et al.,* 2004; *East et al.,* 2004; *Fisher et al.,* 2004; *Fisher et al.,* 2002]. However, because of its extremely low permeability, the drainage distance from the face of the fractures is very small.

Through most of the North Texas area, faults, or karsts, with an orientation of northeast (NE) to south-west (SW) are predominant. Sometimes, they are believed to cause poor results of stimulation, possibly by stealing much of the energy of a fracturing treatment. Induced hydraulic fractures are generally aligned along the NE-SW direction. However, the deviatoric stresses are presumably not very high. This results in significant cross fracturing, during fracturing stimulation.

The counties of Denton and Wise were home to nearly all successful completions until the past few years. This is largely because of the presence of the Viola that separates the Barnett Shale and the Ellenburger, which is usually wet and often an aquifer.

Several of the areas currently under development outside of the core area contain a Barnett Shale interval that is not as well bounded above or below this interval. In addition, the Viola and Ellenburger formations below the Lower Barnett Shale are often completely water-saturated. If a hydraulic fracture grows downward out of the Lower Barnett Shale, then it could conceivably open a conductive path directly into a porous, water-producing interval. This could be extremely detrimental to the relative permeability and subsequent production.

8.1.7 Hydraulic Fracture Geometry

The classical description of a hydraulic fracture is a simple, single, bi-wing, planar crack with the well at the center of the two wings [*Barree et al.,* 2002; *Fisher et al.,* 2002]. In addition, it is often assumed that this fracture would stay primarily within the pay-zone and grows to great length.

However, almost all physical verifications from more than ten years of direct diagnostics of the geometry of fractures performed to date, from core-throughs to mine-backs, have proven this description to be oversimplified and mostly incorrect. In addition, the existing literature discusses numerous cases of incomplete coverage of pay-zones where fractures:

1) may miss entire perforated intervals,
2) only partially cover some intervals,
3) grow primarily out of zone in other intervals,

4) deviate significantly from the well due to connection or link-up problems, and
5) grow into unwanted water or gas intervals nearby.

Generally, fractures can be categorized as traditionally simple, complex, or very complex. An illustration of the different complexities of the fracture geometry is pictured in Figure 8.3. However, it is virtually impossible with existing fracture mapping tools to measure the difference between these types of geometries [*Fisher et al.,* 2004]. If the secondary fractures grow near by and parallel to one another, then they must be inferred from fracture pressure diagnostics.

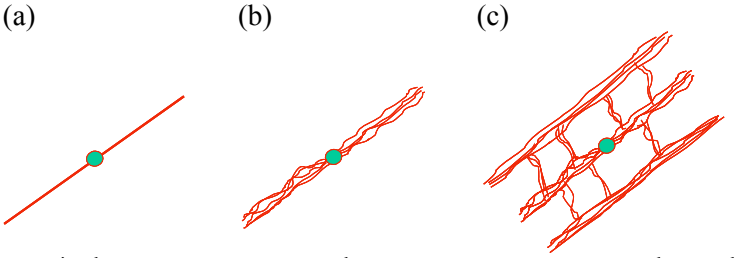

Figure 8.3: Increasing complexity of fracture geometry: (a) simple (most common), (b) complex, and (c) extremely complex (relatively rare) [*East et al.,* 2004; *Fisher et al.,* 2004; *Fisher et al.,* 2002].

Most mapped fractures around the world to date fall into the simple or complex description, with the growth of fractures dominantly occurring in only one planar orientation. Even with relatively simple geometries (i.e., a Perkins-Kern type geometry), fractures can grow asymmetrically, have a variable confinement across geologic interfaces, and change orientation [*Maxwell et al.,* 2002]. However, the growth of fractures in a naturally fractured reservoir can exhibit additional complexities. This is often associated with the interaction between the hydraulic fractures and the pre-existing network of natural fractures.

Because of several factors, including the presence of natural fractures, a fracturing treatment in the Barnett Shale is more likely to resemble the very complex rather than the simple fracture geometry. This allows a network of fractures to be created during a treatment, with many fractures in multiple orientations. This results in great surface areas that can potentially contributing to the production. The length and width of the resulting network is important in determining the total surface area contacted by the fractures, so that the location and spacing of the wells can be optimized. Because of the small drainage distance from the fractures, the density of fractures within this network is very important. There could be opportunities for additional wells to be drilled in less densely fractured areas within a network, or for re-fracturing to be performed that may extend the network or more densely populate it with new fractures.

8.2 Fracture Mapping Results

The stunning success of gas development in the Barnett Shale of north central Texas is largely because of the optimization of hydraulic fracturing in this unusual reservoir environment [*Warpinski et al.,* 2005a; *Coulter et al.,* 2004; *Grieser et al.,* 2003]. In particular, the migration from crosslinked gel, propped-fracture treatments to water fractures with higher rates and lighter proppant loadings has provided both technical and economic benefits by improving connectivity within the reservoir while reducing costs. While these benefits have been observed directly in both gas production and authority for expenditure (AFE) reductions, a full understanding of the mechanisms for these improvements has primarily been provided by microseismic monitoring of the treatments.

A classical hydraulic fracture is generally a planar crack feature that is designed to minimize leakoff into the formation, create extensive fracture length, and provide a propped channel through which hydrocarbons can more easily migrate back to the well. In such a case, the value of high-viscosity fluids that can minimize leakoff, generate width, and effectively carry the proppant to the fracture extremities is clearly founded.

The Barnett Shale, however, is a complicated naturally fractured reservoir where large-volume water fractures pumped at high rates have been demonstrate to effectively stimulate substantial volumes of the reservoir through the development of an interconnected fracture system [*Fisher et al.,* 2004; *Fisher et al.,* 2002; *Maxwell et al.,* 2002]. Evidence for the development of a three dimensional stimulated region, as opposed to a two-dimensional region associated with a classical planar fracture, was first provided by the loading-up of offset wells during water fracture treatments [*Warpinski et al.,* 2005a]. These offset wells, positioned along both the fracture azimuth and perpendicular to it, generally demonstrated improved productivity when the fluids were unloaded and the wells were returned to production.

Microseismic mapping is the technology that has provided the details of the development of the process and the overall size of the stimulated network away from other offset wells. The ability to observe the development of microseismic patterns has given considerable insight into the mechanism for the success of water fractures. In horizontal wells, where many more fracturing configurations are available (e.g., cemented or uncemented, number of stages), microseismic monitoring has been a key provider of information from which to make optimization decisions. However, the monitoring of water fractures in horizontal wells is also a significantly more difficult task because the monitoring must cover the full extent of the well in addition to the full extent of the fracture. One successful solution to this coverage issue is to use two monitor wells.

Microseismic monitoring is essentially a straightforward application of earthquake seismological principles to the mapping of fractures and other processes. It consists of the detection, location, and further analysis of extremely small earthquakes that are induced by the fracturing process [*House,* 1987; *Albright and Pearson,* 1982]. The process by which the micro earthquakes are detected, recorded, analyzed, and used is well known and is discussed in detail in other papers [*Rutledge and Phillips,* 2003; *Warpinski et al.,* 1998]. However, proximity to the fracture region is a necessity because the small earthquakes are not detectable as discrete events at the surface, and the seismic receivers are thus positioned downhole in adjacent wells.

The mechanical behavior of the fracture and reservoir system that generates the microseisms is well established. Typically, microseisms are adequately represented by a double-couple source, which implies a shear slippage that releases stress over some aerial extent. In competent rocks (e.g., the Barnett Shale), the shear slippages occur on pre-existing planes of weakness because of the changes in stress and pore pressure that are induced by the fracturing process. In a classic planar hydraulic fracture, these changes result in a narrow band of microseisms that clearly define the plane of the fracture as well as its extent. However, in the Barnett Shale the behavior is different.

Stress changes are a result of dilation of the fracture and the large amounts of shear that are produced around the crack tip [*Warpinski et al.,* 2004]. Pore pressure changes are because of leakoff into the formation. However, changes in pressure may vary considerably depending on the conditions of the reservoir fluids [*Warpinski et al.,* 2005a]. For example, a hydraulic fracture in a gas reservoir would generally be expected to have a limited width of the microseismic zone, as the formation area pressurized by leakoff of fracturing fluid is limited by the high pore volume compressibility. On the other

hand, liquid-saturated reservoirs with their low compressibility can effectively couple the pressure over large distances, resulting in much wider bands of microseisms.

The microseisms and other seismic activity (collectively known as events) are automatically detected and recorded by use of a standard long-term-average and short-term-average approach. These resulting event files are then further processed to determine which contain microseisms that can be analyzed. The analyzable ones are processed to identify the P-wave (compressional wave) and S-wave (shear wave) arrivals, as well as the particle motion of these waves. When there is only a single vertical well, the analysis of the P and S arrivals provides only the distance to the event and the elevation of the event. The particle motion data is required to provide the directional information (e.g., P-wave particle motion points back towards source). With two observation wells, a more direct triangulation approach can be used to produce a full three-dimensional location. In either case, however, the seismic receivers must still be oriented to accurately use the particle-motion data (even in two-well monitoring there are still many events that may only be detected on one well, and the particle motion is useful for some elements of two-well processing).

While the location analysis is very straightforward [*Nelson and Vidale,* 1990; *Vidale,* 1990], the determination of the velocities of each of the layers through which the seismic energy propagates is significantly more problematic. The best data available usually comes from a dipole sonic log and perforation timing data. The dipole sonic logs provide detail of the velocity structure. However, unfortunately this works only for vertically directed waves (whereas most of the travel associated with microseisms is usually horizontal) and under the wrong conditions (stress concentrations around well, invaded zone with altered saturations, higher frequency, and possibly under different pressure conditions if the well is re-fractured). As a result, dipole-sonic derived velocities are likely to be in error by several percent. Perforation timing measurements can provide information to calibrate the dipole-sonic results. However, this is only feasible if the offset well locations are accurately known relative to the perforation location (i.e., seldom) and if the perforations are in appropriate locations (e.g., not just shallow string-shots used to orient the receivers). However, they cannot provide the level of detail obtained from logs. The greatest source of error in microseismic analysis is likely because of an inappropriate velocity model. However, this situation can often be remedied with advanced velocity calibration and optimization techniques.

A successful microseismic mapping test requires acceptable positioning of the receivers (both lateral and vertical distance from the fracture), a relatively noise-free monitoring environment (quiet borehole), high quality tri-axial seismic data sampled at rates much faster than the dominant frequency of the data, accurate well locations, orienting of the receivers, and an accurate velocity structure. In some cases (of which the Barnett Shale can be one), it is also helpful to have some additional seismic modeling to sort through the various arrivals (e.g., head waves, reflections). Typically, arrays of 12 receivers spread over 300 to 500 ft of vertical aperture are used in a single offset well. However, recently mapping tests have been performed by use of two offset-well arrays.

This section describes the orientation of hydraulic fractures (section 8.2.1 below), vertical wells (section 8.2.2 on page 108), and horizontal wells (section 8.2.3 on page 112).

8.2.1 Hydraulic Fracture Orientation

The behavior of microseismic activity associated with water fractures in the Barnett Shale suggests a process that is significantly more complicated than the typical classical case [*Warpinski et al.,* 2005a]. A hydraulic fracture may clearly initiate in the direction of the maximum horizontal stress (NE). However, other planes (both NE and sub-parallel NW planes) quickly display activity that suggests that a fracture network is being activated and dilated. The rapid extension of both NE and NW planes indicate that fluid is moving through them at fast rates, implying high permeability. However, this permeability must be generated by the fracturing process because a reservoir with a highly permeable fracture network would respond readily to more modest stimulation procedures and not need large water fractures.

Thus, from the microseismic data, the inferred process for these water fractures is the following:
1) The water fractures start as a hydraulic fracture propagating in the northeast direction.

2) The low-viscosity water begins to seep into very tight northwesterly oriented, natural fractures (probably re-healed or calcite filled fractures) and eventually increases the pressure sufficiently to induce shear slippage (the microseisms that are detected), which causes overriding of asperities and an increase in permeability.
3) As more fluid can move into this natural fracture, the pressure increases farther along its length, additional slippage occurs, and the process snowballs.
4) Because the Barnett Shale apparently has very small stress anisotropy, the pressure eventually becomes sufficiently high that these natural fractures dilate into fully fluid-accepting hydraulic fracture branches.
5) These northwest-oriented fractures then intersect other natural fractures that are sub-parallel to the original northeast hydraulic fracture and induce them to open because of pressurization.
6) The result is a network of interconnecting hydraulic fracture branches in NE and NW planes.

Interestingly, the dilation of the NW fractures seems to make the process so efficient. However, in other environments this process has been termed fissure opening and is often thought to result in disastrous consequences (e.g., premature screen-out and damage to the natural fractures) [*van Batenburg and Hellman,* 2002; *Economides and Nolte,* 2000]. In the Barnett Shale, the use of water seems to enhance this process by encouraging the initial pressurization of the cross-cutting natural fractures, low proppant loadings probably ensure the avoidance of screen-outs, and the lack of a gel system to remain stuck permanently in the natural fractures (when they close after shut-down) minimizes any damage. Thus, it would appear that there are several factors that have come together to produce the results achieved in this reservoir.

Microseismic mapping is currently the most common diagnostic technology used in the Barnett Shale [*East et al.,* 2004]. Most of the recent microseismic mapping has been performed with extremely high-resolution vertical seismic profiling (VSP) type geophone sensors [*Fisher et al.,* 2004]. However, in some instances, suitable offset wells are not available for microseismic mapping, and surface tiltmeters are used to determine the effectiveness and orientation of the placement of the fractures.

In the Barnett Shale, the primary orientation of the hydraulic fractures is NE-SW [*Fisher et al.,* 2002]. This has been verified from both surface tiltmeter and microseismic mapping.

Additionally, the natural fractures identified from borehole imaging surveys in this area are oriented orthogonal to the primary hydraulic fractures, NW-SE. Surface tilt mapping demonstrated that these crosscutting natural fractures were activated, or opened, during a hydraulic fracturing treatment, and represented a significant portion (i.e., 20 to 60%) of the total created fracture volume.

8.2.2 Vertical Wells

From the depth of the fracturing treatments, the expected fracture complexity, and the great area encompassing the number of wells stimulated in each field, ~ 30 surface tiltmeter sites were required in each of the mapping areas [*Fisher et al.,* 2004; *Fisher et al.,* 2002].

Fracture Network

Previous fracture mapping projects had identified that fracture growth in vertical wells was extremely complex, with major fracture growth in at least two vertical orientations [*Maxwell et al.,* 2002' *Johnson et al.,* 1998], as mentioned above. This type of multi-planar fracture growth is relatively uncommon, and has only been measured in a handful of reservoirs to date [*Fisher et al.,* 2004].

Surface tilt mapping was used to determine the primary and secondary orientation of the fractures, and the fractional volume of the hydraulic fracturing slurry placed in each orientation [*Fisher et al.,* 2002].

An example of an extremely complex fracture geometry as displayed in Figure 8.3c is typical of hydraulic fracturing in the Barnett Shale. The long axis of the fracture network or network, that is oriented N40E in the core area, is referred to as the

length of the network. The short axis of the rectangle from NW-SE is typically referred to as the width of the network. For vertical wells, these network dimensions can approach a length of ~ 1 mi and a width of ~ 500 to 1,200 ft.

A typical fracture network from a vertical well in the core area of the Barnett Shale is displayed in Figure 8.4. The microseismic events are displayed as orange markers on this plan view. The gross fracture area is immediately obvious. The wide shaded rectangle represents the primary length, as obtained from downhole tilt mapping, and the orientation, as obtained from surface tilt mapping, of the fracture network. The crossties indicate the quantity of fluid that was placed into the secondary, natural fracture orientation. Each crosstie represents 5% of the total volume of slurry. That is, for this hydraulic fracture, the crossties represent 45% in the NW direction. As can be observed on this treatment, the width of this fracture network of ~ 900 ft is very great.

A new technique was developed to determine the growth of multiple fractures with time. Small sequential increments, in this case 40, of microseismic events can be analyzed with time. They are fit into a linear regression model to identify events that occur sequentially and appear to be related to a specific fracture structure. Then, the length and orientation of the many fracture segments in the order that they are created can be determined. These sequential linear structures, representing the minimum number and size of likely fracture segments, are highlighted with green lines in Figure 8.5. These segments verify the primary and secondary azimuths of the fractures measured by surface tilt mapping.

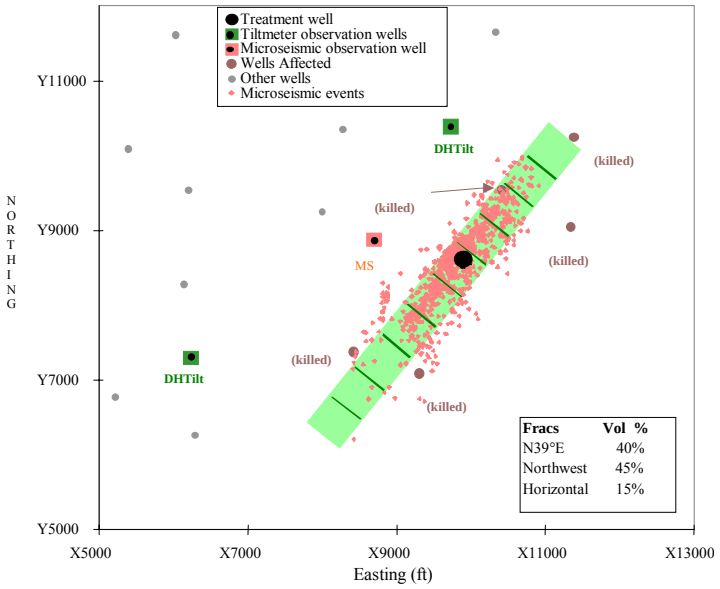

Figure 8.4: Plan view of mapped field for single treatment in vertical well displaying orientation of fracture network, and tilt-measured fracture volume in various fracture planes fractures for core area of Barnett Shale [*Fisher et al.,* 2002].

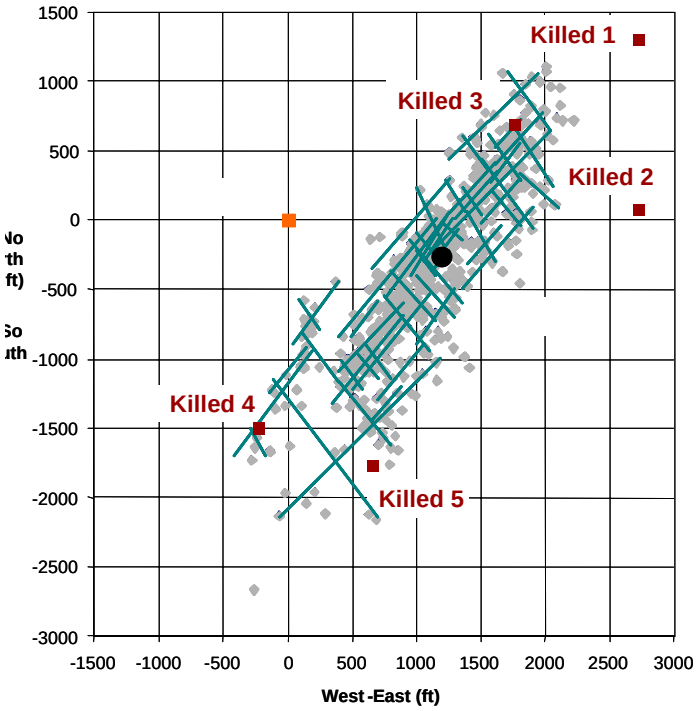

Figure 8.5: Plan view of fracture segments for single treatment in vertical well (black circle) with fracture segment size and complexity in orientations of hydraulic (NE-SW) and natural (NW-SE) fractures for core area of Barnett Shale [*Fisher et al.,* 2004; *Fisher et al.,* 2002]. Offset observation well is marked in orange.

The fracture network has a length of more than 4,000 ft, and a width of ~ 1,000 ft. The total length of the fracture network (i.e., the total length of the fracture segments of all mapped fractures) on this treatment was ~ 30,000 ft.

The five red squares just outside of the fracture network display the locations of wells that were temporarily killed by the hydraulic fracturing treatment on this vertical well. A number of near by wells were killed or affected because of the

fracture-to-well or fracture-to-fracture intersections during this treatment. This provided physical evidence of the geometry of these fracture networks.

The microseismic results from seven mapped fracturing treatments in the Lower Barnett Shale are displayed in Figure 8.6. There were four observations wells for this dataset. The location of the observation wells was taken into account to remove any bias caused by the position of each observation well relative to the fracture. Several gaps in the fracture network are visible. They could be because of lithologies that are microseismically a-seismic, or a lack of fracture network in these local areas. The gaps may thus be targets for re-hydraulic fracturing treatments, or even new drilling locations to drain this field more completely.

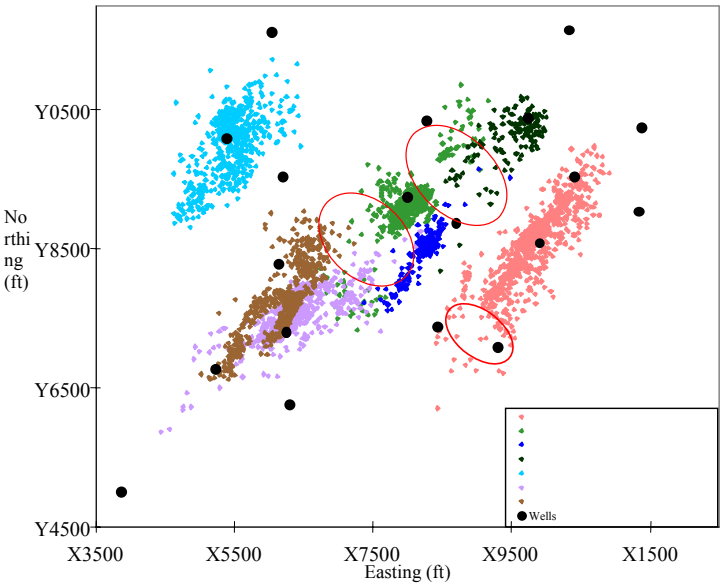

Figure 8.6: Plan view of seven vertical well fracturing treatments in one field illustrating gaps or sand traps in several fracture networks [*Fisher et al.,* 2002].

The geometries of the hydraulic fractures from 16 hydraulic fracturing treatments were obtained from hydraulic fracture mapping. Two different treatment designs were performed in these areas: two separate stages, targeting the Lower and Upper Barnett Shale independently, and combination treatments targeting both Lower and Upper Barnett Shale with a single treatment. The lengths of the fracture network, in general, are longer on the individual stage treatments than on the combination hydraulic fracturing, and the width of the network is greater on the individual treatments than on the combination hydraulic fracturing.

Containment

The fracturing treatment as displayed in Figure 8.7 is mostly confined in the Lower Barnett Shale. Downhole tiltmeters placed past the tip of each wing of the network were used to determine the half-length of the network. The half-length of the fracture network of ~ 2,500 ft is very great. The microseismic monitor well was located near the center of the fracture. It was unable to observe out to the very ends of the network, because of attenuation of the microseismic signals over these extremely long distances. This fracturing treatment covered the entire targeted pay-zone. It created a wide and complex network with fractures growing in multiple orientations. The smaller internal ovals display the geometry (i.e., the height and length) of the fractures measured by downhole tiltmeters at the ends of the network. The individual points are microseismic events measured by an array perpendicular to the center of the fracture network. The large translucent shaded area is the integrated fracture geometry from combining the highest confidence measurement for each fracture parameter. This geometry was used to create a calibrated 3D fracture model for this area. Combining fracture diagnostic technologies from

different perspectives of location is often useful in ensuring that the entire network is used in maximizing the net present value (NPV).

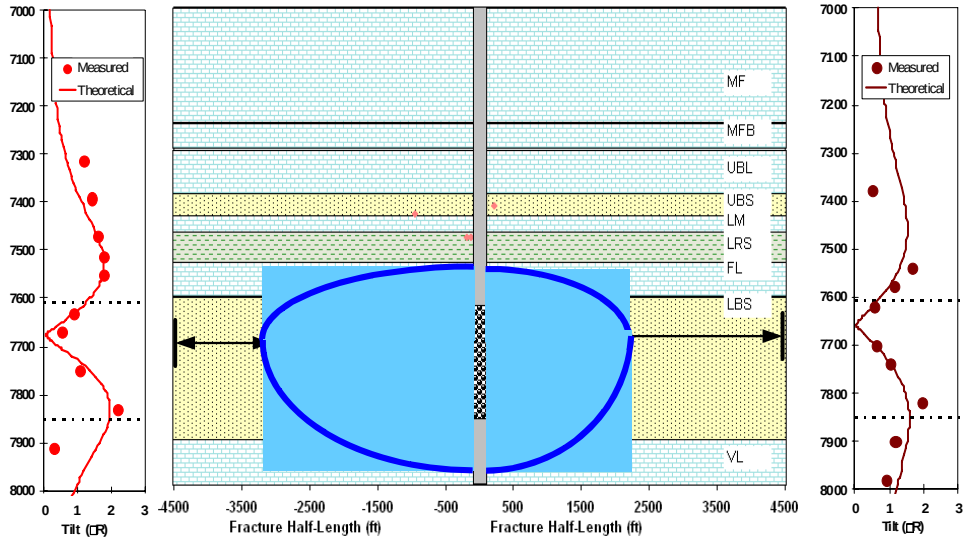

Figure 8.7: Side view of lower Barnett Shale fracturing treatment viewed normal to hydraulic fracture network, as observed from the SE [*Fisher et al.,* 2002].

An example of a longitudinal section view of the microseismic image of two difference fractures is displayed in Figure 8.8 [*Maxwell et al.,* 2002]. The blue zone indicates the depth of the perforated interval in the Lower Barnett Shale, and the green arrow indicates the actual extent of the formation.

(a) (b)

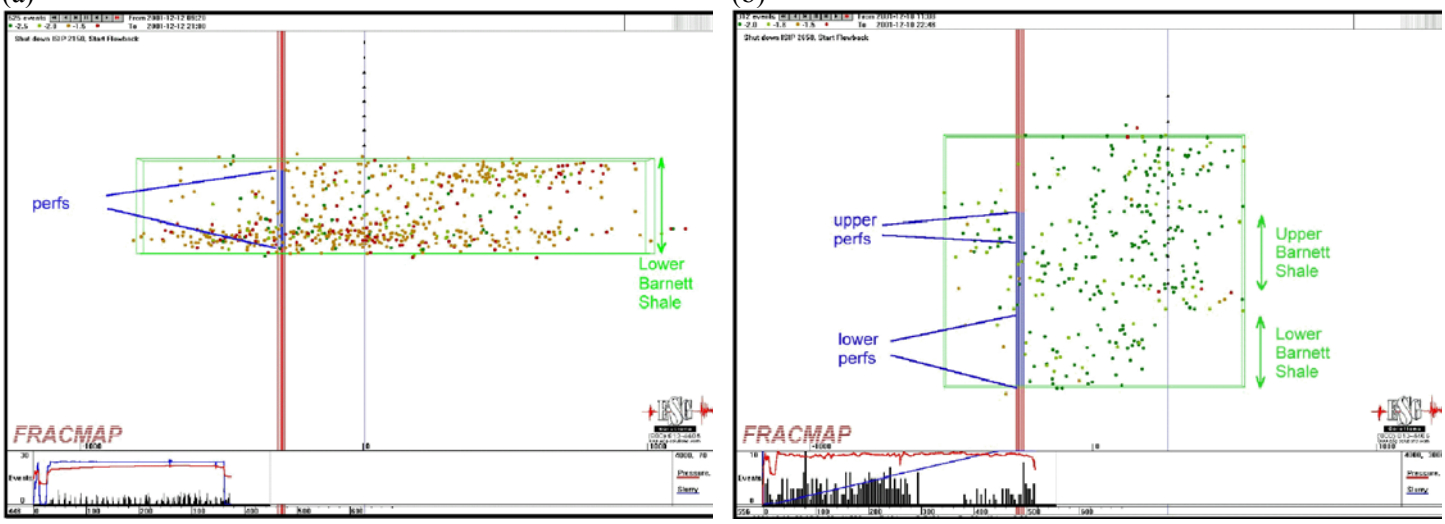

Figure 8.8: Longitudinal section of well stimulation, with fracture: (a) contained, and (b) not contained in Lower Barnett Shale [*Maxwell et al.,* 2002].

When the Lower Barnett Shale was fractured, as displayed in Figure 8.8a, the events are positioned near the perforated interval, and remain contained within the Lower Barnett Shale. The fracture containment could be related to variations in material properties in the Barnett Shale and limestone layers above and below it, or possibly to stress

variations. Alternatively, the apparent containment could be related to the inability of the microseismic system to detect events in the limestone layers above or below the Barnett Shale. The color-coding of the events corresponds to event magnitudes, with green being the smallest and red the greatest event magnitudes. The numerous events with great magnitudes indicate that the seismic deformation is occurring well above the detection limitations of the array. Similar failure mechanisms occurring in the relatively stiffer limestone would tend to result in events of even greater magnitude. This rules out a direct bias related to differences in the material properties.

The case when both the Upper and Lower Barnett Shale were fractured at the same time is displayed in Figure 8.8b. Almost the entire depth interval corresponding to the Lower Barnett Shale was perforated, in addition to the top 100 ft of the Upper Barnett Shale. The microseismicity demonstrates activity in both Barnett Shale units as well as extending some 400 ft above the top of the Barnett Shale. Clearly, the fracture was not contained in the reservoir in this case. This also demonstrates the detectability in the limestone layers outside of the reservoir. The greatest fracture length is achieved in the Forestburg Limestone and formations above the Upper Barnett Shale. Here, the Lower Barnett Shale was the main target for this well, where the least fracture extent is achieved. Hence, the simultaneous hydraulic fracturing of the Upper and Lower Barnett Shale was not effective to maximize fracture length in the Barnett Shale.

8.2.3 Horizontal Wells

Many of the issues of horizontal drilling can be evaluated through the integration of fracture mapping tools (e.g., microseismic mapping) with fracture engineering and production correlations [*Fisher et al.,* 2004].

When the horizontal wells are drilled in the core area where the well control and production of vertical wells are well known, the production of these horizontal wells can thus be directly compared with vertical wells to determine optimum completion strategy before implementing horizontal completions in the fringe areas. Horizontal wells with un-cemented liners and with cemented liners are compared.

Un-cemented Liners

All horizontal wells in the Barnett Shale to date have been cased for borehole stability over the expected long well life and for ease of future procedures for well intervention [*Fisher et al.,* 2004]. In the past, these cased laterals have been, in numbers, almost equally cemented or un-cemented. However, almost all current wells are cemented. The horizontal section can have a length of 1,000 to 4,000 ft or more. The ability to stimulate effectively long un-cemented laterals is the greatest challenge in performing a fracturing treatment on this type of well. Stimulation techniques are used in an attempt to initiate fractures in multiple locations along the well. An example is limited entry diversion treatments, which determine optimum perforation size, spacing, and number and pumping the treatment at an adequately high rate to ensure that all perforations must accept hydraulic fracturing slurry). If this is not successful, then the treatment might simply seek its own preferred location or locations along the lateral, and leave much of the interval unstimulated.

For a typical single-stage, un-cemented horizontal fracturing treatment, previous microseismic mapping studies [*Fisher et al.,* 2002] on vertical wells indicated minimum widths of the fracture network of 500 ft. Therefore, perforation clusters in transverse-oriented horizontal wells are typically separated by a distance of 500 ft between intervals to obtain complete coverage with the fracturing treatments. A typical design uses 50 or 60 holes spaced in four to five clusters along the horizontal section. When the horizontal section becomes longer, multiple stages are required for effective coverage. A typical single-stage, un-cemented horizontal completion is a lower cost treatment than multiple stages. In addition, typical cumulative stimulation volumes could be lower than with multiple staging.

Multiple stages are designed identical to the single stage treatments with the well generally separated into equal sections. The same limited entry design is applied with the spacing between perforations of 500 ft and the number of holes. Composite hydraulic fracturing plugs are set following the first stage treatment to isolate the previously stimulated section of the well. The previously stimulated sections of the reservoir are somewhat isolated from the subsequent stages by a stress diversion effect. The stress diversion effect is present when the reservoir has been supercharged by the previous fracturing treatment. Stress in this region is increased because of locally greater pressure of the fluid, and increased stress

from propped fractures created by the stimulation treatment. These two isolation effects, one mechanical and one because of increased stress, influence the subsequent stage or stages to stimulate reservoir areas that were not treated in the previous stages.

An example of a typical single-stage stimulation treatment in a un-cemented horizontal well is displayed in Figure 8.9. The treatment consisted of a large water fracture that was pumped through five sets of perforations. The half-length of the fracture network at each network location is ~ 1,000 ft, which is less than the length of a typical network of a vertical well. The four widths of the networks average ~ 500 ft each, which is less than the width of an average network on a typical vertical well. However, the cumulative width of the network (i.e., the sum of the four individual widths of the network), is ~ 2,000 ft. This is nearly the same as the length of the lateral of 2,400 ft. If the entire lateral were completely stimulated, then this would be expected. The fractures do not always initiate adjacent to the perforations. Instead, hydraulic fracturing fluid may travel along the well until a weakness in the rock is encountered. At this point, the fracture grows transversely away from the well. This can lead to gaps in the fracture network where less than the entire length of the lateral is stimulated. These gaps in the fracture network equate to smaller overall fracture surface area, and can result in lower well productivity.

A side view of another Barnett Shale fracturing treatment is displayed in Figure 8.10. This is a two-stage fracturing treatment in a un-cemented well. The second stage treatment diverted adequately toward the heel and away from the first stage to cover effectively the entire length of the lateral, and the height of the fracture was confined to the Lower Barnett Shale only. There is no measurable growth downward into the Viola and no upward growth into the Upper Barnett Shale.

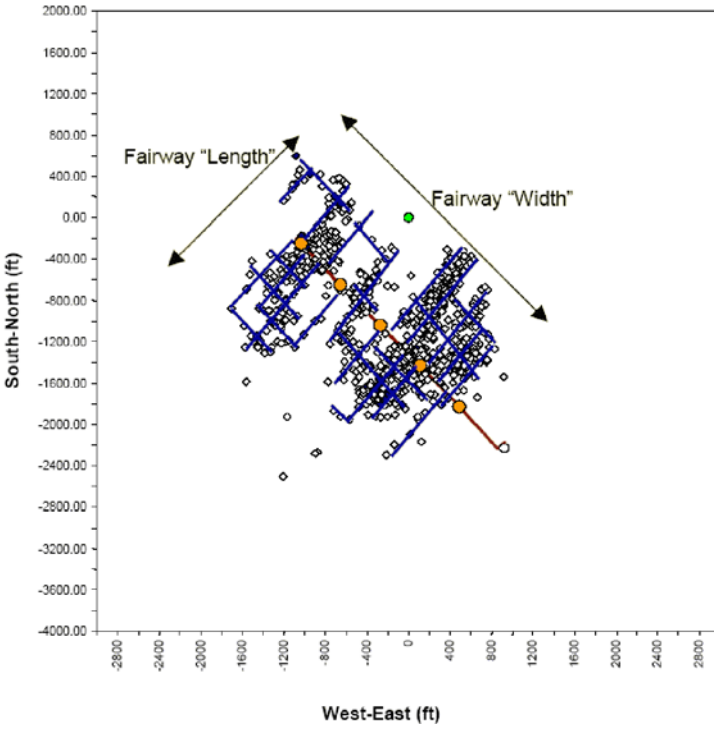

Figure 8.9: Plan view fracture map of horizontal, un-cemented treatment with illustrated fracture structures [*Fisher et al.,* 2004].

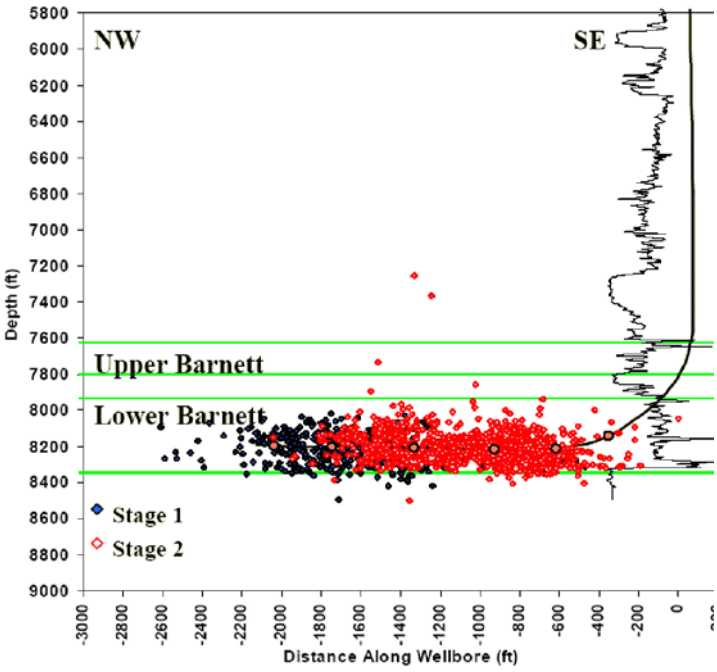

Figure 8.10: Side view fracture map looking normal to un-cemented lateral of treatment with fracture height confined to Lower Barnett Shale. Events displayed are for two fracture stages. Stage 1 treatment (blue filled diamonds) appears to have grown slightly higher than stage 2 (red open diamonds) [*Fisher et al.,* 2004].

Of the eleven wells mapped [*Fisher et al.,* 2004], both cemented and un-cemented, six wells exhibited fracture growth only in the Lower Barnett Shale, while 5 wells had measurable fracture height growth into the Upper Barnett Shale as well. This upward height growth could be more dependent on the thickness and integrity of the Forestburg Limestone interval, than on whether the lateral was cemented or un-cemented. None of the wells in this core area study had appreciable growth downward into the Viola or Ellenburger section.

Cemented Liners

With the casing cemented in place for zonal isolation, cemented horizontal laterals are typically fractured in multiple stages [*Fisher et al.,* 2004]. The number of stages for the cemented wells evaluated in this study ranged from four stages on four separate sets of perforations, to two treatment stages with two to three sets of perforation clusters per stage. The cemented casing would intuitively seem to allow for better control of fracture initiation locations and therefore allow multiple hydraulic fracturing stages to cover more effectively the entire long lateral section. Cemented, multi-stage completions are typically more expensive but achieve greater stimulation rates per foot of pay-zone and may have greater cumulative treatment volumes than a typical single-stage, un-cemented completion.

There have been two strategies utilized on cemented horizontal wells. The first strategy is to perform individual treatments on single perforated clusters. This is achieved by starting at the toe and progressing up to the heel, and isolating the previously stimulated interval or intervals with a composite bridge plug. This method addresses the desire to duplicate the fracture pattern that would be achieved if several vertical wells were drilled instead of the horizontal. This method proved to be cost intensive and led to the second strategy.

The second strategy is to limit the number of stages and stimulate two or three perforation clusters per stage. This hybrid approach proved to be cost effective and deliver satisfactory results.

Pumping rates for a typical hydraulic fracturing stage in a fracturing treatment of a cemented horizontal well are similar to those in un-cemented laterals. When multiple perforation clusters are stimulated in a single stage, they typically have a spacing of 500 ft.

While cemented horizontal wells allow for more control of fracture initiation locations, problems have been encountered in obtaining initiation of fractures. Excessive losses of pressure near the well with accompanying low rates of injection and high treating pressures have been observed in several wells. However, not all, cemented wells. Several steps have been taken to alleviate the problem. These steps include re-perforating, jet cutting holes, acidizing, pumping gel and sand slugs. Each of these procedures has proven to work at different times but none has proven completely successful. These additional steps can add time and cost compared to a problem-free treatment.

A 4-stage cemented Barnett Shale horizontal completion is displayed in Figure 8.11. The microseismic monitor well is on the same pad as the surface location of the treatment well. With the toe of the lateral at a distance of ~ 3,200 ft, the events are smaller in amplitude, or more attenuated, in the first stage, resulting in fewer events positioned at the toe on this treatment. The half-lengths of the fracture network of ~ 1,500 ft to 2,500 ft are greater than for a typical un-cemented treatment. The greater length on the cemented laterals is likely because of the smaller number of fractures initiated from a cemented well versus the many starter cracks expected with a un-cemented lateral. The widths of the fracture network range from 600 to 1,200 ft. This is also greater than for the un-cemented example. Individually, they are in line with typical vertical wells. Hydraulic fracturing volumes were large, averaging ~ 30,500 bbl and 200,000 lbm of sand per stage at rates of 65 bbl/min. The density of fracture along the well is adequate. However, there are still some gaps evident in fracture coverage of the lateral.

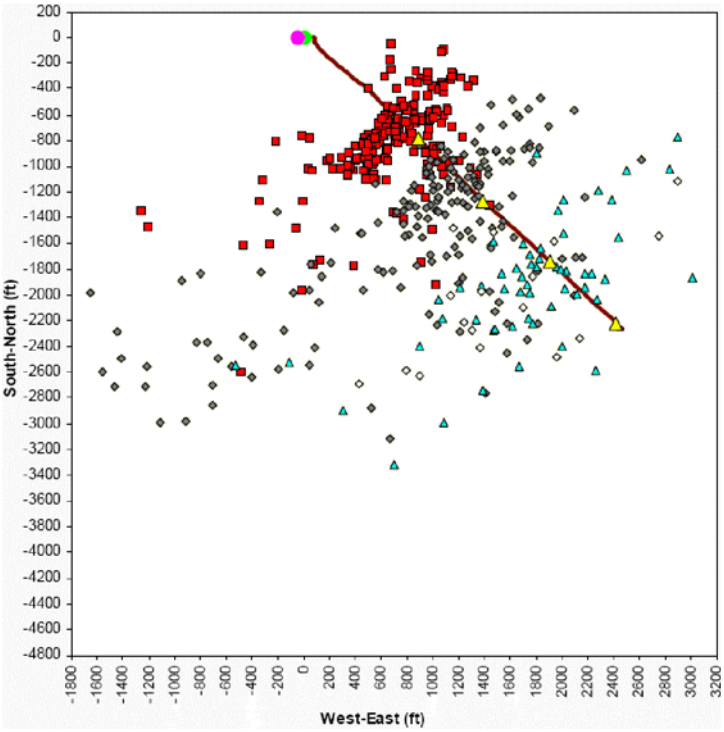

Figure 8.11: Plan view fracture map of typical cemented treatment. Four hydraulic fracturing stages were performed: stage 1 (open diamonds), stage 2 (triangles), stage 3 (filled diamonds) and stage 4 (squares). The first two stages are relatively symmetrical in half-length. However, the last two stages tended to grow preferentially longer to the SW [*Fisher et al.,* 2004].

Stress Shadows

Stress shadowing has been a factor in the success of horizontal treatments in the Barnett Shale [*Fisher et al.,* 2004; *Fisher et al.,* 2002]. On many of the fracturing treatments on horizontal wells, a stress shadow effect is clearly observed in the mapping results [*East et al.,* 2004]. When a hydraulic fracture is opened, the compressive stress normal to the fracture faces is increased above the initial in-situ stress by a quantity equal to the net hydraulic fracturing pressure. This elevation in stress is greatest right at the face of the fracture. However, the perturbation of the stress radiates out into the reservoir for hundreds of feet. The stress shadow that is cast by an open hydraulic fracture is displayed in Figure 8.12. The rate at which this stress perturbation declines with movement away from the face of the fracture is controlled by the smallest aerial fracture dimension (i.e., height or length). In the Barnett Shale, the heights of fractures are generally much less than the lengths of the fractures. Hence, the distance impacted by the stress shadow is controlled by the height of the fracture. The stress shadow becomes quite small when the offset distance is a factor of ~ 1.5 greater than the fracture height. In the core area of the Barnett Shale, the heights of fractures are typically ~ 300 to 400 ft. Hence, it is expected that the stress shadow to dissipate at a distance of ~ 500 ft away from the opening of a fracture. Experience supports this estimated shadow distance, as evidenced by the regularly spaced crosscutting fractures that tend to appear at intervals of ~ 500 ft regardless of the location of the perforation cluster.

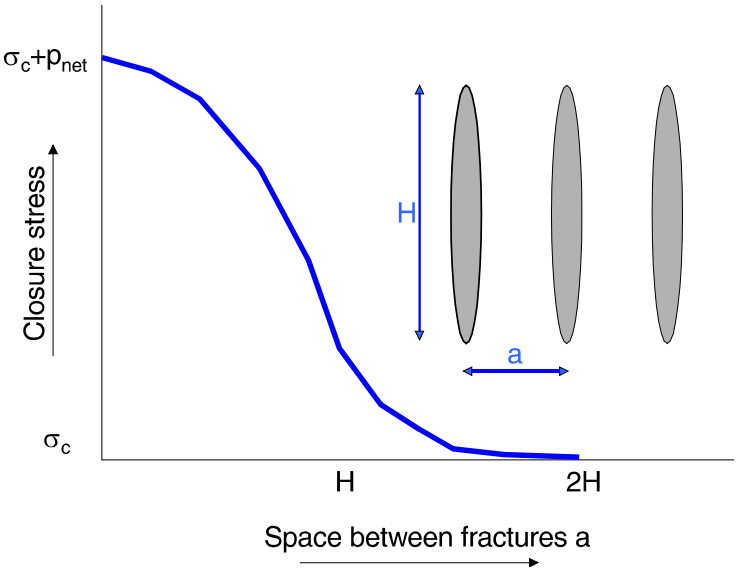

Figure 8.12: Relationship between closure stress increase as a function of distance away from fracture (stress shadow) expressed in terms of fracture height [*Warpsinki and Branagan,* 1989].

Stress shadow effects have been discussed for more than 15 years and documented with fracture mapping data for 10 years [*Minner et al.,* 2003; *Minner et al.,* 2002; *Wright et al.,* 1997; *Wright et al.,* 1995; *Warpsinki and Branagan,* 1989]. However, they were confined to special cases of tightly spaced wells, and were mostly the result of long-term production and injection operations [*Fisher et al.,* 2004]. However, these stress-shadow effects are critical to the design of completions and fracturing treatment strategies for horizontal wells [*East et al.,* 2004]. Yet, the importance of stress shadows remains underappreciated.

Stress shadows in horizontal well hydraulic fracturing have two major impacts [*East et al.,* 2004; *Fisher et al.,* 2004]: First, the increased compressive stress near a fracture tends to close-off or inhibit the initiation of near by parallel fractures. This provides a natural diversion mechanism along the well. If perforation clusters or fracture initiation points are too close together, then stress shadows tend to inhibit fracture growth along the mid-section of horizontal wells. Instead, fracture growth at the heel and toe of wells is encouraged. Second, the increase in the magnitude of the local minimum stress tends to encourage fracture growth in orthogonal directions. Even when the orientation of fractures from vertical wells is relatively uniform, stress shadow effects often induce orthogonal fracture growth when stimulating long intervals in horizontal wells. These impacts are illustrated in Figure 8.13.

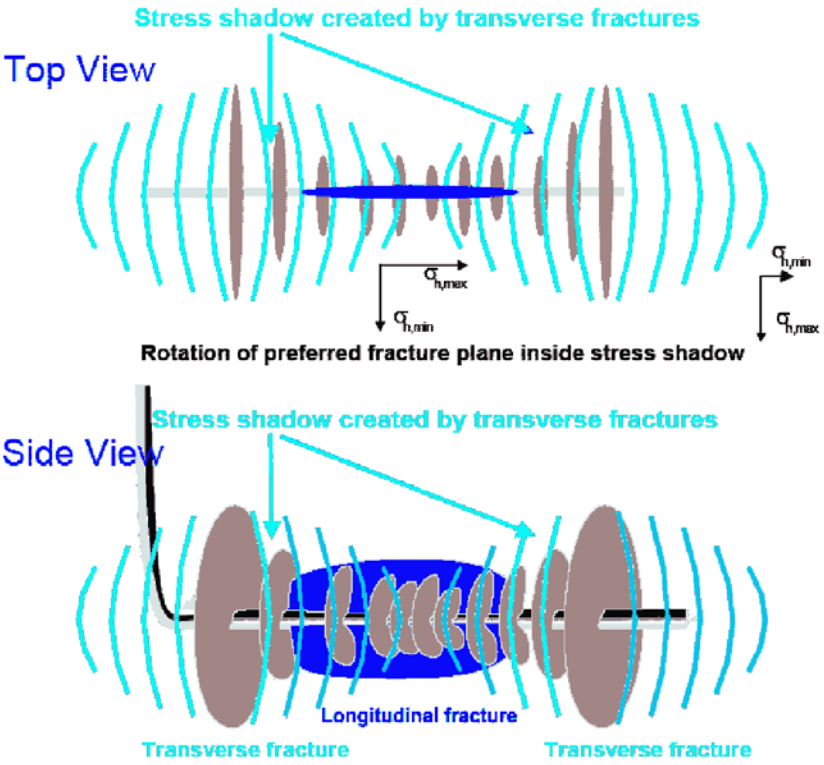

Figure 8.13: Stress shadow effects on transverse fracture growth [*Fisher et al.,* 2004].

Both effects are important for completions from horizontal wells. The growth of orthogonal vertical fractures, or fracture networks, occurs even in vertical wells in the Barnett Shale because of a low in-situ horizontal deviatoric stress and the presence of natural fractures orthogonal to the current maximum stress direction, which is NE-SW. Stress shadows from simultaneously growing and competing fractures that have initiated along a horizontal well tend to enhance further fracture growth in the orthogonal direction, which is NW-SE. This enhancement is positive because the contact area of the reservoir (i.e., the size of the network), and density of the network are both believed to contribute to the productivity of the well.

Recently, the mechanisms of the alteration of a stress field in the surroundings of a created hydraulic fracture that could potentially affect other hydraulic fractures created from near by wells was discussed [*Soliman et al.,* 2004]. If multiple fractures are created from a single well, then this effect could be more significant. Examples are creating multiple transverse fractures from a horizontal well, or multiple fractures intersecting a vertical well at different depths. The presence of casing versus open-hole completion could also make a difference. From earlier solutions [*Sneddon,* 1946; *Sneddon and Elliott,* 1946], the effect of the presence of multiple fractures on the pressure of hydraulic fracturing, the magnitude of the stress field, and even the potential change of the orientation of the stress were presented. Depending on the dimensions of the fracture, the distances between the various already created fractures exhibit a greater pressure of treatment, and may even cause changes in the orientation of the stress in space. The effect could be adequately significant so that it should be considered in the design and optimization of the number of fractures.

Real-time Aid

Five completion designs for horizontal wells were changed on the fly because of the availability of real-time mapping results [*Fisher et al.,* 2004]. The fracture geometry for two completions from horizontal wells (uncemented, two-stage and cemented single stage) is displayed in Figure 8.14.

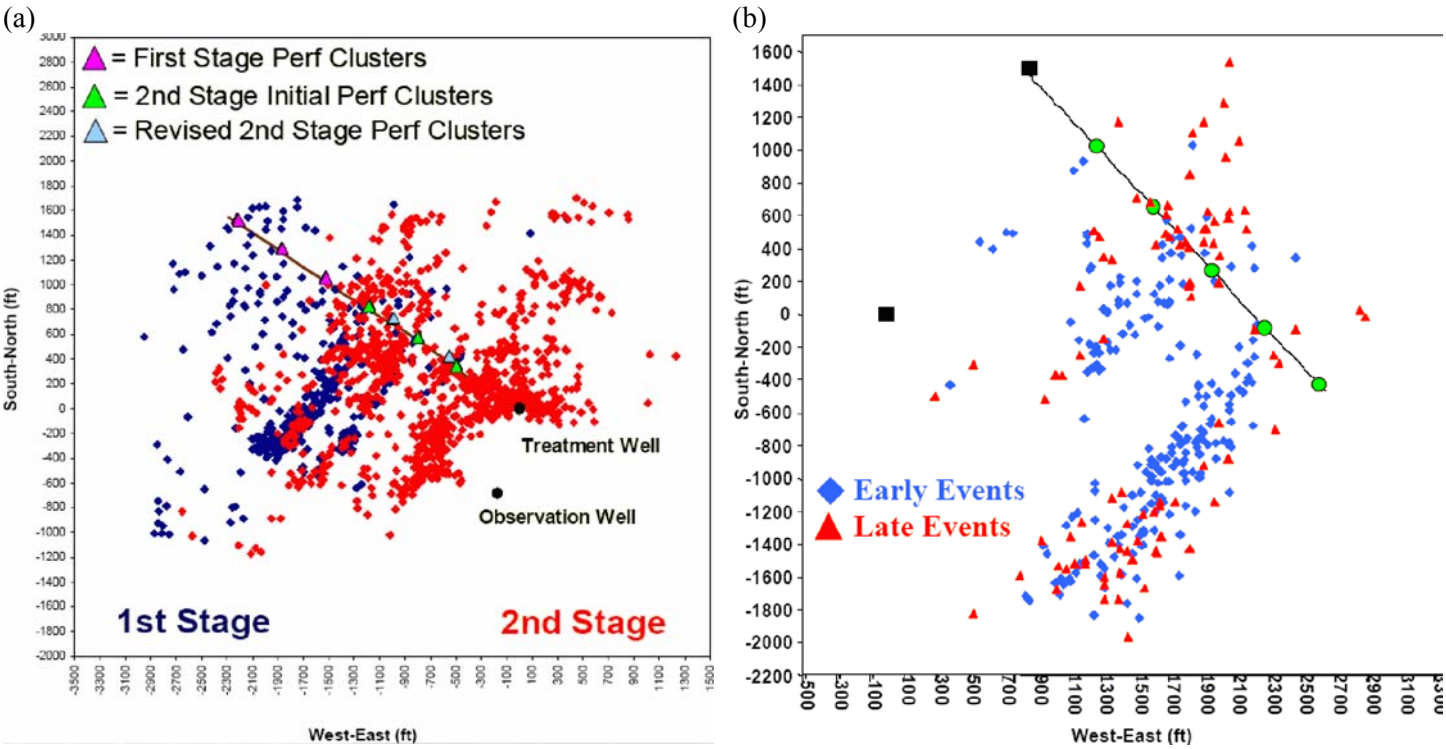

Figure 8.14: Fracture geometry for two horizontal well completions: (a) First and second stage from a two-stage cemented well; and (b) single-stage, un-cemented well, before and after pumping proppant slugs [*Fisher et al.,* 2004].

Cemented Liner

One of the horizontal wells with a cemented liner was re-designed to change the spacings between two separate fracturing stages, as displayed in Figure 8.14a [*Fisher et al.,* 2004]. As the first stage was being pumped, microseismic data indicated that the fracture network exhibited substantial growth in an area that was to be perforated and fractured in the second stage. That information was used to alter the location of the perforation clusters on the second stage, and thus increase the probability of the second hydraulic fracturing treatment contacting a different (and thus greater portion) of the reservoir than the first treatment. The perforations of the second stage shifted ~ 300 ft toward the heel, and reduced from three to two clusters compared to the original design. This allowed the movement of the second stage hydraulic fracturing away from the area that was already stimulated by the first stage treatment.

Un-cemented Liner

The results of another single stage, horizontal well with a un-cemented liner are displayed in Figure 8.14b. During the treatment, the early hydraulic fracturing events were mostly positioned near the center, and especially near the toe of the lateral [*Fisher et al.,* 2004]. Consequently, a series of sand slugs were pumped in an effort to redirect the treatment toward the perforation clusters at the heel and center of the lateral. The proppant slugs were partially effective. Indeed, a greater percentage (~ 50%) of late-job microseismic events was positioned near the center and heel than had been generated during the early part of the treatment before the sand slugs.

8.3 Water Fracturing in Barnett Shale

Two different types of water fractures were pumped [*Mayerhofer et al.,* 1997]:

1) Treated water (i.e., either 10 lbm/1,000 gal of gel or water with friction reducer only, 50% pad, constant sand concentration of 0.5 lbm/gal, and tail-in with a ramp with a concentration of sand of 0.5 to 2.0 lbm/gal for the last 1 to 5% of the job (depending on gross height); and
2) linear gel fluid (i.e., either 10 lbm/1,000 gal of gel or water with friction reducer as pad, followed by 20 lbm/1,000 gal of gel), 50% pad, and a ramp with a concentration of sand of 0.5 to 2.0 lbm/gal through the proppant-laden stage.

The treatments of the second type were pumped in formations with greater reservoir permeability.

A typical match of the net pressure of a water fracture and a conventional propped fracture is displayed in Figure 8.15. The net pressure of the water fracture has a flat trend and a low net pressure, which indicates an adequate extension of the fracture. The net pressure of the conventional propped fracture increases throughout the treatment, which demonstrates a growing resistance, most likely within a region near the well.

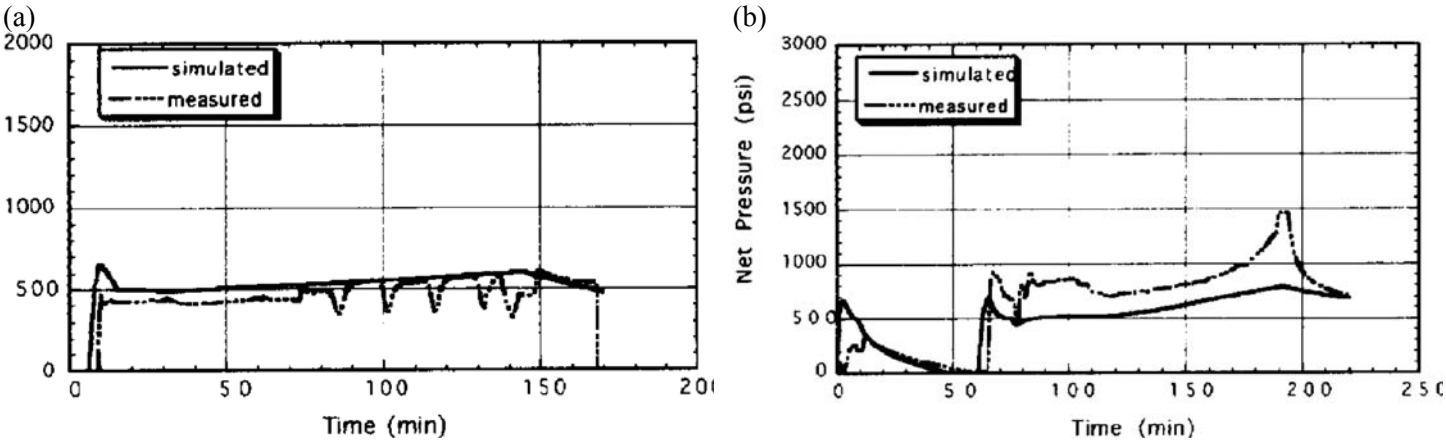

Figure 8.15: Net pressure match of (a) water, and (b) conventional hydraulic fracturing treatment [*Mayerhofer et al.,* 1997].

The results for the matches are listed in Table 8.1. The length of the propped fracture of the conventional fracture is shorter than that of the water fracture, which was pumped with 20% less quantity of fluid and less weight of proppant pumped. The history of the net pressure indicates that fluids with low viscosity result in a better extension of the fracture. Under the assumption that proppant does not settle or convect, the dimensionless conductivity of the fracture of water fracture from one of the wells was calculated, by use of a value of the permeability of the reservoir of 0.005 mD, to be 24. While these assumptions appear questionable, the resultant conductivity is perfectly adequate.

Table 8.1: Results of net pressure match of (a) water, and (b) conventional hydraulic fracturing treatment [*Mayerhofer et al.,* 1997].

fracture	propped fracture length (ft)	average proppant concentration (lbm/ft^2)	pumped proppant weight (lbm)
water	906	0.2	75,000
conventional propped	796	1.13	506,000

In the early days of hydraulic fracturing, similar treatments were performed with fluids with low viscosity, and low concentrations of sand. The total volumes of the fluids, however, were very small. In general, the results were satisfactory. However, it was believed that the productivity would only be acceptable for a few months, and could be improved with treatments that are more massive by using greater volumes of fluid and sand. In the Austin Chalk,

water-fracturing treatments are pumped with no proppant at all, and very large volumes of fluid and high rates of injection are very successful. The mechanism is still not fully understood [*Meehan,* 1995; *Meehan and Pennington,* 1982].

For a water fracture pumped at a rate of injection of 56 bbl/min during a time interval of 6 hr, the microseismic events are displayed in Figure 8.16. For the individual microseismic events, the average accuracy of the location is ~ 45 ft. The displayed events are all above a certain threshold magnitude, such that the microseismic images correspond to a uniform detection over the microseismic volume [*Maxwell et al.,* 2000]. Without these criteria, a bias of location would exist near the treatment well where an increased sensitivity results in the recording of numerous events of smaller magnitude. This type of analysis is crucial to ensure that the microseismic images are not missing hydraulic fracturing in certain regions, and that the event distribution is representative.

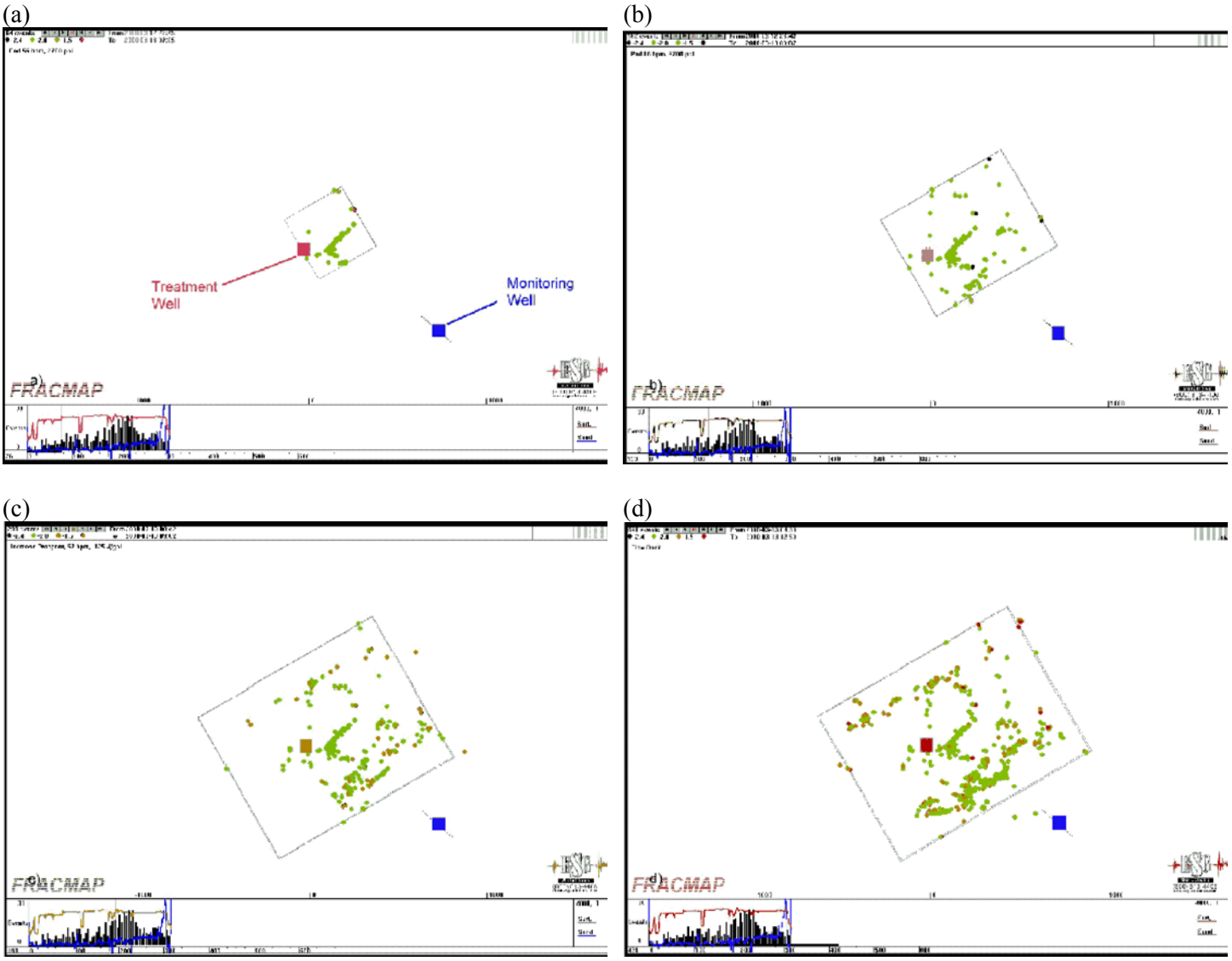

Figure 8.16: Plan view of well stimulation, with fracture growth during four periods: (a) 80 min, (b) 130 min, (c) 190 min, and (d) end of treatment. Microseismic event locations scaled by magnitude [*Maxwell et al.,* 2002].

The events are distributed over three main parallel lineations. They trend NE-SW, parallel to the anticipated orientation of the fracture. They have a spacing of ~ 300 ft. The lineations are interpreted as the result of the interaction of the hydraulic fracturing slurry with pre-existing natural fractures in the reservoir. Between the three main features that are oriented

NE-SW, a number of other less extensive lineations of events can also be observed. One dominant orientation is NW-SE, which is believed to be conjugate fracture sets that feed the slurry into the main NE-SW features. In depth, the events are all contained within the Barnett Shale, which is the target zone.

The seismicity initially migrates out from the treatment well in a NE orientation. It then starts to move in a SE direction towards the most southern main lineation. As this lineation develops, the events also begin to move NW towards the most northern main lineation. During the last half of the job, the most northern and southern lineations continue to extend in the NE and SW directions. This series of images were the first verification from the field that the stimulations were creating complex hydraulic fractures, or that the hydraulic fractures were influenced by pre-existing natural fractures. This has now been clearly established as the case for stimulation treatments in the Barnett Shale. The degree of complexity as displayed in Figure 8.16 is characteristic of the various images of different stimulations in the Barnett Shale, although the ultimate geometry varies remarkably.

Another example of these complex fractures is the effect of stimulating a well that was inadvertently drilled within the depleted zone of a neighboring well. Because of the complex fractures, the area of drainage of various wells is probably significantly more complicated than originally thought. The area of drainage could extend a significant distance perpendicular to the usual NE-SW orientation of the fractures. Before these microseismic images, this drainage in the NE-SW orientation was thought to be the norm in the field. However, the drainage associated with the treatment imaged with the well described in Figure 8.16 would tend to produce a net area of drainage that extends much further in the NW-SE. Tight infill drilling associated with future production strategy can then occasionally result in a well that has been inadvertently drilled into a depleted reservoir that is associated with anomalous drainage.

Chief Oil and Gas began drilling and completing wells in the Barnett Shale in 1996 [*Coulter et al.,* 2004]. Because then and until the end of 2003, they have drilled 182 wells. Most of these wells were in the counties of Denton and Tarrant in Texas. All but two of these wells have been stimulated by use of water fracturing. The early treatments contained only small quantities of sand. However, with time the quantity of sand used in the treatments was increased. A comprehensive database was created of these treatments, as well as the production response from each well. The analysis of this database resulted in information to guide the selection of the particle size and quantity of sand used for future treatments.

Several hydraulic fracturing treatments were mapped. Various degrees of complex hydraulic fracturing behavior were observed [*Coulter et al.,* 2004]. The results from microseismic mapping of one of the hydraulic fracturing treatments from a horizontal well is displayed in Figure 8.17a. The general network demonstrates a trend in the NE-SW orientation, as displayed in Figure 8.17a. However, it is also possible for the general trend of the fracture networks to be oriented in a direction other than that expected. A hydraulic fracturing treatment from a vertical well was mapped, as displayed in Figure 8.17b. The induced fracture networks were interpreted to be oriented ~ 90° from that expected. The interpretation of the induced patterns of the fracture that was created during the hydraulic fracturing of this well is displayed in Figure 8.18. The complexity of some of the patterns of the created fracture is presented in Figure 8.19. Not only are complex fracture networks created, but also the height of the fracture could be unpredictable in some areas. A fracture initiated in the Lower Barnett Shale can extend up into the Upper Barnett Shale, as displayed in Figure 8.19. This does not always happen. The prediction of its occurrence can be difficult. When only the Lower Barnett Shale exists, the heights of the fractures can usually be predicted with some certainty.

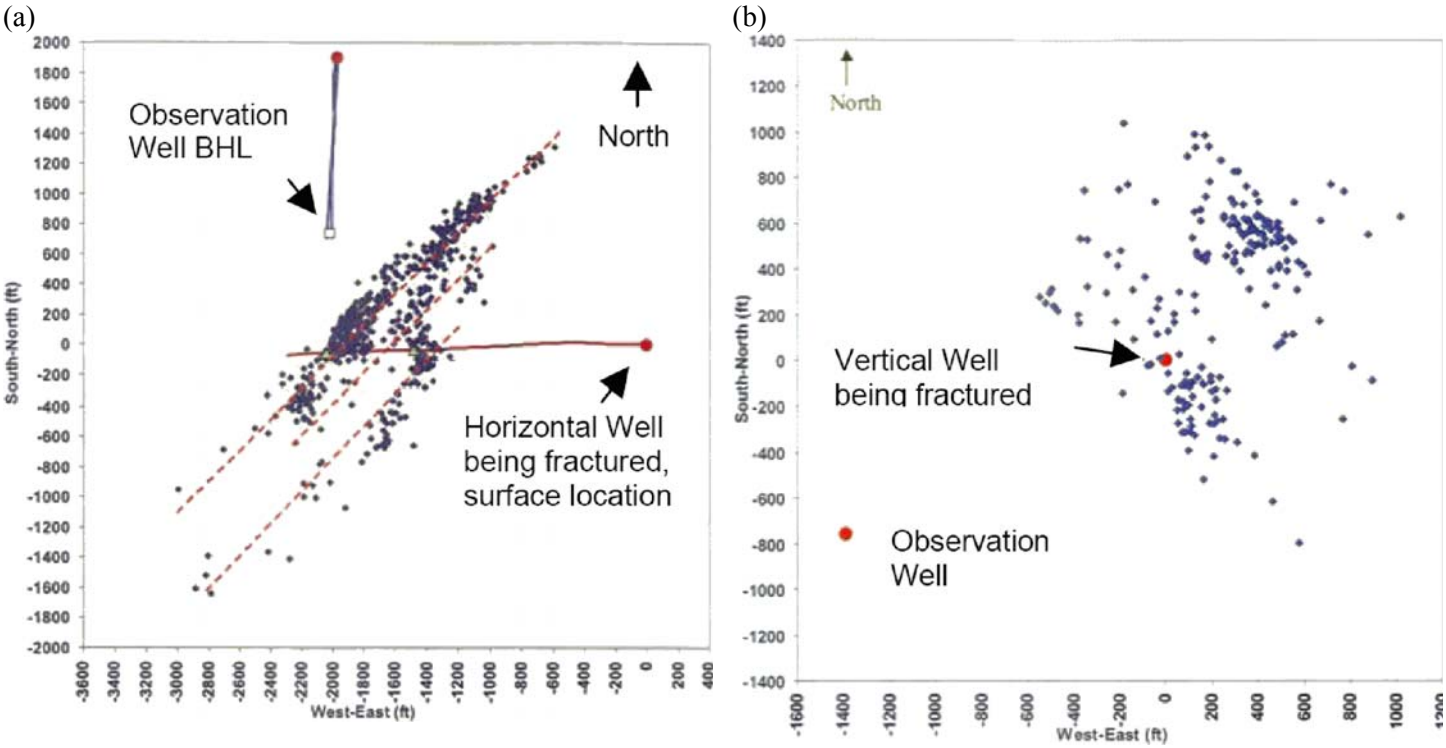

Figure 8.17: Complexity of hydraulic fracture from: (a) horizontal well, oriented as expected; and (b) vertical well, oriented ~ 90° from that expected. Microseismic events displayed as dark circles [*Coulter et al.,* 2004].

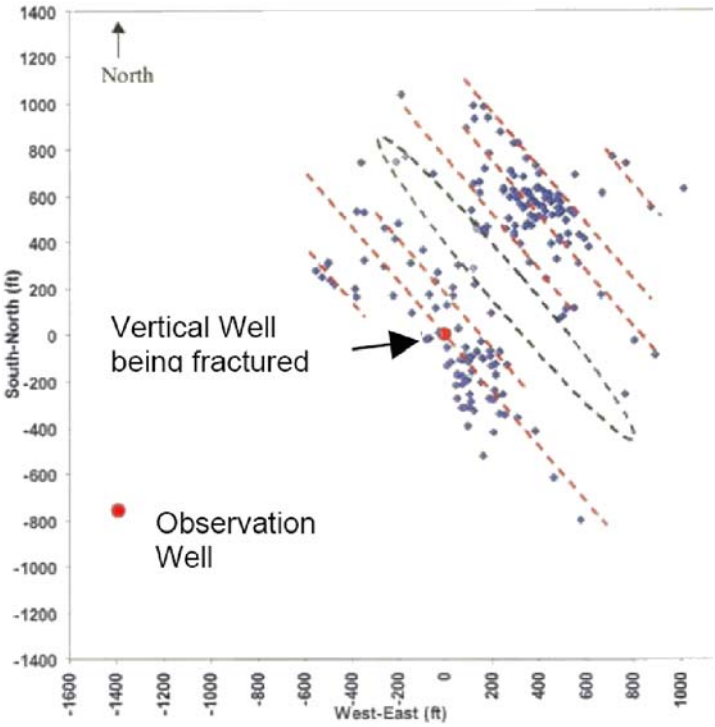

Figure 8.18: Interpretation of induced fractures from Figure 8.17 [*Coulter et al.,* 2004].

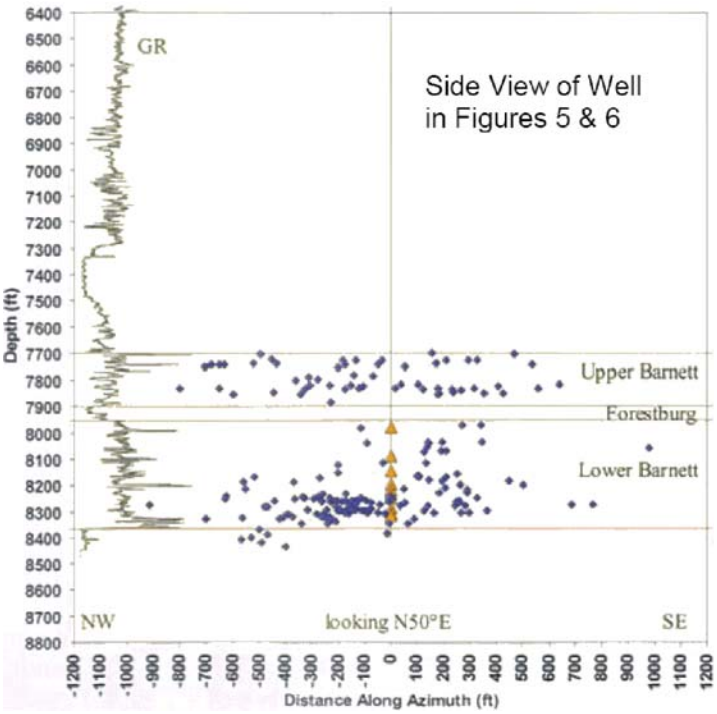

Figure 8.19: Side view of fracture in Figure 8.17 and Figure 8.18, with induced fracture extension into Upper Barnett Shale from Lower Barnett Shale perforations [*Coulter et al.,* 2004].

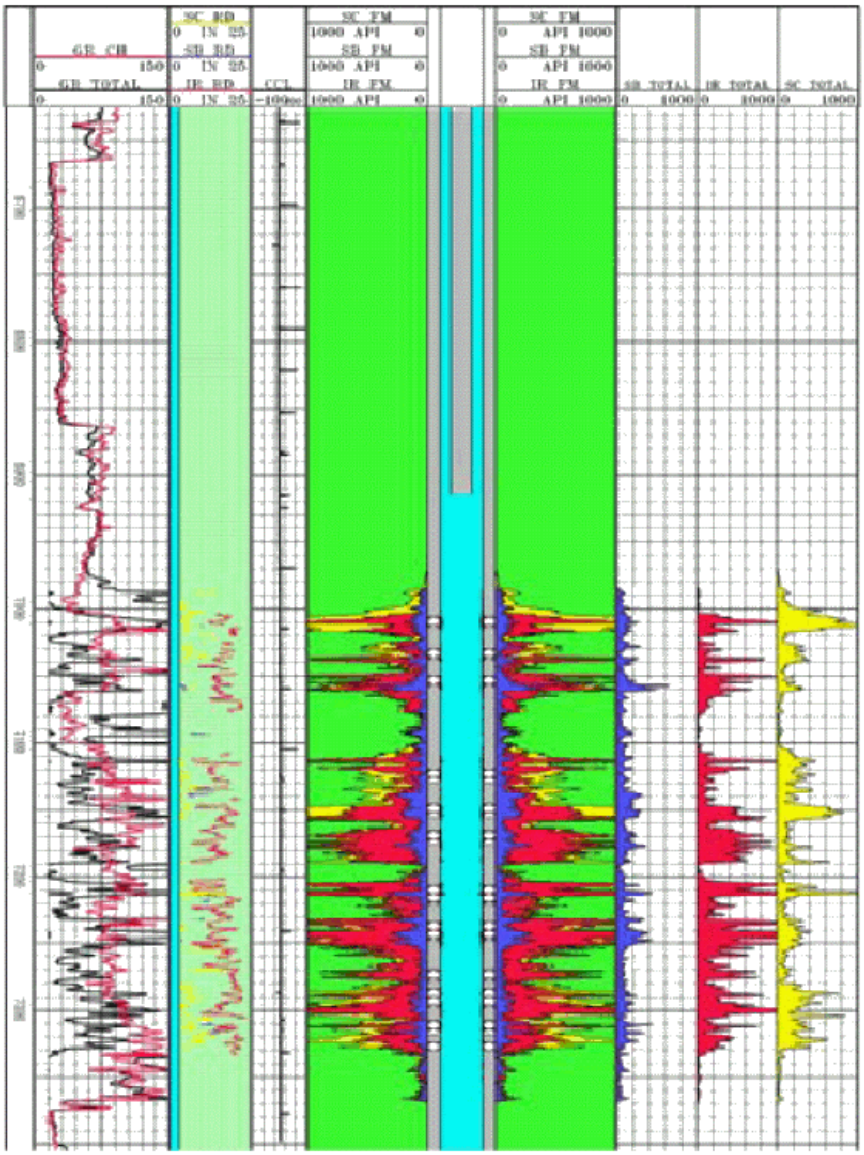

Figure 8.20: Tracer log of fractured well in Lower Barnett Shale, with induced fracture containment in Lower Barnett Shale [*Coulter et al.,* 2004].

An example of a fractured well with only the Lower Barnett Shale existing is displayed in Figure 8.20. Three isotopes were used to trace the pad fluid and each of the applied proppant types [*Coulter et al.,* 2004]. At the well, a satisfactory containment of the fracture was achieved.

8.4 Correlation of Fracture Parameters to Production

The correlations of the fracture parameters to the production parameters are studied, for vertical wells (section 8.4.1 below), horizontal wells (section 8.4.2 on page 128), and water fracturing (section 8.4.3 on page 131).

8.4.1 Vertical Wells

The correlations between the cumulative production of gas and the length of the fractures and the width (i.e., the complexity and total surface area) of the fracture network are displayed in Figure 8.21. The trends (i.e., growth) of the half-length of the fractures and the length of the network as a function of the volume of the fluid in the Lower Barnett Shale are displayed in Figure 8.22.

(a) (b)

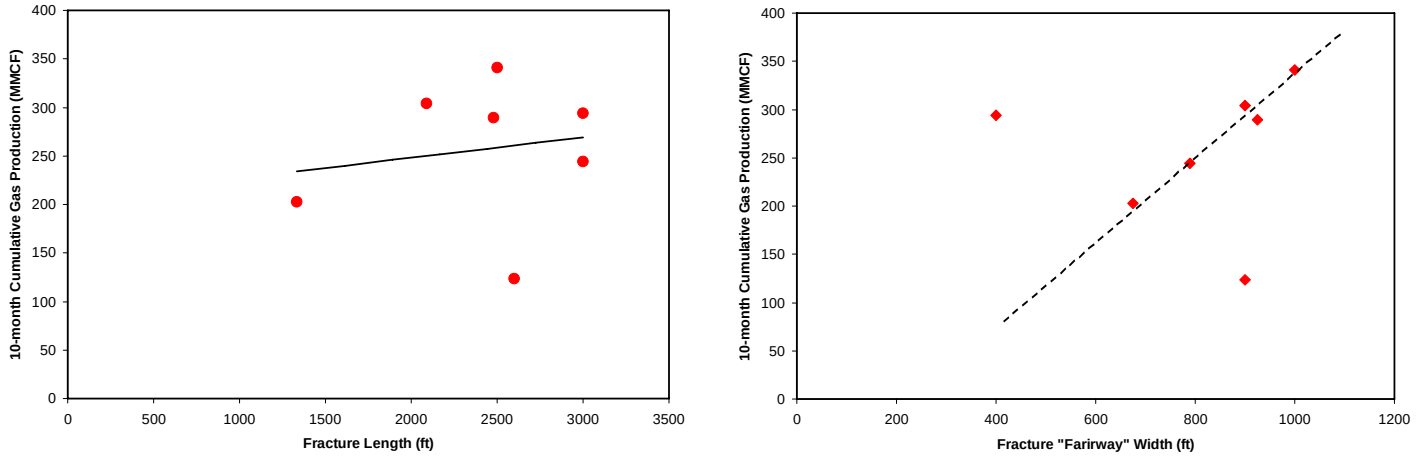

Figure 8.21: Correlation between cumulative gas production and: 33 (a) fracture length (no correlation), and 35 (b) fracture network width, i.e., complexity and total fracture surface area (positive correlation) [*Fisher et al.,* 2002].

(a) (b)

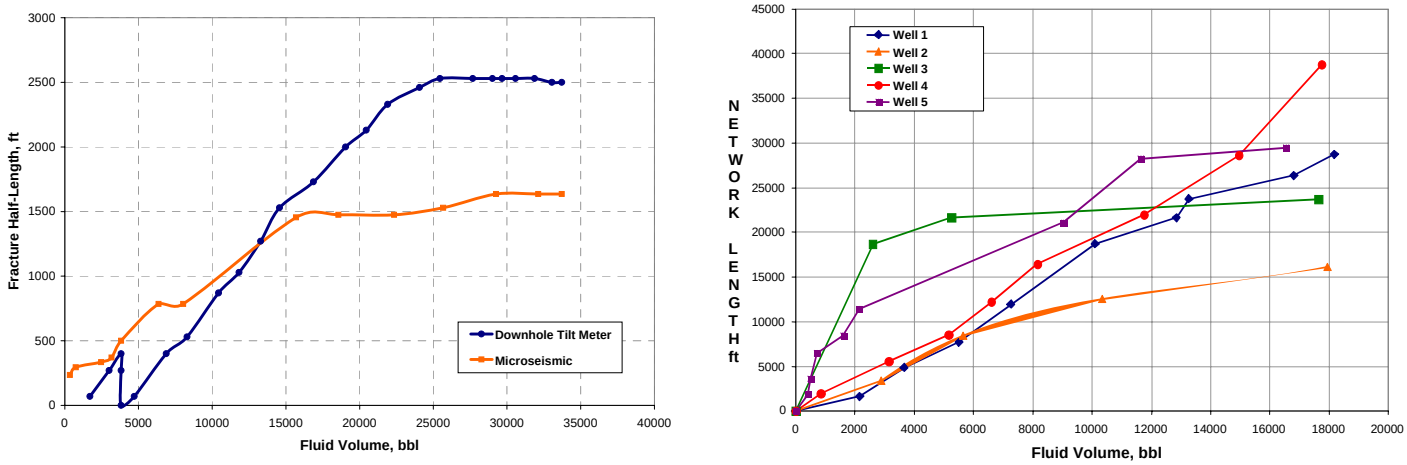

Figure 8.22: Trends (i.e., growth), as a function of fluid volume: (a) fracture half-length, and (b) network length in Lower Barnett Shale [*Fisher et al.,* 2002].

The productivity of the wells was not greatly influenced by the conventional half-length of the fracture, as displayed in Figure 8.21a. This is exactly the opposite of what is generally expected from a reservoir with a low permeability [*Fisher et al.,* 2002]. Consequently, other fracture parameters and their influence on productivity were evaluated.

The lack of the growth of the length of the fracture in the later parts of the treatment appeared to justify the reduction of the volumes of the treatment until the fracture network was evaluated in more detail. The width of the fracture network was observed in both the surface tiltmeters (i.e., the NW component, and in the microseismic activity where growth was observed in a wide band of events). A wider fracture network results in a better productivity from the well, as displayed in Figure 8.21b.

The growth of the half-length of the fracture network was evaluated as a function of the volume of the fluid, as displayed in Figure 8.22a. The half-length of the fracture stops growing for nearly all fractures after a significant quantity of fluid is pumped. The half-length measured from microseismic mapping is shorter because of the position of the observation well and the attenuation of acoustic signals over these very great lengths of the network. However, both mapping methods indicated an arresting of the half-length of the fracture before the end of the treatment.

The total length of the fracture network was determined from the sum over time of the segments of the fracture structure determined by microseismic imaging. Significant individual fracture networks were developing as each treatment progressed. The entire fracture network system continued to grow with additional pumped volume, as displayed in Figure 8.22b. In most cases, network length grows with incremental treatment volume. Therefore, to improve well productivity, a greater network of fractures is desirable, independent of the conventional half-length of the fracture.

Summarizing, the half-length of the fracture network is not a critical parameter influencing early production. The mapping data demonstrates that individual hydraulic fracturing stages in the Barnett Shale typically produce longer and wider fracture networks. In contrast, correlations between the volumes of the treatment and the created half-length of the fracture network are not strong. The correlations between the volume of the treatment and the width of the network and between the width of the network and the early production indicate that greater hydraulic fracturing treatments tend to produce greater surface areas, and that this has a favorable effect on production.

The daily production rates of four different wells are displayed in Figure 8.23. The production for well A (Figure 8.23a) is initially relatively high, and it is maintained at a more uniform rate than for the other wells (which have a more significant hyperbolic decline) [*Maxwell et al.,* 2002]. This high rate of production could be related to an extensive contact between the reservoir and the network of fractures, as can be observed by the complexity of the fracture network as displayed in Figure 8.16 on page 120.

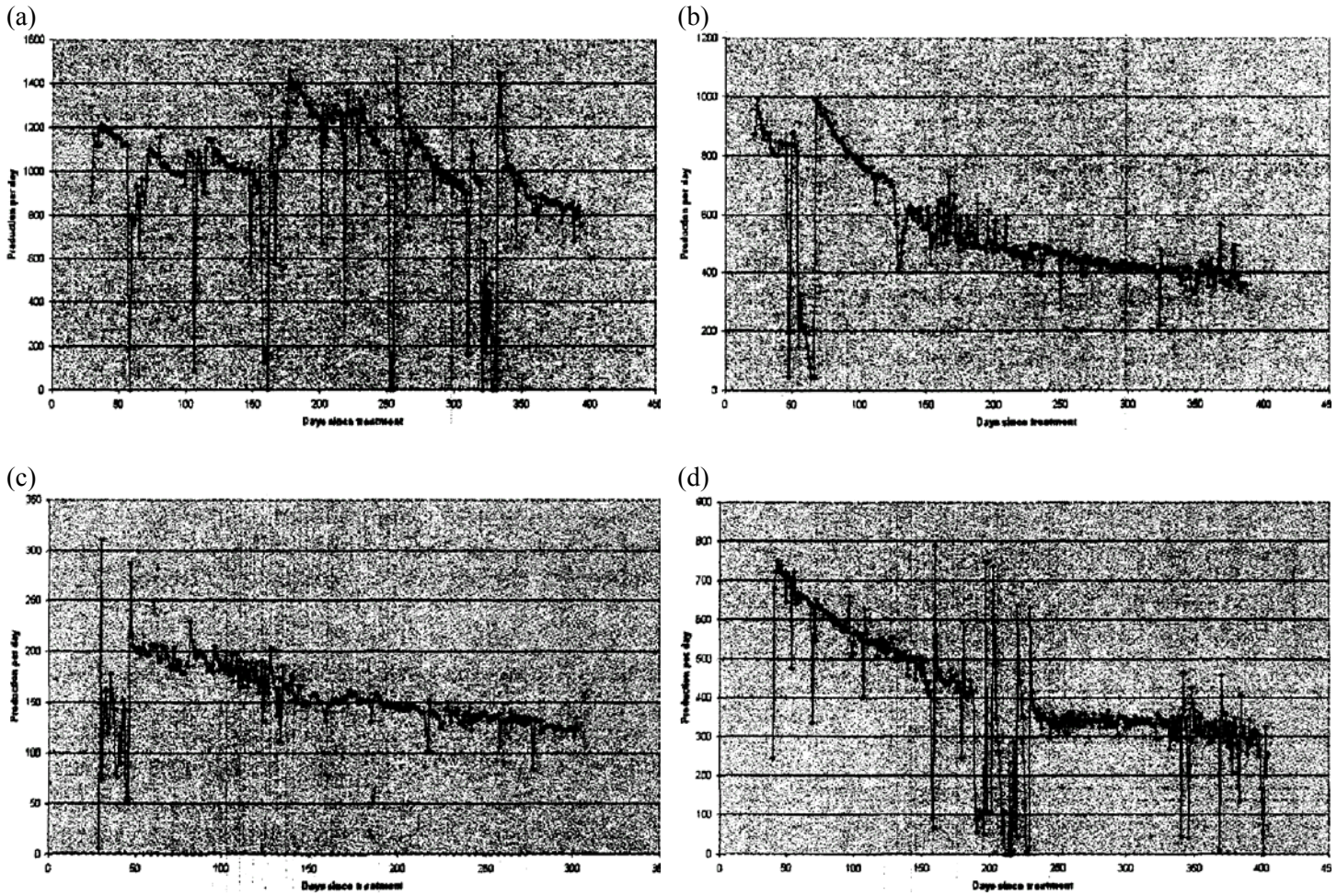

Figure 8.23: Daily production rates for: (a) well A (displayed in Figure 8.16 on page 120), (b) well B, (c) well C, and (d) well D [*Maxwell et al.,* 2002].

The relatively moderate rate of production for well B is displayed in Figure 8.23b. There is evidence that the treatment stimulated parallel fractures in a network of fractures, at least near the treatment well. However, the fractures are much less extensive and more closely spaced, compared to the wider geometry of the network of fractures found for well A. This can perhaps explain the differences in production between the two wells.

The very poor production of well C, where the fracture grew into the monitoring well, is displayed in Figure 8.23c. The very poor production is indicative of all the examples of fractures that encountered a depleted zone near a neighboring monitoring well, or generated a fracture geometry that is oriented parallel to the natural fractures in the NW-SE direction.

The production of well D, which has the second lowest production of these examples, is displayed in Figure 8.23d. Although the fracture image indicates that a network of fractures was stimulated, it may have interacted with the networks of fractures of the neighboring wells. Compared to, e.g., well B, the extent and spacing of the discrete fractures appear to be more extensive, although the production rates are lower. This well was a case study to examine the hydraulic fracturing behavior with a tight spacing of the wells.

In general, however, the various rates of production can be attributed with the differences in characteristics of the networks of fractures. Numerous other stimulations have also been imaged over the last two years, in various parts of the field. Although there are numerous factors that ultimately influence the rate of production, generating a wide fracture zone appears to be a critical factor in the performance of the wells. This appears to be the case when comparing, e.g., well A and

B. The imaging experience also includes cases at very close spacings of the wells, where the interaction of the networks of fractures from neighboring wells are likely to be important. In a few cases (e.g., well C), unfavorable orientations of the networks of fractures have apparently limited the production potential.

A satisfactory positive correlation was observed between the width of the fracture network and the cumulative production [*Fisher et al.,* 2004]. A cumulative production during a period of ten months was more than adequate to predict well the estimated ultimate recovery (EUR) in the Barnett Shale.

8.4.2 Horizontal Wells

Numerous comparisons were made of the parameters of the horizontal wells to the average daily rate of production for the best consecutive six months of production [*Fisher et al.,* 2004]. These 23 horizontal wells comprised all the horizontal wells drilled in the core area with more than six months of production. Almost half of these 23 wells (eleven) were mapped with microseismic imaging. These wells are separated from the total population and discussed in further detail. The calculated average rate of production for all correlations is the daily average of the best six months of production. The geometry and area of contact with the reservoir for cemented versus un-cemented hydraulic fracturing stages can be compared directly.

The correlations between the length of the lateral and the volume of fracturing treatment, and the average rate of production are displayed in Figure 8.24. The correlation between the length of the lateral and the average rate of production (Figure 8.24a) is weak. There is no correlation between the volume of the fracturing treatment and the average rate of production (Figure 8.24b). Generally, greater volumes of the fracturing treatment were used for the wells with a greater length of the lateral. Hence, there are no definitive correlations evident between the length of the lateral and the volume of the fracture versus the rate of production, as displayed in Figure 8.24. Numerous other comparisons of production with parameters (e.g., number of treatment stages, injection rate, proppant concentration, number of perforation clusters, and proppant volume) were performed with similar lack of correlativity.

(a) (b)

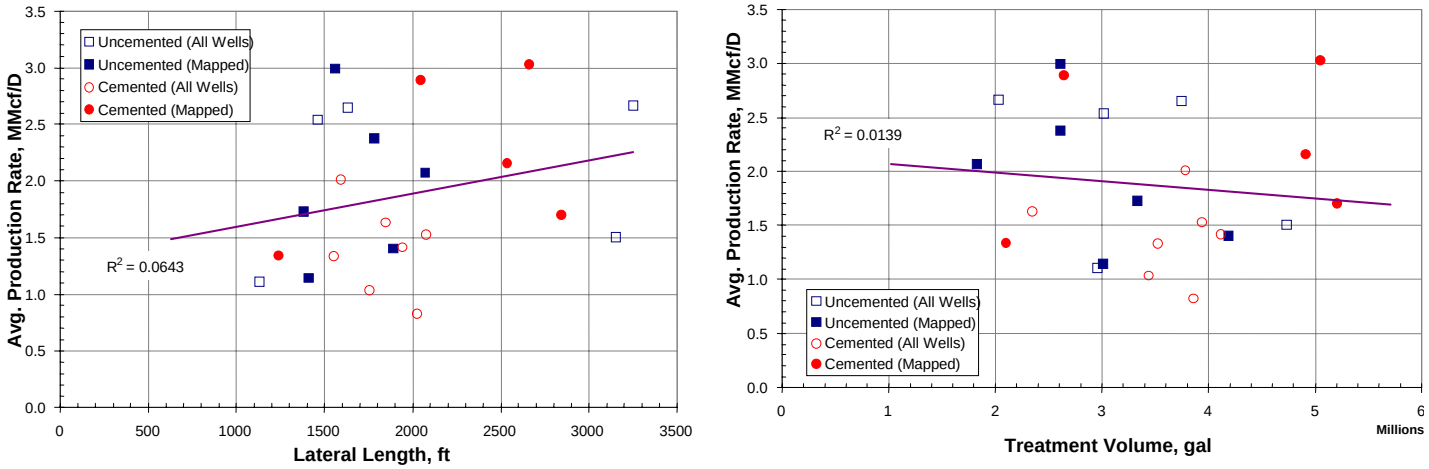

Figure 8.24: Correlation with average production rate for: (a) lateral length (weak correlation), and (b) treatment fluid volume (no correlation) [*Fisher et al.,* 2004].

A different approach was then taken utilizing cumulative frequency graphs [*Fisher et al.,* 2004]. They are often useful in separating variances in behavior within a population of data. These graphs plot the rates of production in ascending order with the individual wells evenly separated for easy viewing. The cumulative frequency graph for all 23 horizontal wells plus 7 vertical wells in this same core area is displayed in Figure 8.25 for the average daily rate of production, and the average daily rate of production normalized by the length of the lateral (to eliminate the potential bias of the rate of production from longer laterals). The horizontal wells outperform their vertical neighbors by a factor of 2 to 3, as displayed in Figure

8.25a. For the horizontal wells, a significant group of the un-cemented wells outperformed the cemented wells in this same area, as displayed in Figure 8.25b.

(a) (b)

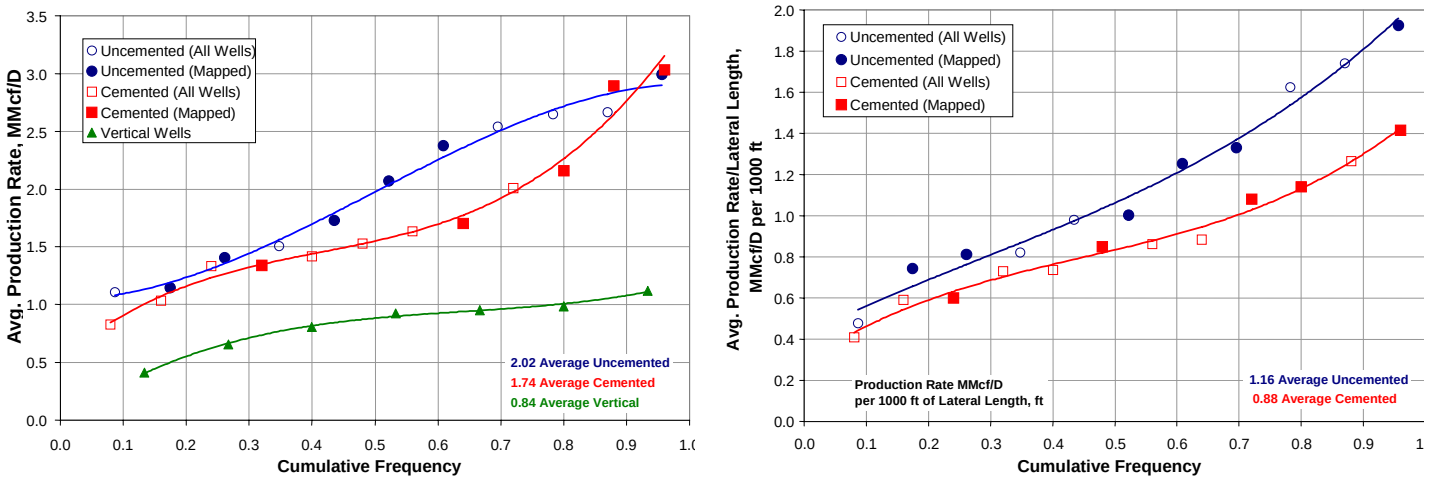

Figure 8.25: Cumulative frequency distribution for 23 horizontal wells and 7 vertical wells of: (a) average production rate, and (b) average production rate normalized by lateral length (only for horizontal wells) [*Fisher et al.,* 2004].

A similar benefit of the un-cemented lateral's average daily production rates normalized with treatment volume is illustrated in Figure 8.26. Thus, for both lateral length and treatment volume variations, un-cemented laterals within the total horizontal population appear to outperform neighboring cemented wells.

The remainder of correlations reported here deal with a subset of the total 23 horizontal well population. These eleven wells represent all the microseismic mapped horizontal wells in the core area with more than six months of production as of the date of this study. As can be observed in the previous three graphs, these 11 mapped wells are representative of the total population of 23 wells in terms of productivity, lateral length, and treatment volume. The following graphs compare and contrast directly measured hydraulic fracture dimensions between various treatment and well completion scenarios.

The correlation of average daily production for the best six months of all mapped horizontal treatments and seven neighboring vertical well treatments versus fracture network length is displayed in Figure 8.27. The summed, or cumulative, fracture network length was derived for all the above treatments by use of the same methodology as described in Figure 8.5 on page 109. As can be observed, a satisfactory correlation exists between total fracture network size and well productivity.

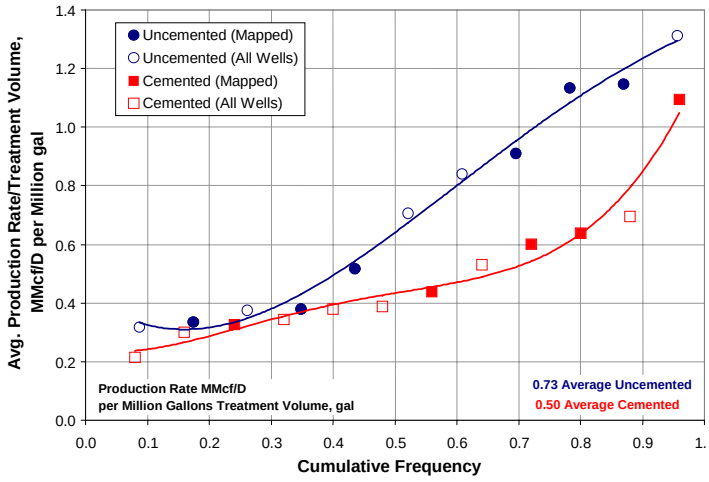

Figure 8.26: Cumulative frequency distribution of average production rate normalized by treatment volume [*Fisher et al.,* 2004].

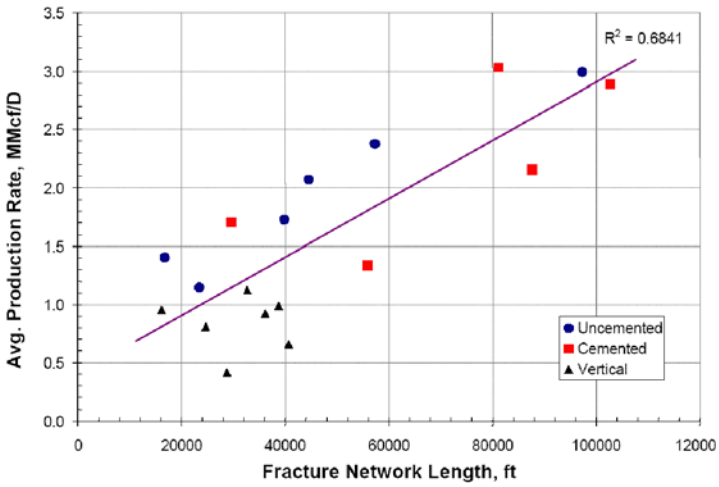

Figure 8.27: Cumulative length of individual fracture segments correlates to improved well productivity [*Fisher et al.,* 2004].

The correlations between the sum of the product of the length (tip to tip) and the height of all fractures on both sides of the lateral well and the width of the fracture network, and the average rate of production is displayed in Figure 8.28.

(a)

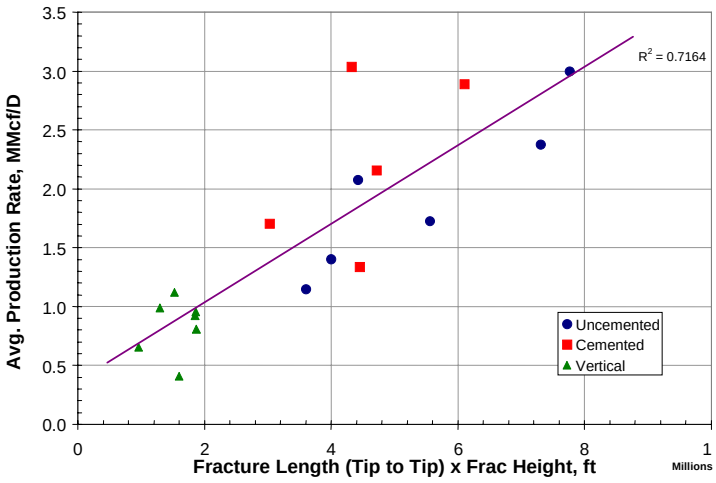

(b)

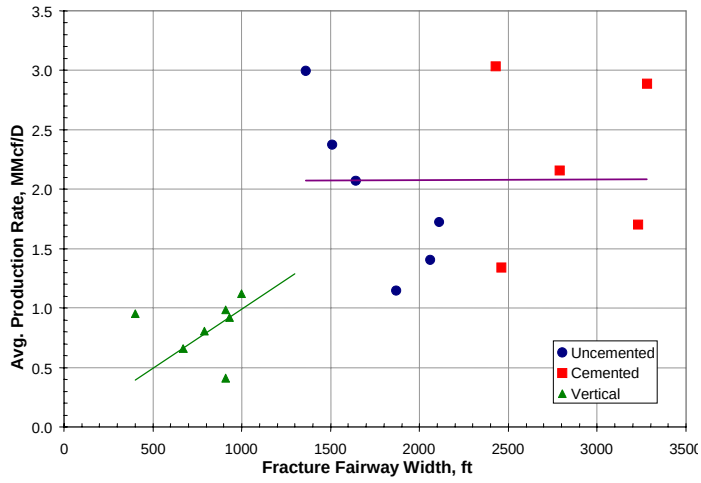

Figure 8.28: Correlations with average production rate: (a) product of total fracture length (tip to tip) and fracture height, and (b) fracture network width [*Fisher et al.,* 2004].

The correlation between productivity and classical fracture half-length is illustrated in Figure 8.28a. Fracture length (tip to tip) as displayed above can be defined as the sum of all fracture half-lengths on both sides of the lateral well. That is, taking the simple fracture half-length perpendicular to the well (NE-SW) for each created network and summing them. This graph further normalizes fracture length with fracture height to account for variances in pay-zone height contacted by the fracture. As can be observed, this is also a strong correlation (i.e., more fracture area of contact means better productivity). Interestingly, as previously reported, fracture half-length does not correlate strongly to productivity on the vertical wells [*Fisher et al.,* 2002].

The poor correlation between productivity and apparent fracture network width on horizontal wells is illustrated in Figure 8.28. Fracture network width is defined here as the distance across a given fracture network from NW-SE (i.e., the short axis of each fracture network rectangle). For horizontal wells, the fracture network widths are not as easily defined or measured as on vertical wells because of interaction and overlap between multiple fracture networks emanating from each perforation cluster. As can be observed here, and as was previously reported [*Fisher et al.,* 2002], there is a satisfactory fit with the data on vertical wells. The difficulty in defining and measuring network width may have led to the poor correlation on these horizontal wells. In vertical wells, fracture network width may serve as a satisfactory proxy for total network contact area. However, with horizontal wells, the variability in network density is much greater and hence network width of itself is not a very satisfactory proxy for total network contact area.

The correlation between the difference between average rate of production and the length of the lateral and the width of the network, and the gross contact volume in the reservoir is displayed in Figure 8.29.

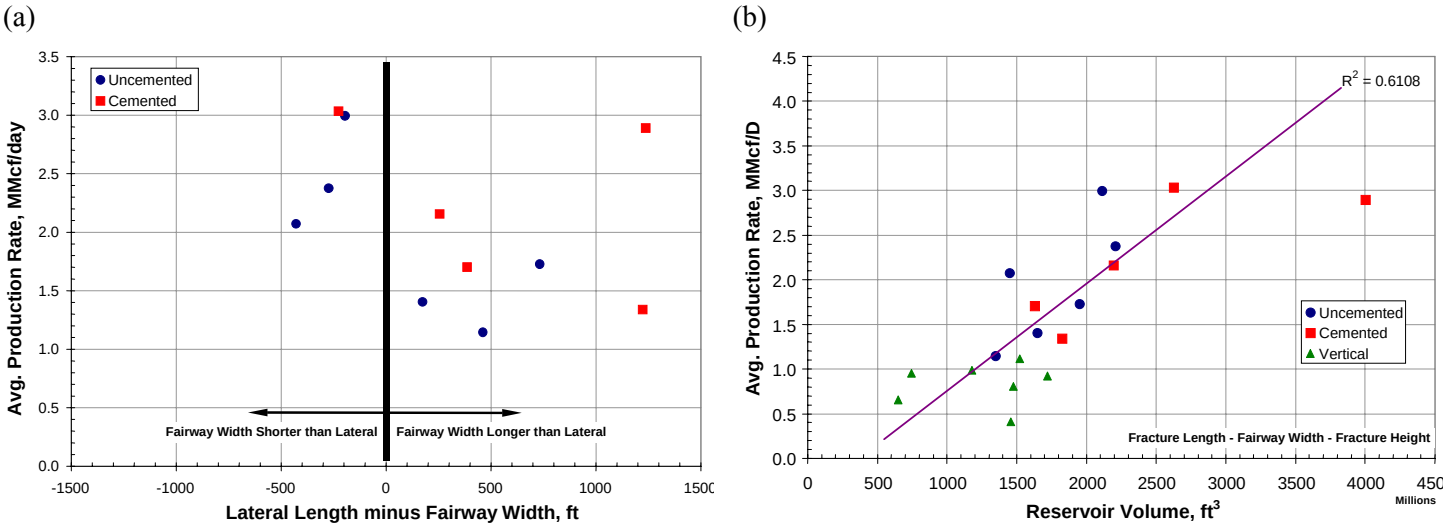

Figure 8.29: Correlation with average production rate for: (a) difference between lateral length and network width, and (b) reservoir volume [*Fisher et al.,* 2004].

If the entire lateral were completely stimulated end-to-end, then the cumulative width of the fracture network is equal the width of the lateral (0 on the ordinate axis in Figure 8.29a). If the entire lateral is not stimulated, then the cumulative width of the fracture network is less than the length of the lateral. Conversely, if the network of fractures extended beyond the heel or toe (i.e., some fractures grew beyond the end of the horizontal lateral section), then the cumulative width of the network of fractures is greater than the length of the lateral. It appears that ~ 0.5 of the treatments stimulated more than the total length of the lateral, as displayed in Figure 8.29a. However, the goal is not just to stimulate the entire length of the lateral. It is also required to achieve an adequate density of the network of fractures along the entire length of the lateral.

The gross volume of the fractured reservoir is defined as double the product of the average half-length of the fracture network, the cumulative width of the fracture network, and the height of the fracture network. The total volume of the reservoir in contact with the network of fractures is immense, as displayed in Figure 8.29b. A typical volume of the reservoir of 2.2×10^9 ft^3 corresponds to more than 50,500 acre-ft of reservoir potentially in contact with the network of fractures from a single horizontal well.

8.4.3 Water Fracturing

Because of the heterogeneity of the Barnett Shale and the unpredictability of hydraulic fracturing treatments, attempting to correlate the results with the variables of treatments (e.g., fluid volumes and sand quantities) is challenging [*Coulter et al.,* 2004]. Volumes of treatment and concentrations of sand were selected, from early results. These criteria were retained until

a adequate number of wells had been treated, so that the criteria could be evaluated. Early results indicated that the quantity of sand was important for satisfactory production.

A study of the hydraulic fracturing treatments for the years before and including 2003 indicate that greater treatments yielded better results. With this respect, the selection of the volume of hydraulic fracturing fluid or the weight of proppant is most significant.

The cumulative quantity of gas produced during a period of 180 and 360 days versus the quantity of fluid and the weight of proppant used in the hydraulic fracturing treatments is displayed in Figure 8.30 and Figure 8.31. There is a great scatter of data for the number of wells displayed. Based upon the complexity of the hydraulic fracturing treatments in the Barnett Shale, this scatter of data can be expected. However, the general trend of the data does indicate that greater weights of sand used in these treatments yields better production results. The positive influence of greater volumes of fluid is not evident. The positive benefit demonstrated for the quantity of sand was encouraging. Consequently, the quantity of sand used in these treatments was continually increased.

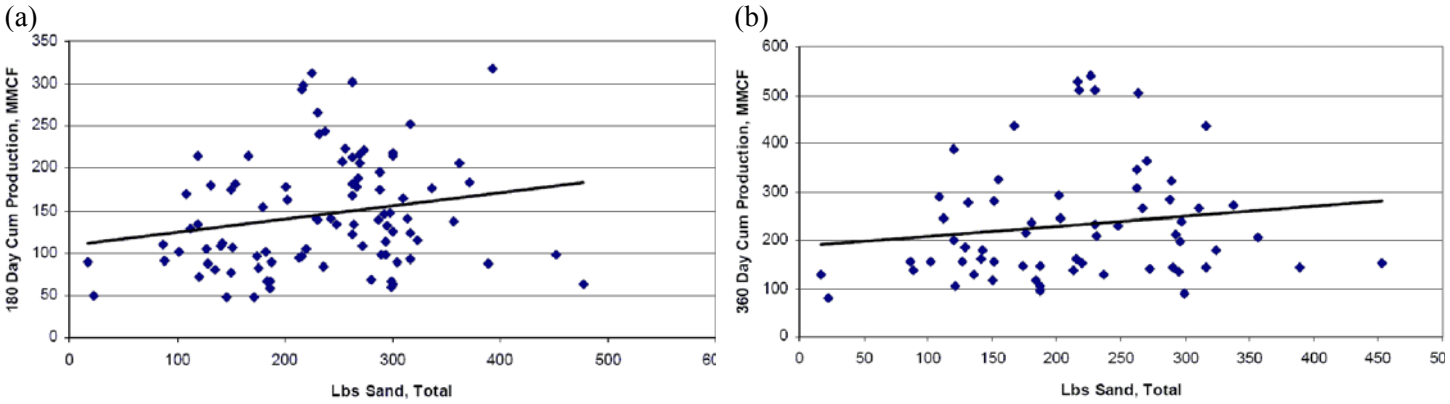

Figure 8.30: Cumulative gas production versus total sand weight for all wells during (a) 180 and (b) 360 days [*Coulter et al.,* 2004].

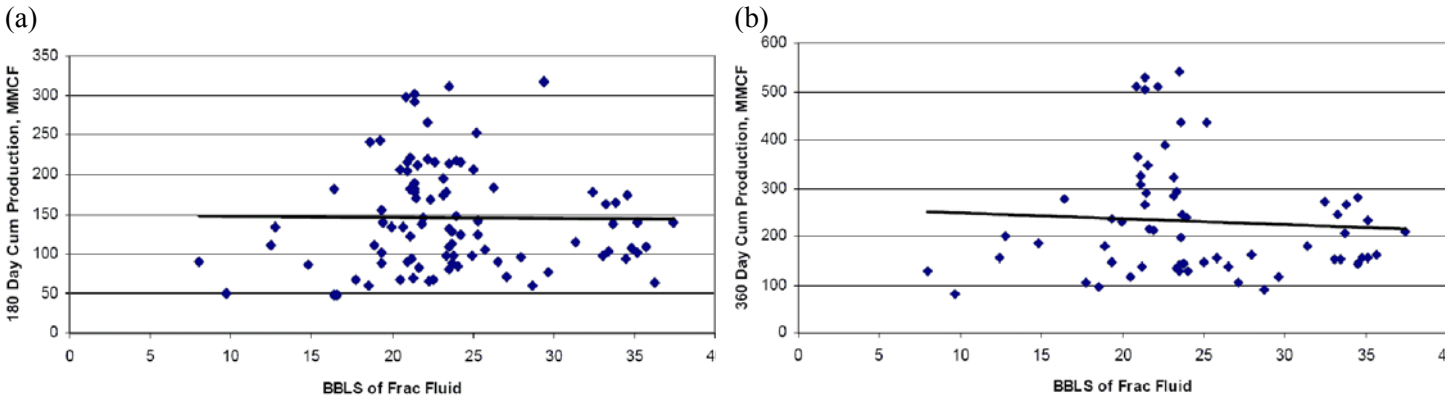

Figure 8.31: Cumulative gas production versus total fluid volume for all wells during (a) 180 and (b) 360 days [*Coulter et al.,* 2004].

The type of proppant utilized in most all cases was 75% of finer 40 to 70 mesh sand followed by 25% of coarser 20 to 40 mesh sand. The reason for by use of the finer 40 to 70 mesh sand was to allow greater quantities of sand to be placed, and for proppant to be carried further by the water with low viscosity.

Additionally, hydraulic fracturing treatments in the Barnett Shale have demonstrated better-sustained production results with greater net pressure of hydraulic fracturing created during the hydraulic fracturing treatment. It is not fully understood why better production results are achieved for greater net pressure during the hydraulic fracturing treatment. However, one possibility is that wider fracture networks are created. With a greater width of the fracture network resulting from greater net pressures, natural fractures must be opening during the hydraulic fracturing treatments. The stress sensitivity of the reservoir is an issue in many reservoirs, particularly those with natural fractures [*Buchsteiner et al.,* 1993]. Because the Barnett Shale is slightly over-pressured, sensitivity to stress is expected. With natural fractures opening during hydraulic fracturing treatments, it would be advantageous to prop these open during production. With the use of a fine proppant (e.g., 40 to 70 mesh sand), there is a much greater probability for the proppant entering these induced fractures than for coarser proppant. Thus, greater quantities of fine proppant may have a benefit in arresting the sensitivity to stress (i.e., arresting rapid declines of production). Following the finer 40 to 70 mesh sand with the coarser 20 to 40 mesh sand provides for near -well conductivity of the fracture. The benefits of high concentrations proppant have been reported in earlier work [*Cooke,* 1973; *Coulter and Wells,* 1972].

With early results demonstrating that the quantity of sand is important, these quantities were increased and each new quantity of sand was evaluated against production results. During this same period, the volumes of the fluid were also varied. By the end of 2003, a database containing adequate hydraulic fracturing treatment and production information for 85 wells was collected [*Coulter et al.,* 2004]. Consequently, a more thorough analysis could be conducted. With the available data, analyses were conducted to evaluate cumulative production during times of 180 and 360 days, as well as data of the decline of production, versus the quantity of sand and the quantity of fluid pumped. The results displayed in Figure 8.30 and Figure 8.31 represent all wells with no discrimination as to, e.g., quality of rock and geologic setting. However, the results do display an overall general trend demonstrating that greater quantities of sand give better results than great quantities of fluid. However, the great scatter of data prompted further analyses.

Porosity-Height Comparisons

The initial quality of the wells was evaluated by use of a calculated porosity-height, or ϕ–h, value [*Coulter et al.,* 2004]. This porosity-height value is calculated from logs of porosity (i.e., neutron density). It is from the number of porosity feet where the calculated porosity exceeds 10%. For the wells studies, the ϕ–h values varied from 4.24 to 15.97. The wells were then grouped by porosity-height. These groups were:

1) ϕ–$h < 8$ with 22 wells,
2) $8 < \phi$–$h < 10$ with 34 wells,
3) $10 < \phi$–h with 29 wells, and
4) $12 < \phi$–h with 13 wells.

The wells in the third group include some of the same wells that were included in the fourth group. All wells in these groups had at least 180 days of production. A lesser number had produced for 360 days. From the porosity-height, wells in the first group are of poorer quality. All the analyses conducted for this group of wells resulted in the same indication that the quantity of sand pumped in the hydraulic fracturing treatment was of more value than the quantity of fluid pumped. Examples of the cumulative production of gas versus the quantity sand and fluid during a time of 360 days are displayed in Figure 8.32. Again, the data is scattered. However, they demonstrate a better general trend for the quantity of sand than for the quantity of fluid.

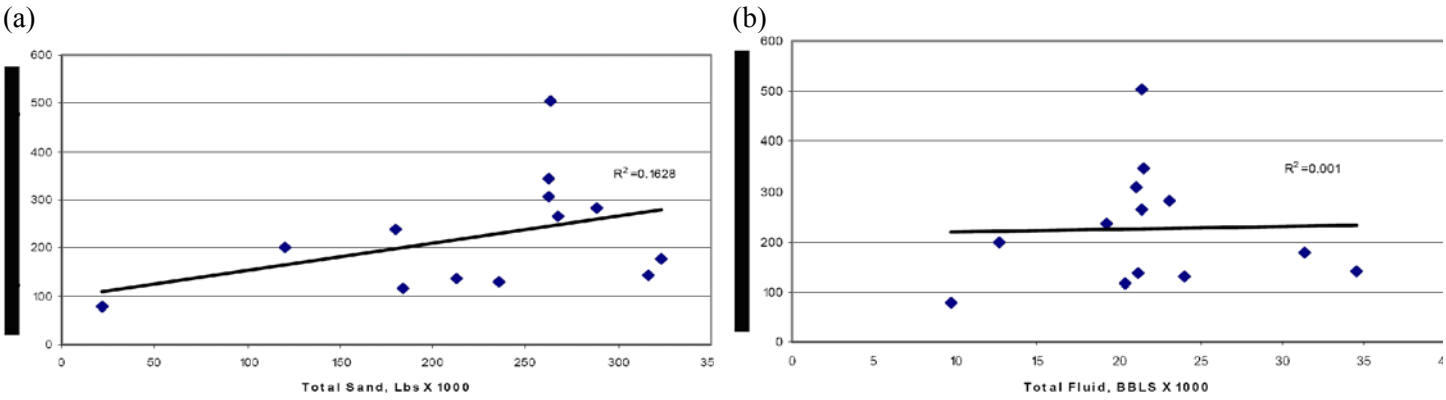

Figure 8.32: Cumulative gas production versus for wells with ϕ–h < 8 during 360 days versus: (a) sand weight, and (b) fluid volume [*Coulter et al.,* 2004].

The wells in the second group yielded similar results with slightly less scattering of the data. The wells in the third group consisted of wells with better than average porosity-height. Again, a general trend of better cumulative production during a time of 180 days versus a greater quantity of sand is evident, as displayed in Figure 8.33a. A general negative relationship between the cumulative production during a time of 180 days to the quantity of fluid pumped is evident, as displayed in Figure 8.33b. A significant negative correlation of the performance of the well versus the quantity of fluid is displayed in this plot, for the wells outlined in red. Most of the treatments with greater volume were for wells with an Upper and Lower Barnett Shale and two hydraulic fracturing stages.

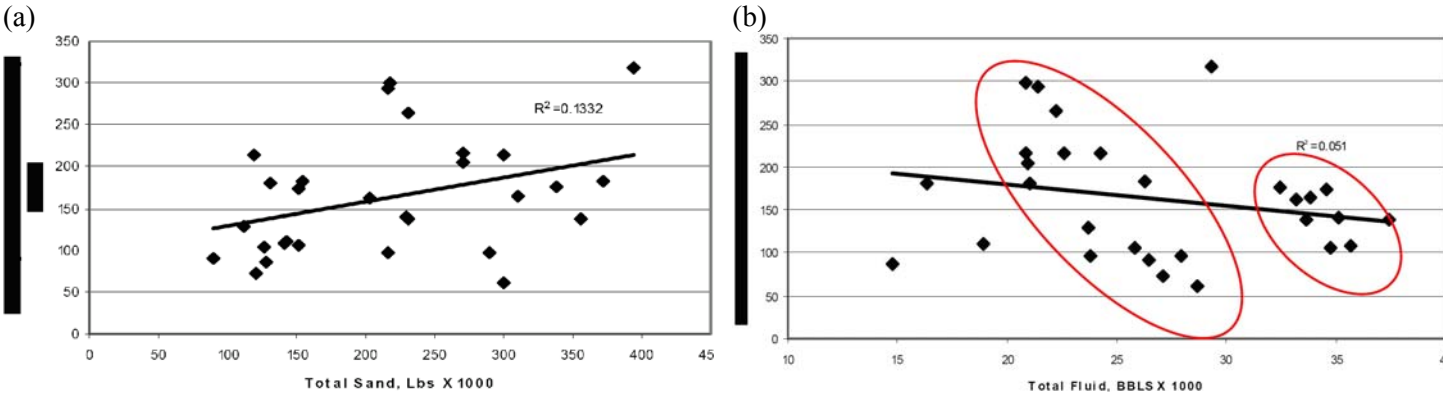

Figure 8.33: Cumulative gas production for wells with 10 < ϕ–h during 180 days: (a) versus sand mass, and (b) fluid volume used in treatment [*Coulter et al.,* 2004].

The 13 wells in the fourth group with much better than average ϕ–h, were analyzed in the same manner as the wells in the prior group, as displayed in Figure 8.34.

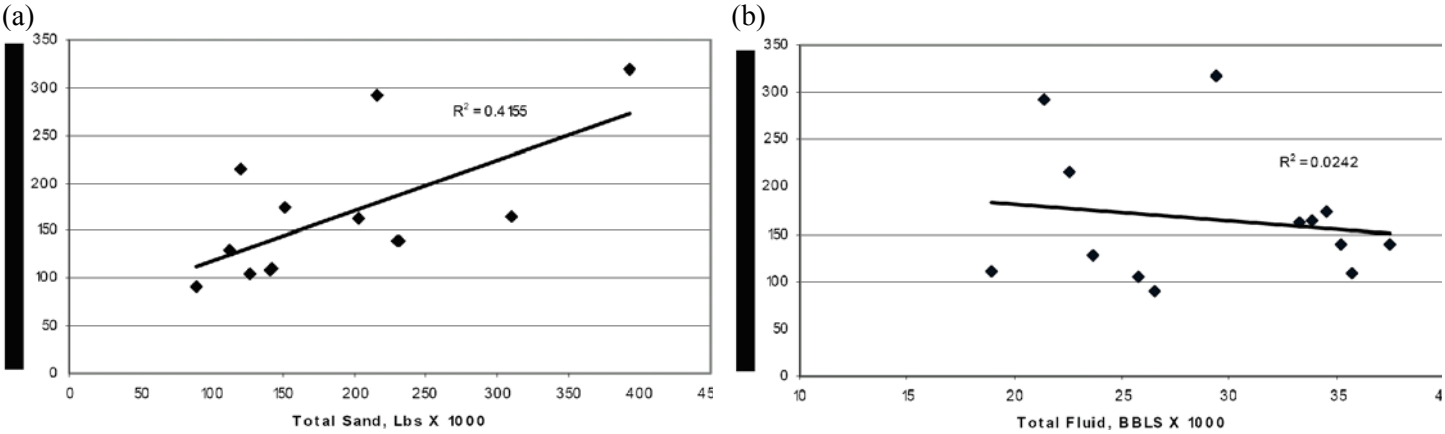

Figure 8.34: Cumulative gas production for wells with 12 < ϕ–h during 180 days versus: (a) sand mass, and (b) fluid volume used in treatment [*Coulter et al.,* 2004].

Additionally, the relative decline of the wells for this group is compared to the quantity of sand fluid pumped, as displayed in Figure 8.35. As these analyses indicate, the quantity of sand is more important than the quantity of fluid.

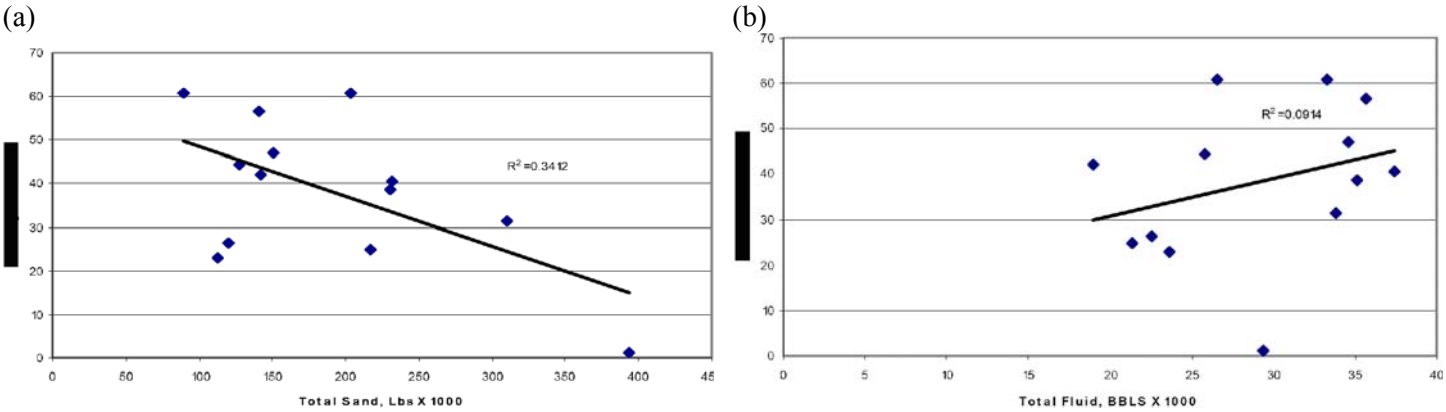

Figure 8.35: Relative production decline for wells with 12 < ϕ–h during 180 days versus: (a) sand mass, and (b) fluid volume used in treatment [*Coulter et al.,* 2004].

Porosity-Height per Unit Length Comparisons

In an attempt to refine further the data set, the data of porosity-height per unit length, or ϕ–h/ft, was compared to the thickness of the interval contributing to the production [*Coulter et al.,* 2004]. The height of the fracture was considered equal to this interval. The 85 wells were grouped by the magnitude of the porosity-height per unit length. Examples of these results for one such group are displayed in Figure 8.36. The cumulative production during a time of 180 days versus the total quantity of sand pumped can be described by a satisfactory best fit, as displayed in Figure 8.36a. The quantity of fluid versus the production for these same wells indicates a very poor correlation, as displayed in Figure 8.36b.

(a) (b)

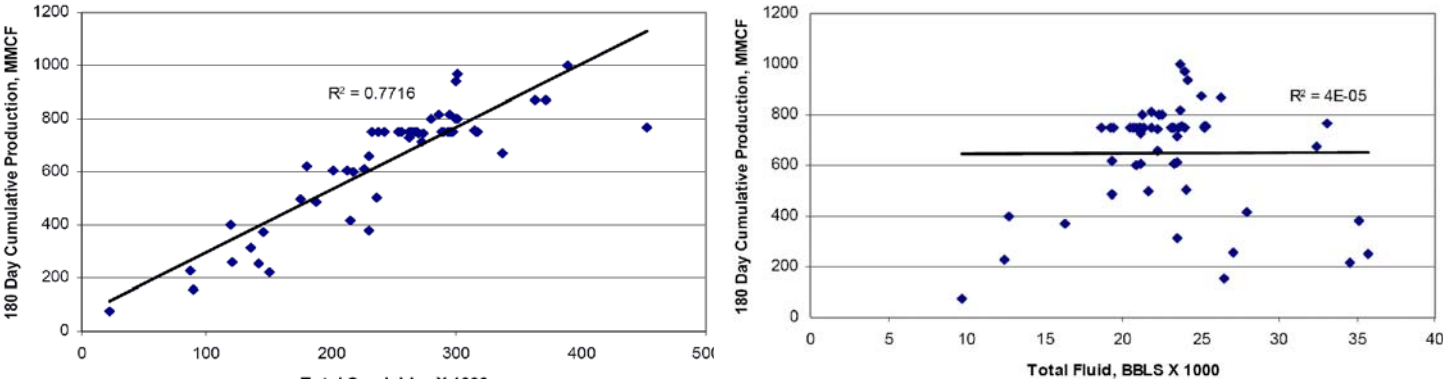

Figure 8.36: Cumulative gas production for wells with $2 < \phi\text{–}h/\text{ft} < 3$ during 180 days versus: (a) total sand mass, and (b) fluid volume used in treatment [*Coulter et al.,* 2004].

Net Pressure Increase Comparison

Other analyses were conducted throughout this study [*Coulter et al.,* 2004]. Figure 8.37 is an example of one analysis approach. That approach was to analyze the net pressure increase during the hydraulic fracturing treatments. The cumulative production trend for 90 days is improved with greater net hydraulic fracturing pressure, as indicated by Figure 8.37. Greater volume treatments and greater rates of injection generally result in greater increases of net pressure. With greater volumes creating greater net pressures, it is logical to assume that the volume of the fluid is important.

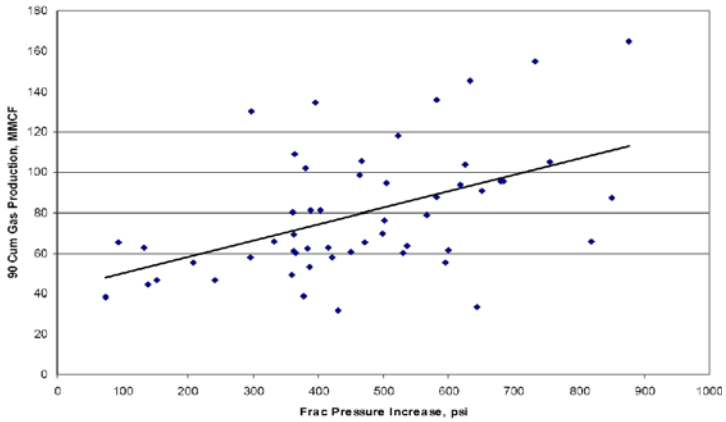

Figure 8.37: Net fracture pressure increase versus cumulative production during 90 days [*Coulter et al.,* 2004].

Summarizing, the reported analyses have indicated that the quantity of sand is more important in longer-term well performance than the quantity of fluid. Based upon that conclusion, the quantity of sand used in these treatments was continually increased over time. With water fractures, the concentrations of proppant pumped are low. In many cases, it is necessary to increase the quantity of fluid to place more sand. However, the reported results recently encouraged the increase of the quantity of sand pumped in these wells by 25% without any increase in the volume of the fluid. There have been no problems in placing the additional proppant.

8.5 Two-Well Mapping Approach

While most microseismic mapping is performed with a multi-level array in a single offset well, the large aerial extent of water fractures generated in horizontal wells makes it very difficult to obtain full mapping coverage on long horizontal segments [*Warpinski et al.,* 2005a]. With two monitor wells, however, the mapping coverage can be optimized to view the entire extent of the fracture system that is being created. This coverage is usually obtained with one well near the toe of the horizontal well and another near the heel. However, may also consist of two wells that are normal to the horizontal-well trajectory.

If the timing is accurate, the microseismic can be acquired separately on each of the two arrays. However, it has been found to be more convenient to acquire all data on one system to minimize handling, processing, and potential errors in timing. Events are detected the same way as on a single array and stored in separate event files that are processed for arrivals and polarization information.

Events that are only detected on one well are processed by standard single-well analysis techniques described above. Events detected on both wells, however, can use other analysis techniques that take benefit of the spatial separation.

For a constant velocity medium (which does not apply to the Barnett Shale), the data can be analyzed by use of a linearization approach [*McEvilly and Majer,* 1982]. If one or both of the monitoring wells are deviated, then their approach is particularly useful. If both wells are vertical, then a more direct analysis that does not reduce the number of equations can be formulated by a joint regression of the separate P and S distance equations from each well. Once the unknown distance from the first well and distance from the second well are obtained, simple geometric relations allow the determination of the two possible locations (there are always two possible locations) and the polarization information is used to decide which one is the appropriate location.

Most often, however, velocity structure must be taken into account. A 3D approach is used [*Warpinski et al.,* 2005a; *Rutledge and Phillips,* 2003; *Hole,* 1995; *Vidale,* 1990]. For one or more deviated wells, there is only one solution point. For two vertical wells, there are again two possible solution points and the polarization information is used to decide the correct one. Thus, even for two-well data it is necessary to have the receivers oriented and to obtain adequate-quality polarization data to find the correct solution point.

While it would seem intuitive that two-well monitoring is more accurate than single well monitoring, this is only true if the receiver locations at depth are accurately known and if an adequate velocity structure can be developed. If there are no deviation surveys of the monitor wells (providing an accurate distance between the two wells), then there exists the potential for considerable error in the event locations. Similarly, an inadequate velocity structure can cause considerable problems in locating the events. It is always good practice to locate the orientation perforations or string-shots to assure at least a reasonable accuracy for events near the calibration shots.

This section describes the analysis of the stimulated reservoir volume (SRV) (section 8.5.1 below), and tests performed in the Barnett Shale (section 8.5.2 on page 138).

8.5.1 Stimulated Reservoir Volume (SRV) Analysis

The microseismic data have a wealth of information that defines many characteristics of the stimulated region. However, the results are most useful if they can be applied in a quantitative sense [*Warpinski et al.,* 2005a]. An empirical approach has been developed to relate the size of the stimulated region with gas production based upon data from the core Barnett area. This approach is called the stimulated reservoir volume (SRV) analysis.

The SRV uses the spatial dimensions of the microseismic activity to generate a stimulated reservoir volume. This reservoir volume is then plotted against production from that well, averaged over the first six months, and compared with other wells

that have been mapped. The resultant comparison, which has an adequate correlation from data obtained to date, is displayed in Figure 8.38.

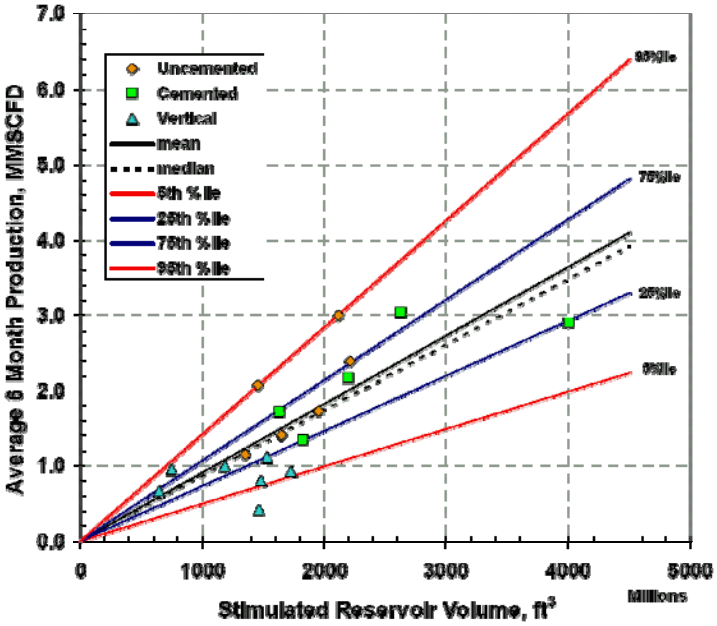

Figure 8.38: Stimulated Reservoir Volume (SRV) [*Warpinski et al.,* 2005a].

Given this correlation, the objectives of a well design and stimulation should be to optimize the SRV and then to push stimulation design to increase the gas flow rate over the average from previous tests. This analysis is used on the Barnett examples given here.

8.5.2 Barnett Shale Tests

Devon has conducted several two-well monitoring tests in the Barnett Shale that provide valuable information on stimulation results. However, they also provide valuable information on various monitoring aspects [*Warpinski et al.,* 2005a]. The following two cases present examples of the results and comparisons between two- and single-well monitoring.

Case 1: Water Fracture Re-fracturing Treatment after Gel Stimulation

One of the more interesting dual-array monitoring tests consisted of a series of stimulations of a horizontal well over a several month period [*Warpinski et al.,* 2005a]. The original stimulation consisted of a propped, gel treatment in a longitudinally oriented well to assess if improvements could be made in horizontal well productivity by changing the stimulation approach. After several months of poor productivity, the well was re-fractured by use of a conventional water fracture. Operational problems resulted in an initial, short, terminated injection, followed the next day by the intended water fracture. These various stimulations were monitored by use of dual arrays and provided some useful information on fracture behavior, stimulation effectiveness, and microseismic accuracy.

Gel Stimulation

Results and the geometric setup for the propped, gel stimulation that was conducted first are displayed in Figure 8.39. The well was drilled along a northeast-southwest azimuth to generate a longitudinal fracture, with the surface location to the southwest [*Warpinski et al.,* 2005a]. The treatment consisted of a crosslinked gel stimulation pumped at 70 bbl/min for ~ 3 hr, with sand concentrations ramped up to ~ 3.0 lbm/gal. Total volumes were 11,600 bbl of 25-lbm crosslinked gel and 700,000 lbm of sand. The initial fracture pressure gradient was 0.61 psi/ft, rising to ~ 0.71 psi/ft at the end of the

treatment. The monitoring wells were situated to the southeast and northwest so that full coverage of the toe and heel regions around the well could be obtained. Hundreds of events were analyzed for these plots, with a majority of the events being detected at least in part on both arrays.

In general, the microseismic data demonstrate that most of the well was stimulated, although activity around the toe of the well (northeast area) is less than other parts of the well. The large mass of events near the heel-to-center region of the well is somewhat because of bias (both wells can detect events from this area making small events easily analyzable). However, also appears to reflect a higher level of activity around the three perforated zones closest to the heel. With the exception of a group of events offset to the northwest by ~ 500 to 700 ft, most of the activity suggests longitudinal fracturing with only modest activation of natural fractures, resulting in a narrow stimulated network (at a distance of less than 500 ft from the well in many sections of the lateral). Height growth appeared to be minimal, with few events observed above or below the Lower Barnett.

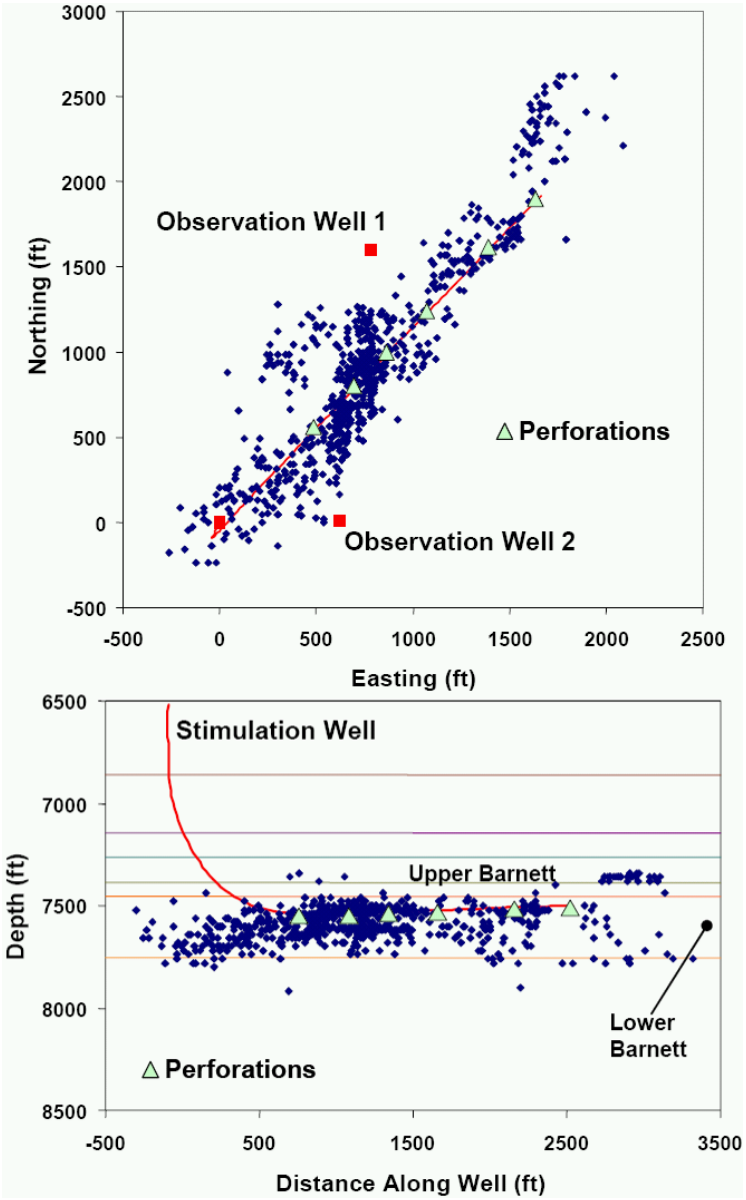

Figure 8.39: Results from dual-monitoring-array solutions of the gel and proppant stimulation [*Warpinski et al.,* 2005a].

These results can be compared with separate, single-well, event locations for those events that have sufficient arrivals on an array to be accurately positioned (by ignoring the data from the other well). Plan-view maps for those events detected from the northwest well (top) and those events detected from the southeast well (bottom) are displayed in Figure 8.40. Some patterns emerge immediately. First, it is clear that the single-well locations produce similar maps to the two-well locations, with the exception of events that are too distant to be observed on both arrays. Secondly, the events that are close to the observation wells are positioned relatively close to where they are situated based upon two-well locations. However, as the events are farther removed, the positions begin to diverge somewhat. Third, the far distant events demonstrate a wider spread because far events have lower signal-to-noise ratios and consequently have poorer resolution of the particle motion for determining the azimuth to the event. In this particular case, the mapping could have been performed fairly well by using only the NW well. However, would have given biased results by use of only the southeast well. As always, optimizing the location of the observation well is important for fracture mapping.

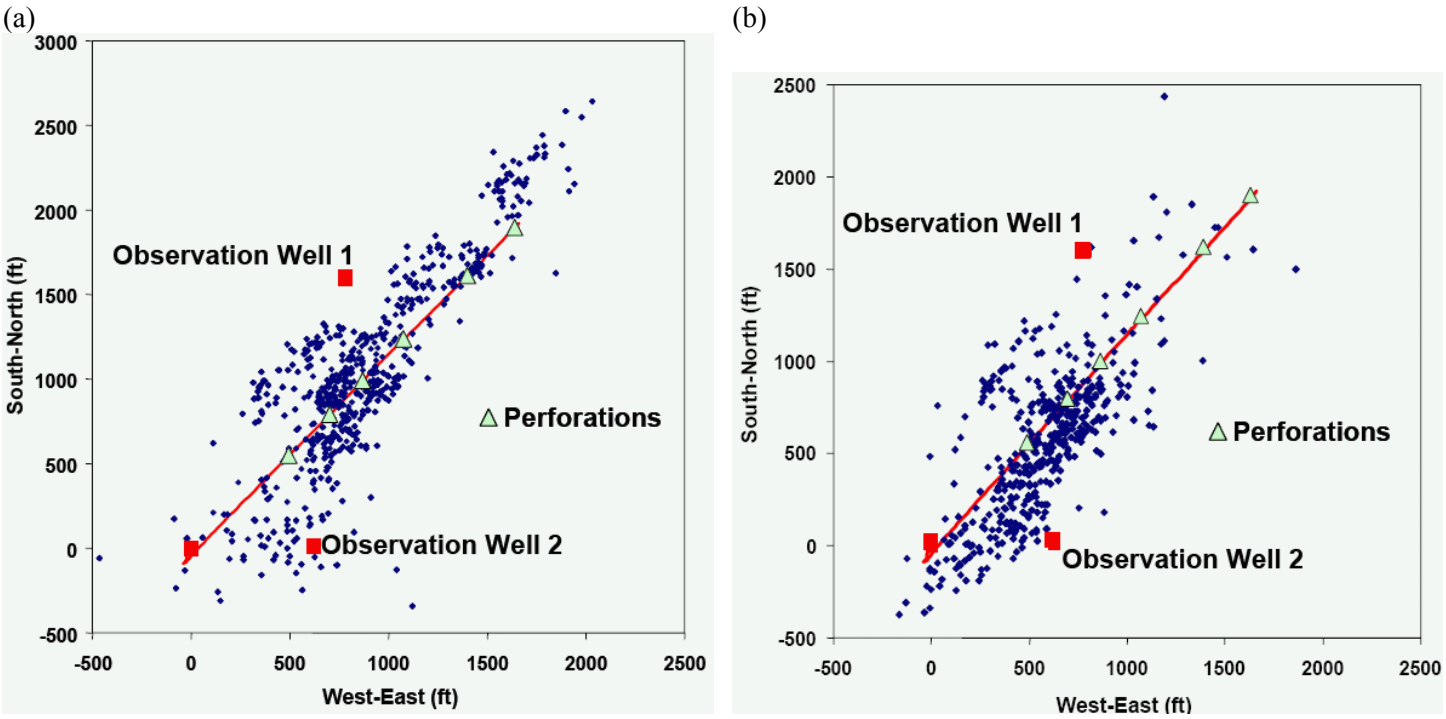

Figure 8.40: Single-well event locations for gel stimulation. Data from: (a) observation well 1, and (b) observation well 2 [*Warpinski et al.,* 2005a].

Water Fracture Re-fracturing Treatment

As mentioned previously, post gel-fracture production was less than expected and a decision was made several months later to re-fracture the well by use of more typical water fracture procedures [*Warpinski et al.,* 2005a]. The planned water fracture was terminated after less than two hours of injection when it was found that the desired injection rate could not be met with the equipment on site. However, this failed re-fracture treatment provided some information on the initial behavior of a water fracture in this previously gel-treated interval.

The plan-view and side-view maps for this treatment are displayed in Figure 8.41a. In fact, this short injection looks similar to the initial part of the gelled-treatment. Most of the activity is near the well, in the same location as most of the microseismic activity in the gelled fracture.

Significantly more interesting is the full re-fracturing, which was conducted the following day. For most of the treatment, this injection was pumped at 125 to 130 bbl/min. However, the injection was tapered off to near 90 bbl/min at the end. This is the result of pressure limitations of the treatment conductor. The total period of the injection was 6.5 hr and the volumes pumped were 60,000 bbl of slickwater and 385,000 lbm of sand. The initial fracture pressure gradient was 0.7 psi/ft, rising to 0.77 psi/ft at the end of the injection. The maps from this treatment are displayed in Figure 8.41b. In this injection, the observed microseisms outline a much greater aerial extent of the process than was achieved with the gel stimulation. The stimulated networks have a width of ~ 1,500 ft and a length of 3,000 ft, with somewhat of a limited zone in the NE. It also appears the treatment broke into the previous hydraulic fractures from each of the monitor wells.

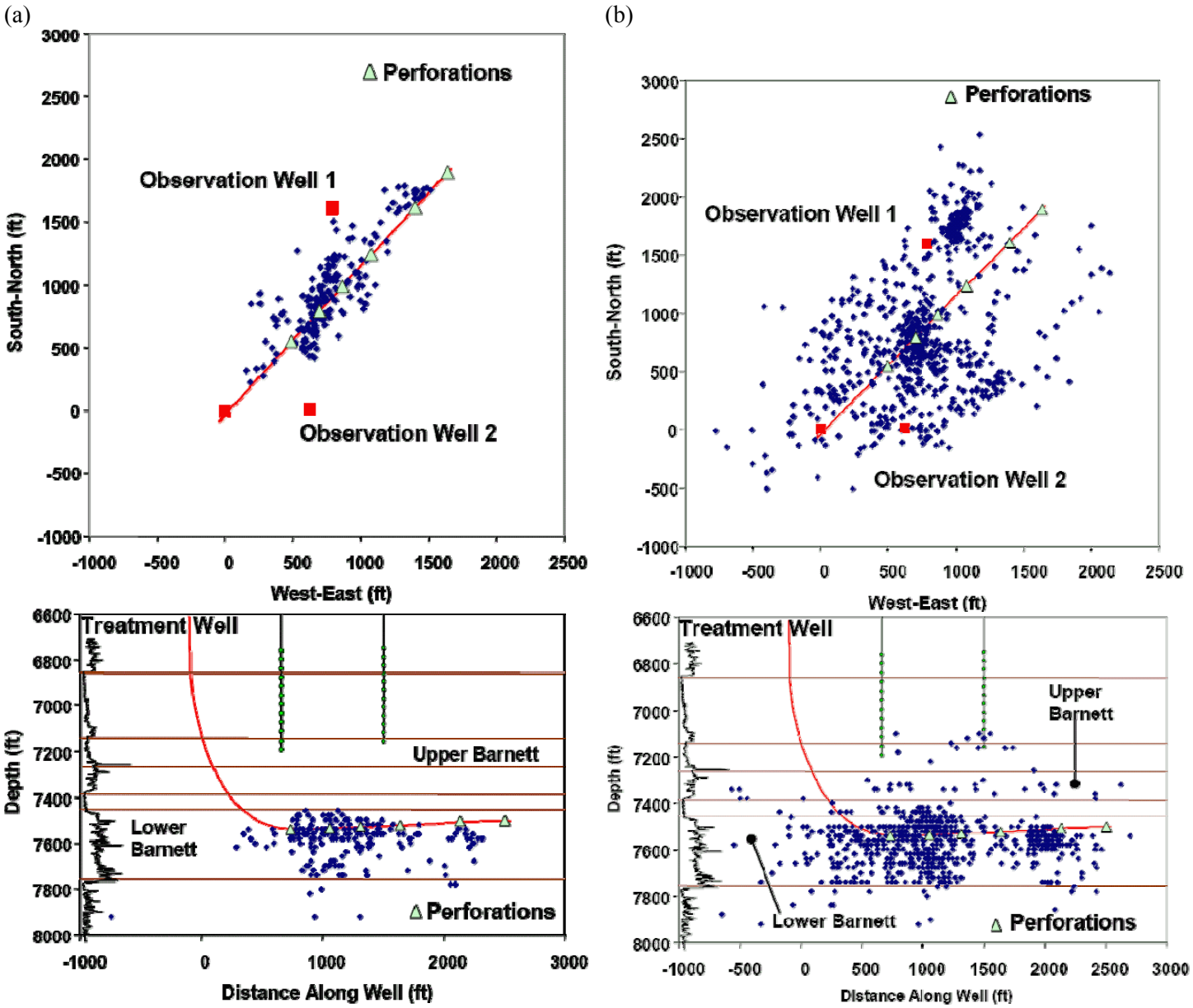

Figure 8.41: Microseismic maps for re-fracturing: (a) terminated, and (b) completed [*Warpinski et al.,* 2005a].

Fracture height growth was considerable, with activity in the upper Barnett Shale and even into the Barnett limestone above the upper Barnett. Some downward growth is also displayed, into the Viola below the lower Barnett.

An edge view of the microseismic events (looking down the length of the well) is displayed in Figure 8.42a. This perspective displays the width of the network relative to height coverage. While there are clearly favored zones, the coverage is over most of the interval throughout the stimulated volume.

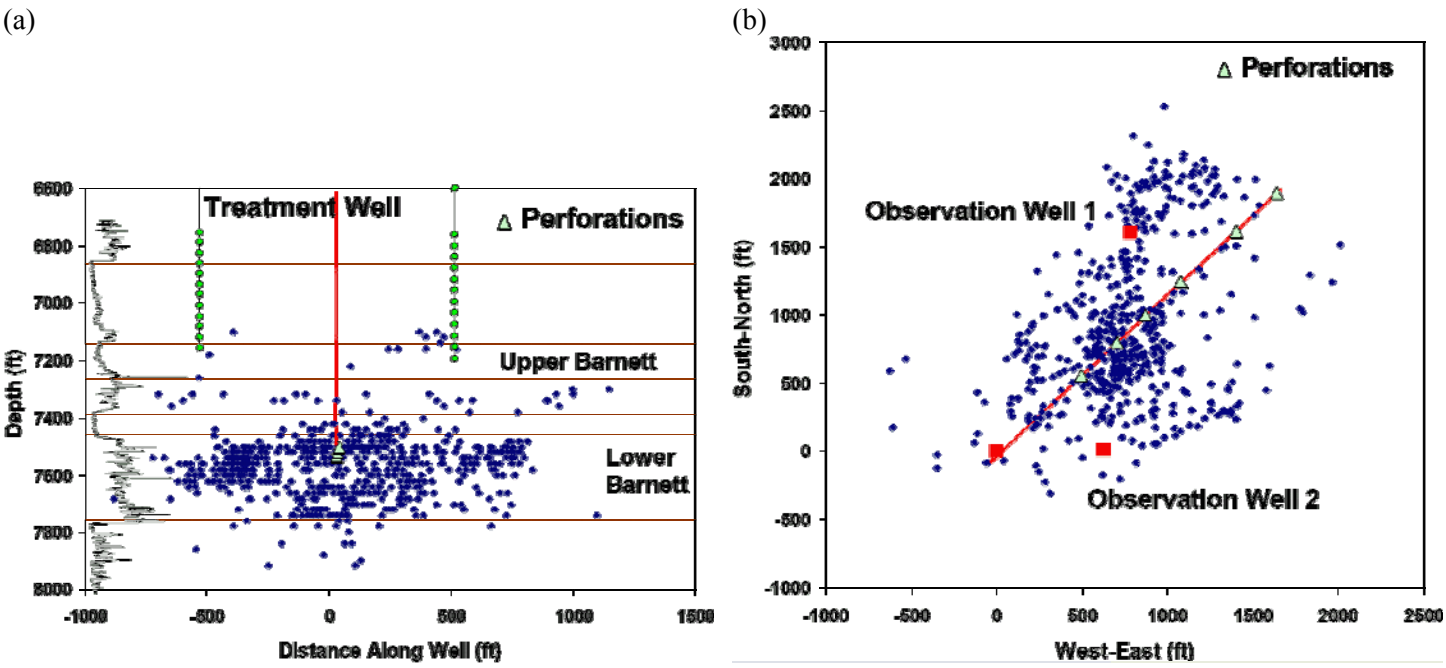

Figure 8.42: Event locations for water fracture re-fracturing treatment. (a) Edge view of two wells, and (b) plan view of single well [*Warpinski et al.,* 2005a].

A plan view plot of just single-well locations, as determined from the northwest well (the most favorable observation point), is displayed in Figure 8.42b. Again, the map is similar to the two-well location plot. However, there are some differences and omissions at far distances.

The velocity structure used in these analyses is displayed in Figure 8.43 as a gray-scale image. Generally, there are very slow shaley layers (e.g., the upper and lower Barnett) and very fast carbonates. This extreme velocity structure results in some very complicated waveforms at the receiver.

Clearly, the re-fracturing treatment successfully stimulated a much greater volume of rock than the initial gel treatment, and demonstrated patterns of development that suggested the opening of both northeast and northwest trending fractures. It appears that the water fracture system is significantly more effective at activating the natural fissures to the NW/SE. The water fracture created an SRV of ~ $1{,}450\times10^6$ ft^3 compared with only 430×10^6 ft^3 in the gel fracture.

Other Diagnostic Results

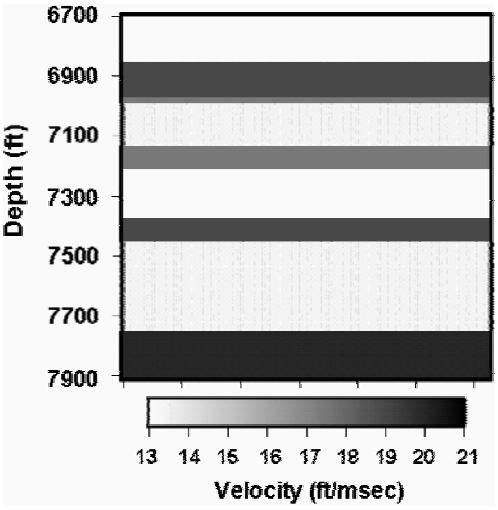

Figure 8.43: Grayscale velocity model for gel stimulation and re-fracturing test [*Warpinski et al.,* 2005a].

While the microseismic results are the primary diagnostic information, other diagnostic information is routinely obtained, including behavior of offset wells and chemical markers. In these tests, there was some interference observed in the two observation wells because of the gel fracture. However, significantly more interference because of the water fracture (as would be expected from the microseismic locations). Chemical markers also demonstrated direct connectivity between the water fracture and the two monitor wells. A third, nearby well also experienced interference, and it produced chemical markers after the water fracture.

Production Results

The production data for this well is displayed in Figure 8.44. Initial production after the gel stimulation dropped rapidly from 975×10^6 ft^3/d, reaching ~ 350×10^6 ft^3/d after approximately six months [*Warpinski et al.,* 2005a]. Some interference between the test well and the observation wells can be observed. As previously mentioned, the SRV for the gel stimulation was calculated to be ~ 430×10^6 ft^3, which is much lower than typical water fractures, and suggests a six-month average production of around 500×10^6 ft^3/d. This is fairly close to the average measured gas rate.

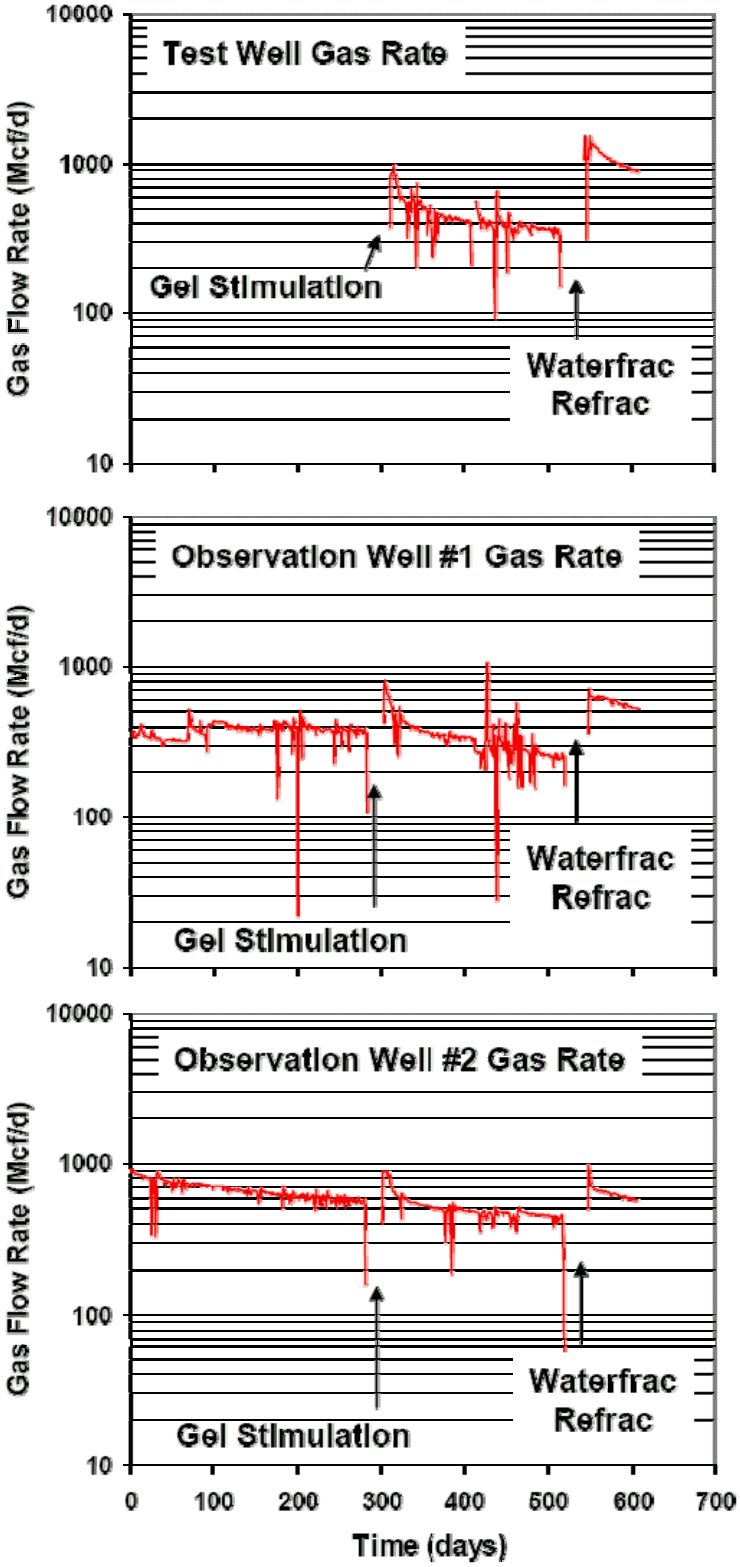

Figure 8.44: Production data associated with the first case [*Warpinski et al.,* 2005a].

Production after the water fracture re-stimulation, however, is indicative of the successful stimulation of a much greater volume of new reservoir. Initial rates exceeded $1{,}500\times10^6$ ft^3/d, whereas the highest rate observed after the gel stimulation was 975×10^6 ft^3/d. Even after the six months of depletion following the gel stimulation, the water fracture was still significantly outperforming the gel stimulation. The rates in the offset wells were increased by 40% and 100%. However, this increase is similar to that achieved after the gel stimulation).

With an SRV for the water fracture of more than three times greater than that of the gel stimulation it is expected that the initial gas production be much improved. The average rate for the initial six month of production after the re-fracturing is nearly $1{,}000\times10^6$ ft^3/d. Because a longitudinal, stimulated well behaves conceptually similar to a vertical well, this production is right in line with the predictions displayed in (Figure 8.38 on page 138).

Case 2: Single-Stage Longitudinal Stimulation of a Horizontal Well

A second example of two-well-monitoring was another longitudinal stimulation of a horizontal well. However, in this case a water fracture was used for the initial treatment [*Warpinski et al.,* 2005a]. In this case, ~ 19,000 bbl of slickwater and 400,000 lbm of sand were injected at an average rate of 91 bbl/min and average wellhead treating pressure of ~ 4,300 psi. The injection started at 120 bbl/min. However, the injection rate was dropped to 80 bbl/min for more than half of the stimulation, because of equipment problems. The total treatment time was a slightly more than 3.5 hr.

The plan-view and side view maps of the stimulation results are displayed in Figure 8.45a. This injection resulted primarily in a large concentration of fracturing activity around the heel of the well (to the SW), with only limited evidence of stimulation in the northeast half of the well. The plan-view data also suggest that the fracture broke into the previous hydraulic fracture plane from the second observation well. Some limited height growth is observed. However, this is not sufficient to suggest any major growth out of the lower Barnett.

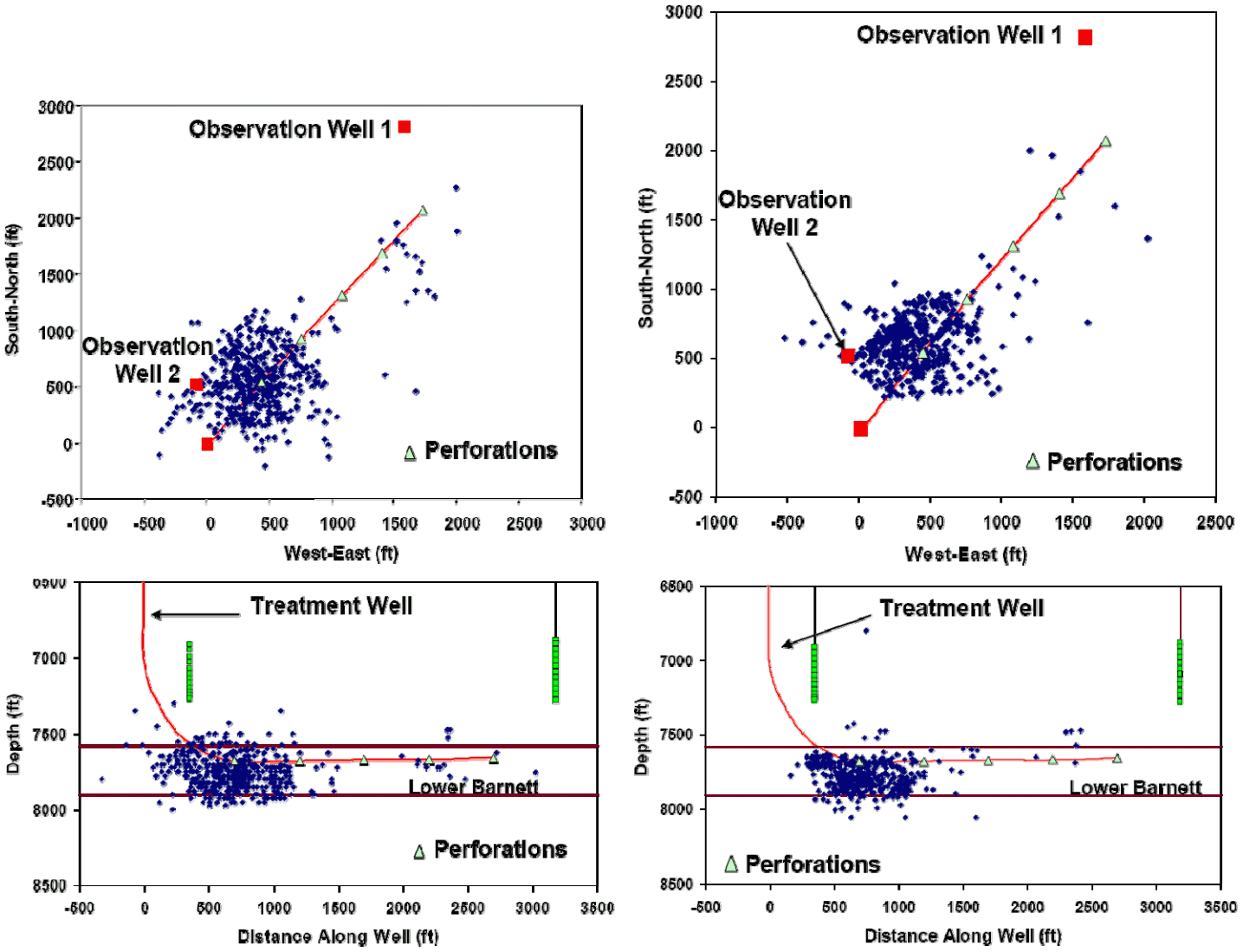

Figure 8.45: Single stage maps for case 2 water fracturing in longitudinal well: (a) two-well, and (b) single well [*Warpinski et al.,* 2005a].

The stimulated reservoir volume for this test is ~ 410×10^6 ft, a relatively small number. Clearly, the single-stage treatment at a relatively low rate failed to stimulate the entire well.

An edge-view plot of the microseismic activity, that is, looking parallel to the well azimuth from the southwest, is displayed in Figure 8.46. There is adequate coverage of the entire lower Barnett in the heel region, and some indication of high events lining up along discrete planes (further suggesting some upward growth).

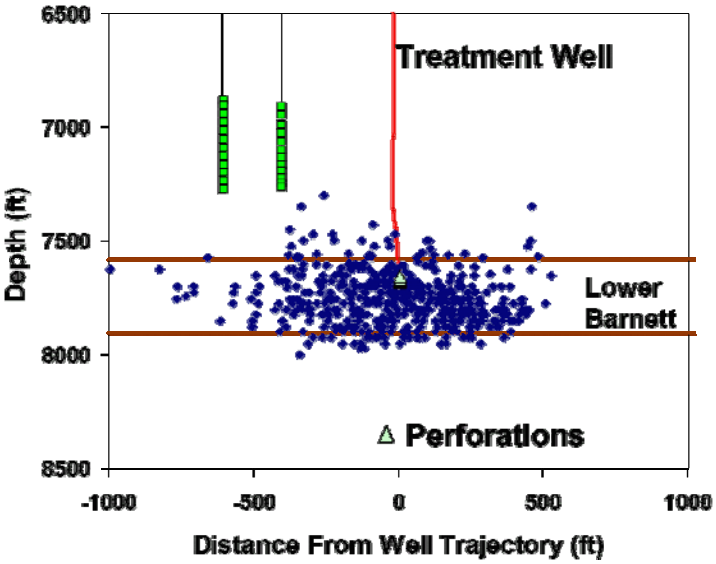

Figure 8.46: Edge view of single stage water fracture for case 2 [*Warpinski et al.,* 2005a].

The single-well solution is a little surprising and is displayed in Figure 8.45b. This solution uses events detected at observation well 2. While the overall picture is not much different, the single-well maps demonstrate a narrower zone of microseismic activity (in map view) than the two-well maps given in Figure 8.45a. Usually, single well solutions have more scatter because they rely on the particle motion of the incoming waves to provide the direction to the source. Weak events, with low signal-to-noise ratios, tend to have greater scatter because the particle motion can be significantly affected (more so than the arrival time). In this case, however, the single well events are almost all very close to the monitor well and the directionality should be relatively accurate. The two-well events, however, need to use arrivals from the distant observation well 1. Difficulties in detecting head waves and complex wave interactions (e.g., overlapping of reflections and direct arrivals), make some of those arrivals more susceptible to error. Hence, in cases such as this, where events are very close to the monitor well, the single well events have the potential to be more accurate. On the other hand, the depth obtained from the two-well data is likely to be better constrained and more accurate than the depths obtained from the single-well data with the receivers positioned above the reservoir.

Production Results

The production results from this water fracture are displayed in Figure 8.47. The average six month of production is a little more than 650×10^6 ft^3/d [*Warpinski et al.,* 2005a]. The SRV analysis suggests that it should be in the 250×10^6 to 600×10^6 ft^3/d range, so the results are slightly better than expected. However, these results are certainly poorer than usually achieved with the stimulation of a water fracture in a horizontal well.

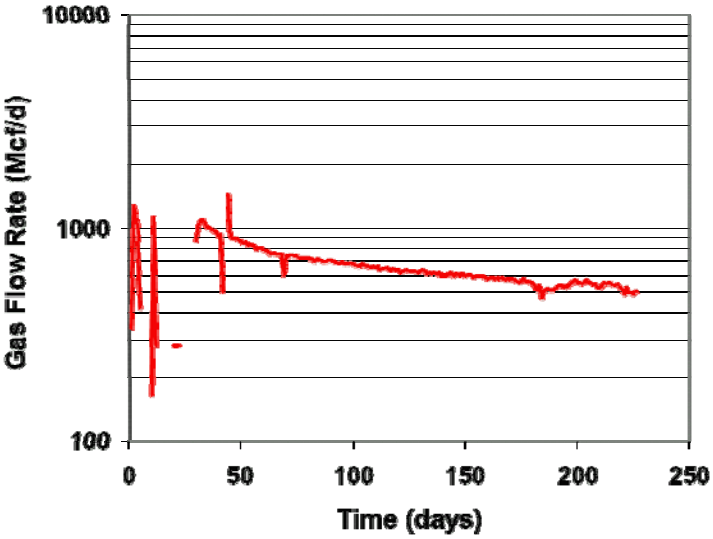

Figure 8.47: Production results after case 2 water fracturing [*Warpinski et al.,* 2005a].

8.5.3 Discussion

The optimal mapping of microseisms with respect to accuracy, coverage, and cost depends greatly on available monitoring locations relative to the treatment well, receiver depths, accuracy of the monitor-well locations, the ability to determine correctly the velocity structure, the locations of the microseisms, and noise issues [*Warpinski et al.,* 2005a].

Aerial coverage is probably the most significant factor when deciding on a potential 2-well mapping test. Monitor wells near the toe and heel of a horizontal well allow for a greatly expanded view of the induced microseisms. However, if the single well is suitably oriented, then they seldom produce significant differences in the maps compared to a single well. Yet, if a single well is not in an adequate viewing position, then the single-well results can give a biased picture of the stimulation.

Obtaining an accurate velocity structure is a key element in fracture mapping, both for single-well and for dual-array tests. One adequate test of the velocity structure is the ability to locate the perforations. This should always be performed as a quality control (QC) measure.

In normal situations in the Barnett Shale, noise is not an issue unless the fracture breaks into a monitor well location or if there is nearby drilling or seismic survey activity. If the drilling depth at the time of monitoring is near the Barnett Shale, drilling activity is particular problematic, because the low velocity Barnett Shales act as wave-guides. Recently, Simultaneous Operations (SIMOPS) types of treatments, where both the treatment and observation wells are drilled from the same pad, have been used. In situations with SIMOPS, it is often necessary to take additional measures to reduce background noise.

Production data from the first case supports the microseismic results. The gel treatment stimulated a relatively small volume and gas flow rates were well below average rates for this area. The water fracture stimulated a much large volume and the resultant gas flow rates were superior. Interference with the observation wells also matched the microseismic data [*Warpinski et al.,* 2005a].

The production results from the first case are consistent with the SRV analysis. The low SRV from the gel fracture yielded low gas rates and the much higher SRV from the water fracture improved rates considerably, even though the reservoir had been produced for six months. Similarly, the production from the second case is only slightly above the range predicted by the SRV analysis.

Summarizing, it can be concluded that:

1) Dual-array mapping has been found to be an effective tool for monitoring stimulations in long horizontal wells. Two optimally placed observation wells allow for extended aerial coverage and better resolution of the internal structure of the microseismic activity, as well as improved accuracy of the depth of the microseisms.
2) Mapping and production data for both a gel stimulation and a water fracture conducted in the same well demonstrate that the water fracture provided superior results in terms of volume stimulated and gas production.
3) The stimulated reservoir volume (SRV) analysis developed from the microseismic data can be used to quantify expected production, and thus aid in the early optimization of the stimulation procedures and materials.

9 APPENDIX B: PHYSICS OF FRACTURE GROWTH

This section describes the physics of the growth of hydraulic fractures in terms of existing hydraulic fracturing simulators (section 9.1 below), hydraulic fracturing (section 9.2 below), simulations of the geometry of hydraulic fractures (section 9.3 on page 154), strongly coupled reservoir simulators that incorporate hydraulic fractures (section 9.4 on page 159), fractured reservoir simulators (section 9.5 on page 163), an overview table of the various simulators (section 9.6 on page 167), features of current simulators (section 9.7 on page 170), a definition of EGS systems (section 9.8 on page 170), the representation of hydraulic fractures (section 9.9 on page 171), capabilities of current simulators (section 9.10 on page 171), components of simulators that need to be developed (section 9.11 on page 172), the approach to develop these components (section 9.12 on page 172), and the direct incorporation of measurements (section 9.13 on page 185).

9.1 Hydraulic Fracturing Simulators

Fracture growth in a complex fracture network can be approximated by oilfield fracture models. Such models can be used for fracture treatment design, analysis, and post-fracturing evaluation. They have been used to develop calibrated models of fracture growth for environments similar to the Barnett Shale. However, a methodology must be developed to account for some of the fracture growth physics in EGS applications, and the longer time scale associated with EGS applications in comparison to the fracture treatments (i.e., modeling longer-term impact on fracture growth).

9.2 Hydraulic Fracturing

Hydraulic fracturing refers to a stimulation treatment to create a high permeability communication between a well and a low permeability reservoir [*Economides and Nolte,* 2004]. For this purpose, fluids are injected into (parts of) the reservoir at high pressure. This creates a fracture to initiate at the well, and to propagate into the reservoir. After the treatment has been completed, proppants that are added to (some of) the fluids keep the fracture open.

This section describes hydraulic fracturing in terms of the principal variables (section 9.2.1 below), the critical processes for geothermal reservoirs (section 9.2.2 below), and predictions from field data (section 9.2.3 on page 152).

9.2.1 Principal Variables

Hydraulic fracturing is controlled by six principal variables [*Smith et al.,* 2001]:
controllable:
1) fluid viscosity; and
2) pump rate; and

unknown:
3) fracture geometry (generally, the in situ stress profile relative to the net pressure is the major controlling factor for the maximum fracture height or containment);
4) leakoff (typically characterized by a coefficient for linear leakoff out of the fracture; this includes wall building characteristics of the fluid systems, effects of natural fractures, and the behavior of leakoff additives);
5) tip effects (the apparent fracture toughness controls the net pressure at the fracture perimeter that is required to propagate the fracture); and
6) the Young's modulus (i.e., the stiffness of the rock).

These variables are related by the governing equations (i.e., conservation of mass, momentum and energy) and constitutive relationships (i.e., between the crack opening over the length of the fracture and the net pressure, and for the fracture propagation criteria) [*Mack and Warpinski,* 2000; *Meyer,* 1989].

9.2.2 Critical Processes for Geothermal Reservoirs

Building upon the six principal variables for hydraulic fracturing of oilfield reservoirs, the processes that are critical for the hydraulic stimulation of geothermal reservoirs, in contrast to most conventional hydraulic stimulations in oilfield reservoirs,

are leakoff and heat transfer between the fractures and the surrounding reservoir, and near-well friction losses. In addition, the ability to simulate multiple fractures (parallel, perpendicular, or oblique with respect to each other) is important.

Leakoff

The leakoff of fracturing fluid from a hydraulic fracture into the reservoir can be divided into subsequent stages [*Mack and Warpinski,* 2000]:
1) Spurt loss with a high leakoff rate (i.e., displacement and compressibility of reservoir fluid),
2) a decreasing leakoff rate (i.e., invasion of formation by filtrate or fracturing fluid, and build-up of an external filter cake), and
3) dynamic leakoff with a steady-state leakoff rate (i.e., build-up of external filter cake stops, because of the high-velocity of fluid in the fracture that prevents further polymer deposition).

Heat Transfer

As the fracturing fluid penetrates the hydraulic fracture, heat transfer occurs between fracturing fluid and rock [*Mack and Warpinski,* 2000]. This is important as the properties of the fracturing fluids depend on the temperature. It is generally assumed that:
1) The temperature gradient in the direction perpendicular to the fracture wall is much greater than those in other directions, and
2) the heat conduction in the fluid is much less than the heat conduction in the host rock and the heat convection of the fracturing fluid.

Near-well Friction Losses

Near-well friction losses are detrimental to the success of hydraulic fracturing because they [*Mack and Warpinski,* 2000]:
1) Increase the net pressure, and
2) increase the likelihood of unplanned screen-outs caused by the limited fracture width near well.

These friction losses are because of the following reasons:
1) Well communication (i.e., perforations),
2) tortuosity (i.e., fracture turning and twisting),
3) perforation phasing misalignment and induced rock pinching, and
4) multiple fractures.

9.2.3 Predictions from Field Data

Field data from hydraulic fracturing operations exist primarily in the form of pressure response curves [*Carter et al.,* 2000]. It is difficult to define the actual hydraulic fracture geometry from this data alone, however. Therefore, models are used to evaluate and predict the location, direction, and extent of the hydraulic fractures.

The time-dependent fracture geometry depends on the distribution of the pressure, caused by the flow of fluid and proppant within the fracture [*Mack and Warpinski,* 2000]. Because the relationship between the pressure gradient and the flow rate is highly sensitive to the width of the fracture, the geometry and fluid flow are tightly coupled. The complexity of solving a model of hydraulic fracturing lies in the close coupling between the different processes.

In locations where the magnitude and direction of the in situ stress field is known, and the well is aligned with one of the far-field principal stresses, the hydraulic fracture geometry can be predicted and controlled with reasonable accuracy. For wells that are not aligned with such a direction (i.e., deviated wells), the fracture geometry is usually more complex and more difficult to model, especially close to the well where the local stress field is significantly different from the far-field stresses.

To validate the models, only limited data are available on typical treatments. For commercial treatments, the pressure history during treatment is usually the only data available for validation. However, even in these cases, if the bottom-hole pressure must be inferred from the surface pressure, then the quality of the data can be problematic. The bottom-hole pressure is also not sufficient to determine uniquely the fracture geometry in the absence of other information (e.g., derived from tiltmeters and microseismic analysis). A successful simulator should match both treating pressure and fracture geometry.

9.3 Hydraulic Fracture Geometry Simulations

Efficient numerical simulation of fully 3D hydraulic fracturing requires [*Carter et al.,* 2000]:
1) A capability for representing and visualizing the complex well and fracture geometries; this includes modeling of the geometry and topology for fracture propagation, automated meshing and remeshing, visualization of response information, and post-modeling analysis information.
2) a method for solving the non-linear coupling between the equations for the fluid flow in the fracture and the deformation and propagation of the fracture; this consists of stress analysis procedures, and fluid flow simulation capabilities; and
3) a method for coupling the structural response with the fluid flow, including rules for determining hydraulic fracture propagation direction and extent.

Numerical simulations range in spatial dimension from two-dimensional (2D) to three-dimensional (3D), depending on the degree of complexity of the geometries of the wells and the fractures, the capability of the available model, and the required accuracy of the predictions.

For the 2D models, the layers surrounding the fractured zone are not considered [*Mack and Warpinski,* 2000]. In contrast, for the pseudo (planar) 3D and 3D models, data about the properties of the surrounding zones are used to predict the rate of growth into the layers surrounding the target zone. The three principal types of models for hydraulic fracturing that include height growth are thus categorized according to their major assumptions:
1) 2D (section 9.3.1 below),
2) pseudo (planar) 3D where the coupling between the 2D fluid flow field in the fracture and the 3D elastic response of the rock is approximated (section 9.3.2 on page 155),
3) planar 3D where the 2D fluid flow field in the fracture is coupled to the 3D elastic response of the rock (section 9.3.3 on page 156), and
4) fully 3D (section 9.3.4 on page 158).

The 2D, pseudo (planar) 3D, and planar 3D hydraulic fracturing simulators work very well in many cases where the geometry of the fracture is easily defined and constrained to a single plane. However, there are instances where a fully 3D simulator is necessary for more accurate modeling.

For the pseudo (planar) 3D and the fully 3D models, the overall approach is to subdivide the hydraulic fracture into discrete elements, and to compute the solution of the governing and constitutive equations for these elements [*Clifton,* 1989]. These equations consist of:
1) Elasticity equations that relate the pressure on the fracture faces to the fracture opening,
2) fluid-flow equations that relate the flow of the fluid in the fracture to the pressure gradients in the fluid, and
3) a fracture criterion that relates the intensity of the stress state ahead of the fracture front to the critical intensity necessary for tensile fracture of the rock.

The theoretical model itself is only a small part of the hydraulic fracturing software system. It should incorporate realistic and general physics. Other requirements for such software systems are computer hardware and software design constraints. As computing power continues to improve, it becomes possible to execute increasingly sophisticated models during treatment execution either at the well site or remotely. There are other software design issues (e.g., robust execution with a wide variety of parameter values, straightforward importing and exporting, superposition of actual data on model output, and graphical display) that are required for a useful software system for real-time applications.

9.3.1 2D

The 2D models are applicable only to fully confined fractures [*Mack and Warpinski,* 2000]. They convert a 3D solid and fracture mechanics problem into a 2D (i.e., plane strain) problem by assuming:
1) Plane strain in the horizontal direction, the Geertsema-deKlerk (GdK) model is valid if the fracture height is much greater than the length, or if complete slip occurs at the boundaries of the pay-zone; and

2) each vertical cross-section acts independently, the Perkins-Kern-Nolte (PKN) model is valid if the length is much greater than the height.

The 2D models require the specification of the fracture height, or the assumption that a radial fracture develops. That is, they are not able to simulate both vertical and lateral propagation independently [*Carter et al.,* 2000]. This is a significant limitation, because the fracture containment is not always obvious from logs and other data. In addition, the fracture height usually varies from the well (where the pressure is highest) to the tip of the fracture. This limitation can be remedied by the use of pseudo (planar) 3D and planar 3D models.

9.3.2 Pseudo (Planar) 3D

Pseudo (planar) 3D models attempt to capture the significant attributes and behavior of planar 3D and fully 3D models without the computational complexity [*Carter et al.,* 2000; *Mack and Warpinski,* 2000; *Clifton,* 1989]. They have been developed from the 2D models by removing the assumption of constant and uniform fracture height [*Warpinski et al.,* 1994]. That is, the height is a function of position along the fracture as well as time. The major assumption is that the fracture length is much greater than the height. The pseudo (planar) 3D models use equations from simple geometries (e.g., radial, elliptical) to compute the fracture width as a function of position and pressure, and to apply the fracture propagation criterion to the length and height. That is, they cannot handle fractures of arbitrary shape and orientation. 3D models are required for this purpose. The pseudo (planar) 2D models use linear elastic fracture mechanics, the power law for the time-dependent fluid rheology, and the classical leakoff model [*Core Lab,* 2003]. They can be used to model fracture height growth through multiple layers of rock with differing stresses and properties. Consequently, the Young's modulus, stress, toughness, and layer thickness are needed for zones above and below the target zone [*Schlumberger,* 2002; *Schlumberger,* undated]. The two main types of pseudo (planar) 3D models are cell-based, and lumped. They assume either 1D fluid flow along the fracture length [*Warpinski et al.,* 1994], or pseudo 2D (i.e., streamline) fluid flow along the fracture length and height [*Carter et al.,* 2000; *Mack and Warpinski,* 2000], respectively. They allow for proppant settling. The computed fracture geometries are similar for the various simulators. However, they are different from those of GOHFER [*Core Lab,* 2003].

Cell-based

The cell-based, pseudo (planar) 3D models include E-StimPlan by NSI Technologies [*Smith and Klein,* 1995], and Fracturing Computer-aided Design and Evaluation (FracCADE) by Schlumberger [*Schlumberger,* 2002; *Schlumberger,* undated]. In cell-based models, the fracture length is divided into a number of discrete, connected cells [*Mack and Warpinski,* 2000]. This is directly analogous to the planar 3D models, except that only one direction is discretized instead of two. They use the local cell geometry to relate the fracture opening with the fluid pressure. The fracture height and width are dependent only on the pressure in the cell with respect to the stress profile and formation data. They do not prescribe a fracture shape. The two principal assumptions are:
1) plane strain at any cross section (i.e., each cross section or cell acts independently); and
2) horizontal fluid flow along the length of the fracture (i.e., neglecting vertical flow and the variation of the horizontal velocity as a function of vertical position).

These two assumptions allow the uncoupling (and hence simplification) of the solid and fracture mechanics solution from the 1D fluid flow [*Mack and Warpinski,* 2000]. These assumptions are valid for reasonably contained fractures, which are long relative to their height (as in the 2D PKN model). The assumption of 1D fluid flow results in the inability of pseudo (planar) 3D models to represent:
1) The effect of variations in width in the vertical direction on fluid velocity;
2) local dehydration, which is approximated as simultaneous dehydration over the entire height of the fracture;
3) leakoff after tip screen-outs, when fluid flow through the proppant pack is ignored; and
4) proppant settling resulting from convection or gravity currents.

It is also assumed that the stress profile in the rock mass is locally constant.

Lumped (Overall Fracture Geometry Parameterization)

The lumped, pseudo (planar) 3D models include FracproPT by Pinnacle Technologies, Inc. [*Cleary and Fonseca,* 1992; *Cleary et al.,* 1991; *Cleary,* 1980a; *Cleary,* 1980b], and MFrac by Meyer and Associates [*Hagel and Meyer,* 1992; *Meyer et al.,* 1990; *Meyer,* 1986; *Meyer,* 1989]. In lumped models, the governing and constitutive equations are simplified by assuming a self-similar fracture shape (i.e., one that is the same as time evolves, except for a length scale) [*Mack and Warpinski,* 2000]. In addition, a spatial averaging (i.e., integral) approach reduces the partial differential equations to ordinary differential equations in time. The undetermined, lumped coefficients of the governing equations are chosen from physical and mathematical considerations, and calibrated from fully 3D solutions of simpler problems, simulations with fully 3D models, and experimental and field data. The fracture shape is generally assumed to consist of two half-ellipses of equal lateral extent, but with different vertical extent, joined at the center. The horizontal fracture length and vertical tip extensions at the well are computed at each time step, and the assumed shape is matched to these positions. That is, these models use a parametric representation of the total fracture geometry. They attempt to include truly 3D fracture behavior from history matching and the lumped parameters. In addition, the lumped models make the inherent assumptions that fluid flow is along 2D streamlines from the perforations to the edge of the ellipse, and that the 2D streamlines have a particular shape that is derived from simple analytical solutions. The key characteristics of lumped models are:

1) The physics of the problem is realistic and general,
2) the computation time is much faster than the treatment time to allow for repetitive execution during pressure history matching, and
3) the use of improved estimates of parameters obtained in real time (i.e., during the treatment) [*Crockett et al.,* 1989].

Consequently, they are used extensively for the application of pressure data during a treatment. However, if calibrated models can be supported by the correct physics, then they can work in the long term.

9.3.3 Planar 3D

Planar 3D models are based on the assumption that the fracture is planar and oriented perpendicular to the far-field minimum in-situ stress [*Mack and Warpinski,* 2000]. The complexities that result in deviations from this planar behavior are not considered. These models solve the basic equations of mass balance, elasticity, height growth, and fluid flow using implicit finite difference or finite element solutions for a fracture that is constrained a single plane. The fracture width is calculated using 3D elastically coupled displacement (i.e., the total displacement at a point is the integration of all displacement increments caused by all local forces). Thus, the fracture width is calculated correctly for a complex geometry. In contrast, for pseudo 3D models, the width and height growth at each point along the fracture is a function of the net pressure at that point alone. Fracture propagation is calculated for all points around the fracture perimeter. In contrast, for pseudo 3D models, the major part of the fracture propagation is into the zone where the fracture initiates.

They formulate the physics rigorously, assuming [*Warpinski et al.,* 1994]:

1) Planar fractures of arbitrary shape in a linearly elastic formation,
2) 2D fluid flow and proppant convection in the fracture,
3) time-dependent power-law fluid rheology,
4) typically linear fracture mechanics for fracture propagation, and
5) a fracture tip advancement that is proportional to the stress intensity factor on the fracture tip contour.

In essence, the hydraulic fracture is divided into a number of equal elements [*Mack and Warpinski,* 2000]. The solution of the governing and constitutive equations for these elements is computed. As the fracture boundary extends, the elements distort to fit the new shape. One difficulty with such a solution is that the elements can develop large aspect ratios and small angles. The numerical schemes typically used to solve the equations do not usually perform well with such shapes.

Planar 3D models simulate fracture growth through complex geologic environments (e.g., formations with varying values of stress, strength, modulus, and fluid loss). They are also able to compute the correct width from the correct mass balance and fluid efficiency. However, such models are computationally demanding. Consequently, they are generally not used for

routine designs. They should be used where a significant part of the fracture volume is outside of the fracture initiation zone, or where the fluid flow has a more vertical than horizontal orientation. Such cases typically arise when the stress in the layers around the target zone is similar to or lower than that within the target zone.

The planar 3D models include:
1) TerraFrac by TerraTek [*Clifton and Abou-Sayed,* 1979; *Clifton and Abou-Sayed,* 1981; *Clifton and Wang,* 1988; *Clifton and Wang,* 1991a; *Clifton and Wang,* 1991b],
2) HYFRAC3D by Lehigh University [*Advani et al.,* 1990] (discontinued),
3) GOHFER by Core Laboratories [*Barree,* 1991; *Barree,* 1983], and
4) E-StimPlan 3D from NSI Technologies (recently available) [*Smith and Klein,* 1995; *Smith et al.,* 2001; *Smith et al.,* 2004].

The planar 3D models TerraFrac and HYFRAC3D incorporate similar assumptions and formulate the physics rigorously, assuming planar fractures of arbitrary shape in a linearly elastic formation, 2D flow (finite element scheme) in the fracture, power-law fluids, and linear fracture mechanics for fracture propagation [*Warpinski et al.,* 1994]. Their difference is in the numerical technique used to calculate fracture opening. TerraFrac uses an integral equation representation, while HYFRAC3D used the finite element method. Both models use a fracture tip advancement that is proportional to the stress-intensity factor on the fracture tip contour.

TerraFrac subdivides the fracture into discrete elements and solves the governing equations for these elements. These governing equations consist of:
1) 3D elastic equations that relate pressure on the fracture faces to the fracture opening,
2) 2D fluid flow equations that relate the flow in the fracture to the pressure gradients in the field, and
3) a fracture criterion that related the intensity of the stress state ahead of the fracture front to the critical intensity for mode 1 fracture growth.

TerraFrac provides the following distinctive features:
1) 2D fluid flow for both proppant and temperature distribution;
2) multiple states having different fluids, proppants, and rates, with fluid and proppant properties as functions of temperature if desired;
3) multiple layers, each having different in-situ stress, Young's modulus, fracture toughness, Poisson's ratio, and leakoff;
4) poro-elastic and thermo-elastic capabilities for water-flooding and other applications;
5) a robust mesh generator to handle a wide variety of fracture geometries and a quasi-Newton method to solve the non-linear system of equations for the fluid pressures (this approach provides fast convergence and high accuracy); and
6) a post shut-in calculation capability for which no additional assumptions are made (only the injection rate changes).

HYFRAC3D uses a finite element code that is based on a set of coupled mass continuity, fluid momentum, constitutive elasticity, and fracture mechanics equations governing planar hydraulic fracture propagation in a multi-layered reservoir. A mapping technique of the baseline mesh defined on a unit circle to arbitrarily shaped fracture geometries is used in the numerical scheme to track the moving fracture front.

E-StimPlan 3D is a hydraulic fracture simulator for fracture design and analysis in complex situations (e.g., involving height growth, proppant settling, foam fluids, and tip screen-out). The model has complete fluid and proppant tracking that allows optimum fluid selection and scheduling based on time and temperature histories. Fracture height growth is calculated through multiple layers, and it includes proppant settling and bridging calculations. A fracture analysis and history-matching module provides history matching of measured net treating pressures to yield the most accurate possible estimation of actual fracture geometry and behavior. In addition, simulations during fracture closure (i.e., pressure decline) aid in pressure decline analysis for fluid loss in complex geologic situations.

Finite-Difference Scheme

GOHFER (Grid Oriented Hydraulic Fracture Extension Replicator), in contrast to other planar 3D models, avoids the problem of grid distortion by dividing the layered reservoir into a stationary grid of equal-size rectangular elements, which are defined over the entire region that the fracture may cover [*Mack and Warpinski,* 2000; *Warpinski et al.,* 1994; *Barree,* 1991]. As the failure criterion is exceeded, the elements ahead of the failed tip are opened to flow, and they become part of the fracture. Two limitations of this approach are:

1) The number of elements that participate in the simulation increases as the simulation proceeds, so that the initial number could be small and results in inaccuracy, while the final number could be large and results in excessive computational demands; and
2) the general size of the fracture must be estimated in advance of the simulation to optimize the number of elements.

In addition, the following simplifications are used:

1) A simplified method for representing modulus contrasts, and
2) a tensile strength criterion is used for fracture extension, rather than a fracture mechanics effect.

This failure criterion compares the tensile-stress distribution around the fracture perimeter with an assumed maximum allowable tensile stress of the formation normal to fracturing plane. However, the fracture-induced stress in the formation near the tip of a fracture varies with the square root of the distance from the tip. Hence, the failure criterion is grid-resolution dependent. The fracture width is computed by superposition by use of the surface displacement of a semi-infinite half-space under normal load (i.e., the Boussinesq solution). It uses non-linear fracture mechanics (in contrast to other planar 3D models) [*Core Lab,* 2003].

The application of planar 3D models to EGS is further discussed in section 9.12.3 on page 179.

9.3.4 3D

For relatively unconfined fracture growth in a complex in-situ stress profile [*Warpinski et al.,* 1994], when the fracture geometry is not easily defined and constrained to a single plane, a fully (non-planar) 3D model is necessary for more accurate modeling [*Carter et al.,* 2000]. Fully 3D models make no assumptions about the orientation of the fracture [*Mack and Warpinski,* 2000]. For example, perforation patterns, restricted flow, and tortuosity in the near-well region, and deviated wells may cause a fracture to initiate in a particular direction before re-orienting into a final preferred orientation (i.e., perpendicular to the far-field minimum in-situ stress). That is, such fractures are generally non-planar with arbitrary fracture front shapes, and re-orient during propagation. For deviated wells, the complex stress state and fracture geometry can limit the fracture width at the well and hinder the injection of proppant into the fracture leading to premature screen-out. Nevertheless, the benefits of drilling inclined wells are significant. Therefore, the ability to model hydraulic fracturing from deviated wells is of ever-increasing importance to the petroleum industry. The attractive features of fully 3D modeling are obtained at the increased costs of obtaining additional information on formation properties, and demanding computational requirements [*Clifton,* 1989]. They generally require a specialist to obtain and interpret the results. They are most applicable in research environments, to study details of fracture initiation and near-well complexities, rather than overall fracture growth. The application of planar 3D models to EGS is further discussed in section 9.12.3 on page 179.

9.4 Fully Coupled Hydraulic Fracturing Reservoir Simulators

Fully coupled hydraulic fracturing reservoir models include Geosim by Taurus Reservoir Solutions [*Bagheri and Settari,* 2005; *Ji et al.,* 2004] and STARS by Computer Modeling Group (CMG) [*CMG,* 2005]. Similar to petroleum reservoirs that are not affected by natural fractures, naturally fractured reservoirs can be greatly influenced by the geomechanical behavior of rocks. Moreover, the role of geomechanics could be even more crucial owing to the presence of natural fractures, which could be more sensitive to stress than the rock matrix. These natural fractures are affected by stress disturbances because of fluid injection, which result in their opening, closure, and re-orientation. These variations in geomechanical properties of the fractures affect the magnitude and direction of their permeability. The fracture permeability is a controlling factor in management of naturally fractured reservoirs. To capture this behavior, it is inevitable to consider geomechanical factors in modeling of fluid flow in naturally fractured reservoirs. Most dual porosity models used in the industry that couple fluid flow behavior in naturally fractured reservoirs fail to account for deformability of rock and fractures. These models use simple pressure-dependent relations for rock compressibility while fracture permeabilities are usually treated statically throughout the simulation of the entire reservoir life.

In uncoupled conventional hydraulic fracturing models, the fracture propagation is usually modeled from a mass balance of the injected fluid, and the reservoir coupling with the fracture is simplified to a 1D or 2D analytical leakoff model [*Ji et al.,* 2004]. In contrast, in coupled models, a mass balance constraint is used, by coupling the fracture mechanics, fracture propagation, reservoir flow and heat transfer. The coupling between the fracture and the reservoir is obtained by treating the fracture flow as a boundary of reservoir flow, and numerically solving the leakoff of the injected fluid. However, the following problems occur when the conventional models for fracture propagation are coupled to reservoir models:

1) The conventional reservoir coupling of a fracture with a 1D or 2D analytical or numerical leakoff model lends itself easily to construct dynamic grid for the fracture. However, coupled models generally require a dynamic fracture propagating through a stationary reservoir stress grid. This creates grid effects that result in oscillation of fracture growth with time, and limiting the stability of the model, especially in full field reservoir simulations with coarse grids.
2) When the volume of fluid in a fracture is small compared to the injected volume of fluid because of high leakoff, this can cause a singularity of the mass balance or the fluid volume constraint in the facture. This in turn, causes convergence problems in the conventional fracture propagation predictions, and changes of far-field stress and reservoir pressure (which in turn influences the fracturing mechanics). Consequently, a strongly coupled simulation of the reservoir flow, fracture propagation, and resulting stress change is needed.
3) The theory of coupling geomechanics and reservoir engineering in fractured rocks published in the literature is built on the single-porosity poro-elastic theory of Biot [*Bagheri and Settari,* 2005]. Different approaches have been proposed to extend Biot's single porosity theory to dual porosity models. Models that incorporate the coupling are based on either partial or full coupling, with different benefits and disadvantages. The most rigorous approach is represented by the fully coupled fracture and reservoir model. However, to avoid the disadvantages of the fully coupled approach and to achieve a great flexibility for modeling the complex history, a partially de-coupled, iterative approach needs to be used.

This section describes the partially de-coupled model Geosim (section 9.4.1 below), and the three-phase and multiple-component thermal and steam additive simulator STARS (section 9.4.2 on page 160).

9.4.1 Partially De-coupled Model

Geosim is a partially de-coupled reservoir, geomechanics, hydraulic fracturing, and reservoir damage model that includes the strong coupling between reservoir flow and formation stress, deformations, compaction or stress-dependent properties, or interactions with fractures resulting from stimulation treatments [*Taurus,* 2003]. The main objective of this model is to address the effect of geomechanics on existing fracture flow properties (i.e., porosity and permeability) [*Bagheri and Settari,* 2005]. Other effects (e.g., the creation of new fractures by matrix failure, fracture slip, fault reactivation) are not treated. The methods for representing the dynamic fracture propagation take into consideration the mutual influence between dynamic fracture propagation and reservoir flow, treat the fracture as a highly permeable part of the reservoir, and use a single common grid system to model dynamic fracture propagation and reservoir flow in a fully coupled manner [*Ji et al.,* 2004]. The model has been implemented in a reservoir simulator, as a first step in developing a fully coupled

geomechanical fracturing model. The physical system that is solved consists of the reservoir grid as a subset of the finite element stress grid, which cover the overburden, flanks, and possibly base rock.

The simulation is modular and consists of the reservoir model, the stress-strain model, the fracture model, and the damage model, depending on the problem to be solved. The system is controlled by the reservoir simulator. The temperature model is necessary for most problems involving water injection. The modeling of the geomechanical response of the formation allows optional stress codes to be utilized. The principal module is a poro-elastic and thermo-elastic model that treats elasticity and plasticity. A variety of fracture types and configurations can be represented in the model. Fractures can be specified directly through data or imported from associated simulation. This includes the modeling of the following features:

1) Static or dynamic fractures;
2) full thermal treatment;
3) vertical or horizontal fractures;
4) non-linear rock mechanics with failure; and
5) multi-fractured horizontal or vertical wells.

The damage caused by the quality of the produced water is modeled by a relationship between permeability reduction and injected water throughput.

Several methods of coupling between the host reservoir model and the stress model can be used to optimize the performance of the system while representing the essential physics of the coupled processes. These range from the rigorous coupling between stress, flow, and heat to loosely coupled treatment. Both the pore volume coupling (i.e., compaction or porosity enhancement) and coupling through flow properties (permeability changes because of stress or creation of fractures) can be represented [*Taurus,* 2003]. Two methods of fracture coupling are available:

1) The fracture growth is modeled by transmissibility multipliers in the fracture plane, which are a function of effective stress. This provides rigorous coupling with reservoir flow and stress.
2) The time-dependent fracture growth can be generated by conventional fracturing software. In this method, fracture mechanics can be solved rigorously. However, the coupling to the flow and stress field is weak.

If the initial distribution of fractures and their mechanical properties are known, then fracture flow properties are calculated internally [*Bagheri and Settari,* 2005]. Depending on the distribution of fractures (i.e., oblique), the geomechanical model described here must be coupled with a flow model capable of handling full permeability tensor. In this case, changes in fracture permeability result in the change in the magnitude as well as the direction of the principal permeabilities. However, fractures that are oriented parallel to the coordinate axes result in a simple, diagonal permeability tensor. The model computes the stress, deformation, and flow (pressure, saturation, and temperature).

9.4.2 Three-phase and Multiple-component Thermal and Steam Additive Simulator

STARS is a three-phase multi-component thermal and steam additive simulator. Grid systems could be Cartesian, cylindrical, or variable depth/variable thickness [*CMG,* 2005]. Two-dimensional and three-dimensional configurations are possible with any of these grid systems. Some of the relevant features of STARS are:

1) Naturally fractured reservoirs: The flow in naturally fractured reservoirs can be simulated with four different models, dual porosity (DP), dual permeability (DK), multiple interacting continua (MINC), or vertical refinement (VR), depending on the process or mechanisms to be studied. The basic approach idealizes the fractured reservoir as consisting of two parts: fracture and matrix. The fractures, with small storativities, are the primary conduits of fluid flow, whereas the rock matrices have low fluid conductivities but greater storativities.
2) Fully implicit wells: Wells are solved in a very robust fashion. The bottom-hole pressure and the block variables for the blocks where the well is completed are solved fully implicitly. If a well is completed in more than a single layer, then its bottom-hole pressure is solved in a fully coupled manner (i.e., all completions are accounted for). This eliminates convergence problems for wells with multiple completions in highly stratified reservoirs. In addition, a comprehensive well control facility is available. An extensive list of constraints, e.g., maximum, minimum bottom-hole or wellhead

pressures, rates, gas / oil ratio (GOR) can be entered. As a constraint is violated, a new constraint can be selected according to the user's specifications.

3) Discretized well: The growing acceptance of horizontal well technology has raised questions that reservoir simulation models need to address. In particular, the impact of long well transients, viscous pressure drop, and multiphase flow patterns in creating non-uniform injectivities and productivities along the well are of concern. STARS provides an efficient and consistent method for handling these questions by discretizing well flow and solving the resulting coupled well/reservoir flow problem simultaneously. Appropriate multiphase flow correlations are used to adjust well flow patterns in an explicit fashion at the end of each time step.
4) Geomechanical model: Several production practices depend critically on the fact that the producing formation responds dynamically to changes in applied stresses. These include plastic deformation, shear dilatancy, and compaction drive in cyclic injection/production strategies, injection induced fracturing, as well as near-well formation failure and sand co-production. A geomechanical model consisting of three sub-modules is available for treating aspects of the above problems. The coupling between the geomechanical model and the simulator is done in a modular and explicit fashion. This increases the flexibility and portability of the model, and decreases computational costs.

Several models have been introduced to handle the processes that govern the fluid and heat flow in fractured reservoirs. To model these processes effectively, the viscous, capillary, gravitational, and diffusive effects must be quantified. The importance and interaction between these forces depend on the type (i.e., geometry) of the fractured reservoir and the recovery strategy. In all models, the reservoir is divided into matrix and fracture interacting continua with a superimposed computational grid. In general, each grid block may contain several fracture and matrix continua (i.e., elements) which are lumped together. When a fractured reservoir exhibits substantial matrix heterogeneities, this lumping may lead to erroneous results. Therefore, one must be careful when choosing grid block sizes. Generally, the models could be classified into two groups:

1) Dual Porosity Models: It is assumed that the fracture network is the primary continuum for fluid flow. The low permeability, high storativity matrix is considered a sink or a source to the fracture, which is appropriate for well-fractured reservoirs that have complete matrix discontinuity. The models could be sub-divided according to their abilities to treat the fluid and heat flow.
   a) Standard dual-porosity model (DP): This is the simplest model to describe the behavior of fractured reservoirs. The matrix and the fracture communicate through a single exchange term. There is no direct communication between inter-block matrices (i.e., neighboring blocks are connected through fracture flow only). The fluid or heat inside matrix can be transferred only to fracture. It is assumed that fracture and matrix within a grid block are at the same depth and, therefore, it is not possible to simulate gravity drainage effects with this model. A quasi steady state is assumed inside each matrix element that may lead to incorrect results in reservoirs with large matrix elements, particularly at the initial stages of reservoir depletion because of delayed matrix response.
   b) Multiple interacting continua model (MINC): This model was proposed for geothermal reservoirs and later was applied to hydrocarbon reservoirs. The matrix element is divided into several nested volume domains that communicate with each other. Therefore, e.g., pressure, saturation, and temperature gradients are established inside matrix, allowing transient interaction between fracture and matrix. Because of the matrix discretization, the transmissibility for matrix-fracture flow is higher than in DP or dual permeability models for the same matrix size. This results in earlier and increased matrix-fracture response. Semi-analytical approaches to modeling this transient behavior are not considered.
   c) Vertical refinement model (VR): This model is used to consider gravitational effects and the gravity drainage mechanism. In this model matrix is refined in the vertical direction, accounting for transient flow behavior in the matrix. Complete phase segregation in the fracture is assumed. The matrices communicate with only the fracture in the off-vertical directions, and with each other in the vertical direction. The matrix sub-blocks as well as the fracture have different depth and, hence, this model is suitable to simulate the gravity drainage process as well as processes with phase segregation inside the matrix. Similar to the MINC model, the fracture and matrix start communicating earlier because of smaller matrix sub-blocks. Other semi-analytical approaches to modeling gravity drainage are not considered.
2) Dual permeability models (DK): The fracture network and the matrix are both considered in the fluid and heat flow. These models are suitable for moderately to poorly fractured reservoirs or fractured brecciated reservoirs where the assumption of complete matrix discontinuity is not valid. They are also used for problems that require capillary

continuity. The standard dual permeability model is similar to DP model. However, it has an additional communication between matrices of the adjacent grid blocks. Gravity drainage can be simulated only to a certain degree, because of the quasi steady-state assumption inside matrix blocks. This degree varies with the complexity of a process, and it would be quite low for thermal heavy oil/bitumen recovery, where the oil mobility is strongly temperature dependent. In this case, models with additional vertical matrix refinement should be used.

9.5 Fractured Reservoir Simulations

For the hydraulic stimulation of natural fractured reservoirs, the relation between width and pressure could be severely modified with respect to the single fracture model. To describe a fracture network system, it is possible to track its entire growth history. Such simulations have been performed for research purposes with models that incorporate natural fractures as joints in between blocks that form the elements. However, it is impractical to perform such a simulation for design purposes. Moreover, it appears that for correct modeling of fracture propagation, the effect of new fracture generation needs to be included, which adds to the computational effort.

Fractured reservoir models describe static fractures (i.e., fractures that do not propagate, but that open because of the effective stress profile in the reservoir). These models can be used to simulate the opening of natural fractures in EGS.

Alternatively, techniques that have been developed for modeling fluid flow in fractured rock masses [*Dershowitz et al.,* 1992] could be applied. In fracture flow problems, one approach, i.e., Discrete Fracture Models (DFM) is to generate a fracture network from statistics, such that it mimics the observed patterns. For hydraulic fracturing, probably only a few parameters would be needed to describe the hydraulic fracture network. The height growth and length growth of the fracture system should of course depend on the stress and the formation properties (including lamination or interaction with natural fractures). The density of the fracture network should agree with the geometry of a single planar fracture in 3D. Then, the conductivity of the network is modeled by assigning statistically determined fracture conductivity. Of course, the effect of stress and the interaction in the network needs to be taken into account. The development of such a model would be a strong deviation from anything that has been developed for hydraulic fracturing modeling for propped stimulations in the oilfield.

This section describes fracture reservoir simulations for geothermal applications (section 9.5.1 below) and general use (section 9.5.2 on page 164).

9.5.1 Geothermal

Geothermal fractured reservoir simulators include HEX-S by GEOWATT AG (Swiss Geothermal Expert Group) [*Kohl and Mégel,* 2005a]. The hydro-mechanical code HEX-S has been developed to simulate the stimulation processes in a fractured reservoir during massive injection into a borehole [*Kohl and Mégel,* 2005b]. It computes the reaction of the reservoir permeability because of the opening of pre-existing fractures during a borehole injection. The model takes into account the aperture change of each fracture in the model because of the corresponding overpressure resulting from the injection. The propagation of the overpressure in the reservoir as well as the development of the highly anisotropic reservoir permeability because of the fracture apertures is calculated as a time-dependent process. Hence, the reaction of the reservoir permeability to an arbitrary injection rate history can be calculated.

The permeability distribution depends essentially on the location, orientation, aperture, and extent of the incorporated fractures. An arbitrary number of both, stochastic and deterministic, fracture sets can be defined. Because it is assumed that in most cases an induced microseismic event represents the shear failure of a part of a fracture surface area (i.e., slip patch), the locations of the calculated shearing events can be compared with the microseismic clouds. In contrary, possible mode I events (i.e., normal stress variations) remain unidentified. Every fracture or fracture zone is represented by a circular plane subdivided into a number of circular slip patches with small, predefined radii. The aperture of each specific slip patch contributes to the final permeability distribution. Starting from an initial value, the aperture change of a fracture depends on the orientation, the local effective stress field, and its defined mechanical parameters. Each fracture zone is defined either deterministically or stochastically, with following detailed properties [*Kohl and Mégel,* 2005a; *Kohl and Mégel,* 2005b]:
Deterministic fracture zones consist of slip patches with defined positions, radii, orientations, and classes of mechanical behavior. The essential information is generally derived from borehole logs. However, may also be the result of post–experimental interpretation of individual, microseismically active planar structures.
Stochastically generated fracture zones have random locations and orientations. Input parameters for the stochastic generation are the statistical distribution of the orientation of fracture zones seen in borehole logs. For a specific starting value of a random sequence, a model with a specific distribution of fracture zone locations is generated. Each stochastically

generated model has the same distribution of orientations of fracture zones. Typically, stochastically generated fracture zones are used at locations with little information (i.e., at greater distance from the boreholes). The distribution and orientation is calculated from statistical evaluation of the observed fractures intersecting the boreholes. The model domain is filled–up until a predefined fracture (or slip patch) density is reached.
The initial aperture of each slip patch is proportional to its radius and orientation to the local stress field and adjusted with an overall factor in such a way that the entire reservoir model has a predefined average permeability.

The implemented aperture laws for the fractures or slip patches are of the analytical kind. The aperture of a fracture depends on the following parameters:
1) The mechanical properties of the fracture,
2) the fluid pressure in the fracture space, and
3) the normal and the shear stress on the fracture plane.

The effective normal stress and the effective shear stress on the plane of a fracture are derived from the three regional principal stress components and the fluid pressure at the fracture location. Depending on the pore and fracture fluid pressure, the fracture aperture at a given location is assumed a function of three different opening processes:
1) Compliance only: Under the condition of low effective shear stress, only a compliant reaction of the fracture walls to fluid pressure affects the aperture. The condition for this behavior is the Mohr-Coulomb criterion. The aperture increase is treated as reversible, and it vanishes as soon the pressure declines after the end of injection.
2) Compliance and shearing: If the effective shear stress at the fracture walls exceeds the friction resistance and the effective normal stress still is positive, then the fracture fails. This portion of the aperture increase is considered irreversible when injection test has stopped and the pressure field in the reservoir has reached its ambient value.
3) Jacking and shearing: When the effective normal stress becomes negative, the fracture walls separate and the friction forces acting on them disappear. In addition to the shear aperture change, a contribution from jacking conditions arises. Clearly, this contribution is considered fully reversible. Although the shear induced, mode II, aperture change of a fracture is the only permanent effect after an injection test has ended, the contributions from jacking and compliance are also of major importance for the propagation of the pressure front during the stimulation process.

The time-dependent pressure computation includes local mesh refinement at specified locations in the reservoir domain (e.g., boreholes) [*Kohl and Mégel,* 2005a]. Iteratively, the local hydraulic conductivity is derived from the apertures of the intersecting slip patches by a specific mapping procedure, and the pressure and the new apertures of the slip patches are then computed.

The time-dependent pressure calculation is performed with a new finite element (FE) algorithm. The main benefits of the FE algorithm are in efficient and flexible formulations:
1) Local mesh refinement at specified locations in the reservoir domain (e.g., boreholes),
2) utilization of an implicit time-step procedure for transient calculation, and
3) easy extension to further physical processes or constitutive laws.

The hydraulic conductivity for each element is derived from the apertures of the intersecting slip patches by a specific mapping procedure. The intersection of the discrete fractures with the continuous FE grid is calculated by use of a rock-to-fracture volumetric index (RFVI). The mapping results in individual FE volumes of strongly anisotropic properties. Thereby, the hydraulic properties of the FE grid are modified after each time-step. The pressure is computed and the new apertures of the slip patches are determined. When the hydraulic conductivities of the elements have been updated from the corresponding slip patch apertures, a next time-step is carried out.

9.5.2 General Use

In addition to the specialized hydraulic fracturing simulators, which model the opening of natural fractures in a reservoir, several general (geo)mechanical simulators can be used. Such simulators can be divided by their discretization scheme in:
1) 3D finite elements methods (3D FEM), and
2) 3D discrete elements methods (3D DEM).

Finite Elements

Finite elements simulations include ABAQUS [*ABAQUS,* 2005a; *ABAQUS,* 2005b] ABAQUS is from the 3D finite elements method (3D FEM). It can simulate a wide variety of linear and nonlinear problems. For example, it can simulate numerous physical phenomena (e.g., transient 3D heat transfer, dynamic stress and displacement, and 3D pore fluid flow and pore pressure). Coupling between different physical phenomena (e.g., thermo-mechanical, pore fluid flow-mechanical, and fluid-structural) can also be simulated. A variety of methods is provided to specify initial conditions, boundary conditions, loads, and predefined fields for various analysis types. It is possible to prescribe conditions point-by-point or, by use of sets and surfaces, over entire regions of the model at once. Several different types of constraints can be defined including multi-point constraints (linear or nonlinear), surface-based constraints, and an innovative ability to embed elements inside other elements.

Discrete Elements

Discrete elements simulations include 3DEC by HCItasca [*Itasca,* 2005]. 3DEC (3D Distinct Element Code) is from the 3D discrete element method (3D DEM). 3DEC is a three-dimensional numerical program from the distinct element method (DEM) for discontinuum modeling. The model simulates the response of discontinuous media (e.g., a jointed rock mass) subjected to either static or dynamic loading. The discontinuous medium is represented as an assemblage of discrete blocks. The discontinuities are treated as boundary conditions between blocks. Large displacements along discontinuities and rotations of blocks are allowed. Individual blocks behave as either rigid or deformable material. Deformable blocks are subdivided into a mesh of finite difference elements. Each element responds according to a prescribed linear or nonlinear stress-strain law. The relative motion of the discontinuities is also governed by linear or nonlinear force-displacement relations for movement in both the normal and shear directions. 3DEC has several built-in material behavior models, for both the intact blocks and the discontinuities, which permit the simulation of response representative of discontinuous geologic (or similar) materials. 3DEC is from a Lagrangian calculation scheme that is well suited to model the large movements and deformations of a blocky system. The distinguishing features of 3DEC are:

1) The rock mass is modeled as a 3D assemblage of rigid or deformable blocks.
2) Discontinuities are regarded as distinct boundary interactions between these blocks. Joint behavior is prescribed for these interactions.
3) Continuous and discontinuous joint patterns can be generated on a statistical basis. A joint structure can be built into the model directly from the geologic mapping.
4) 3DEC uses an explicit in-time solution algorithm that accommodates both large displacement and rotation and permits time domain calculations.
5) The graphics facility permits interactive manipulation of 3D objects. In the graphics screen mode, the user can move around inside the model and make regions invisible for better viewing purposes. This allows the user to build the model for a geotechnical analysis and instantly view the 3D representation. This greatly facilitates the generation of 3D models and interpretation of results.

For the simulation of a geothermal stimulation, the model is used to make the coupled hydro-mechanical computations. These computations allow for the simulation of the interactions between the mechanical process (i.e., deformations, stresses) and hydraulic process (i.e., pressures, apertures) in a solid cut by discrete discontinuities. This corresponds to a realistic geometry of the fracture network intersecting the blocks [*Gentier et al.,* 2005]. These blocks are considered deformable. The model is from a discretization of the blocks into tetrahedral elements and the fractures into elementary domains. The modification of the pressure field results in a modification of the actual stresses applied to the surrounding formations, which may themselves cause changes in the openings of the fractures and hence of the pressure field. Because the calculation method in 3DEC is incremental with preset time steps, equilibrium in the model is assumed to occur when the pressure and stress fields no longer change between two consecutive time steps. The numerical model takes into account only a parallelepiped volume centered on the open-hole of each well. At this stage, the open-hole of each well is considered as vertical.

The conceptual model of the modeling of a hydraulic stimulation is a homogeneous impermeable granitic mass crossed by a primary network of discontinuities constituted by hydrothermal fractured zones formed by the tectonic and hydrothermal

history of the site. On this primary network is superimposed a secondary network of discontinuities constituted mainly of more or less isolated fractures without a strong tectonic history. As a consequence, the rock mass is divided into blocks whose size is dependent on the density of the fracture network. The fracture networks introduced in the models are limited in a first step to a few fracture planes that are determined from the analysis of all the available data in the considered well. The location and the orientation of the fractures are more or less constrained according to the quality of the basic data. The physical model associated with the conceptual model is the following:

1) The rock matrix constituting the blocks is considered as homogeneous with an elastic behavior;
2) the mechanical properties are those of standard granite; and
3) the matrix is impermeable.

The fracture zones are infinite planes whatever their geological and tectonic natures. All the fractures have the same mechanical behavior. The normal mechanical behavior is elastic-linear while the fracture is in compression. The tensile strength is equal to zero. The tangential mechanical behavior is elasto-plastic. It follows the failure criteria of Mohr-Coulomb with dilation effects. The effect of dilation appears as soon as the maximum shear strength is reached. Fluid flow occurs exclusively through the fracture network and obeys a cubic law. As a first step, a set of hydro-mechanical parameters equivalent for all the fractures has been defined to obtain the correct order of magnitude for the hydro-mechanical responses of the various hydraulic stimulation tests in the wells of the upper reservoir.

For the initial conditions, it is assumed that the initial stresses are equal to the natural stress, and that the distribution of the initial pressures in the fracture network is obeying a hydrostatic field. For hydro-mechanical boundary conditions, the hydrostatic pressure is assumed and mechanical boundary conditions are assumed with no displacement at the boundaries of three of the six faces of the rectangle volume and stresses imposed on the three others. At the beginning of each simulation, the distribution of the fracture pressures is verified to obey the hydrostatic field as it was assumed. The simulation of the hydraulic test is carried out by adding an overpressure in the open part of the well. Then, the flow rate injected throughout the fracture network is computed when hydro-mechanical equilibrium is reached. The overpressures considered in each well correspond to those applied during the in situ hydraulic stimulation tests.

9.6 Overview Table

An overview of the properties of the various simulators is presented in Table 9.1.

Table 9.1: Overview of properties of simulators.

simulator	**E-StimPlan**	**FracCADE**	**FracproPT**	**MFrac**	**GOHFER**	**E-StimPlan 3D**	**Geosim**	**STARS**	**HEX-S**	**ABAQUS**	**3DEC**
hydraulic fractures (*s*tatic, *d*ynamic)	d	d	d	d	d	d	s, d	s	s	s	s
• fracture geometry (*P*seudo, 2D, 3D, *c*ell, *l*umped, *p*lanar)	P3D c	P3D c	P3D l	P3D l	3D p	3D p	3D p	3D	2D	3D	2D
• fracture mechanics (*l*inear *e*lastic, *n*on-*l*inear)	le	le	le	le	nl	le	le	×	×	×	×
• tip effects	fracture toughness	?	composite layer parameter	over-pressure parameter	process stress	fracture toughness	?	-	-	-	-
discrete fractures	✓	✓	✓	✓	✓	✓	✓	✓	✓	✓	✓
aperture function of normal stress	✓	✓	✓	✓	✓	✓	✓	✓	✓	✓	✓
aperture function of shear	×	×	×	×	×	×	×	×	×	✓	✓
natural fractures	✓	×	×	×	×	✓	2D	✓	2D	3D	2D
fluid flow (streamline)	2D	2D	2D, s	2D, s	2D	2D	✓	✓	✓	×	✓
flow rate function of aperture	✓	✓	✓	✓	✓	✓	✓	×	✓	✓	✓
channeling (within fractures)	✓	✓	✓	✓	✓	✓	×	×	×	✓	×
• fluid rheology (*N*ewtonian, *p*ower *l*aw, *C*arreau, *t*ime-dependent)	pl t	pl t	pl t	pl t	C t	pl t	N	N	N	N	N
multiple-phase flow (liquid, gas)	×	×	×	×	×	×	×	✓	?	×	×
porous flow in matrix	✓	✓	✓	✓	✓	✓	✓	✓	×	✓	×
• leakoff (*c*lassical, *n*umerical, 1D, 2D, 3D)	c	✓	c n 1D	c 1D 2D	n	c	n 3D	?	✓	n 3D	×
• spurt loss	✓	✓	✓	✓	✓	✓	×	×	-	✓	×

• filtrate	✓	✓	✓	✓	✓	✓	×	×	-	×	×
• filter cake	✓	✓	✓	✓	✓	✓	×	×	-	×	×
• dynamic	✓	✓	✓	✓	✓	✓	×	×	-	×	×
• compressible reservoir fluid	?	?	✓	✓	?	?	?	×	×	×	×
• poro-elasticity	?	?	✓	?	?	?	✓	×	×	×	×
tracer transport	×	×	×	×	×	×	×	×	×	✓	×
near-well friction	✓	✓	✓	✓	✓	✓	×	×	×	✓	×
• perforations	✓	✓	✓	✓	✓	✓	-	-	-	✓	-
• tortuosity	✓	✓	✓	✓	✓	✓	-	-	-	×	-
• multiple fractures	×	×	×	✓	×	×	-	-	-	✓	-
proppant transport											
• convection (*s*treamline)	2D	2D	2D s	2D s	2D	2D	×	×	×	×	×
• settling	?	✓	✓	?	?	?	×	×	×	×	×
• bridging	?	?	?	?	?	?	×	×	×	×	×
• tip screen-out							×	×	×	×	×
heat transfer (*well*, *f*racture, *r*eservoir)	f	f r	w f r	w f r	?	f	f r	r	?	r	r
• fluid convection in *f*	1D	✓	1D	✓	×	1D	✓	✓	✓	×	×
• fluid conduction in *f*	?	?	×	?	?	?	?	✓	✓	×	×
• fluid convection in *r*	?	?	1D	✓	?	?	✓	✓	✓	?	?
• fluid conduction in *r*	×	1D	×	✓	×	×	?	✓	✓	×	×
• rock conduction	×	1D	×	✓	×	×	✓	✓	✓	✓	✓
thermo-elasticity	×	×	×	×	×	×	×	×	×	×	×
mineral deposition/dissolution	×	×	×	×	×	×	×	×	×	×	×
reservoir (*2D*, *3D*, *a*nalytical, *n*umerical)	3D n	2D n	2D n	2D a	×	3D n	3D n	3D n	3D n	3D n	3D n
3D	✓	×	×	×	×	✓	✓	✓	✓	✓	✓
irregular grid	×	×	×	×	×	×	✓	✓	✓	✓	✓
• wells (*v*ertical, *h*orizontal, *o*blique)	v h	v h o	v	v h	v	v h	v	h	v	v h o	v h o
• multiple layers	✓	✓	✓	✓	✓	✓	✓	✓	×	✓	✓
• multiple fractures per perforation cluster or reservoir layer	×	×	×	✓	×	×	×	✓	✓	✓	✓
• coupling with fractures (*w*eak, *s*trong)	w	w	w	w	w	w	s	s	s	s	s
analysis											
• automatic net pressure history matching	✓	✓	✓	✓	✓	✓	×	×	×	×	×
• real-time data acquisition	✓	✓	✓	✓	×	✓	×	×	×	×	×
• fracturing test	✓	×	✓	✓	×	✓	×	-	-	-	-

• downhole friction step-down test	✓	×	✓	✓	×	✓	×	×	×	×	×
• pressure build-up well test	✓	×	×	×	×	✓	×	×	×	×	×
simulator	**E-STimPlan**	**FracCADE**	**FracproPT**	**MFrac**	**GOHFER**	**E-STimPlan**	**Geosim**	**STARS**	**HEX-S**	**ABAQUS**	**3DEC**

9.7 Features of Current Simulators

The basic features of conventional *geothermal* simulators are [*Sanyal et al.,* 2000]:
1) Multiple-phase fluid flow including phase change, relative permeabilities, and capillary pressure effects,
2) heat transfer, and
3) tracer transport in porous and fractured media.

For conventional hydrothermal resources (hot water, steam and two-phase reservoirs in porous or fractured rock), reservoir simulation is a routine activity. Hydrothermal simulators have been used to model complex fracture systems in an approximate way. However, hydrothermal simulators cannot accurately model certain aspects of fractures, either artificially created or enhanced, particularly the dynamic aspects. Consequently, they have not been used extensively for modeling artificially fractured systems.

9.8 EGS System Definition

The general concept of EGS is a reservoir consisting of a porous medium, generally with a natural fracture network, perhaps intersected by highly conductive, hydraulically induced artificial fractures. Flow occurs primarily in fractures and is dependent on fracture apertures, which in turn could be functions of fluid pressure and thermal contraction in the adjacent rock. In EGS, the main challenges are improving permeability through enhancement of natural fractures or creation of artificial fractures, and optimizing heat recovery through injection. Heat is removed by the sweep of injection fluid through the fracture system.

The premise is that the behavior of EGS is dominated by fracture flow. Consequently, the special features that would be desirable or required of any practical numerical simulator for EGS are, in addition to those of conventional geothermal simulators:
1) Explicit representation of fractures;
2) change in fracture aperture because of effective stress;
3) shear deformation and associated jacking of the fractures;
4) relationship between fracture aperture and fracture conductivity, including the potential for turbulent flow in the fractures;
5) channeling of fluid flow within fractures;
6) thermo-elastic effects;
7) chemical reaction between water and rock (i.e., mineral deposition and dissolution); and
8) coupling of the reservoir model with a well model.

The well-known simulators that have been used or can he used to model EGS are reviewed with regard to these features. While each of these simulators has many of the capabilities listed above, none has all of them. In addition, each

simulator has its strengths and weaknesses. A single type of model may not be suitable for all EGS projects or at every stage of a given project. Therefore, the need for developing a single, all-purpose simulator for EGS applications is perhaps less urgent than taking benefit of the strengths of the various available simulators to solve a particular problem.

Much can he learned about modeling EGS reservoirs from the experience gained in the modeling of artificially fractured systems in connection with hot dry rock (HDR) projects, which lie at one extreme of the EGS spectrum. Some of the simulation methods developed for HDR systems have applications in the broader area of EGS reservoirs. These HDR simulators are better at handling the dynamic aspects of fractures but lack certain other critical features (e.g., the ability to handle two-phase flow).

9.9 Fracture Representation

Fractures can be represented as [*Sanyal et al.,* 2000]:

1) An effective continuum approach is justified when the matrix and the fractures remain in approximate thermodynamic equilibrium (i.e., only when there are relatively low temperature gradients in the rock). For a typical situation in which the rock matrix is relatively impermeable, approximate equilibrium is only valid if the active fracture spacing and flow rates are sufficiently small, because of the relatively low hydraulic conductivity of the rock.
2) Explicit modeling of fractures is more appropriate in artificially fractured systems and in many low permeability systems, because the actively flowing fractures are widely spaced. This can be accomplished by:
   a) A discrete fracture model, or
   b) a porous-medium model with sufficient grid refinement and the application of appropriate permeabilities.

9.10 Current Capabilities

The current capabilities of simulators relative to the desired EGS features are [*Sanyal et al.,* 2000]:

1) Explicit representation of fractures: All geothermal and hydrothermal models can be used to simulate fractures at some level. The mathematical formulation and the complexity of the representation may differ between the simulators. Evidently, all hydraulic fracturing and fractured reservoir models describe discrete fractures explicitly. However, all hydraulic fracturing models and the hydraulic fracturing reservoir model can only describe a single fracture per reservoir layer. That is, multiple fractures are not truly implemented. While the fractured reservoir models can describe multiple fractures, their location and properties are determined deterministically or stochastically before fluid injection.
2) Fracture opening as a function of effective stress: This is important in reservoirs in which the natural permeability is low or when permeability enhancements are being modeled. Many of the geothermal and hydrothermal models include approximations of this mechanism, either through permeabilities that are a function of stress or by discrete fracture modeling. Evidently, all hydraulic fracturing models and the hydraulic fracturing reservoir model allow the fractures to open and propagate as a function of effective stress. However, the fractured reservoir models allow fracture opening as a function of effective stress. However, do not describe fracture propagation.
3) Shear deformation and associated jacking of the fractures: This feature is similar to the previous one and is subject to similar limitations. None of the hydraulic fracturing and hydraulic fracturing reservoir models describes this feature. However, it is included in the fractured reservoir models.
4) Relationship between fracture aperture and fracture conductivity: This feature requires the fluid flow in the fracture to be a function of the fracture aperture. In essence, all reviewed simulators have this feature. In discrete fracture models, the fluid flow in the fractures is described by the cubic law. In contrast, in porous flow models, fluid flow in the fracture is described by Darcy's Law. The cubic law is only valid for single-phase fluid flow. Evidently, all hydraulic fracturing, hydraulic fracturing reservoir, and fractured reservoir models account for this type of relationship.
5) Channeling of fluid inside fractures: Obtaining sufficient detailed knowledge to identify successfully when channeling in fractures is occurring require input from other technologies (e.g., tracers and fracture detection methods). These technologies are under development. However, may not be achievable in the near future. Only one geothermal model can describe this mechanism approximately, with user-define material properties). Evidently, all hydraulic fracturing models and the hydraulic fracturing reservoir model describe this mechanism. However, none of the fractured reservoir models considers this.

6) Thermo-elastic effects: The stress in the rock because of temperature change, in addition to the fluid-pressure stress, can alter the fracture aperture, which changes the fluid flow in the fracture. Because the aperture cannot be measured directly, it must be inferred through the transient and steady state flow simulation, and by comparison with tracer data. Once such inferences are made, two of the geothermal models are equipped to handle thermo-elastic effect around individual fractures, while a third handles this by use of a global stress. Thermo-elastic effects are not implemented in any of the hydraulic fracturing, hydraulic fracturing reservoir, and fractured reservoir models. Of the hydraulic fracturing models, only FracproPT and MFrac describe heat transfer in the fracture and the reservoir. Similarly, the hydraulic fracturing reservoir model, and the fractured reservoir models implement such heat transfer.
7) Mineral deposition and dissolution: Reactive chemical transport simulation in geothermal reservoirs is a major topic, particularly if all typical chemical species are included. One of the geothermal models includes simple chemical dissolution and deposition, and such a feature is being developed for one of the hydrothermal models. None of the hydraulic fracturing, hydraulic fracturing reservoir, and fractured reservoir models describes this mechanism.
8) Tracer module: All geothermal and hydrothermal simulators provide tracer modules. In contrast, none of the hydraulic fracturing, hydraulic fracturing reservoir, and fractured reservoir models incorporates such a feature.
9) Multiple-phase flow: None of the geothermal models provides multiple-phase liquid and gas flow capability. In contrast, all the hydrothermal simulators have this feature. In addition, none of the hydraulic fracturing, hydraulic fracturing reservoir, and fractured reservoir models truly describes multiple-phase liquid and gas flow. However, the hydraulic fracturing models can describe multiple-phase liquid and proppant transport, and most describe foams to some extent.

Summarizing, none of the *geothermal*, *hydrothermal,* and *fractured reservoir* models incorporate hydraulic fracture propagation. Consequently, they cannot be used for hydraulic stimulation of EGS. In contrast, none of the *hydraulic fracturing* models describes fluid flow and heat transfer in porous and naturally fractured reservoirs very accurately, because they are limited to near-fracture processes. In addition, they do not incorporate natural fractures and the propagation of multiple fractures from the same perforation into the same reservoir layer, and thus not fracture networks. The *hydraulic fracturing reservoir* model does account for fluid flow and heat transfer in porous reservoirs. However, its fracture propagation criterion is not from fracture mechanics. The *fractured reservoir* models are able to describe fluid flow and heat transfer. However, they are too general to handle the complexities of fracturing and reservoir fluids. None of the *hydraulic fracturing* and *hydraulic fracturing reservoir* models describes thermo-elasticity.

9.11 Components to be Developed

Consequently, the following components need to be developed to account for fracture growth physics in EGS applications:
A two-dimensional algorithm for heat transfer between the fractures and the reservoir: This extends the existing one-dimensional algorithms heat transfer for heat transfer near the fracture face. This addition is necessary to account for the longer time scale associated with EGS applications, which requires a model of heat transfer in both horizontal directions for a vertical fracture, not just in a direction perpendicular to the fracture plane.

1) A two-dimensional algorithm for leakoff from the fractures into the reservoir, that extends the existing 1D algorithms for leakoff.
2) An empirical model for fracture growth orientation and fracture complexity from a 3D state of stress, rock mechanical characteristics, natural fracture orientation, and fracture treatment characteristics.
3) An improvement of the modeling of the fracture closure stress changes (i.e., back-stress) because of an increase in reservoir pore pressure and a reduction in reservoir temperature throughout the fracture treatments.
4) An improvement of the pressure dependent leakoff functionality: In naturally fracture reservoirs, fluid leakoff from a main fracture can accelerate dramatically once the fracture pressure in the main fracture exceeds the maximum horizontal stress because of the opening of fissures.
5) An approximate visualization of the fracture network in the reservoir, in addition to the overall fracture geometry.

9.12 Approach

A useful simulator for EGS needs to include elements of hydraulic fracture propagation, fluid flow, and heat transfer in the fractures and the reservoir, and thermo-elasticity. To obtain such a simulator, it is in principle possible to combine a

hydraulic fracturing model with a *reservoir* model. For example, because of the *hydraulic fracturing* models only FracproPT and MFrac describe heat transfer in the fracture and the reservoir, it may make sense to couple either one to the oilfield *hydraulic fracturing reservoir* models Geosim or STARS. Alternatively, they can be coupled to one of the *geothermal* or *hydrothermal* models (which have the benefit of potentially being able to describe thermo-elasticity, tracer transport, multiple-phase liquid-gas flow, and mineral deposition and dissolution), in particular HEX-S. While coupling with the general use *fractured reservoir models* ABAQUS and 3DEC could be possible, they are generally not sufficiently flexible with regard to complex fluid flow, heat transfer, and in particular multiple-phase liquid-gas flow.

This section describes the approach for 2D heat transfer (section 9.12.1 below), 2D leakoff (section 9.12.2 on page 176), 3D fracture growth (section 9.12.3 on page 179), back stress (section 9.12.4 on page 181), pressure dependent leakoff (section 9.12.5 on page 181), and natural fracture networks (section 9.12.5 on page 181). Finally, the direct incorporation of measurements (section 9.13 on page 185) is discussed.

9.12.1 2D Heat Transfer

The properties of many fracturing fluids demonstrate some dependence on temperature [*Economides and Nolte,* 2004]. In a typical fracturing treatment, the temperature of the fracturing fluid is different from the temperature of the reservoir. As the fluid penetrates farther into the fracture, heat transfer occurs between the fracturing fluid and the rock, resulting in a change of the temperature of the fracturing fluid and of the reservoir near the fracture. Typically, the temperature gradient in the direction perpendicular to the fracture wall is much greater than the gradients in other directions. Consequently, the temperature gradients in the other directions can be neglected for short time scales. However, for longer time scales, they need to be taken into account. In addition, heat conduction in the fluid can be ignored because it is small relative to both conduction in the rock and transport of heat with the convecting fluid.

Governing Equations - Approach 1

A simple approach is given by [*Smith et al.,* 2004], where the governing equations are expressed directly in terms of temperature:

The energy continuity for the reservoir (assuming that the fluid and rock come to thermal equilibrium instantaneously)

$$\left(\rho C_p\right)_{\mathrm{r}} \frac{\partial T}{\partial t} + \left(\rho C_p\right)_{\mathrm{l}} v \cdot \nabla T - \nabla \cdot k_{h,\mathrm{r}} \nabla T = 0 \tag{9.1}$$

where $(\rho C_p)_{\mathrm{r}}$ is the heat capacity of the rock-fluid, $(\rho C_p)_{\mathrm{l}}$ is the heat capacity of the leakoff fluid, v is the fluid velocity in the reservoir, and $k_{h,\mathrm{r}}$ is the thermal conductivity of the rock; and

the energy continuity for the fracture (in difference form)

$$\left(\rho C_p\right)_{\mathrm{l}} \frac{\partial T}{\partial t} + \frac{1}{V_{\mathrm{f}}} \nabla \cdot A_{\mathrm{f}} v \left(\rho C_p\right)_{\mathrm{l}} \nabla T - 2 \frac{A_{\mathrm{r}}}{V_{\mathrm{f}}} k_{h,\mathrm{r}} \nabla T = 0 \tag{9.2}$$

where V_{f} is the local fracture volume, A_{f} is the local fracture cross sectional area and A_{r} is the local fracture-reservoir surface area (i.e., the factor of 2 is required because of leakoff from both faces of the fracture).

The continuity equations are solved for the temperature. The solution assumes that the reservoir temperature is symmetric on both sides of the fracture. The well temperature is the inner boundary condition for the fracture, and the outer boundary conditions are constant reservoir temperature.

Governing Equations - Approach 2

The governing equations that are used to describe the transport behavior in a reservoir can take many forms depending on the effects that are considered in the model. The diffusion terms of gravity, capillary force and conduction are not considered. Thus, the mass and heat transport in the reservoir occurs through the flowing phases only. For a 2D two-phase black-oil model, assuming that the water and oil components are always in the water and oil phases, and neglecting conduction, the general thermal governing equations are given by [*Pasarai and Arihara,* 2005a; *Pasarai and Arihara,* 2005b]:

The mass continuity for the fracturing fluid component f

$$-\nabla\cdot\left(\rho_{\mathrm{f}}\vec{u}_{\mathrm{f}}\right)+q_{\mathrm{f}}=\frac{\partial\left(\phi\rho_{\mathrm{f}}S_{\mathrm{f}}\right)}{\partial t} \tag{9.3}$$

the mass continuity for the reservoir fluid component r

$$-\nabla\cdot\left(\rho_{\mathrm{r}}\vec{u}_{\mathrm{r}}\right)+q_{\mathrm{r}}=\frac{\partial\left(\phi\rho_{\mathrm{r}}S_{\mathrm{r}}\right)}{\partial t} \tag{9.4}$$

the energy continuity for the fracturing and reservoir fluid component, f and r, respectively

$$-\nabla\cdot\left(\rho_{\mathrm{f}}H_{\mathrm{f}}\vec{u}_{\mathrm{f}}+\rho_{\mathrm{r}}H_{\mathrm{r}}\vec{u}_{\mathrm{r}}\right)+q_{\mathrm{r}}H_{\mathrm{f,HF}}+q_{\mathrm{r}}H_{\mathrm{r,HF}}=\frac{\partial}{\partial t}\left[\phi\left(S_{\mathrm{f}}\rho_{\mathrm{f}}U_{\mathrm{f}}+S_{\mathrm{r}}\rho_{\mathrm{r}}U_{\mathrm{r}}\right)+\left(1-\phi\right)U_{\mathrm{R}}\right] \tag{9.5}$$

where ρ is the density, q is the mass flow rate (i.e., given by the leakoff model of the hydraulic fracture; section 9.12.5 on page 181), ϕ is the porosity, S is the saturation, t is the time, H is the enthalpy, U is the internal energy, HF represents the hydraulic fracture, R represents the host rock. The flux velocity is given by Darcy's law as

$$\vec{u}_{\mathrm{f\,or\,r}}=-k\left(\lambda_{\mathrm{f\,or\,r}}\nabla p\right) \tag{9.6}$$

where p is the total pressure. The phase mobility is given by

$$\lambda_{\mathrm{f\,or\,r}}=\frac{k_{\mathrm{R,f\,or\,r}}}{\mu_{\mathrm{R,f\,or\,r}}} \tag{9.7}$$

where k is the relative permeability, and μ is the viscosity.

Functional Dependencies of Fluid Properties on Temperature and Pressure

The functional dependencies of the fluid properties on temperature and pressure are described as [*CMG,* 2003]:

The phase densities ρ are modeled by the correlation

$$\rho_{\mathrm{f\,or\,r}}=\rho_{\mathrm{f\,or\,r,std}}e^{c_{\mathrm{f\,or\,r}}\left(p-p_{\mathrm{std}}\right)-a\left(T-T_{\mathrm{std}}\right)-\frac{1}{2}b\left(T^{2}-T_{\mathrm{std}}{}^{2}\right)} \tag{9.8}$$

where c is the compressibility, a and b are the thermal expansion coefficients, and std refers to standard conditions.

The phase viscosity may be specified using the correlation

$$\mu_{\text{f or r}} = a_{\text{vis}} e^{\frac{b_{\text{vis}}}{T}} \tag{9.9}$$

where T is in absolute degrees, a_{vis} and b_{vis} are empirical parameters with values determined from two viscosity measurements at different temperatures.

The enthalpies can be calculated based on liquid heat capacity or vapor heat capacity. For example, in the case of the latter, the enthalpy of the liquid phase (i.e., fracturing and reservoir fluid) enthalpy is given by

$$H_{\text{f or r}} = H_{\text{g}} - H_{\text{vap}} \tag{9.10}$$

where the gas phase enthalpy is given by

$$H_{\text{g}} = \int_{T=T_{ref}}^{T} C_{\text{g}} dT \tag{9.11}$$

the heat capacity of the gas phase is expressed by a correlation with four coefficients c_1 to c_4

$$C_g = c_1 + c_2 T + c_3 T^2 + c_4 T^3 \tag{9.12}$$

and the vaporization enthalpy is given by

$$H_{\text{vap}} = h_{\text{vap}} \left(T_{\text{cr}} - T \right)^{e_{\text{vap}}} \tag{9.13}$$

where h_{vap} and e_{vap} are constants, and T_{cr} is the critical temperature.

While temperature effects on relative permeability play a significant role in thermal simulations, they are generally neglected. Thus, the influence of temperature in the simulation model is purely through changes in fluid viscosity and density. In addition, capillary pressure can be ignored.

Mesh Grid Discretization Approach

The general tendency for the simulation of heat transfer has been to use the fully implicit finite difference method to solve the mass and heat transport. The method has been proven favorable to handle rapidly changing properties and complex physical mechanisms encountered in the processes. However, this method is limited in the mesh grid size due to restrictions in computational power. In addition, if care is not taken in the choice of the numerical scheme, then the method could also predict erroneous results. Local grid refinement is a natural process to handle this situation but requires a great amount of memory and high computational cost. Moreover, simple methods with a reasonable balance between the detailed physical model and the computational efficiency are not available [*Pasarai and Arihara,* 2005a; *Pasarai and Arihara,* 2005b].

Streamline Approach

An alternative approach to solve the problem is to use the streamline method [*Pasarai and Arihara,* 2005a]. Because fluid transport occurs along streamlines rather than between discrete grid blocks on which the reservoir pressure field is solved, the problems associated with the fully implicit finite difference method are minimized and the simulations can be executed much faster. It is highly efficient in solving large, geologically complex systems where flow is controlled by heterogeneity and well positions [*Pasarai and Arihara,* 2005b]. The speed advantage is related to both the ability to take longer time steps and the fact it does not need to invert the very large linear equation systems as resulted in the fully implicit method [*Pasarai and Arihara,* 2005b].

The streamline method is an ideal tool for quick assessment of process optimization where pressure changes are slow [*Thiele et al.,* 1997; *Batycky et al.,* 1997; *Huang et al.,* 2004]. Consequently, streamlines can be updated infrequently. The resulting simulations run very fast. If dramatic pressure changes take place, then the streamlines may need to be updated more often. A fast numerical solver for the pressure equation is of paramount importance for this situation. A multi-grid solver for the highly efficient solution of large linear systems of equations with sparse matrices was used to solve the matrix system resulting from discretization of the pressure equation.

For the thermal streamline simulator, a field pressure equation is derived for defining the streamlines from the equations for the fracturing fluid and reservoir fluid components, taking into account the fluid and the rock compressibility. Then, the water saturation and the heat transport equations along the streamlines were formulated. The major difference lies in the numerical scheme to solve these transport equations. For the flow simulation, the formulated streamline transport equations were solved simultaneously for each streamline. For the heat transfer simulation, the sequential solution method was selected to speed up the 1D solver. For each streamline, the streamline mass transport equation is solved first assuming temperatures are unchanged, followed by the streamline energy equation.

9.12.2 2D Leakoff

The most basic process in hydraulic fracturing is fluid leakoff because it determines directly the mass balance. Because FracproPT was developed for low permeability gas reservoirs, it is still limited in its leakoff modeling. The assumption of linear Carter leakoff (i.e., with the leakoff velocity perpendicular to the fracture faces) seems justified because the fluid pressure reduces to zero (i.e., pore pressure) near the fracture tip. However, even for moderate permeability, this assumption breaks down and 2D leakoff becomes important. This can significantly modify the fluid efficiency and fracture dimensions. Moreover, in oil reservoirs there is a significant back stress, which might be misinterpreted as a high net pressure. Of course, these problems have been dealt with for modeling water injection (by use of both analytical and numerical solutions to model the pressure distribution in the reservoir). To extend the model for water injection, an appropriate leakoff model and stress model should be incorporated.

Modeling water fracturing can be performed in the leakoff controlled regime, where the influence of poro-thermo-elasticity is small and the leakoff can be modeled by the 1D Carter law. However, in many cases the fracture is small with respect to the pressure disturbance and the cooled zone. Consequently, a rigorous coupling of the leakoff to the reservoir flow is needed. In addition, the stress changes because of cooling and pore pressure need to be considered. The modeling capability should be improved in this respect because even for propped fracturing 2D fluid leakoff and the back stress can be important. This would also allow for improved reservoir monitoring.

Fluid leakoff from hydraulic fractures is normally described by a 1D (Carter) fluid-flow model. In its simplest form, the leakoff rate within this model is, for a propagating fracture of constant height h, given by the equation

$$Q(t) = 4hC_T \int_{x=0}^{L(t)} \frac{dx}{\sqrt{t-\tau(x)}} \tag{9.14}$$

where Q is the leakoff rate at time t; h is the fracture height, L is the fracture length, respectively; C_T is the total leakoff coefficient; and τ is the first time of exposure of x to injection fluid.

It is well known that only if the fracture propagation rate is large compared to the leakoff diffusion rate, then the 1D Carter model works properly. If this is not the case, then the use of the 1D Carter model can lead to overestimation of fracture length (by as much as up to two orders of magnitude [*Koning,* 1988; *Settari,* 1980]). In this case, the 1D Carter model needs to be replaced by a proper description of the reservoir fluid flow around the fracture [*Koning,* 1988; *Settari,* 1980; *van den Hoek et al.,* 1999; *Gheissary et al.,* 1998]. In addition, for hydraulic fracture stimulation [*Mayerhofer et al.,* 1993; *Hannah et al.,* 1994; *Wong et al.,* 1993; *Fan and Economides,* 1995; *Fan,* 1997; *Valko and Economides,* 1997; *Ma and Yew,* 1999] in high-permeability reservoirs, leakoff rate may be high enough compared to fracture propagation rate to the extent

that using the 1D Carter model is not justified anymore. This is especially true for those cases in which the reservoir flow contribution to total leakoff is the controlling factor, as can be the case for fracture stimulation [*Mayerhofer et al.,* 1993; *Fan,* 1997; *Valko and Economides,* 1997].

A number of efforts have been undertaken to improve upon the 1D Carter model by incorporating 2D (nonlinear) reservoir flow effects. To date, however, none of the efforts addressing nonlinear leakoff fluid flow around a hydraulic fracture have resulted in a model that can be used for a fracture propagating at arbitrary, not necessarily constant, velocity. That is, there is no model that can be used to describe the growth of a fracture that propagates through a multilayer reservoir, with stress contrasts (i.e., leading to at least temporary retardation or acceleration of fracture growth) and rock mechanical property contrasts, and that can also be used to describe the fracture closure after shut-in. There is no model, moreover, that in its simplicity is comparable to the 1D Carter model, and as such is easy to implement into any hydraulic fracturing code.

To overcome these deficiencies, an exact numerical solution has been derived of the transient elliptical (leakoff) fluid flow equation around a hydraulically induced fracture propagating with any, not necessarily constant, velocity and based on an arbitrary fracture growth history [*van den Hoek,* 2002]. This solution (i.e., the leakoff rate profile around the fracture) at any time interval affects the fracture volume balance and pressure, and, therefore, the fracture propagation rate in the next time interval. The numerical solution is presented in the description of the numerical leakoff model to come.

A simple analytical formula for elliptical leakoff rate is presented in the description of elliptical leakoff. This formula approximates the numerical results within a few percent, both during fracture growth and after shut-in. This formula can be easily incorporated into any existing hydraulic fracture model, and it is applicable over the entire range of fluid leakoff rates (i.e., from low-permeability fracture stimulation to high permeability water-flood fracturing).

Description of Numerical Leakoff Model

The numerical leakoff model is an exact solution to the transient elliptical diffusivity equation with a moving source boundary condition (i.e., fracture) [*van den Hoek,* 2002]. Previous work in this area focused on static fractures [*Gringarten et al.,* 1974; *Kucuk and Brigham,* 1981]. The numerical solution can be characterized by the following points:
Transient solution of the elliptical diffusivity equation for leakoff flow from a growing fracture.
The model computes the time-dependent leakoff rate for any (not necessarily constant) fracture growth rate based on an arbitrary fracture growth history: This computed leakoff rate at any time interval affects the volume balance and pressure and, therefore, the propagation rate in the next time interval.
Fractures with high (approximately infinite) conductivity: However, the solution methodology is not necessarily restricted to this case.
Description of pressure-dependent leakoff includes the full pressure history during propagation and after shut-in by means of a convolution.
2D elliptical leakoff flow around a fracture is considered representative for reservoirs with small kv/kh (where kv is the vertical permeability and kh is the horizontal permeability): This is true for most cases. However, if k_v and k_h are of the same order, then it may be required to consider 3D (ellipsoidal) leakoff flow around the fracture.

Approximate Description of Elliptical Leakoff

An approximate expression of the elliptical leakoff rate for variable injection rate is presented and compared with numerical results.

Static Fractures

An approximate solution to the transient elliptical diffusivity equation [*Gringarten et al.,* 1974] relates the pressure in a stationary infinite conductivity fracture to the fracture length L, leakoff rate Q, and leakoff time t

$$\Delta p_{\mathrm{D}} = \tfrac{1}{2}\sqrt{\pi t_{\mathrm{D}}}\left[\operatorname{erf}\left(\frac{0.134}{\sqrt{t_{\mathrm{D}}}}\right)+\operatorname{erf}\left(\frac{0.866}{\sqrt{t_{\mathrm{D}}}}\right)\right]+0.067E_1\left(\frac{0.018}{t_{\mathrm{D}}}\right)+0.433E_1\left(\frac{0.750}{t_{\mathrm{D}}}\right) \tag{9.15}$$

where E_1 is the exponential integral function, the dimensionless pressure difference between the fracture and the far-field reservoir is given by

$$\Delta p_{\mathrm{D}} = \frac{\Delta p}{\left(\frac{\mu Q}{2\pi k h}\right)} \tag{9.16}$$

the dimensionless time is given by

$$t_{\mathrm{D}} = \frac{\lambda t}{L^2} \tag{9.17}$$

and

$$\lambda = \frac{k}{\phi \mu c} \tag{9.18}$$

Here, μ is the viscosity of the reservoir fluid, k is the permeability of the formation, ϕ is the porosity of the formation, and c is the compressibility of the reservoir fluid.

Propagating Fractures: Constant Injection Rate

The following substitutions can be made [*Koning,* 1988]

$$\Delta p_{\mathrm{D}} \rightarrow \frac{1}{Q_{\mathrm{D}}} \qquad t_{\mathrm{D}} \rightarrow \frac{1}{L_{\mathrm{D}}{}^2} \tag{9.19}$$

with the dimensionless leakoff rate given by

$$Q_{\mathrm{D}} = \frac{\left(\frac{\mu Q}{2\pi k h}\right)}{\Delta p} \tag{9.20}$$

and the dimensionless fracture length given by

$$L_{\mathrm{D}} \rightarrow \frac{L}{\sqrt{\lambda t}} \tag{9.21}$$

This yields an expression relating fracture length to injection rate for a propagating (i.e., non-static) fracture in a homogeneous reservoir and for constant injection rate (i.e., leakoff rate for leakoff dominated fracture growth). This expression yields results very close to another model [*Settari,* 1980] that was specifically developed for propagating fractures under constant injection rate.

Propagating Fractures: Variable Injection Rate

Combination of equation 9.15 and the substitutions (equation 9.19) results in an elliptical leakoff rate from a fracture propagating in a homogeneous reservoir with constant injection rate. The next step is to further generalize this approach to eventually yield an expression that may be considered applicable to fracture propagation for variable (e.g., intermittent) injection rate and to fracture closure after shut-in. In other words, the purpose is to develop an approximate expression that can be considered an elliptical generalization of the linear Carter model as given by equation 9.14. To this end, we start by rewriting equation 9.15 in a more convenient form by applying the first of the substitutions of equation 9.19. The result is

$$Q_{\mathrm{D}} = \left\{ \tfrac{1}{2}\sqrt{\pi t_{\mathrm{D}}}\left[\operatorname{erf}\left(\frac{0.134}{\sqrt{t_{\mathrm{D}}}} \right) + \operatorname{erf}\left(\frac{0.866}{\sqrt{t_{\mathrm{D}}}} \right) \right] + 0.067 E_1\left(\frac{0.018}{t_{\mathrm{D}}} \right) + 0.433 E_1\left(\frac{0.750}{t_{\mathrm{D}}} \right) \right\}^{-1} \tag{9.22}$$

where the dimensionless time t_{D} is given by equation 9.17. The pressure-dependency of the leakoff rate as computed by equation 9.22 is explicitly incorporated by equation 9.20.

As a next step, the methodology in [*Koning,* 1988] is followed in order to determine an elliptical leakoff rate for the case of variable injection rate. The following substitution is made in equation 9.22

$$\frac{1}{\sqrt{t_{\mathrm{D}}}} \rightarrow \frac{2}{\pi\sqrt{\lambda}} \int_{x=0}^{L} \frac{dx}{\sqrt{t - \tau(x)}} \tag{9.23}$$

The substitution of equation 9.23 for the dimensionless time t_{D} in equation 9.20 may be considered as a generalization to variable injection rate of the substitution of equation 9.17 for t_{D} in equation 9.22. The substitution of 9.17 in equation 9.22is only valid for constant injection rate. The impact of variable injection rate (and, therefore, of variable fracture growth rate) on equation 9.23 is exhibited via the times $\tau(x)$ of first exposure of fracture length x to injection fluid.

It appears that in high-permeability fracturing, elliptical leakoff results in fracture dimensions, which can be significantly (up to one order of magnitude) smaller than fracture dimensions using linear Carter leakoff. Using elliptical leakoff can significantly reduce fracture size sensitivity to formation permeability with respect to using linear leakoff.

9.12.3 3D Fracture Growth

For the past two decades, hydraulic fracture design has relied principally on pseudo 3D hydraulic fracturing models (section 9.3.2 on page 155). The main, current hydraulic fracturing simulators (e.g., FracproPT, StimPlan, MFrac, and FracCADE) approach the 3D reality in different ways. However, they describe a highly simplified geometry. Planar 3D models (section 9.3.3 on page 156) have been available for a long time (e.g., TerraFrac, GOHFER). However, they appear to be applicable only in special circumstances. Recently, a new planar 3D fracture model has become available (E-StimPlan 3D). To the best of our knowledge, full 3D models (section 9.3.4 on page 158) with a user-friendly interface, user support and a significant user base are not currently available (i.e., existing full 3D models are either academic or proprietary, and are only used by the developers for research purposes or have been discontinued). Unfortunately, planar and especially full 3D models are currently too computationally demanding for routine use. That is, if a brute force method is the most convenient solution, then the general mesh for 3D fracture propagation makes sense. However, if it leads to slow simulation, then it is sub-optimal.

Planar 3D Models

Planar 3D models (section 9.3.3 on page 156) can be used for analyzing the effects of complex geologic environments on fracture propagation and geometry, for a fracture that is constrained a single plane. Planar 3D models simulate fracture growth through formations with varying values of stress, strength, modulus, and fluid loss. They are able to compute the correct width from the correct mass balance and fluid efficiency.

The main differences between planar 3D models (section 9.3.3 on page 156) and pseudo 3D models (section 9.3.2 on page 155) are:

1) The fracture width is calculated using 3D elastically coupled displacement (i.e., the total displacement at a point is the integration of all displacement increments caused by all local forces). Thus, the fracture width is calculated correctly for a complex geometry. This is critically important for areas such as fracture re-entrant areas. In contrast, for pseudo 3D models, the width and height growth at each point along the fracture is a function of the net pressure at that point alone.
2) Fracture propagation is calculated for all points around the fracture perimeter. In contrast, for pseudo 3D models, the major part of the fracture propagation is into the zone where the fracture initiates.

While the current planar 3D models can potentially simulate more complex fracture geometries, they are currently limited to single, planar fractures. In addition, the application of 3D state-of-stress, 3D rock mechanical properties, and the presence of natural fractures is currently not supported.

3D Fracture Geometry

Any rigorous linear elastic mechanics solution for 3D fracture geometry needs to follow the stress-strain relationship (i.e., the generalized, 3D, anisotropic Hooke's law) [*Jaeger and Cook,* 1976]

$$\vec{\sigma} = \vec{\vec{C}}\vec{\varepsilon} \tag{9.24}$$

where $\vec{\sigma}$ is the stress vector, $\vec{\vec{C}}$ is the elastic constants or stiffness matrix, and $\vec{\varepsilon}$ is the strain vector. The stiffness is a property of the solid body (i.e., it depends on the material, its shape, and the boundary conditions).

To compute the strain from the stress, the stress-strain relationship is rewritten to

$$\vec{\varepsilon} = \vec{\vec{C}}^{-1}\vec{\sigma} = \vec{\vec{S}}\vec{\sigma} \tag{9.25}$$

where the elastic moduli or compliance matrix is defined as

$$\vec{\vec{S}} = \vec{\vec{C}}^{-1} \tag{9.26}$$

GOHFER uses an existing analytical solution to compute the compliance matrix directly and thus efficiently. However, this introduces the limitations of square mesh grid elements, and a uniform Young's modulus.

E-StimPlan 3D inverts the stiffness matrix a single time before the main computations to preserve a more rigorous solution. This allows for the simulation of a layered Young's modulus, and arbitrary mesh grid geometry. In addition, E-StimPlan 3D provides a fully implicit solution where all the factors affecting fracture geometry (i.e., fluid flow, fluid rheology, fracture width, tip effects, and fracture propagation and height growth) are solved simultaneously.

Application to EGS

Planar 3D models (and to a limited extent full 3D models, due to their computational expense) can be used as a basis to develop an empirical model for fracture growth orientation and fracture complexity based on:

1) 3D state-of-stress (refer also to section 9.12.4 on page 181),
2) rock mechanical characteristics,
3) natural fracture orientation (refer also to section 9.12.5 on page 181), and
4) fracture treatment characteristics.

9.12.4 Back Stress

As fluid leaks out of the fracture into the reservoir, the pressure and temperature changes in the affected part of the reservoir. Consequently, that part of the reservoir dilates or contracts, and a back stress develops. This increases the effective closure pressure. These effects are referred to as poro-thermo-elastic [*Economides and Nolte,* 2004]. The poro-thermo-elastic effects are generally small. However, they could be important in some cases [*Nolte et al.,* 1993]. Although the additional pressure results in an increased net pressure in the fracture, it generally has little effect on fracture geometry.

The equation for the stress change due to changes in reservoir pressure and temperature is [*Smith et al.,* 2004]

$$\Delta\sigma_{yy} = \frac{E}{1+\nu}\frac{\partial^2\phi}{\partial y^2} + A_p\Delta p + A_T\Delta T \tag{9.27}$$

where σ_{yy} is the stress perpendicular to the fracture face, E is Young's modulus, v is Poisson's ratio, Δp is the pressure change for the initial reservoir pressure, and ΔT is the temperature change from the original reservoir temperature.

The potential ϕ is the solution to the Poisson Equation

$$\nabla^2\phi = -A_p\Delta p\frac{1+\nu}{E} - A_T\Delta T\frac{1+\nu}{E} \tag{9.28}$$

where the poro-elastic constant is defined as

$$A_p = \frac{1-2\nu}{1-\nu}B \tag{9.29}$$

and B is Boit's constant. The thermo-elastic constant is defined as

$$A_T = \frac{E\alpha_T}{1-\nu} \tag{9.30}$$

where α_T is the thermal expansion coefficient.

These two equations are solved for the change in fracture closure stress. The new stress is included in the calculation of the coupled pressure- width in the fracture.

9.12.5 Pressure Dependent Leakoff from Natural Fractures

One of the key issues in designing a fracture treatment is accurate knowledge of how rapidly fluid leaks out of the fracture into the reservoir [*Economides and Nolte,* 2004]. Without this information, it would be impossible to design a treatment that provides a specified fracture geometry. Mini-fracture treatments are performed to estimate the leakoff coefficient. Three separate leakoff processes are distinguished [*Carter,* 1957]:

1) Displacement and compressibility of reservoir fluid (section 9.12.2 on page 176),
2) invasion of the formation by filtrate or fracturing fluid, and
3) buildup of an external filter cake.

Rather than considering the three processes, leakoff can also be divided into three periods [*Williams,* 1970]:

1) During the initial period, when the filter cake has not formed, the leakoff rate is controlled by the resistance of the formation to flow of the fracturing fluid, and the leakoff is rapid.

2) This is followed by a decreasing leakoff rate when the external filter cake builds up.
3) Finally, the cake stops building, because the high-velocity fluid in the fracture prevents further polymer deposition, and a steady-state leakoff rate occurs. This last stage is referred to as dynamic leakoff.

The leakoff of the fracturing fluid is pressure dependent if it is controlled by:
1) The wall-cake,
2) the filtrate, or
3) the movement of the reservoir fluid (section 9.12.2 on page 176).

In addition, the creation of a fracture network has a profound effect on pressure-dependent leakoff. Current hydraulic fracturing models are incapable of *a priori* simulation of the fracture networks that develop in naturally fractured, low-stress-bias reservoirs (e.g., the Barnett Shale), because of the complexity of these networks. However, the following mitigates this problem:
1) A multitude of fractures have been mapped in the Barnett Shale,
2) similar trends were observed in many of the fractures,
3) the production was related to the stimulated reservoir volume (SRV), and
4) the effects of rate and other parameters were observed.

Consequently, there probably exists a sufficient amount of information and an adequate understanding of the development of the network to formulate a model that allows for the optimization of fracture design, and performs a sensitivity analyses on the various parameters. Such a model requires the introduction of a number of new parameters. However, from the mapping data, it should be possible to calibrate these parameters to yield results that look reasonably similar to the mapped data. Unfortunately, the network model is not able to simulate the details of heterogeneous and anisotropic fracture development that is often observed. However, if the calibration is performed correctly, then the total stimulated reservoir volume should be reasonably accurate.

Fracture Network Model

The envisioned approach to the network model is to execute a standard hydraulic fracturing model (e.g., the calibrated model FracproPT of Pinnacle Technologies, Inc.) to simulate the main hydraulic fracture. These simulation results can then be used as the backbone of the simulation of the network of natural fractures. The fluid leakoff into the network of natural fractures is superimposed on the normal fluid leakoff from the fracture into the surrounding porous reservoir matrix.

Coupling to Existing Hydraulic Fracturing Model

Because the fracture network model requires a number of new parameters, it is reasonable to contain most of the complexity of fracture modeling within the main hydraulic fracture. For example, a simple solution to determining the height growth within the network is to determine it from the height from the main hydraulic fracture with respect to the height of the naturally fractured reservoir layers. In this way, the primary added functionality is the conservation of mass and momentum in the fracture network.

Proppant Transport

The major problem of this approach is proppant transport. It seems reasonable to develop the initial model by assuming that there is no proppant transport into the fracture network (i.e., it only stays within the main hydraulic fracture). For a later version of the model, proppant transport into the fracture network can be accommodated, by developing a reasonable, physically plausible methodology.

Main Hydraulic Fracture Pressurizes Intersecting Network Fractures

The initial network development of a hydraulic fracturing treatment with the main hydraulic fracture starting at a well and propagating in both directions into a naturally fractured reservoir is displayed in Figure 9.1. Early in the treatment, the main hydraulic fracture intersects the first natural fractures, and fluid starts to permeate into those network fractures. It is assumed

that this network consists of two sets of natural fractures that intersect at a certain angle with each other and with the main hydraulic fracture. The spacings for each of the two fracture sets and the deviatoric stress bias (i.e., the difference between the minimum and maximum horizontal stress), which are not common in typical fracture models, need to be specified.

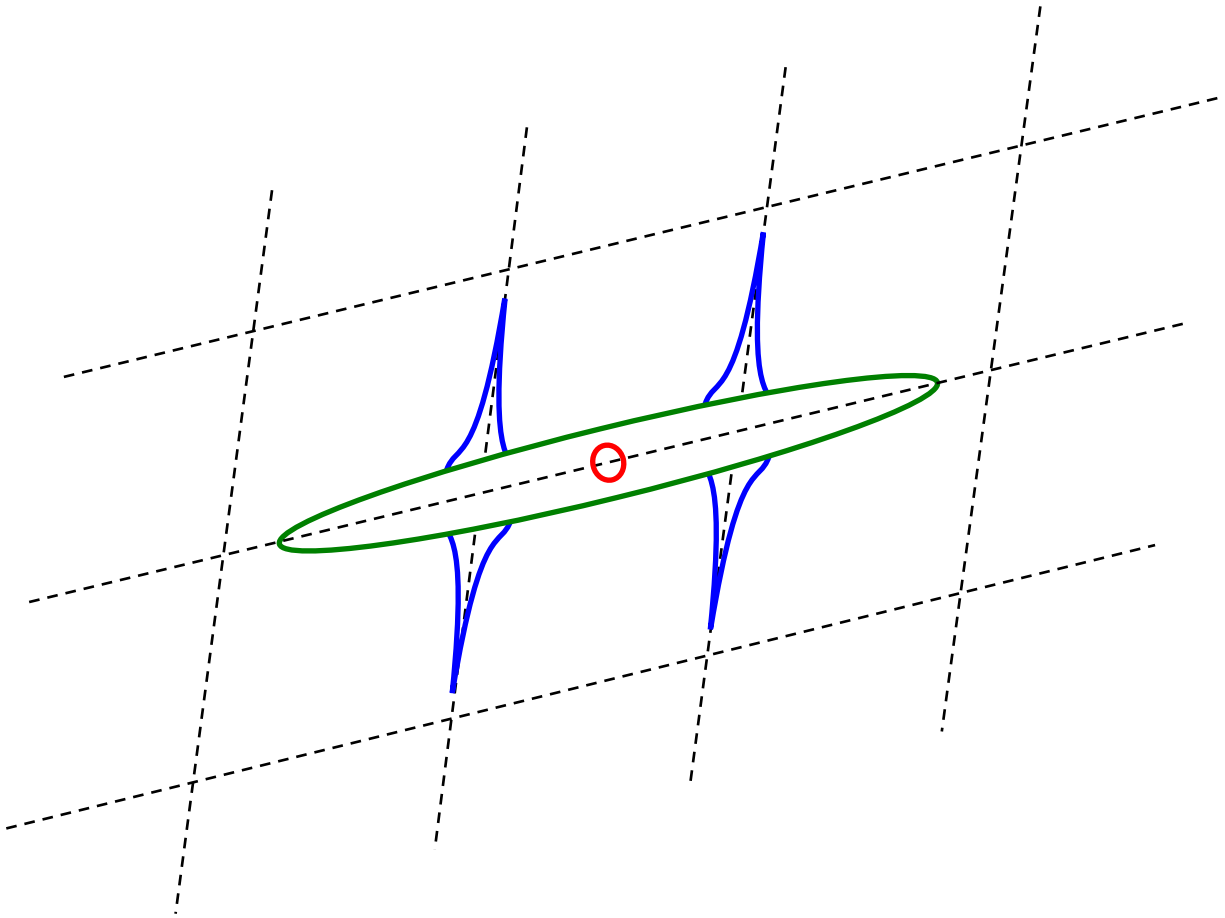

Figure 9.1: Main hydraulic fracture (green ellipse) that initiates from a well (red circle), and intersects the network of natural fractures (black dashed lines) which pressurize (blue lines). This schematic is not drawn to scale.

Opening of Network Fractures

The key to the development of the network model is describing the flow into these natural fractures and allowing the fractures to dilate and eventually open. The ways that elevated pressure could affect natural fractures is displayed conceptually in Figure 9.2. Natural fractures with rough surfaces and minimal mineralization (left side of Figure 9.2) are most likely highly sensitive to the net stress pushing on them:

1) Under initial, ambient reservoir conditions (i.e., the pressure p within the natural fracture equals the initial, ambient reservoir pressure p_i), the effective stress is high, and the open slot pores are most likely deformed and closed. The fracture network permeability is initially equal to that of the natural fracture network in the reservoir, and the value can be quite low.
2) As the pressure in the natural fracture increases because of leakoff of the high-pressure fracturing fluid from the main hydraulic fracture ($p > p_i$), the net closure stress is reduced and the natural fracture porosity opens. In this regime, the leakoff coefficient is highly pressure dependent. The fracture network permebility increases slightly.
3) As the pressure exceeds the closure stress on the natural fracture ($p > p_{fo}$), the entire natural fracture opens, yielding an accelerated leakoff condition. The fracture network permeability increases dramatically. The width of the natural fracture is essentially constant over its length, such that an average value for the width can be used (greatly simplifying the mass and momentum equations).

4) In contrast, vuggy porosity (i.e., lined with mineral precipitates; right side of Figure 9.2) is generally insensitive to stress, and remains unchanged until the pressure exceeds the closure stress and opens the entire natural fracture (i.e., accelerated leakoff).

Interestingly, the situation reverses during cleanup because the well is drawn down to extract stimulation fluids. Consequently, the natural fracture permeability decreases. Thus, stimulation fluids are injected under wide-open natural fracture conditions, but are produced under clamped natural fracture conditions. This makes it difficult to clean up the reservoir.

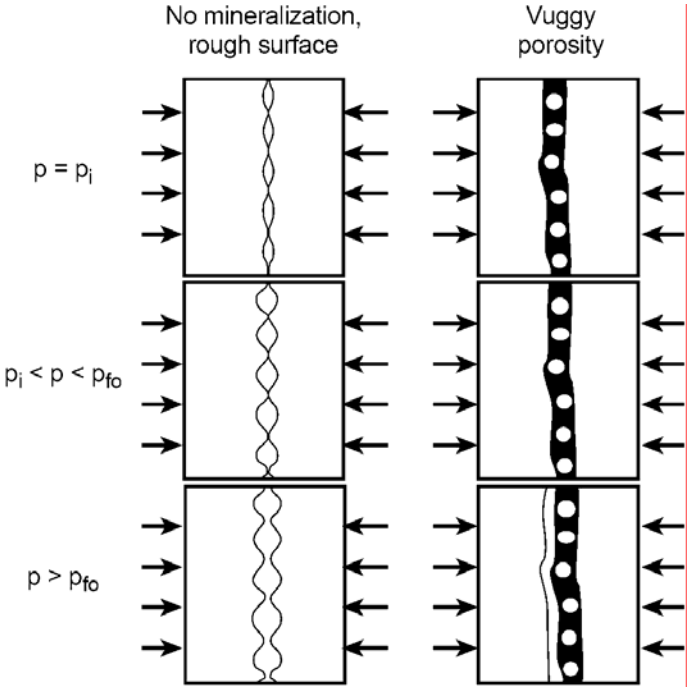

Figure 9.2: The effects of pressure on fracture opening and porosity [*Warpinski,* 1991]. Here, p is the pressure inside the fracture, p_i is the initial (ambient, reservoir) pressure, and p_{fo} is the fracture opening pressure or closure stress.

More precisely, a natural fracture is not expected to open uniformly as it is pressurized on either end (or both ends). Asection of the first natural fracture during the opening process is displayed schematically in Figure 9.1:

1) At the far tip of the natural fracture, the fluid has not yet penetrated into the natural fracture, and it is at its initial permeability.
2) In the middle of the natural fracture, the permeability has begun to increase because of the penetration of the fluid into the natural fracture and the subsequent increase in pressure.
3) Where the natural fracture meets the main hydraulic fracture, the pressure is already sufficiently great that the natural fracture is opening.

Flow between Network Fractures

Once the main hydraulic fracture and the intersecting natural fractures inflate, these natural fractures in turn begin inflating subsequent network fractures at their intersection. Natural fractures that are sub-parallel to the main hydraulic fracture are generally expected to open before the natural fractures that are sub-perpendicular, because they should have slightly lesser stress.

Modified Stress Field

Because of the opening of the main hydraulic fracture and the network of natural fractures, the stress field in the reservoir is expected to change. This affects the appropriate closure stress on the fractures. Consequently, the cumulative effect of the stress that each fracture exerts on all other fractures needs to taken into account.

Model Development and Data Management

Once the model is developed to this extent, the remainder of the model development is simply a further expansion of the network by use of the same principles. It takes a significant amount of accounting (i.e., management of data), and there could be some numerical problems (e.g., instabilities, oscillations). However, it should be possible to develop techniques to minimize such issues.

Application

The analysis is based on calibrating the net model for permeability, calculating reasonable stresses on the network fractures, and obtaining reasonable fracture spacings from fracture mapping data (and other information). The model should then be able to simulate the effect of rate and viscosity on the development of the fracture networks. It is also possible that this model can assist with inversely estimating characteristics of the fracture system to match it with the mapping data. One possible result would be the total surface area contacted by the hydraulic stimulation (e.g., the sum of the areas of all the natural fractures opened in addition to that of the hydraulic fracture).

9.13 Direct Incorporation of Measurements

The reality of routine hydraulic fracturing design is that there is a tremendous gap in data requirement for a simple simulation and the data gathering effort. The single most important issue for hydraulic fracturing design is predicting the fracture height. Although better simulation models can improve the height prediction, the lack of stress and modulus data hampers a meaningful simulation. In practice, an engineer simply selects either contained or uncontained fracture geometry, rather than making a prediction. Consequently, a stronger link between model and observations (e.g., via fracture mapping) would be highly beneficial for the hydraulic fracturing design.

It would be highly beneficial to integrate fully diagnostics of hydraulic fracturing in the stimulation design cycle. Currently, the diagnostics are ahead of the simulation capability in terms of geometry. On the other hand, the diagnostics could be directed to fracture conductivity mapping because that is the critical design objective. Another issue is the verification of true 3D fracture simulation. Insufficient effort is made to verify the results from 3D models against field observations.

It is critical to validate any model with measurements, in particular monitoring via diagnostics. However, a model can only be credible if the link with reality is from the correct physics and fracture geometry. The final goal should be to improve the predictive power of simulations and that can never be achieved by correlations. In the long term, there is no easy solution to difficult problems. A direct link between physical understanding, geological reality, and the modeling approximations needs to be maintained. This also implies that a more sophisticated modeling capability should provide a better approximation to the problem that needs to be solved. It is worthwhile to invest in a true 3D fracture model if it yields a better prediction of height growth, proppant pack geometry, and final conductivity. However, if such a state-of-the-art model deviates significantly from observations, this may not be a feasible approach. For this purpose, the discrepancy between 3D fracture models and observations needs to be studied. Few data sets can be used for such a comparison.

10 APPENDIX C: ALTERNATIVES TO THE BARNETT SHALE

In addition to the Barnett Shale, both vertical and horizontal wells have been used in various other low permeability oil-field reservoirs that are naturally fractured (e.g., the Devonian Shale in West Virginia and Kentucky, the Niobrara Shale in Colorado, the McLure Shale in California, the Bakken Shale in North Dakota, the Austin Chalk in Texas, and the Niobrara in Wyoming). Other applications include low permeability oil-field reservoirs (e.g., the Niobrara Limestone and Codell Sandstone in South Dakota, the Stevens Sandstone in California, and the Palo and Pinto Sandstone in Texas).

This section refers to these reservoirs in terms of limited entry (section 10.1 below), vertical wells (section 10.2 below), horizontal wells (section 10.3 on page 187), and direct hydraulic fracture diagnostics (section 10.4 on page 191).

10.1 Limited Entry

Starting in the early 1960s, excellent results from the limited entry technique were experienced in Texas and New Mexico [*Lagrone and Rasmussen,* 1963]. This method has proven significantly more effective than any other method in treating thick pay-zone sections and in diverting treating fluids to multiple horizons. The limited entry treatment technique is accomplished by:

1) Limiting the number of perforations in a well, and
2) providing sufficient injection rate to require the restricted flow capacity of the perforations to divert the treatment to a greater portion of the perforated interval.

The production performance of wells treated by limited entry completions is superior to that of conventionally treated wells. Gamma-ray tracer logs indicate that most of the pay-zone is being treated even though not all of it is covered by perforations. Results of these simultaneous treatments have been gratifying in both well performance and reduced costs.

10.2 Vertical Wells

Devonian Shale

The results of a study of the effect of various stimulation methods on vertical wells in the Devonian Shale compared the economics of their alternatives [*Zuber* et al., 1987]. It appears that the key factors that determine the optimal stimulation technique are:

1) The anisotropy of the permeability of the formation, and
2) the length of the induced fracture wing.

The conductivity and orientation of the induced fracture are also important.

Niobrara Limestone and Codell Sandstone

In the last several years, the application of the limited entry technique has been extended to massive hydraulic fracturing of the Niobrara Limestone and Codell Sandstone [*Cramer,* 1987]. Limited entry perforating reduces stimulation costs with no apparent effect on production [*Eberhard and Schlosser,* 1995]. A primary concern for treating multiple intervals is to ensure that all zones receive the necessary treatment.

The mechanisms involved in fluid and slurry flow through perforations were investigated [*Cramer,* 1987]. Limited entry design and procedural guidelines for large scale fracturing treatments are analyzed to assist in achieving the desired placement of fluid and proppant into individual zones. Fundamental limitations of the limited entry technique were also analyzed. Analysis of the bottom-hole pressure data of these treatments indicates that proppant alters the mechanical configuration of the perforations, as evidenced by a change in the magnitude of perforation friction in opposition to the Bernoulli constant energy equation. The practical significance of changing pressure drop across perforations in limited entry stimulation treatments is that it alters treatment fluid distribution and injection rate profiles among the multiple

intervals. This can result in zonal shut-off because of insufficient pressure drop or zonal sand-out because of inadequate pad volumes and treating rate.

Currently, some operators simply ratio the number of perforations in each interval to the volume of treatment required for each interval. To ensure that both zones are being treated, a minimum pressure drop is usually used for limited entry design. Changes in the perforation discharge coefficient and diameter during the treatment, combined with changes in the net treating pressure, affect the calculation of the pressure drop over the perforations. To determine the actual pressure drop across the perforations, designers use a real-time calculation. Limited entry treatments pumped in 34 wells that verify the calculations were reviewed. Changes in the perforation discharge coefficient and diameter were analyzed, as well as the effect of proppant concentration and velocity through the perforation. The current calculation used on location to calculate the pressure drop across the perforations was also analyzed.

10.3 Horizontal Wells

The application of horizontal wells has increased tremendously with significant and positive results in the United States of America during the past decade [*Biglarbigi et al.,* 2000]. The pace of horizontal drilling for oil and gas has remained high at 600 to 1,000 wells per year between 1990 and 2000. Most of these wells have been drilled in three formations: the Austin Chalk in Texas (79%), the Bakken Shale in North Dakota (5%), and the Niobrara in Colorado and Wyoming (2%). Wells in other formations constitute 14%.

In low permeability, naturally fractured reservoirs, horizontal wells are believed to be necessary to increase natural gas recovery and to reduce the risk of drilling a dry hole [*Layne and Siriwardane,* 1988]. In a horizontal well, the borehole can cross multiple natural fractures in the reservoir. The orientation of hydraulic fractures created from horizontal wells depends on their orientation with respect to the stress field, and the completion technique [*Soliman et al.,* 2004]. Fracturing horizontal wells could be used to alleviate the following situations:

1) Restricted vertical flow and low productivity of the formation caused by its low permeability;
2) the presence of natural fractures in a direction different from that of the induced hydraulic fractures, with a resulting high probability of interception; and
3) a low stress contrast between the pay-zone and the surrounding layers (fracturing vertical wells would not be acceptable, because the fracture would grow in height as well as length; in contrast, creating transverse or longitudinal fractures from horizontal wells would allow rapid depletion of the reservoir).

Stress Interference

Although fundamentally similar to fracturing vertical wells, fracturing horizontal wells has unique aspects that need to be considered during the design and optimization of fractures to allow for a successful treatment [*Soliman et al.,* 2004]. Differences between horizontal and vertical wells exist in areas of rock mechanics, reservoir engineering, and operational aspects. In terms of rock mechanics, stress interference because of multiple transverse fractures can be significant. This can result in an increase of the fracturing pressure (which is a function of the distance between the fractures relative to their dimensions), and a change in the orientation of the stress field (if the stress contrast between the maximum and minimum horizontal stresses is not great), which can cause significant problems during the fracturing of successive fractures. These considerations should be used in determining the optimum distance between fractures. In contrast, stress interference because of multiple vertical fractures from a vertical well is less likely to change the orientation of the stress field. However, it can increase the breakdown and extension pressures of the fractures.

Devonian Shale

A series of stimulations were designed to open and propagate natural fractures known to exist along a horizontal well, and to induce hydraulic fractures [*Overbey et al.,* 1988]. The locations of the fractures were determined by radioactive tracers. The fractures appeared in zones other than the one pumped into. This indicates the opening and propagation of natural fractures with two or more orientations. Pressure testing and gas sampling of the isolated zones confirm that communication between fractures was accomplished along a significant part of the borehole by stimulation of a single section.

The concept that multiple hydraulic fractures from horizontal wells can increase gas recovery efficiency over vertical stimulated boreholes was tested [*Yost et al.,* 1987a]. Geologic mapping was used to define the orientation and potential for production of fracture networks [*Mroz and Schuler,* 1990]. Two directional well site evaluations were used to select the sites and to design the geometry of the well. Three-dimensional models were developed for each site, and they were demonstrated to be an economical tool for defining and developing a producing reservoir.

From a comparison of the predicted economics and gas production from unstimulated and stimulated horizontal, high-angle, and vertical wells, it appears that horizontal drilling is the optimal method with as much as a 46% improvement in production performance compared to high-angle drilling (which results in a slight improvement) and vertical drilling [*Zammerilli,* 1989].

To assess the effectiveness and economic feasibility of applying horizontal drilling and stimulation techniques to enhance the production of natural gas, a horizontal well in the was successfully drilled and completed [*Bellinger,* 1991]. Six completion zones were established:
1) An open-hole and slotted liner section at the bottom;
2) three zones isolated by external packers with access to the formation through sliding sleeves, and
3) two zones which were cemented.

It appears that such a well allows for the development of additional reserves.

The significance of enhanced production from a horizontal well in a field that was partially depleted was studied [*Yost and Overbey,* 1989]. The performance of multiple hydraulic fracturing treatments along a horizontal well was evaluated. Pre-fracturing flow and pressure data, hydraulic fracturing treatments, and post-stimulation flow and pressure data were analyzed. Average field production from 72 wells was used as baseline data for the analysis. Under current reservoir pressure conditions, the horizontal well produced at a rate of a factor of 7 times greater than the current field average for stimulated vertical wells. This increase in production suggests that horizontal wells, in strategically placed locations within partially depleted fields, can significantly increase reserves.

Appropriate locations for a horizontal well in a multiple site reservoir were selected from favorable geology, high flow capacity (from reservoir data from more than 38 wells), minimum interference of adjacent wells, a high expected production efficiency (also compared to vertical wells), and reasonable access in a rugged terrain [*Yost et al.,* 1987b]. The evaluation of the interference and production efficiency was from a three-dimensional gas flow simulator capable of modeling the porosity, permeability and desorption of the fracture and the matrix. Directionally drilling to intersect the natural fracture system (from regional mapping trends), horizontal coring to determine the spacing of the natural fractures and the creation of multiple horizontal fractures through the cemented casing was applied. It appears that horizontal wells can be realized in naturally fractured formations. However, extensive reservoir studies are required to increase the probability of success in achieving significant production enhancement.

The design and predictions of the geometry of hydraulic fractures for horizontal wells were analyzed [*Layne and Siriwardane,* 1988]. Current models and theories of hydraulic fracturing address failure mechanisms and the propagation of a single crack from a vertical well. These theories have been adapted to predict the pressure, flow rate, and induced fracture geometry for each natural fracture that is intersected by fracturing fluid in the horizontal well. A model for tubing/annulus flow was coupled with a model for hydraulic fracturing that predicts the three-dimensional geometry of multiple fractures propagating from a horizontal well. Additionally, a model for the prediction of the distribution of the pressure and flow rate along the lateral extent of the well was developed. Stimulation data from individual zones along a horizontal well was tested and simulated. Predicted results were compared with in situ fracture diagnostics from gas and foam-sand stimulation treatments. Radioactive tracers confirmed that both fluid pressure and stress perpendicular to the fracture affect the distribution of the injection rate along the well. Both of these factors were used as governing mechanisms for the prediction of the geometry of the fracture in the model simulation. Predictions from these models and tracer logs confirm that the single crack theory for fracture propagation is not applicable for stimulations that are initiated along an isolated part of a horizontal borehole.

Niobrara Shale

To identify potential locations for horizontal wells in the Niobrara Shale, the following techniques were integrated [*Stright and Robertson,* 1995]:
1) Surface and subsurface geologic data,
2) analysis of structural deformation from second-derivative maps overlaid on production data, and
3) dimensionless type curves from reservoir simulation models.

The evaluation of the spacing and economics of drilling horizontal wells suggests that in some instances, it could be more economical to drill vertical rather than horizontal wells.

McLure Shale in California

In the McLure Shale, horizontal wells have been completed with an uncemented liner and a single hydraulic fracture treatment. The well was aligned with the preferred fracture orientation, with the intention of initiating and propagating a simple longitudinal fracture along the lateral [*Minner et al.,* 2003]. Compared to vertical wells in the adjoining North Shafter field, these horizontal wells greatly improve the ability to place hydraulic fracture treatments, and to improve the economics of the wells by accessing a greater volume of reservoir per well. However, the long completion interval and the uncemented liner unavoidably add uncertainty to the distribution of the fracture treatment along the lateral. To determine whether by use of limited entry perforation effectively stimulates the entire target lateral interval, surface tiltmeter mapping of hydraulic fractures was used to evaluate fracture growth during the nine fracture treatments. The actual fracture growth pattern appeared to be very complex, with vertical fracture components in two orthogonal directions, and a significant horizontal fracture component. Almost half of the fracture volume was contained in transverse fracture components, while one-third of the fracture volume was in longitudinal components, and the remaining in horizontal fractures. This complex, multiple component fracture growth is believed to be because of a small in-situ stress bias, combined with the impact of the completion technique (i.e., preferential longitudinal initiation, and treatment-induced stress changes) and the misalignment of natural fractures with the current stress field. There was less fracture treatment volume in the mid-lateral than expected from the design of the perforation cluster, possibly because of the interference of stress from the transverse fractures. Although the uncemented liner technique did not achieve the original intent of longitudinal fracture dominance, reasonable lateral coverage was achieved. Changes in the character of the fracture growth occurred during five of the nine treatments. Most of these changes appeared to be associated with proppant bridging. From 1-year cumulative production, the limited dataset is suggestive. However, not conclusive, that horizontal and transverse fracture growth is preferable to longitudinal fracture growth.

Devonian Shale, Palo Pinto Sandstone, and Stevens Sandstone

Long, horizontal sections have been used increasingly in the Devonian Shale, the Palo Pinto Sandstone, and the Stevens Sandstone [*McDaniel et al.,* 1999]. Historically, such wells have been stimulated with several separate fracture treatments, requiring expensive well operations between fracture stages. Successful zonal isolation for each fracture stage has been a primary reason for the success of this technique. Several operators reduced the completion costs by extending the application of limited entry fracturing techniques to very long sections of highly deviated or horizontal wells, while ensuring effective fracture stimulation of each perforated section. Many special innovations have been introduced recently for enhancing the applicability of limited entry fracturing in long, open-hole completions and in some uncemented liner applications.

Bakken Formation in Montana

In the shales and dolomites of the Bakken Formation, an evolution in the horizontal drilling and completion methodology has resulted in significant improvements in well productivity [*Wiley et al.,* 2004]. Although the horizontal wells can produce at economic rates without stimulation, hydraulic fracturing increases well productivity significantly. The wells were drilled for longitudinal fracture orientation. The original wells had cemented liners and used the limited entry technique to distribute the fracture treatment. Later, un-cemented liners and a modified fracture treatment with diverter stages were used. The most effective way to complete and hydraulically fracture these laterals was evaluated. In addition,

the improvements in proppant distribution along the well caused by changes in fracture treatment design and its impact on well productivity were analyzed.

Austin Chalk in Texas

In the Austin Chalk, the application of horizontal wells was tested for use [*Shelkholeslami et al.,* 1991]. Three short and seven medium radius wells were drilled successfully. Well plans, bottom-hole assemblies, trajectory control, telemetry, mud systems, hydraulics, hole cleaning, casing design, cementing, problems encountered, formation evaluation, completions, and reservoir response were analyzed.

Most horizontal wells in the Austin Chalk in Texas have been completed as open-hole laterals because the advent of horizontal drilling [*Bell et al.,* 1993]. This horizontal configuration makes stimulating the entire length of the lateral zone extremely difficult. Natural fractures and the horizontal profile preclude the use of conventional hydraulic fracturing techniques.

Nibrara in Wyoming

Vertical and horizontal wells in the Niobrara have been stimulated by injecting large volumes of water at high rates to improve productivity [*Johnson and Brown,* 1993]. This stimulation technique was applied to the Niobrara because it has features that are similar to that of the Austin Chalk. The most important similarity is that productivity requires connection to an adequate natural fracture system.

Antrim Shale in Michigan

Re-stimulation

Similar to the Barnett Shale, the presence of multiple intersecting sets of natural fractures is the primary control on well deliverability for the Antrim Shale in Michigan. Consequently, it must be stimulated to be economical [*Hopkins et al.,* 1998]. However, because of the shallow depths and the natural fractures, the geometry of the resulting hydraulic fractures is complex, and the determination of the optimal fracture treatment or completion methodology is not straightforward. In contrast to the Barnett Shale, the Antrim Shale is under-pressured and contains coexisting mobile water, free and adsorbed gas [*Reeves et al.,* 1993b]. The technical areas that require attention include the frequently disappointing stimulation results achieved with hydraulic fracturing.

The effectiveness of hydraulic fracturing was determined from the following sources:
1) Pressure transient modeling,
2) microseismic imaging to determine the created fracture geometry, and
3) the cutting of multiple core holes to core the created hydraulic fractures.

The integrated results suggest that fracture growth is very complex. A series of sub-vertical fractures were created that were parallel to the maximum principle stress and defined a zone of fracturing. The fractures grew asymmetrically in height above the top perforation and appeared to follow a tortuous path along the directions of the joint-sets. Two oblique core holes encountered eight propped hydraulic fractures. Several of the cored propped fractures had varying azimuths, suggesting that pre-existing natural fractures were propped during the fracture treatment.

The Gas Research Institute (GRI), currently the Gas Technology Institute (GTI), targeted the Antrim Shale for research aimed at enhancing the well performances through improved completion, stimulation and production practices with field research projects to study [*Reeves et al.,* 1993b; *Reeves et al.,* 1993a]:
1) The cost effectiveness of commonly applied single-stage fracture treatments compared to individual treatments for each zone,
2) the potential for re-stimulation to improve the performance of existing wells identified through pressure transient testing as problematic; and

3) the potential application of alternative, low-cost stimulation methods (i.e., comparing acid bailout treatment, high-energy gas fracturing and hydraulic fracturing).

The selection consisted of two open-hole completions to evaluate single-stage treatments, and two cased-hole completions to evaluate multiple-stage treatments. Pre- and post-stimulation pressure transient testing, mini-fracture, bottom-hole treating pressure data, and post-fracturing borehole camera surveys were conducted. Preliminary results indicate that single-stage fracture treatments do contact both shales. However, the stimulation achieved in each zone has not been clearly defined yet.

A significant increase in gas production of the re-stimulated well was achieved. Consequently, there appears to be considerable scope for improving the performance of existing wells through selective re-stimulation.

Post-stimulation pressure transient testing, production testing, and stimulation diagnostics have been applied. Preliminary results indicate that hydraulic fracturing provides superior production results. The lower costs of the alternative treatments, however, may still make them attractive under certain reservoir conditions.

10.4 Direct Hydraulic Fracture Diagnostics

In addition to the Barnett Shale, direct hydraulic fracture diagnostics have also been applied to the Devonian Shale in West Virginia, the McLure Shale in California, the Bossier Sands, and the Cotton Valley in Texas, and the Clinton County Carbonates in Kentucky.

Devonian Shale

Microseismic Imaging of Vertical Wells

In the Devonian Shale, microseismic imaging was applied to a vertical well to evaluate the height and orientation of a hydraulic fracture [*Fix et al.,* 1991]. The technique was used in the Comprehensive Study Well 2 of the Gas Research Institute. This was the first application of the microseismic fracture mapping procedure in the Appalachian Basin, and the first time that the seismic data were collected in a gas-filled well and after a well had been produced for an extended period of two years. It was performed as part of Institute's efforts to understand growth and orientation of fractures in the Devonian Shale. A series of hydraulic fracture diagnostic tests were performed on the well before the microseismic imaging experiment. The comparison between the analyses of the results of microseismic imaging and of other diagnostic tests indicates that they are both consistent for the interpretation of the top of the hydraulic fracture. However, that there is a discrepancy between the results of the analysis for the bottom of the hydraulic fracture.

Downhole Tiltmeter Mapping of Vertical Wells

Surface deformations occurring around a vertical well undergoing hydraulic fracturing stimulation were analyzed by downhole tiltmeter mapping to obtain a description of the geometry and the development of the resulting fracture [*Evans et al.,* 1982]. Significant upward and lateral growth of a near-vertical fracture aligned with the proposed direction of maximum tectonic compression is inferred to take place initially. However, after some time after the fracturing fluid (i.e., nitrogen gas) had been injected, fracture growth in a horizontal plane abruptly began, and vertical growth ceased. No indication of this breakout is evident in the wellhead pressure or flow rate records.

McLure Shale

Surface Tiltmeter Mapping of Vertical Wells

Core data, tiltmeter mapping at the surface, and post-fracturing analysis in the McLure Shale indicated that the limiting factor for hydraulic fracturing from a vertical well was reservoir quality [*Ganong et al.,* 2003]. This suggests that project

viability required significant cost pruning. The differences between the new Rose Field and its nearest analog, the North Shafter Field, were studied, allowing for improved engineering practice.

To determine whether by use of limited entry perforation for a horizontal well with an uncemented liner and a single hydraulic fracture treatment effectively stimulates the entire target lateral interval, surface tiltmeter mapping of hydraulic fractures was used to evaluate fracture growth [*Minner et al.,* 2003]. The actual fracture growth pattern appeared to be very complex, with vertical fracture components in two orthogonal directions, and a significant horizontal fracture component. The fracture volumes that were contained in the various fracture components, and the fracture treatment distribution across the lateral were determined.

Bossier Sands

Microseismic Imaging

In the hot Bossier Sands, extensive sets of data have been collected for microseismic fracture mapping [*Sharma et al.,* 2004; *Griffin et al.,* 2003]. Both water and hybrid fracturing treatments were applied. Microseismic mapping was conducted successfully at bottom-hole temperatures of 300°F and depths of 12,000 to 13,000 ft. In the Bossier Sands, out-of-zone fracture height growth in this area is primarily the result of natural fractures. These natural fractures can act as a barrier to hydraulic fracture growth and as a leak when hydraulic fractures grow through it.

Cotton Valley

In the inter-bedded sands and shales of the Cotton Valley, extensive sets of data have also been collected for a variety of fracture diagnostic tools. Both conventional propped sand fracturing and water fracturing treatments were applied [*Rutlegde et al.,* 2004; *Rutledge and Phillips,* 2003; *Rutledge and Phillips,* 2002; *Mayerhofer et al.,* 2000; *Rutledge et al.,* 1998]. In addition, a methodology that uses full tri-axial waveform analysis of the microseismic signals was used to obtain seismic source parameters, which characterize failure modes during hydraulic fracturing. This information could potentially be used for a detailed description of fracture geometry, growth, and complexities. This may also give some indications about created versus propped lengths of fractures. The fractures are vertically contained within the individual targeted sands, suggesting little or no hydraulic communication between discrete perforation intervals over the stimulated section. The microseismic mapping indicates that water fractures exhibit mostly shear-type failures and conventional propped fractures have a greater volumetric failure component, which indicates more propped fracture width.

Within the top of the Upper Cotton Valley, a system of vertical fractures trending sub-parallel to the maximum principal stress is pressurized. This results in long, narrow fingers of stimulated rock. This is consistent with activation of known natural fractures that are isolated within individual sands and trend sub-parallel to the expected hydraulic fracture orientation in the direction of the maximum principal stress. Stimulation improves connection by hydraulic extension and intersection, resulting in a mesh network of low-angle dilational jogs. Shearing on the natural fractures accompanying adjacent extension enhances and sustains the volume increases. Some fracture offsets or orientation changes are encountered and pressurized, and these tend to concentrate stress and choke off fluid flow. Although these structural heterogeneities cannot be avoided, the adverse effects of impeding proppant transport and fracture growth at such features could be lessened with lower proppant concentrations.

Treatments within the base of the Upper Cotton Valley indicate that a more heterogeneous fracture system is pressurized. Again, the prevalent natural fractures in the reservoir are activated. The interpretation is that the induced seismicity is primarily controlled by the geometry of the natural fractures. Contrary to previous interpretations [*Urbancic and Rutledge,* 2000], the character of deformation is found to be independent of treatment design and position from the treatment well. By implication, it is expected that the effectiveness of shear-induced fracture propping is independent of the treatment fluid.

Austin Chalk and Clinton County Carbonates

Microseismic Imaging

In two sites in the Austin Chalk, and during primary production in the 76 field, Clinton County Carbonates, microseismic imaging was used to define fracture orientation and extent during hydraulic stimulation. At the base of the Austin Chalk, microseismic imaging defined elongated fracture zones at the stimulated depths, extending from the stimulation wells parallel to the regional fracture trend [*Phillips et al.,* 1998]. However, the widths of the stimulated zones differed by a factor of 5 between the two Austin Chalk sites, indicating a large difference in the population of ancillary fractures. Post-stimulation production was much higher from the wider zone. In the Clinton County Carbonates, microseisms defined low-angle, reverse-fault fracture zones above and below a producing zone. Associations with depleted production intervals indicated the mapped fractures had been previously drained. Drilling demonstrated that the fractures contained brine. The seismic behavior was consistent with poro-elastic models that predicted slight increases in compressive stress above and below the drained volume.

Antrim Shale in Michigan

Microseismic Imaging

In the Antrim Shale in Michigan, the effectiveness of hydraulic fracturing was determined from the following sources [*Hopkins et al.,* 1998]:
1) Pressure transient modeling,
2) microseismic imaging to determine the created fracture geometry, and
3) the cutting of multiple core holes to core the created hydraulic fractures.

The integrated results suggest that fracture growth is very complex. A series of sub-vertical fractures were created that were parallel to the maximum principle stress and defined a zone of fracturing. The fractures grew asymmetrically in height above the top perforation and appeared to follow a tortuous path along the directions of the joint-sets.

Mesaverde Sandstone in Colorado

Downhole Tiltmeter Mapping and Microseismic Imaging

In the Mesaverde Sandstone in Colorado, a series of hydraulic-fracture experiments by use of downhole tiltmeter mapping was conducted at the Multi-Site facility of the Department of Energy and Gas Research Institute [*Warpinski et al.,* 1997]. The deformation of the reservoir in response to hydraulic fracture opening was measured, and validating information on the accuracy of microseismic imaging of the fracture geometry was provided. Comparisons of the two techniques were excellent for all tests. In addition to the confirmation of the height, however, the downhole tiltmeters also provided other important information, e.g.:
1) A value of the minimum in situ stress from the actual measurement of fracture opening,
2) a measure of the fracture width during the treatment,
3) a measure of residual width after the treatments, and
4) a validation of the correct situ modulus for hydraulic fracture modeling.

The relative shape of the deformation curves at closure, compared to that measured during the injection, gives a measure of proppant placement within a fracture.